Mucosal Associated Invariant T cells and related CD161 expressing T lymphocytes

Joannah R. Fergusson

St. Edmund Hall





This thesis is submitted for the degree of Doctor of Philosophy,
Infection, Immunology and Translational Medicine,
University of Oxford

Supervisor:
Prof. Paul Klenerman, MRCP, FRCP, DPhil

Supported by wellcome trust

Mucosal Associated Invariant T cells and related CD161 expressing T lymphocytes

Joannah R. Fergusson, St Edmund Hall

Submitted for DPhil in Infection, Immunology and Translational Medicine, Trinity Term 2014

Abstract

The C-type lectin CD161 is expressed by a large number of T lymphocytes, with approximately a quarter of both T cell receptor (TCR)αβ+ and TCRγδ+ T cells expressing this marker. Within CD8+ T cells, a large proportion of these are comprised of Mucosal Associated Invariant T (MAIT) cells, a novel innate-like lymphocyte subset characterised by expression of a semi-invariant TCR together with high levels of CD161 (CD161++). These cells display a phenotype reflective of type 17 CD4+ helper T cells (Th17), which are also hallmarked by CD161 expression. Both MAIT and Th17 cells arise from pre-programmed progenitors, identifiable within umbilical cord blood by expression of CD161. Thus, CD161 appears to identify cells of a pre-determined and distinct phenotype. Whether this reflects a common transcriptional programme, developmentally induced within these cells, and further whether this extends to other CD161 positive T cells, was examined here by mRNA microarray analysis. This analysis identified a shared transcriptional signature and common innate-like function of all CD161 expressing T lymphocytes, and independent of TCR expression or lineage. Furthermore, a population of CD8+ T lymphocytes expressing lower levels of CD161 which overlap phenotypically with CD161++CD8+ MAIT cells was identified by both mRNA microarray analysis and mass cytometry (CyTOF); the CD161+CD8+ T cell population. TCR repertoire analysis, flow cytometry and cell culture experiments were utilised to investigate the origin of this subset, and its phenotype and function in both health and disease investigated in depth. This revealed a pre-programmed, tissue-resident memory population with potent effector functions. Both CD161++ MAIT and CD161+CD8+ T cells expressed high levels of the drug efflux pump MDR1, previously described to confer drug resistance to certain malignant cells. The significance of expression of this pump was hence investigated to determine its potential affect on the success of a variety of clinical therapies.

Acknowledgements

Professor Klenerman
Thank you to my supervisor, Paul. Firstly, for the opportunity to work within his lab and, secondly, for making my time here so enjoyable, including all the opportunities he has created for me. I cannot imagine a better supervisor.

Funding
Many thanks to the *Wellcome Trust* for their generous funding, which has enabled me to complete this research. Also, to *Professors Gull* and *Powrie* for accepting me onto the IITM course.

Lab members
The Klenerman lab is full of people who are helpful and fun to work with. A big thank you to the postdocs, *James* and *Chris*, who always made time for my questions. To my DPhil buddy, *Ayako*, and to my office mates, *Alba* and *Matt*. Thank you to all who donated blood, and especially to *Kathleen Gärtner* who travelled all the way back from Paris to donate blood for the stimulated microarray. Thank you to *Lucy Walker* for guidance on the MDR1 work. Also, thanks to *Clare Marchant* for technical advice.

Teachers
Thank you to all the teachers who taught me to love science and encouraged me to apply firstly to university, and subsequently for a PhD. These include *Mr Moncrieff*, *Mr Barber* and *Mrs McMillian*; *Ann Pullen and Gabi Braun*; *Vicki Fleming* and *Ruth Simmons*.

Friends
Many people have supported me through this DPhil – listening and sympathising, faithfully praying, and being part of various good memories over my time in Oxford. Thank you to *Helen*, *Jacqui*, *Sarah*, *Christine*, *Emma*, *Mary*, *Ruth*, *Annette*, *Ivy*, *Anja*, *Serena* and *Georgia*. I have made friends for life here, and am grateful to you all.

Family
Last, but by no means least, I wish to thank my wonderful family. For numerous tearful phone conversations, where they provided both a sympathetic ear and advice about lab matters – despite mostly not understanding what I was on about! And for all the love and support you've provided. I can never thank you enough.

"Not to us, O Lord, but to your name be the glory,
because of your love and faithfulness"
Psalm 115:1

Table of Contents

THESIS CONTRIBUTIONS 1

ABBREVIATIONS 2

1. INTRODUCTION 3

1.1 INNATE VS. ADAPTIVE IMMUNITY 4
1.1.2 T CELL MEMORY 4
1.1.3 TISSUE-RESIDENT MEMORY 8
1.2 INNATE-LIKE LYMPHOCYTES: BRIDGING INNATE AND ADAPTIVE IMMUNITY 9
1.2.1 TCRγδ+ T CELLS 9
1.2.2 INVARIANT NATURAL KILLER T (iNKT) CELLS 11
1.2.3 MUCOSAL ASSOCIATED INVARIANT T (MAIT) CELLS 12
1.3 CD161 14
1.3.1 CD161 AND A TYPE 17 PHENOTYPE 14
1.3.2 CD161 AND MEMORY PHENOTYPE 16
1.3.3 CD161 IN MOUSE MODELS 17
1.3.4 LECTIN-LIKE TRANSCRIPT 1 (LLT1): THE LIGAND FOR CD161 19
1.3.5 THE FUNCTION OF CD161 19
1.3.6 CD161 AND TISSUE HOMING 20
1.3.7 CD161 AND DISEASE 20
1.4 AIMS OF THESIS 23

2. MATERIALS AND METHODS 24

2.1 CELLS 24
2.1.1 PBMC SEPARATION, FREEZING AND THAWING 24
2.1.2 CELL SELECTION 24
2.2 FLOW CYTOMETRY 25
2.2.1 SURFACE STAINING 25
2.2.2 DEXTRAMER STAINING 25
2.2.3 INTRACELLULAR CYTOKINE STAINING (ICS) 25
2.2.4 TRANSCRIPTION FACTOR STAINING 26
2.2.5 DATA ACQUISITION AND ANALYSIS 26
2.2.6 CELL SORTING 26
2.3 CELL CULTURE 29
2.3.1 T CELL ACTIVATION 29
2.3.2 MAIT FUNCTIONALITY ASSAY 29
2.3.3 IL-12 AND IL-18 STIMULATION 29
2.4 CYTOMETRY BY TIME-OF-FLIGHT (CyTOF) 30
2.4.1 ANTIBODY LABELLING 30
2.4.2 STIMULATION AND STAINING 30
2.4.3 DATA ACQUISITION AND ANALYSIS 34
2.5 STATISTICAL ANALYSIS 34
2.6 MEDIA AND BUFFERS 34

3. SHARED PHENOTYPE OF CD161 EXPRESSING T CELLS 36

3.1 INTRODUCTION 36
3.2 AIMS 39
3.3 MATERIALS AND METHODS 40

3.3.1 Vβ TYPING BY FLOW CYTOMETRY 40
3.3.2 TCR SEQUENCING 40
3.3.3 CYTOF 41
3.3.4 MICROARRAYS 42

3.4 RESULTS 44

3.4.1 CD161++ CD8+ T CELLS ARE COMPOSED OF BOTH Vα7.2+ MAIT AND Vα7.2− CELLS 44
3.4.2 UNLIKE Vα7.2+ MAIT CELLS, THE Vα7.2− SUBSET IS POLYCLONAL 44
3.4.3 Vα7.2−CD161++ CD8+ T CELLS ARE NOT ACTIVATED IN AN MR1-DEPENDENT MANNER BUT, LIKE MAIT CELLS, RESPOND TO STIMULATION BY IL-12+IL-18 47
3.4.4 Vα7.2−CD161++ CD8+ T CELLS MIRROR THE Vα7.2+ MAIT CELL PHENOTYPE 49
3.4.5 ANALYSIS OF CD161-EXPRESSING CD8+ T CELLS BY CYTOF 51
3.4.6 THE PHENOTYPIC AND TRANSCRIPTIONAL PROFILE OF CD161+CD8+ T CELLS OVERLAPS WITH CD161++CD8+ T CELLS 53
3.4.7 CONSERVED TRANSCRIPTIONAL CHANGES IN CD161-EXPRESSING CD4+ AND TCRγδ+ T CELLS 58
3.4.8 A COMMON FUNCTIONAL CORRELATE OF CD161-EXPRESSION IN ALL T CELL SUBSETS 61
3.5 DISCUSSION 66
3.6 SUMMARY 69

4. CD161+ CD8+ T CELLS: PHENOTYPE AND FUNCTION 103

4.1 INTRODUCTION 103
4.2 AIMS 105
4.3 MATERIALS AND METHODS 106
4.3.1 STUDY SUBJECTS AND CELLS 106
4.3.2 QUANTITATIVE (Q)PCR 107
4.3.3 MRNA MICROARRAY 108
4.4 RESULTS 109
4.4.1 CD161 IS EXPRESSED BY A SUBSET OF ANTI-VIRAL CD8+ T CELLS 109
4.4.2. CD161 EXPRESSION ON CD8+ T CELLS IS LARGELY RESTRICTED TO MEMORY CELLS 111
4.4.3. MICROARRAY ANALYSIS OF CD161+ CD8+ T CELLS REVEALS A MAIT CELL-LIKE PROFILE 113
4.4.4. EXPRESSION OF FURTHER NK CELL RECEPTORS BY CD161+ CD8+ T CELLS 115
4.4.5. CD161+ CD8+ T CELLS ARE POTENT EFFECTOR CELLS 119
4.4.6. CD161+ CD8+ T CELLS ARE THE MAJOR CD161 POSITIVE CD8+ T CELL SUBSET IN THE GUT, BUT NOT THE LIVER 121
4.4.7. PHENOTYPE OF CD161+ CD8+ T CELLS IN PERIPHERAL BLOOD OF HEPATITIS C-INFECTED PATIENTS 126
4.4.8. ANALYSIS OF STIMULATED CD161+ CD8+ T CELLS BY MICROARRAY 131
4.5 DISCUSSION 135
4.6 SUMMARY 140

5. DEVELOPMENT OF CD161+ CD8+ T CELLS 171

5.1 INTRODUCTION 171
5.2 AIMS OF CHAPTER 173
5.3 MATERIALS AND METHODS 174
5.3.1 CELLS 174
5.3.2 Vβ TYPING AND CORRELATIONS 174
5.3.3 CD161− T CELL CULTURE 175
5.3.4 CMV T CELL LINES 175
5.4 RESULTS 176
5.4.1. CD161 IS EXPRESSED EARLY DURING DEVELOPMENT 176
5.4.2. CD161+CD8+ T CELLS DISPLAY A PRE-PROGRAMMED PHENOTYPE IN CORD BLOOD 178

5.4.3. Vβ TYPING OF CD161+ IN COMPARISON TO CD161– CD8+ T CELLS 180
5.4.4. CAN CD161– CD8+ T CELLS BE INDUCED TO EXPRESS CD161? 186
5.5 DISCUSSION 192
5.6 SUMMARY 195

6. MDR1 FUNCTION IN CD161 EXPRESSING CD8+ T CELLS 200

6.1 INTRODUCTION 200
6.1.1 MAIT CELLS AND CHEMOTHERAPY 200
6.1.2 MAIT CELLS AND TRANSPLANTATION 203
6.1.3 UNANSWERED QUESTIONS 203
6.2 AIMS 204
6.3 MATERIALS AND METHODS 205
6.3.1 MDR1 AND DEXTRAMER STAINING 205
6.3.2 EFFLUX ASSAY 205
6.3.3 CYTOTOXICITY ASSAY 205
6.3.4 PROLIFERATION ASSAY 206
6.3.5 MAIT CELL FUNCTIONAL ASSAY 206
6.4 RESULTS 207
6.4.1 MDR1 IS EXPRESSED AT ELEVATED LEVELS ON CD161++ AND CD161+ CD8+ T CELLS 207
6.4.2 CD161 POSITIVE CD8+ T CELLS EXPRESS FUNCTIONAL MDR1 207
6.4.3 MAIT CELLS ARE PROTECTED FROM CYTOTOXICITY DURING EXPOSURE TO DAUNORUBICIN 210
6.4.4 DO ANTI-VIRAL CD161+CD8+ T CELLS HAVE THE POTENTIAL TO PROVIDE PROTECTION AFTER ABLATIVE CHEMOTHERAPY? 213
6.4.5 MAIT CELLS ARE SUSCEPTIBLE TO, BUT REMAIN FUNCTIONAL AFTER, EXPOSURE TO IMMUNOSUPPRESSANTS 215
6.5 DISCUSSION 220
6.6 SUMMARY 224

7. DISCUSSION 227

7.1 T LYMPHOCYTES EXPRESSING CD161 SHARE COMMON FEATURES 228
7.1.1 UTILISING MULTI-DIMENSIONAL DATA 228
7.1.2 RESPONSE TO IL-12 AND IL-18 IS AN INNATE-LIKE CHARACTERISTIC OF ALL CD161 EXPRESSING T CELLS 229
7.1.3 FOCUS ON UPREGULATED, RATHER THAN DOWNREGULATED, GENES 230
7.1.4 CD161 AS A CO-STIMULATORY RECEPTOR; OVERCOMING THE TCR HYPORESPONSIVENESS OF INNATE-LIKE LYMPHOCYTES 230
7.1.5 TCR SIGNALLING AND SELECTION OF INNATE-LIKE LYMPHOCYTES 231
7.1.6 TRANSCRIPTIONAL CONTROL OF THE CD161 PHENOTYPE 233
7.2 CD161+CD8+ T CELLS 236
7.2.1 CD161+CD8+ T CELLS DISPLAY FEATURES OF INNATE-LIKE T LYMPHOCYTES 236
7.2.2 CD161+CD8+ T CELLS REFLECT FEATURES OF MAIT CELLS 236
7.3 CD161 AND DISEASE 239
7.3.1 CD161+CD8+ T CELLS AND TISSUE-SPECIFIC DISEASES 239
7.3.2 A COMMON PATHWAY OF ACTIVATION: PROTECTIVE OR PATHOGENIC? 240
7.3.3 CHALLENGES TO THERAPY POSED BY EXPRESSION OF MDR1 241
7.4 CONCLUDING REMARKS 242

REFERENCES 244

Thesis Contributions

Experiments and analyses presented in this thesis that were performed by persons others than myself are as follows:

Chapter 3

S. Björkander	24 month old PBMC experiments
V. Fleming	CD161+ vs – CD4+ T cell microarray
Y. Kang	CD161++, + and – CD8+ T cell microarray
A. Kurioka	IL12+18 stimulation data included
H. Lockstone	CD4 and CD8 microarray statistical analyses
E. Marchi	Microarray normalisations
E. Newell	CyTOF PCA analysis
N. Rajoriya	CD161+ vs – TCR$\gamma\delta$ T cell microarray
R. Simmons	collaboration on TCR sequencing
L. Swadling	collaboration on CyTOF experiments
C. Willberg	IL12+18 stimulation data included

Chapter 4

M. Hühn	gut lymphocyte phenotyping and analysis
L. Swadling	HCV vaccine patient phenotyping
J. Ussher	CD161+ vs – CD8+ microarray sample preparation
	liver lymphocyte phenotype

Chapter 5

J. Kumar	TCR repertoire correlation analysis
A. Kurioka	perforin and granzyme B cord blood stains
L. Walker	some Vβ staining data included
	cord blood vs. adult GSEA
C. Willberg	24 month old phenotyping

Many thanks to all who contributed to this thesis.

Abbreviations

ABC	ATP-binding cassette
αGalCer	alpha-branched galactosylceramide
AICD	activation induced cell death
AML	Acute Myeloid Leukaemia
APC	antigen presenting cell
ATP	adenosine triphosphate
BSA	bovine serum albumin
CD	Crohn's Disease
CDR	complementarity determining region
ChIP-Seq	chromatin immunoprecipitation sequencing
Clr	C-type lectin related
CMV	cytomegalovirus
CsA	cyclosporine A
CTL	cytotoxic T lymphocyte
CTV	CellTrace™ Violet
CyTOF	cytometry by time-of-flight
D	diversity
DC	dendritic cell
DN	double negative (CD4−CD8−)
E.coli	*Escherichia coli*
FACS	fluorescence activated cell sorting
FCS	foetal calf serum
FES	feature extraction software
FLU	influenza
FMO	fluorescence minus one
FSC	forward scatter
GEM	germline-encoded, mycolyl lipid-reactive T cells
geoMFI	geometric mean fluorescence intensity
GSEA	gene set enrichment analysis
GVHD	graft-versus-host disease
HBV	hepatitis B virus
HCV	hepatitis C virus
HIV	human immunodeficiency virus
HM-BPP	(E)-4-Hydroxy-3-methyl-but-2-enyl pyrophosphate
hr	hours
IBD	Inflammatory Bowel Disease
ICS	intracellular cytokine staining
IFN	interferon
IL	interleukin
iNKT	invariant natural killer T cell
Itk	IL-2-inducible T cell kinase
J	junctional
KIR	killer-cell immunoglobulin-like receptor
LLT1	lectin-like transcript 1
LTNPs	long term non-progressors
MAIT	mucosal associated invariant T cell
MDR1	multi drug resistance 1

MHC	major histocompatibility complex
MIC	MHC class I polypeptide-related sequence
min	minutes
MPA	mycophenolic acid
MS	Multiple Sclerosis
MVA	Modified Vaccinia Ankara
NES	normalised enrichment score
NK	natural killer
NKT	natural killer T cell
ns	not significant
nTreg	natural T regulatory cell
Ocil	osteoclast inhibitory lectin
PAMP	pathogen associated molecular pattern
PBMC	peripheral blood mononuclear cells
PBS	phosphate buffered saline
PCA	principal component analysis
PCR	polymerase chain reaction
PD1	programmed death 1
PHA	phytohemagglutinin
PLZF	promyelocytic leukaemia zinc finger protein
PMA	Phorbol 12-Myristate 13-Acetate
PRR	pattern recognition receptor
qRT-PCR	quantitative real-time PCR
R	receptor
RA	Rheumatoid Arthritis
RAG	recombination-activating gene
Rh123	rhodamine 123
ROR	RAR-related orphan receptor
SSC	side scatter
SEM	standard error of the mean
TAPI-2	TNF protease inhibitor 2
TB	Tuberculosis
TCR	T cell receptor
Th	T helper
TLR	Toll-like receptor
Treg	T regulatory cell
T_{CM}	central memory T cells
T_{EM}	effector memory T cells
T_{N}	naïve T cells
T_{RM}	resident memory T cells
T_{SM}	memory stem T cells
UCB	umbilical cord blood
unstim	unstimulated
V	variable
vsn	variance stabilising normalisation

Note: When referring to specific populations, the level of CD161 expression is indicated, ie. CD161– (no or little expression), CD161+ (intermediate expression) or CD161++ (high expression). The term ‘CD161 positive’ is used to refer to all cells that express CD161, regardless of the level of expression.

1. Introduction

1.1 Innate vs. Adaptive Immunity

The immune system fundamentally needs to achieve two objectives to protect against disease. Firstly, to quickly and efficiently react to an invading pathogen, and ultimately control that pathogen, and secondly to provide protection against re-invasion, 'remembering' how a pathogen was successfully controlled and replicating such a response. These characteristics are broadly conferred by the innate and adaptive arms of the immune system, respectively. The innate immune system is predominantly composed of a network of sentinels, cells such as neutrophils and macrophages with germline encoded receptors (pattern recognition receptors, PRRs) that broadly recognise structures associated with foreign pathogens (pathogen associated molecular patterns, PAMPs) or danger signals associated with tissue invasion (Matzinger, 1994). These cells are posted at or rapidly recruited to potential sites of invasion and both raise the alarm, through the release of cytokines and chemokines, and provide a first line of defence, through such destructive mechanisms as phagocytosis and the release of antimicrobial peptides. Additionally, a crucial role of the innate immune system is the activation of the adaptive arm of defence, through the presentation of antigenic peptides on Major Histocompatiblity Complex (MHC) molecules. The cells of the adaptive immune system, in contrast to those of the innate, express highly diverse, somatically-recombined receptors which specifically recognise the invading pathogen, and as a consequence of recognition undergo clonal expansion to produce an army of effectors; the B and T lymphocytes. This thesis is concerned with the role of T lymphocytes within the immune response.

1.1.2 T cell memory

T lymphocytes develop in the thymus, until they are released as mature T cells which circulate in the bloodstream, migrating through successive lymph nodes scanning antigen presenting cells (APCs) within for presentation of their cognate antigen (Mackay et al.,

1990). At this stage of differentiation, until they have encountered antigen, they are described as 'naïve'. Upon recognition of antigen, a specific T cell is activated to undergo clonal expansion and differentiation into 'effector' cells that perform specialised functions. Classically, these functions have been divided based upon co-receptor expression; CD8+ T cells differentiate into cytotoxic T lymphocytes (CTLs) with the ability to kill infected cells through the release of cytotoxic molecules such as perforin and granzymes, and CD4+ T cells differentiate into T helper (Th) cells of which there are several lineages, including Th1, Th2 and Th17. These lineages are defined based upon the predominant cytokines produced and their characteristic transcription factor expression, and are thought to differentially develop according to the specific cytokine milieu during antigen presentation. For example, the more recently identified Th17 lineage is characterised by production of Interleukin (IL)-17 and expression of the master transcription factor RAR-related Orphan Receptor (ROR)γt (Ivanov et al., 2006), and is thought to develop in the presence of IL-1β and IL-23 (Cosmi et al., 2008).

Following clonal expansion, and generally after removal of the invading microorganism, T lymphocytes undergo extensive contraction. Numbers of pathogen-reactive cells reduce rapidly, due to activation induced cell death (AICD) for example, before reaching a plateau, with a percentage of effector cells remaining (Zimmermann et al., 1996). This pool of long-lasting antigen-specific T cells form a defining attribute of the adaptive immune system, namely their ability to develop immunological memory. Memory is defined as the presence of lymphocytes after removal of antigenic stimulation (Lau et al., 1994; Murali-Krishna et al., 1999; Swain, 1999) together with the capacity to expand and differentiate rapidly upon secondary challenge (Lau et al., 1994; Veiga-Fernandes et al., 2000).

Human memory T cells can be identified by a switch in their expression of the CD45 isoform from CD45RA to CD45RO, yet with reversion to CD45RA possible (Michie et al., 1992). Further phenotypic analysis of human memory cells also revealed a dichotomous heterogeneity based upon expression of the lymph node-homing chemokine receptor CCR7 (Sallusto et al., 1999). Expression of CCR7 by 'central memory' T cells (T_{CM}), together with CD62L, enables them to home to the lymph node where they can proliferate

to initiate secondary responses. T_{CM} cells produce few cytokines except IL-2. On the other hand, CCR7– 'effector memory' T cells (T_{EM}) produce high levels of several cytokines, including IL-4 and Interferon (IFN)-γ and circulate through non-lymphoid tissues (Masopust et al., 2001). Characterisation based upon expression of both CD45RA and CCR7 divides T cells into three CD4+ subsets (CCR7+CD45RA+ naïve, CCR7+CD45RA– and CCR7–CD45RA– memory) and four CD8+ subsets (with an additional CCR7–CD45RA+) (Sallusto et al., 1999), with re-expression of CD45RA associated with terminal differentiation (Hamann et al., 1997).

Key questions regarding T cell memory include discerning the pathway of differentiation, whether linear (from naïve to T_{CM} to T_{EM}) or independent (Ahmed et al., 2009) (see Figure 1-1); the identification of 'memory precursors' (Kaech et al., 2002) - those cells which develop into memory cells; and the hunt for memory cells with stem-cell like qualities capable of repopulating memory pools (Fearon et al., 2001). While the differentiation pathway of memory T cells remains controversial, with evidence supporting both pathways (Kaech and Wherry, 2007), expression of the IL-7 receptor (IL-7R) (Kaech et al., 2003), together with downregulated expression of CD25 (Kalia et al., 2010) and KLRG1 (Sarkar et al., 2008), is thought to distinguish those effector CD8+ T cells which differentiate into memory cells, whether T_{CM} or T_{EM}. Furthermore, a putative human 'memory stem' cell population has recently been described, with the self-renewal capacity and multipotency of stem cells combined with the rapid effector function and gene expression profile of memory cells (Gattinoni et al., 2011).

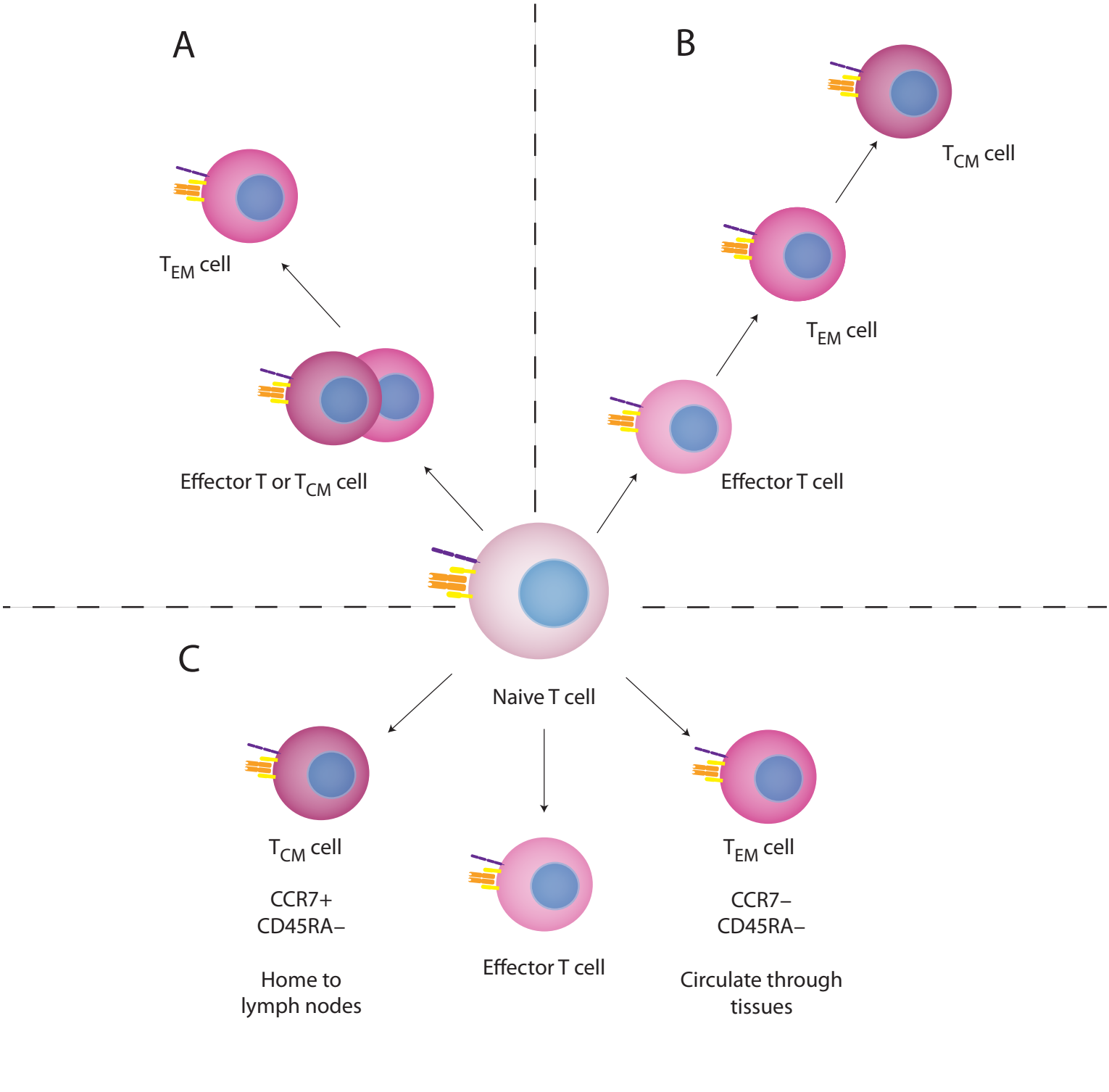

Figure 1-1: Proposed pathways of T cell memory differentiation. **A**) Linear pathway of differentiation by which central memory T cells (T_{CM}) provide a source of effector memory T cell (T_{EM}), with or without an effector T cell stage. **B**) Conversely, a linear differentiation pathway through an intial T_{EM} stage, which may subsequently convert to T_{CM} has also been proposed. **C**) Alternatively, the two memory subsets may be distinct and differentiate through independent pathways as either effector T cells, T_{CM} or T_{EM}.

1.1.3 Tissue-Resident Memory

In addition to the T cell memory subsets already described, a population of memory T cells which, unlike T_{EM}, do not recirculate have been identified in certain peripheral tissues, including the skin (Jiang et al., 2012), gut (Sathaliyawala et al., 2013) and lung (Turner et al., 2014). This population is stably maintained within the respective tissue, independently of their circulating counterparts, and have hence been described as 'tissue-resident memory' T cells (T_{RM}) (Shin and Iwasaki, 2013). Like innate immune cells, T_{RM} cells reside in tissues that form a barrier to invading pathogens and can proliferate *in situ* (Wakim et al., 2008), and these cells can provide anti-viral protection (Ariotti et al., 2014; Schenkel et al., 2014). Transcriptional studies have demonstrated CD8+ T_{RM} to be unique from circulating memory CD8+ T cells (Mackay et al., 2013; Wakim et al., 2012), yet few markers of T_{RM} have been identified to date. However, expression of CD103 (integrin αE), which is expressed on memory CD8+ T cells within many tissues yet low on circulating T cells (Sathaliyawala et al., 2013), identifies T_{RM} within human mucosal tissues such as gut and lung (Sathaliyawala et al., 2013), and has hence been used as a marker of T_{RM} cells. CD103 binds E-cadherin, a molecule expressed on epithelial cells (Cepek et al., 1994), and therefore may function to retain T_{RM} cells within peripheral tissues. It should be noted, though, that CD103 has also been described as a marker of regulatory T cells, of both CD4+ (Lehmann et al., 2002) and CD8+ (Uss et al., 2006) subtype, and therefore it is the combination of CD103 expression together with their stable tissue localization which identifies T_{RM} cells. Although the differentiation pathway of this unique T_{RM} population is largely unknown, it is clear that the specific tissue microenvironment plays an important role (Masopust et al., 2006a).

1.2 Innate-like lymphocytes: bridging innate and adaptive immunity

The division of leukocytes as either innate or adaptive, a paradigm of immunology, has existed from the times of Ehrlich and Metchnikoff. More recently, however, non-conventional T cells that display features of both innate and adaptive immunity have been identified – termed 'innate-like lymphocytes'. Like innate cells these lymphocytes demonstrate rapid effector function upon stimulation, yet express a somatically recombined T cell receptor (TCR), characteristic of adaptive lymphocytes. Yet, unlike conventional T cells, innate-like lymphocytes display a restricted TCR repertoire, often with conserved Variable (V)-Junctional (J) combinations and chain pairings, suggestive of recognition of a limited number of conserved antigens (see Table 1-1).

1.2.1 TCRγδ+ T cells

Perhaps the first innate-like T lymphocytes to be described were the TCRγδ+ population, discovered upon the chance isolation of the γ chain by Saito et al. (1984). Unlike conventional T cells, which express a TCR composed of α and β chains, this population expresses a TCR encoded by the γ and δ loci (with δ located within the α locus) (Hayday, 2000). Although formed by V(D)J recombination, this population displays narrow TCR diversity, constrained by the limited number of germline-encoded genes (although displaying high junctional diversity), and restricted chain pairing, such as that of Vγ9 with Vδ2. Vγ9Vδ2 T cells form the predominant population of TCRγδ+ cells in the human circulation (Triebel and Hercend, 1989), where TCRγδ+ T cells represent 2-10% of T cells (Rajoriya et al., 2014). The other major subset in humans is the Vδ1+ subset which homes to epithelial tissues such as the liver, gut and skin (Bonneville et al., 2010), reflecting the tissue-homing feature of innate-like lymphocytes. Although this subset does not display biased γ chain pairing (Casorati et al., 1989), TCRs within tissues display a high degree of uniformity due to clonal expansion (Chowers et al., 1994; Holtmeier et al., 2001).

	TCRγδ		iNKT	MAIT
Characteristic of Innate-like lymphocytes	**Vγ9Vδ2**	**Vδ1**		
Restricted TCR repertoire	Vγ9 pairs with Vδ2	No Vγ bias, clonal expansion reduces diversity within tissues	Vα24-Jα18	Vα7.2-Jα33/12/20
	Limited germline encoded elements		Vβ11	Vβ2 and Vβ13.2 bias
Non-polymorphic antigen presenting molecules	Butyrophilin 3A1	eg. CD1c	CD1d	MR1
Conserved ligands, examples	Phosphoantigens	MIC-A, MIC-B	glycosphingolipids, aGalCer	5-OE-RU, 5-OP-RU
Rapid effector function	High cytotoxicity	Lower cytotoxicity	Cytotoxicity	Cytotoxicity
	High levels of IFNγ and TNFα	Broad range of cytokines including IL-4 and IL-17	Production of IFNγ and IL-4	IFNγ, IL17
Tissue homing	Circulating, and recruited to tissues	Home to epithelial tissues	Liver, Spleen	Liver, Mucosal tissues
Expression of PLZF	Eidson *et al.* 2011		Savage *et al.* 2008	Savage *et al.* 2008

Table 1-1: Characteristics of innate-like lymphocytes.

The γδ TCR functions much like a PRR, recognising conserved molecules produced by infected or transformed cells. For example Vγ9Vδ2 cells respond to non-peptide phosphoantigens, such as (E)-4-Hydroxy-3-methyl-but-2-enyl pyrophosphate (HM-BPP), produced by certain bacteria during isoprenoid biosynthesis (Hintz et al., 2001; Tanaka et al., 1995). This molecule is presented by Butyrophilin 3A1, a ubiquitously expressed and non-polymorphic antigen presenting molecule (Vavassori et al., 2013). Vδ1+ T cells have also been described to respond to self-antigens presented by the MHC class I-like, non-polymorphic molecule CD1c (Spada et al., 2000), which also presents lipids to T cells (Beckman et al., 1996). Vδ1+ T cells can also respond to cell stress-induced molecules such as MHC class I polypeptide-related sequence (MIC)-A and –B through both the TCR and the Natural Killer (NK) receptor NKG2D (Xu et al., 2011).

TCRγδ+ T cells display a pre-activated phenotype associated with the expression of memory markers (Parker et al., 1990), a feature shared with other innate-like T lymphocytes, and rendering them able to exert rapid effector functions – a defining attribute of innate immunity. These effector functions include the production of various cytokines (Morita et al., 1991), in addition to cytotoxicity conferred by expression of such molecules as granzyme B, CD95 (Fas) (Qin et al., 2009) and granulysin (Dieli et al., 2001). While cytotoxicity is conventionally associated with T cells bearing the CD8 co-receptor (CTLs), TCRγδ+ T cells are largely negative for both CD4 and CD8 co-receptors, although CD4+ and CD8+ TCRγδ+ T cells do exist (Morita et al., 1991).

1.2.2 Invariant Natural Killer T (iNKT) cells

A seminal study of the TCR expression of all double-negative (DN) human T lymphocytes by Porcelli et al. (1993), identified an invariant alpha chain rearrangement of Vα24-Jα18, also found in CD4+ T cells. Subsequent identification of murine thymocytes with a similar TCR bias and which expressed the NK cell marker NK1.1 (Arase et al., 1992), or the equivalent CD161 (NKRP1A) in humans (Exley et al., 1997), led to the christening of this population as invariant NK T (iNKT) cells. The restricted TCR repertoire of this population across donors indicated evolution towards recognition of a limited number of antigens, likely presented by a non-polymorphic antigen-presenting molecule. Indeed, NKT cells

recognise the MHC class I-like molecule, CD1d (Bendelac et al., 1995; Exley et al., 1997) which presents lipid antigens, such as glycosphingolipids from the cell wall of *Sphingomonas* or the surrogate marine sponge ligand alpha-branched galactosylceramide (or αGalCer) (Bendelac et al., 2007). Other members of the CD1 family also present lipid antigens to further unconventional T cells, including germline-encoded, mycolyl lipid-reactive (GEM) T cells recognising CD1b (Van Rhijn et al., 2013) and those recognising CD1a (de Jong et al., 2014) and CD1c, as mentioned above. Interestingly, T cells with diverse TCR expression yet restricted by these same antigen-presenting molecule:ligand complexes have also been described (Gadola et al., 2002; Van Rhijn et al., 2013).

Invariant CD1d-restricted NKT cells are characterised by an intrinsic activated, memory phenotype (Loh et al., 2014; Park et al., 2000), and their ability to produce large amounts of IL-4 in addition to IFNγ (Yoshimoto and Paul, 1994). Central to this phenotype is expression of the transcription factor Promyelocytic leukaemia zinc finger protein (PLZF), encoded by *ZBTB16*, with PLZF-deficient NKT cells displaying a naïve phenotype, reduced expression of NK markers and altered cytokine secretion patterns (Eidson et al., 2011; Kovalovsky et al., 2008; Savage et al., 2008). PLZF is also highly expressed by a further member of the innate-like lymphocyte family; Mucosal Associated Invariant T (MAIT) cells (Savage et al., 2008).

1.2.3 Mucosal Associated Invariant T (MAIT) cells

In addition to the invariant alpha chain of iNKT cells, Porcelli *et al.* (1993) identified a further invariant Vα7.2-Jα33 rearrangement amongst DN T lymphocytes, and subsequently described amongst CD8+ T cells (Tilloy et al., 1999). In fact, this Vα7.2+ population predominantly expresses the CD8 co-receptor, with only about 10% being DN (Walker et al., 2012), and displays semi-invariant Vβ usage with preferential use of Vβ2 and Vβ13.2 (Tilloy et al., 1999; Walker et al., 2012). TCR sequencing has also revealed that a minority of MAIT cells may express Vα7.2 combined with further J regions, including Jα12 and 20 (Reantragoon et al., 2013). Expression of the gut-homing integrin α4β7 and enrichment of Vα7.2-Jα33 transcripts within gut biopsies led to this population being descried as “mucosal-associated” invariant T cells (MAIT; Treiner et al. 2003), yet further

tissue sampling demonstrated more prominent enrichment of MAIT cells within the liver (Dusseaux et al., 2011). This population of invariant T cells was found to be restricted by a non-MHC class I or II, or CD1 molecule (Tilloy et al., 1999), later identified as the MHC class Ib molecule, MR1 (Treiner et al., 2003), ubiquitously transcribed across tissue and cell types (Riegert et al., 1998). Like CD1d, MR1 is highly conserved, displaying inter-species cross-reactivity (Huang et al., 2009) despite the relative absence of a MAIT cell equivalent in conventional lab mouse strains (Tilloy et al., 1999). While the ligand for this antigen presenting molecule remained enigmatic, MAIT cells were demonstrated to display potent antibacterial activity, being activated by a range of bacteria, but not viruses (Gold et al., 2010; Le Bourhis et al., 2010). This pointed to a ligand found in numerous strains of bacteria, identified by the McCluskey lab as a vitamin metabolite originating from the bacterial riboflavin biosynthetic pathway (Corbett et al., 2014; Kjer-Nielsen et al., 2012).

MAIT cells display many similarities to iNKT cells, including a restricted V beta repertoire (predominantly Vβ2 and Vβ13.2; Tilloy et al. 1999; Walker et al. 2012), memory phenotype (uniformly T_{EM}) and tissue location (Dusseaux et al., 2011). In addition, both iNKT (De Santo et al., 2010) and MAIT cells (Davey et al., 2014) modify the activity of innate cells such as neutrophils, and hence display immunomodulatory function. However, in humans MAIT cells are approximately 100-fold more abundant than iNKT cells within peripheral lymphocytes (Gapin, 2009). In addition to their memory phenotype, MAIT cells can be identified by high expression of IL18 receptor (IL18R), the drug efflux pump multi-drug resistance (MDR)1, and high levels of the homodimeric C-type lectin CD161 (Dusseaux et al., 2011).

1.3 CD161

CD161, originally a marker of NK cells (Lanier et al., 1994; Yokoyama and Seaman, 1993), marks both NKT cells (Exley et al., 1997) and MAIT cells (Martin et al., 2009). However, CD161 expression is not unique to these T cell subsets. Lanier et al. (1994) originally identified expression on both CD4+ and CD8+ T cells, with a higher surface density on the latter. Further analysis has identified two CD161 positive CD8+ populations (Billerbeck et al., 2010; Takahashi et al., 2006), with intermediate (CD161+) or high (CD161++) expression levels, and one CD4+ T cell population expressing intermediate levels of CD161 only (CD161+; Takahashi et al. 2006; Kang et al. 2012). The adult CD161++CD8+ T cell subset is predominantly composed of Vα7.2+ MAIT cells (Ussher et al., 2014; Walker et al., 2012), however the functional relationship between the two populations of CD161 positive CD8+ T cells, and the significance of a CD161++ population within CD8+ T cells which appears to be largely absent from the CD4+ population, is yet to be fully defined. A minor fraction of MAIT cells express CD4 (Reantragoon et al., 2013), however, suggestive of a previously unappreciated CD161++CD4+ population. Moreover, CD161 expression is not restricted to TCRαβ-expressing T cells, but is detected on TCRγδ+ T cells also (Maggi et al., 2010; Rajoriya et al., 2014)

1.3.1 CD161 and a type 17 phenotype

The identity of these CD161-expressing T cell subsets remained elusive until mRNA microarray analysis identified CD161 to be significantly upregulated in Th17 clones compared to those of Th1 and Th2 (Cosmi et al., 2008). This helper cell subset is named according to their secretion of IL-17, which is related to their specific expression of RORγt (Ivanov et al., 2006). Type 17 cells can also be identified by expression of the IL-23 receptor (IL-23R) and CCR6 (see Figure 1-2; Annunziato et al. 2007). In peripheral blood, CD161+CD4+ T cells express RORγt, IL23R and CCR6, and thus phenotypically overlap with Th17 cells. Further, IL-17 secreting CD4+ T cells were contained within the CD161+ fraction (Cosmi et al., 2008). As a result, Maggi *et al.* (2010) investigated CD161 expression on other T cells capable of producing IL-17. In all T cell subsets the ability to

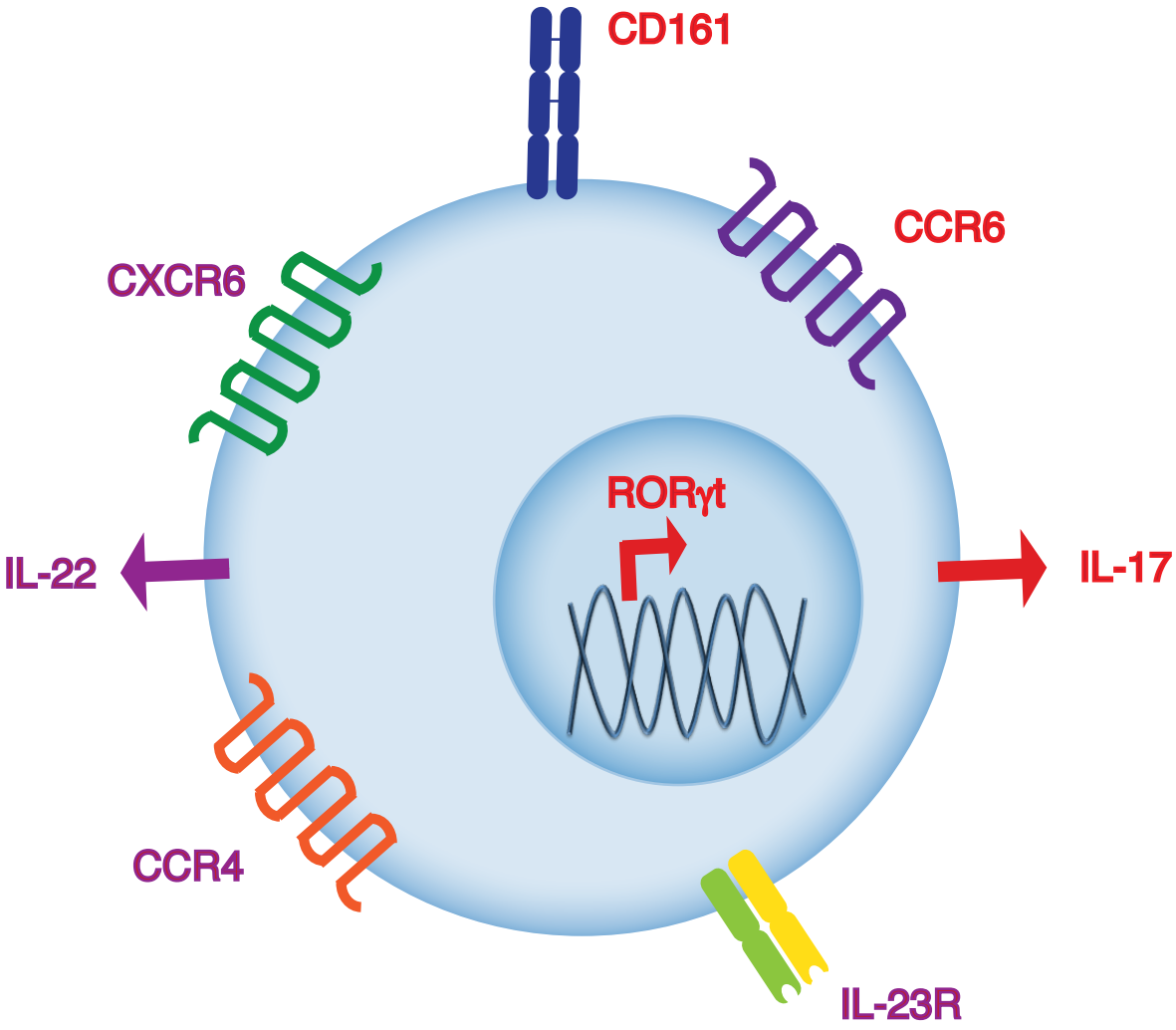

Figure 1-2: Characteristics of a type 17 phenotype. The figure shows the phenotypic attributes of type 17 cells, based on the prototypical T helper (Th) 17 cells. Those specific to Th17 cells are shown in red, while those characteristic of Th17 cells but shared with other cell types are shown in purple. These include a variety of chemokine receptors, cytokine receptors, cytokines and the type 17 transcription factor RORγt.

secrete IL-17 was virtually restricted to those cells expressing CD161, and this was related to their expression of the Th17 transcription factor RORγt. This is true even of CD4+ T regulatory (Treg) cells, with a pro-inflammatory yet suppressive subset capable of secreting IL-17 recently identified, and marked by expression of CD161 (Pesenacker et al., 2013). Furthermore, although Th17 cells display plasticity of phenotype, converting to a more Th1-like or intermediate phenotype under certain inflammatory conditions, they retain expression of CD161 (Nistala et al., 2010), indicating CD161 as a stable marker of type 17 lineage and origin. MAIT cells reflect many of the characteristics of Th17 cells, including upregulated expression of RORγt, CCR6, and secretion of IL-17 (Billerbeck et al., 2010; Dusseaux et al., 2011). Amongst CD8+ T cells, IL-17 secretion was restricted to this CD161++ subset (Billerbeck et al., 2010).

1.3.2 CD161 and memory phenotype

Interestingly, CD161 positive T cells of all lineages display a memory phenotype. This may suggest that CD161 expression is acquired as a result of immune stimulation, and may itself be a memory marker. However, memory CD161– T cells do exist, and do not alter in CD161 expression with anti-CD3/2/28 stimulation or specific peptide re-stimulation (Northfield et al., 2008), implying that CD161 is not simply a marker of activation. Furthermore, CD161 is expressed by a subset of T cells in the foetal liver and on a minor population of CD3+ thymocytes (Lanier et al., 1994; Martin et al., 2009). Both CD161+CD4+ (Cosmi et al., 2008) and CD161++CD8+ (Billerbeck et al., 2010; Martin et al., 2009; Walker et al., 2012) T cells have also been isolated from umbilical cord blood (UCB), where they display a naïve phenotype. These CD161 positive naïve cells appear to represent the precursors of their adult Th17 and MAIT counterparts. When cultured in the presence of Th17-polarizing cytokines, IL-17 production was restricted to the CD161-expressing fractions of these naïve cells, including CD4+, CD8+ and DN subsets (Maggi et al., 2010). These CD161 positive cells, though naïve, are pre-programmed to a type 17 phenotype, already expressing CCR6, IL18R and IL23R, amongst other markers (Cosmi et al., 2008; Walker et al., 2012).

What induces the maturation of these precursor cells to display a memory phenotype, or indeed to express CD161, is not yet known. Naïve CD161−CD4+ T cells transduced with RORγt upregulated CD161, while inhibition of RORγt inhibited CD161 expression in Th17 clones (Maggi et al., 2010), suggesting a role for this Th17 transcription factor in CD161 expression. Yet, the transcription factor PLZF may also be important, with a loss of CD161 expression evident in PLZF deficient iNKT (Eidson et al., 2011; Kovalovsky et al., 2008) and CD8+ T cells (Eidson et al., 2011). PLZF also appears important in the constitutive memory phenotype of these cells; knockout of PLZF results in the development of iNKT cells with a naïve phenotype (Kovalovsky et al., 2008; Savage et al., 2008) and transgenic MAIT cells in mouse models which lack PLZF also display a naïve phenotype (Martin et al., 2009).

1.3.3 CD161 in mouse models

CD161 (NKRP1A) represents the single orthologue of the family of *Nkrp1* genes in rodents. Seven murine *Nkrp1* genes have thus far been identified, termed *Nkrp1a-g* (with *Nkrp1e* and *Nkrp1g* thought to be a pseudogene; (Plougastel et al., 2001b)). In C57BL/6 mice, NKR-P1C carries the NK cell antigenic marker NK1.1 (Glimcher et al., 1977; Koo and Peppard, 1984) and also marks murine NKT cells (Koo and Peppard, 1984; Macdonald, 1995). This NKRP1 receptor may also be expressed during activation of CD8+ T cells (Aust et al., 2009). NKRP1 receptors recognize non-MHC ligands of the C-type lectin related (Clr) family, encoded by genes interspersed within the *Nkrp1* genes themselves (Plougastel et al. 2001; Iizuka et al. 2003; see Figure 1-3). Like other NK cell receptors, *Nkrp1* gene products can be classified as either activating or inhibitory. NKRP1A, C and F contain charged residues within their transmembrane domains, and are therefore considered to be activating receptors, inducing NK cytolytic activity, while NKRP1B and NKRP1D lack charged transmembrane residues and deliver inhibitory signals when crosslinked (Aust et al., 2009). NKRP1B and D appear to be closely related inhibitory molecules, expressed in BALB/c and C57BL/6 mice, respectively, with the *Nkrp1d* gene of C57BL/6 mice suggested to represent a divergent allele of the *Nkrp1b* gene of other strains (Carlyle et al., 2004). Both NKRP1B and D bind the Clr-b protein osteoclast inhibitory lectin (Ocil; Carlyle et al. 2004).

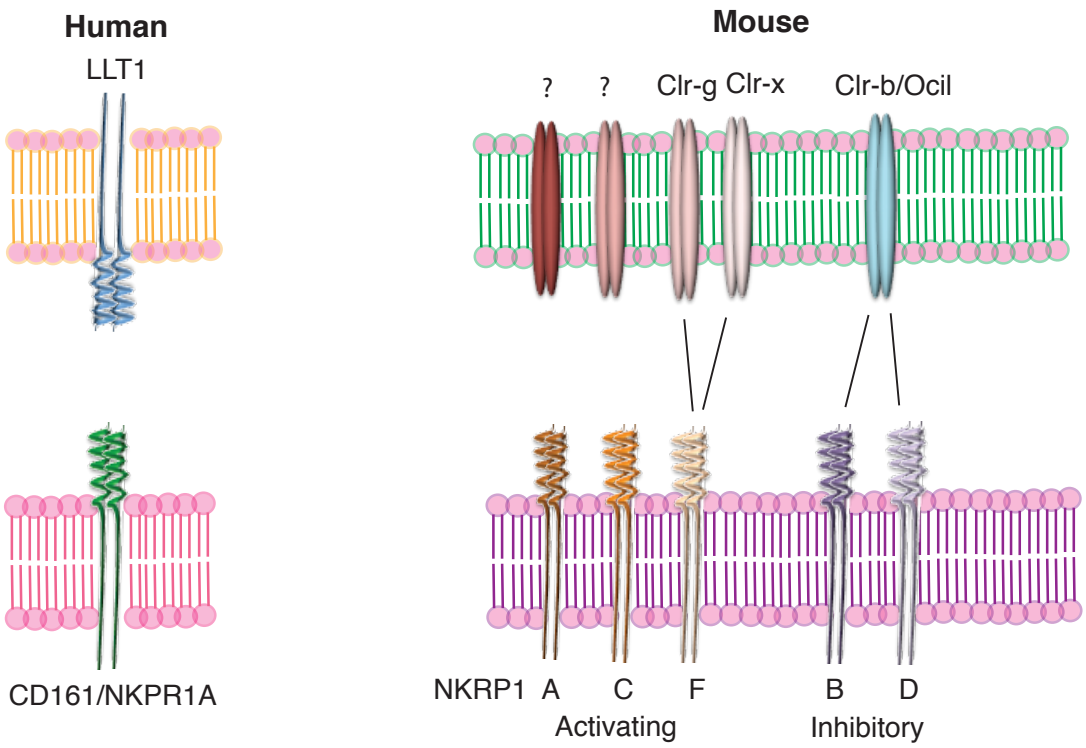

Figure 1-3: Human and Murine NKPR1 molecules and ligands. The single human NKPR1A protein, CD161, binds to LLT1 - the orthologue of Clr-b. The mouse NKRP1 family consists of 5 known proteins: NKPR1A, B and C induce activating signals, while NKPR1B and D are inhibitory. The ligands of NKPR1A and C in the mouse are not yet known, while NKPR1F binds both Clr-g and Clr-x gene products. NKPR1B and D both bind Clr-b (Ocil).

1.3.4 Lectin-Like Transcript 1 (LLT1): the ligand for CD161

The human orthologue of the Clr-b protein Ocil, also known as lectin-like transcript 1 (LLT1), was simultaneously identified by two groups as a ligand for CD161 in humans (Aldemir et al. 2005; Rosen et al. 2005; see Figure 1-3). This interaction is therefore conserved between mouse and man, and suggests that NKRP1B and D represent the closest relations to human CD161. However, unlike its murine counterpart, which has an MHC class I-type pattern of expression (Carlyle et al., 2004), expression of LLT1 appears to be restricted to certain cell types, particularly activated APCs including B cells, plasmacytoid dendritic cells (DCs) and monocyte-derived DCs (Rosen et al., 2008) and also described on NK and T cells (Boles et al., 1999). LLT1, like CD161, is encoded within the NK gene complex of chromosome 12 and is a type II transmembrane receptor (Boles et al., 1999), with signalling upon ligation being bi-directional (Mathew et al., 2004).

1.3.5 The Function of CD161

Identification of LLT1 as the ligand for CD161 has greatly aided the study of the function of this molecule. Despite CD161 transcripts and proteins being identical between NK and T cells, ligation by LLT1 has been described to have opposing effects in these subsets. Crosslinking CD161 inhibited NK cell degranulation (Rosen et al., 2008) and cytotoxicity of CD161+ NK cells was reduced towards LLT1 expressing targets (Aldemir et al., 2005; Poggi et al., 1998; Rosen et al., 2005). Furthermore, IFNγ production by NK cells was also inhibited by LLT1:CD161 ligation, while crosslinking of CD161 enhanced IFNγ production by anti-CD3 activated T cells (Aldemir et al., 2005). Crosslinking of CD161 alone had no effect. A costimulatory role for CD161 has also been described for CD1d-restricted iNKT cells (Exley et al., 1998). Here, crosslinking of CD161 enhanced both IFNγ and IL-4 production by anti-CD3 activated iNKT cells and also enhanced proliferation, while again CD161 alone had no effect. In this case, crosslinking of CD161 also had no effect on CD1d-specific cytolytic activity. This co-stimulatory function has been linked to activation of acid sphingomyelinase, an enzyme involved in the production of the secondary messenger ceramide, capable of activating various cellular signalling

pathways (Pozo et al., 2006). Activation of this enzyme by CD161 ligation is also thought to be involved in the generation of Th17 cells (Bai et al., 2014).

1.3.6 CD161 and Tissue Homing

A role for CD161 has also been suggested in transendothelial migration. In addition to an association with high expression of β1 and β2 integrins (Poggi et al., 1997), both CD161+ CD4+ (Poggi et al., 1997) and CD161+ TCRγδ (Poggi et al., 1999a) T cells migrated more efficiently than their CD161– counterparts. This was inhibited by addition of an anti-CD161 crosslinking antibody. Interestingly, migration occurred without chemotactic stimuli, which may be indicative of a preference of these cells to home to specific tissues. Indeed, both CD4+ and CD8+ CD161 positive T cells make up more than half of T cells in the healthy human intestine (O'Keeffe et al., 2004) and CD161 positive CD8+ T cells appear to home to the liver (Ishihara et al., 1999). MAIT cells specifically comprise a major population in the liver (Dusseaux et al., 2011), and to a lesser extent in mucosal tissues such as the gut and lung (Treiner et al., 2003).

1.3.7 CD161 and Disease

This tissue distribution implicates CD161 positive cells in a range of tissue-specific diseases, in either control or pathogenesis. For example, presence within the lung, together with anti-bacterial reactivity, suggests a role for MAIT cells in pulmonary infections such as tuberculosis (TB). A lower proportion of circulating MAIT cells was detected in patients with active TB infection compared to those with latent infection (Gold et al., 2010), and MR1 knockout mice displayed a higher bacterial load in the lung at early timepoints following *Mycobaceterium bovis* BCG infection than wildtype mice (Chua et al., 2012). MAIT cells display reactivity against a range of bacteria *in vitro*, and provide protection against infection with these bacteria *in vivo* (Georgel et al., 2011; Le Bourhis et al., 2010; Meierovics et al., 2013). In addition, MAIT cells are also involved in viral disease, with MAIT cells specifically depleted in the circulation and colon of Human Immunodeficiency Virus (HIV)-infected patients (Cosgrove et al., 2013; Greathead et al., 2014; Leeansyah et al., 2013; Wong et al., 2013). Their potential to respond to viruses is

also implied by their ability to mount TCR-independent responses to cytokines (Ussher et al., 2014). Moreover, they are not simply connected to infectious disease. Infiltration of MAIT cells has been detected in tumour tissue (Peterfalvi et al., 2008), which may prove particularly important given the demonstration that MAIT cells are resistant to chemotherapy through expression of the drug efflux pump MDR1 (Dusseaux et al., 2011; Turtle et al., 2009). MAIT cells have also been detected in brain lesions of Multiple Sclerosis (MS) patients (Annibali et al., 2011; Illes et al., 2004), where they have been suggested to play an immunoregulatory role (Croxford et al., 2006; Miyazaki et al., 2011). While long thought a Th1-driven disease, Th17 cells, which express CD161, are now also regarded as pathological in MS (Goverman, 2009) and CD161+ TCR$\gamma\delta$+ T cells were significantly expanded in the peripheral blood of MS patients (Poggi et al., 1999a). Indeed, polymorphisms in CD161 itself have been implicated in MS, presented by the International Multiple Sclerosis Genetics Consortium as one of the non-MHC candidate risk loci (The International Multiple Sclerosis Genetics Consortium, 2007).

The presence of CD161 positive T cells, including both CD4+ and CD8+ subsets, in the healthy intestine (O'Keeffe et al., 2004) also suggests a role for these cells in immune regulation in the gut, and therefore in inflammatory conditions of the bowel (inflammatory bowel disease: IBD), such as Crohn's Disease (CD). MAIT cells were enriched in inflamed bowel tissue, in comparison to healthy tissue, concomitant with a reduction of MAIT cells in the peripheral blood (Serriari et al., 2014). These MAIT cells also produced more IL-17 than in healthy donors. This is reflected in CD4+ T cells, with increased production of IL-17 in CD161+CD4+ T cells in the blood of CD patients, and gut sections from these patients showing a 20-fold increase in CD161+CD4+ T cells compared with control specimens (Kleinschek et al., 2009).

However, CD161++ MAIT cells are more prominently located within the healthy liver (Dusseaux et al., 2011), and are further enriched in chronic Hepatitis C virus (HCV) infection (Billerbeck et al., 2010). CD161+CD4+ T cells are also enriched in the liver during chronic HCV infection, composing the predominant hepatic CD4+ T cell population (Kang et al., 2012). Furthermore, CD8+ T cells specific for both HCV and Hepatitis B virus (HBV) are enriched in expression of CD161, compared to those specific for

cytomegolvirus (CMV) or influenza (FLU) (Northfield et al., 2008). As MAIT cells are unable to recognise viral peptides in the context of MHC class I, as determined by tetramer staining (Dusseaux et al., 2011), this is likely reflective of an enrichment in CD161+CD8+ T cells. However, the phenotype and function of this population has not yet been investigated.

It is clear, therefore, that CD161 positive T cells of different lineages are implicated in a variety of diseases, including both infectious and non-infectious. Yet without a full description of the functional differences of CD161 expressing T cells compared to those which lack CD161, their role within disease can only be implied. Further, the significance of shared expression of CD161, expressed early, across these T cell subsets is not yet known. Expression of CD161 may identify cells with a common phenotype and function, such as has been shown for IL-17 secretion (Maggi et al., 2010), and which may prove important in the disease setting.

1.4 Aims of Thesis

1. Undertake a direct comparison of CD161 positive T cells to identify common features in addition to shared expression of CD161
2. Determine the phenotype and function of the CD161+CD8+ T cell population, firstly in health and subsequently in disease
3. Investigate the origin of CD161+CD8+ T cells – are they, like MAIT cells, apparent from birth?
4. Investigate the role of MAIT cells in disease settings where MDR1-associated drug efflux may provide resistance to treatment

2. Materials and Methods

2.1 Cells

Peripheral blood mononuclear cells (PBMC) were obtained from adults (whole blood leukocyte cones, NHS Blood and Transplant, UK), 24 month olds (prospective birth cohort (Saghafian-Hedengren et al., 2010)) and umbilical cord blood (UCB) samples (Stem Cell Services, NHS Blood and Transplant, UK). Details of further study subjects used for individual experiments are detailed in the methods section of the relevant chapter.

THP1 cells (ECACC, UK) were maintained at 2 x10^5 cell/ml in THP1 culture medium (see 2.6).

2.1.1 PBMC separation, freezing and thawing

Whole blood, diluted with Phosphate Buffered Saline (PBS), was layered over Lymophoprep separation medium (Axis Shield Diagnostics) and centrifuged at 2200rpm for 22min at room temperature. Following this, the PBMC layer was removed by Pasteur pipette and washed twice at 1700rpm for 7min and 1500rpm for 5min, respectively, in R10 (see 2.6). Cells were counted by Trypan Blue (Sigma) exclusion, and aliquoted in freezing mix (see 2.6) for freezing in liquid nitrogen. Aliquots were stored until required, whereupon vials were partially thawed in a 37°C water bath and the contents transferred to a 50ml falcon. 10mls of R10 was then added dropwise at intervals, and then topped up to 50ml and centrifuged at 1500rpm for 5min. Cells were re-washed and resuspended in R10.

2.1.2 Cell selection

CD8+ T cells were isolated from PBMC using CD8 microbeads (Miltenyi Biotec) and MS or LS MACS columns (Miltenyi Biotec), as determined by cell number, following the manufacturer's instructions. Purity was consistently >90%.

Naïve and memory T cells were isolated using the negative and positive fractions, respectively, from the naïve pan T cell isolation kit (Miltenyi Biotec), following the kit's protocol.

2.2 Flow cytometry

2.2.1 Surface staining

Cells were washed and resuspended in PBS and fluorochrome-conjugated antibodies added at the optimal dilution (Table 2-1). Cells were incubated at 4°C for 20min before being washed in PBS and fixed in 2% formaldehyde (Sigma) for at least 20min at room temperature. After fixation, cells were washed and resuspended in PBS for flow cytometric analysis.

2.2.2 Dextramer staining

For staining of anti-viral responses, MHC class I dextramers presenting NLVPMVATV (CMV), GLCTLVAML (EBV) or GILGFVFTL (FLU) (Immudex) were added at 1:10 dilution for 10mins at room temperature, in the dark. Following this incubation, surface antibodies were added as above. Fixation was performed with methanol-free 2% paraformaldehyde (Sigma).

2.2.3 Intracellular cytokine staining (ICS)

Following fixation as above, cells were washed with PBS, followed by 1X permeabilsation buffer (eBioscience) and then incubated with antibodies at the optimal dilution (Table 2-1) in 1X permeabilisation buffer for 30min at room temperature. Cells were then washed in PBS and resuspended for flow cytometry analysis.

2.2.4 Transcription factor staining

For nuclear stainings such as for transcription factors, cells were stained with the Foxp3/Transcription Factor Staining Buffer Set (eBioscience). Briefly, after surface staining, cells were wash and incubated with Fixation/Permeabilisation working solution for 30-60min at room temperature. After washing twice in this buffer, cells were then resuspended in 1X permeabilisation buffer containing antibodies targeting intracellular and nuclear proteins and incubated for >30min at room temperature. Cells were subsequently washed and resuspended in PBS.

2.2.5 Data acquisition and analysis

Data were acquired on a MacsQuant (Miltenyi Biotec) or LSRII (BD Bioscience) and analysed using FlowJo software (Treestar, Inc.). Gating strategies generally followed that shown in Figure 2-1. Expression of various markers was determined according to the corresponding fluorescence minus one (FMO) sample or isotype control.

2.2.6 Cell sorting

CD8+ T cells were enriched from PBMC, modifying the ratio of MACS buffer to CD8 MicroBeads to 40:10 per 10^7 cells. Enriched CD8+ T cells were washed and resuspended in PBS and surface stained in 100μl, scaling up the antibody concentrations accordingly. After washing and resuspension in PBS, specific cell subsets were sorted on a MoFlo Legacy or MoFlo XDP (Beckman Coulter).

Marker	Fluorochrome	Clone	Company	Dilution
Annexin V	FITC	n/a	Miltenyi Biotec	1:20
Caspase 3	PE	CCP32	BD Bioscience	1:5
CCR6	PerCPCy5.5	11A9	BD Bioscience	1:25
CCR7	PE	3D12	eBioscience	1:100
	PerCPCy5.5	G043H7	BioLegend	1:100
CD103	FITC	Ber-ACT8	BD Bioscience	1:50
CD14	APCCy7	HCD14	BioLegend	1:100
CD158a/h-biotin	Streptavidin-PO	11PB6	Miltenyi Biotec	1:3.3
CD158b	FITC	CH-L	BD Bioscience	1:50
CD158e1/e2	APC	Z27.3.7	Beckman Coulter	1:25
CD16	FITC	eBioCB16	eBioscience	1:100
	PECy7	3G8	BioLegend	1:100
CD160	Alexa647	BY55	BioLegend	1:50
CD161	APC	191b8	Miltenyi Biotec	1:100
	BV421	HP-3G10	BioLegend	1:100
	PE	191b8	Miltenyi Biotec	1:100
CD244	PerCPCy5.5	C1.7	BioLegend	1:5
CD3	APC	OKT3	eBioscience	1:50
	APCCy7	HIT3a	BioLegend	1:100
	eFluor450	UCHT1	eBioscience	1:100
	FITC	UCHT1	BioLegend	1:50
	PECy7	UCHT1	eBioscience	1:100
CD4	PerCPCy5.5	OKT4	eBioscience	1:100
	VioG	VIT4	Miltenyi Biotec	1:25
CD45RA	BV421	HI100	BioLegend	1:100
	PerCPCy5.5	HI100	BioLegend	1:100
	PECy7	HI100	BioLegend	1:100
CD56	BV421	HCD56	BioLegend	1:100
CD62L	PECy7	DREG-56	BioLegend	1:50
CD8	AF700	RPA-T8	BD Bioscience	1:50
	eFl450	OKT8	eBioscience	1:200
	PerCP	RPA-T8	BioLegend	1:100
	PerCPCy5.5	RPA-T8	BD Bioscience	1:100
	VioG	BW135/80	Miltenyi Biotec	1:25
CD94-biotin	Streptavidin-PO	DX22	Serotec	1:5
CXCR6	Alexa647	TG3/CXCR6	BioLegend	1:10
Granzyme B	AF700	GB11	BD Bioscience	1:50
	APC	GB11	Invitrogen	1:50
IFNα	FITC	MMHA-1	PBL	1:100

IFNγ	AF700	E27	BD Bioscience	1:100
	FITC	45-15	Miltenyi Biotec	1:100
IL-2	PerCPCy5.5	MQ1-17H12	BD Bioscience	1:100
IL18Rα	PE	H44	eBioscience	1:50
KLRG1	FITC	13F12F2	Kindly provided by H. Pircher	1:100
Live/Dead	nIR	n/a - amine reactive	Invitrogen	1:1250
MDR1	PE	UIC2	BioLegend	1:50
NKG2A	APC	Z199	Beckman Coulter	1:50
	PE	Z199	Beckman Coulter	1:10
NKG2C	PE	134591	R&D Systems	1:10
NKG2D	FITC	1D11	AbD Serotec	1:5
NKp30	APC	AF29-4D12	Miltenyi Biotec	1:50
NKp44-biotin	Streptavidin-FITC	2.29	Miltenyi Biotec	1:5
NKp46	PE	9E2/NKp46	BD Bioscience	1:10
NKp80	PE	4A4.D10	Miltenyi Biotec	1:50
Perforin	FITC	δG9	BD Bioscience	1:50
	Pacific Blue	B-D48	BioLegend	1:50
PLZF	APC	6318100	R&D Systems	1:10
RORγt	PE	Q21-559	BD Bioscience	1:25
TCRαβ	APC	IP26	eBioscience	1:50
	PECy7	IP26	BioLegend	1:50
TCRγδ	APCVio770	11F2	Miltenyi Biotec	1:50
	FITC	IMMU510	Beckman Coulter	1:20
	PC5	IMMU510	Beckman Coulter	1:20
TNFα	PECy7	MAb11	BioLegend	1:100
Vα7.2	APC	3C10	Miltenyi Biotec	1:50
	FITC	3C10	Miltenyi Biotec	1:50
	PE	3C10	Miltenyi Biotec	1:50
	PECy7	3C10	Miltenyi Biotec	1:50

Table 2-1: Antibodies used in flow cytometry

2.3 Cell culture

2.3.1 T cell activation

For activation through the TCR, PBMC were cultured with anti-biotin beads coated with anti-CD2-biotin, anti-CD3-biotin and anti-CD28-biotin at 10μg/ml at a bead-to-cell ratio of 1:2, according to the T cell Activation/Expansion kit (Miltenyi Biotec).
Phorbol 12-Myristate 13-Acetate (PMA) and ionomycin stimulations were performed by adding 1X cell stimulation cocktail (eBioscience; equivalent to 0.081μM PMA + 1.34μM ionomycin) to 100μl R10 containing 3μg/ml Brefeldin A (eBioscience) and 2μM monension (eBioscience), unless otherwise specified.

2.3.2 MAIT functionality assay

THP1 cells were incubated with paraformaldehyde-fixed *E. coli* (DH5α, Invitrogen) at 25 bacteria per cell overnight (8 x10^4 THP1s : 2 x10^6 *E.coli* per well). The following morning, these THP1 cells were washed and PMBCs (24 month donors) or sort-purified CD8+ T cells (adults, sorted on a MoFlo, Beckman Coulter) were then added for a 5h co-culture. Anti-MR1 antibody (clone 26.5, kindly provided by T.H. Hansen) or IgG2a isotype control (BD Bioscience) was added at 10μg/ml. 3μg/ml Brefeldin A (eBioscience) was added for the final 4hrs of incubation and IFNγ production assayed by ICS.

2.3.3 IL-12 and IL-18 stimulation

PBMC were incubated with IL-12 (Miltenyi Biotec) and IL-18 (R&D Systems) each at 50ng/ml overnight. 3μg/ml Brefeldin A (eBioscience) was added for the final 4hrs of incubation and IFNγ production assayed by ICS.

2.4 Cytometry by Time-Of-Flight (CyTOF)

2.4.1 Antibody labelling

Purified antibodies were labelled with heavy metal-preloaded maleimide-coupled MAXPAR® chelating polymers according to instructions provided by DVS Sciences. The panel of antibodies and heavy metal isotopes used are shown in Table 2-2.

2.4.2 Stimulation and staining

Cryopreserved cells were thawed and rested overnight at 37°C. Dead cells were then removed by ficoll density centrifugation. For stimulation, cells were cultured for 3hrs with 150ng/ml PMA + 1mM Ionomycin in the presence of brefeldin A (eBioscience), monensin (eBioscience), anti-CD107 antibodies (see Table 2-2) and 10μM TNF protease inhibitor 2 (TAPI-2) (VWR International), a metalloproteinase inhibitor that prevents stimulation-induced cleavage of CD62L. Following stimulation cells were resuspended in cytometry buffer for 1hr at room temperature. Cells were then stained with fluorescently-tagged primary antibodies for 30min on ice. Cells were then washed before staining with a prepared cocktail of metal-conjugated surface-marker antibodies including secondary antibodies against the fluorescent tags. Staining was again performed for 30mins on ice. Cells were again washed, then resuspended in metal-labelled Live/Dead marker (20μM maleimido-mono-amine-DOTA in PBS). After 30min on ice, cells were washed extensively before overnight fixation in PBS + 2% paraformaldehyde (Electron Microscopy Sciences) at 4°C. The next day, cells are washed twice in intracellular staining permeablization buffer (eBioscience) and stained with a cocktail of intracellular antibodies on ice for 45min. Cells are then washed and labelled for 20min with 250nM iridium interchelator (DVS Sciences) suspended in PBS + 2% paraformaldehyde. Finally, cells are washed two times in each cytometry buffer, PBS and distilled water before dilution to achieve an acquisition rate <500 events/s on the CyTOF instrument.

Base Panel	Atomic Mass	Clone	Company
“cell length”	N/A	N/A	N/A
DNA	191, 193	N/A	DVS Sciences
Live/Dead	103, 115	N/A	DVS Sciences
CD3	Cd-122	S4.1	Invitrogen
CD3	Sn-141	S4.1	Invitrogen
CD8	Nd-146	SK1	BioLegend
CD4	Sm-149	SK3	BioLegend
CD13	Dy-156	WM15	BioLegend
CD33	Dy-156	P67.6	Santa Cruz
CD19	Gd-157	HIB19	BioLegend
TCR$\gamma\delta$-FITC	Dy-162	FIT-22	BioLegend
Phenotypic/ Functional Markers	**Atomic Mass**	**Clone**	**Company**
CD5	Nd-143	UCHT2	BioLegend
CCR7	Er-168	150503	R&D Systems
CD107a+b	Eu-153	H4A3/4	BD Bioscience
CD127	Ho-165	A019D5	BioLegend
CD161-APC	Er-167	191b8	Miltenyi Biotec
CD27	Gd-154	LG.7F9	eBioscience
CD28	Dy-160	CD28.2	Beckton Dickinson
CD38	Dy-161	HIT2	BioLegend
CD40L	Tb-172	24-31	eBioscience
CD45RA	Sm-148	HI100	eBioscience
CD45RO	Nd-144	UCLHL1	BioLegend
CD56	Tb-159	NCAM16.2	BD Bioscience
CD57	In-115	HCD57	BioLegend
CD62L	Yb-174	PE001	BioLegend
CTLA4	Nd-145	BNI3	Beckton Dickinson
GM-CSF	Sm-147	BVD2-21C11	BioLegend

Granzyme B	Eu-151	GB11	AbCam
HLA-DR	Yb-171	L243	BioLegend
IFNγ	Yb-170	4S.B3	eBioscience
IL-2	Er-166	MQ1-17H12	eBioscience
MIP1β	Sm-150	D21-1351	BD Bioscience
Perforin	Yb-176	DREG-56	BioLegend
TNFα	Sm-152	Mab11	eBiosciences

Table 2-2: Panel of antibodies and heavy metal isotopes used in CyTOF

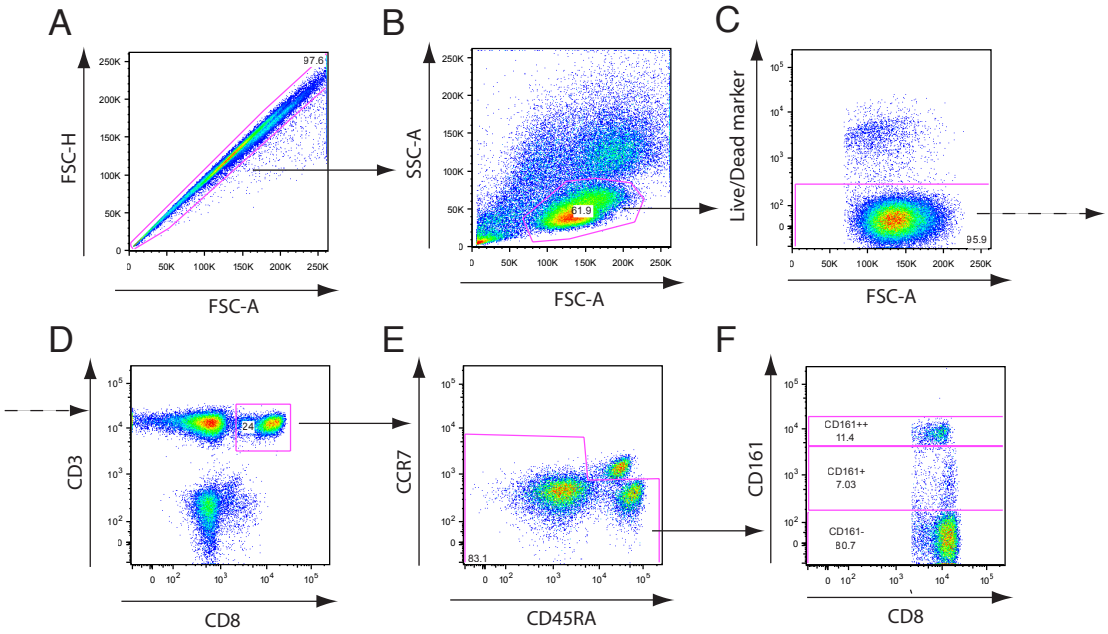

Figure 2-1: Flow cytometry gating strategy. Singlets were gatted on forward scatter (FSC) properties (**A**) and then lymphocytes gated in relation to size (FSC) and granularity (side scatter; SSC) (**B**). Dead cells were excluded (Live/Dead negative) (**C**) and CD8+ T cells gated according to expression of CD3 and CD8 (**D**). Naive cells were then excluded as CCR7+CD45RA+ cells (**E**). The division of these cells into CD161 subsets is then shown (**F**).

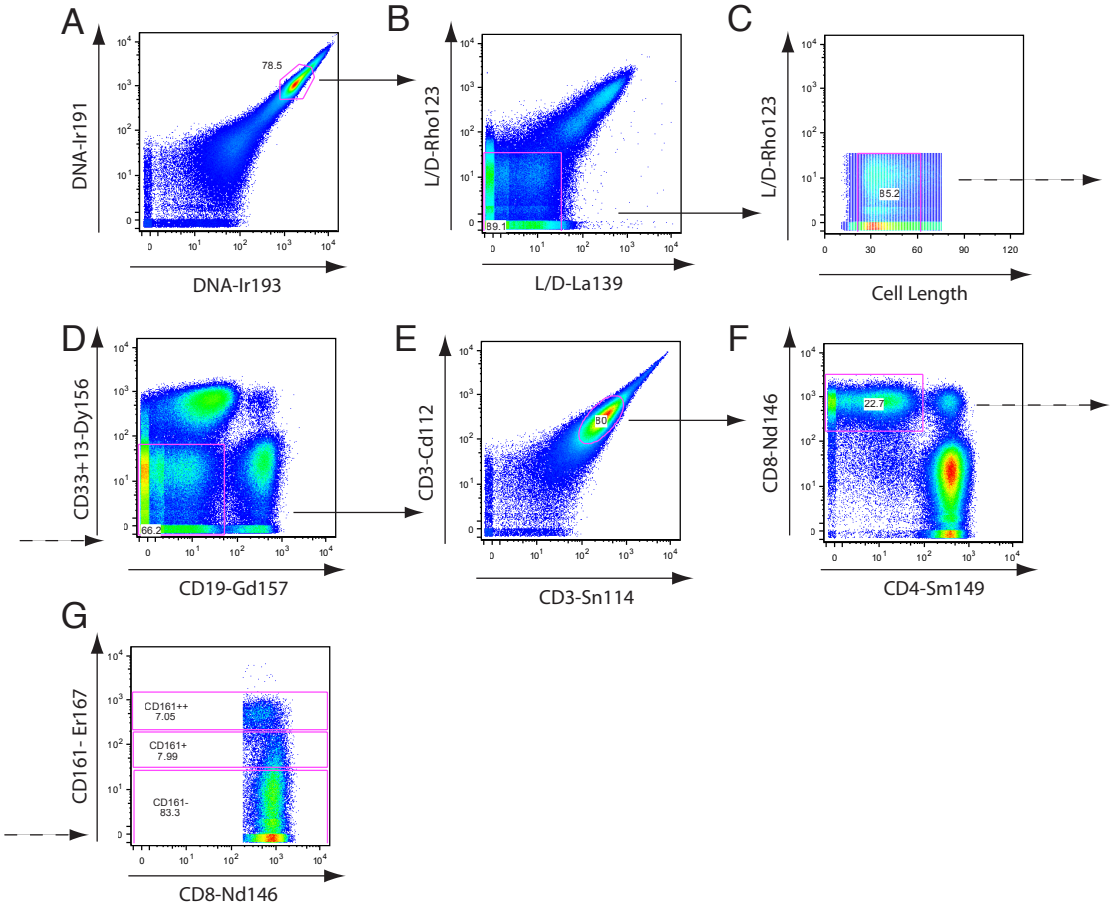

Figure 2-2: Mass cytometry (CyTOF) gating strategy. DNA content is used to identify individual cells (**A**). Cells are also gated by exclusion of a live-dead viability stain (**B**) and for uniformity in the length of signal received by the ion detector (**C**). Lymphocytes are gated by exclusion of myeloid cells (CD33+13) and B cells (CD19) (**D**). T cell are gated on expression of CD3 (**E**) and CD8+ T cells as CD8+CD4– (**F**). The division of these cells into CD161 subsets is then shown (**G**).

2.4.3 Data acquisition and analysis

CyTOF data were acquired and analysed on the fly, using dual-count mode with noise-reduction mode turned off. All other settings were either default setting or optimized with tuning solution as instructed by DVS Sciences. Analysis was performed on FlowJo software (Treestar, Inc.), following the gating strategy shown in Figure 2-2. For principal component analysis (PCA) live CD8+ T cell events were exported and analysed with scripts written in Matlab. Matlab scripts produced text files which were converted back to FCS files for analysis of principal components using FlowJo software.

2.5 Statistical analysis

Statistical analysis was performed using Prism version 6 software (GraphPad). Data are represented as mean ± standard error of the mean (SEM). **** $p<0.0001$, ***$p<0.001$, **$p<0.01$, *$p<0.05$, ns = not significant, as stated in figure legends. CD161−CD8+ T cells are displayed as red, CD161+ as blue and CD161++ as green throughout.

2.6 Media and buffers

CyTOF cytometry buffer

PBS+0.05% sodium azide + 2mM EDTA + 2% FCS

R10

RPMI medium 1640 (Gibco)

10% heat inactivated (56°C, 60min) fetal calf serum (FCS; Gibco)

2mM L-Glutamine (Gibco)

1X Penicillin-Streptomycin solution (Gibco)

(equivalent to 50,000U Penicillin, 50mg Streptomycin)

Rh10

RPMI medium 1640 (Gibco)

10% heat inactivated (56°C, 60min), filtered human serum (Sigma)

2mM L-Glutamine (Gibco)

1X Penicillin-Streptomicin solution (Gibco)

(equivalent to 50,000U Penicillin, 50mg Streptomycin)

Freezing mix

90% heat inactivated FCS

10% DMSO (Sigma)

MACS buffer

PBS + 0.5% heat inactivated FCS + 2mM EDTA (Sigma)

Efflux buffer

RPMI medium 1640 (Gibco) + 1% Bovine Serum Albumin (Sigma)

THP1 culture medium

R10 + 50μM β-mercaptoethanol (Sigma)

5X TBE buffer

54g Trizma Buffer (Sigma)

27.5g Boric Acid (Sigma)

10ml 5M EDTA (Sigma)

up to 1L dH_2O

3. Shared phenotype of CD161 expressing T cells

3.1 Introduction

Innate-like lymphocytes span both innate and adaptive immune responses, displaying features of conventional lymphocytes, namely T and B cells, in addition to characteristics of innate cells, such as NK cells. NKT cells, for example, home to extra-nodal tissues and show immediate effector functions, while maintaining the adaptive feature of a somatically recombined antigen receptor (Bendelac et al., 2007). However, these antigen receptors are of limited diversity and recognise conserved epitopes, and can, therefore, be viewed more as pattern recognition receptors (Kronenberg, 2005).

MAIT cells are an innate-like subset of human T cells, identified by their invariant expression of the TCR α chain Vα7.2, conventionally recombined with Jα33, but with a minority recombining with Jα12 or 20 (Reantragoon et al., 2013; Tilloy et al., 1999). This TCR, paired with a biased Vβ repertoire, is restricted by the MHC class Ib antigen presenting molecule MR1, which is non-polymorphic and highly conserved between mammals. MR1 presents a riboflavin precursor (Kjer-Nielsen et al., 2012) capable, via non-enzymatic reactions with other small molecules (Corbett et al., 2014), of binding MR1 and activating MAIT cells. This metabolite is produced by a variety of bacteria, implicating MAIT cells in the control of bacterial infections (Chua et al., 2012; Georgel et al., 2011; Gold et al., 2010; Le Bourhis et al., 2010). However, a role for MAIT cells has also been suggested in a number of inflammatory conditions, including MS (Annibali et al., 2011; Miyazaki et al., 2011). This may be related to their high expression of IL18R (Dusseaux et al., 2011; Le Bourhis et al., 2010) and consequent activation by TCR-independent cytokine stimulation through

the synergistic effects of IL-12 and IL-18, as has recently been described (Ussher et al., 2014).

While originally identified within the DN T cell fraction (Porcelli et al., 1993), MAIT cells in humans are predominantly CD8+ (Walker et al., 2012), although around 10% are DN and a small fraction of CD4+ MAIT cells also exists (Reantragoon et al., 2013). Independently of co-receptor usage, and in addition to the expression of Vα7.2, MAIT cells are also identified by their high expression of the C-type lectin receptor CD161 (CD161++) (Dusseaux et al., 2011; Martin et al., 2009).

Originally a marker of NK cells (Yokoyama and Seaman, 1993), Lanier et al. (1994) also identified CD161 (KLRB1, NKRP1A) expression on subsets of T cells, including both CD4+ and CD8+ lineages, with two populations expressing intermediate (CD161+) or high (CD161++) levels apparent in the latter (Takahashi et al., 2006). While the vast majority of CD161++CD8+ T cells are Vα7.2+ MAIT cells, a population of CD161++ Vα7.2– cells exists, which also display an innate ability to respond to cytokine stimulation by IL-12 and IL-18 (Ussher et al., 2014). To what extent this population shares further features of CD161++ MAIT cells, including restriction to MR1, has not yet been explored. In addition to these populations of CD4+ and CD8+ TCRαβ+ T lymphocytes, a subset of TCRγδ+ T cells also expresses CD161 (Battistini et al., 1997; Maggi et al., 2010). TCRγδ+ T cells are themselves an example of innate-like lymphocytes, responding to non-polymorphic antigens such as microbial HMB-PP (Eberl et al., 2003; Hintz et al., 2001) and demonstrating rapid cytokine release, with stimulation through CD161 described to induce IFNγ release by this subset (Battistini et al., 1997).

CD161 binds LLT1 (Aldemir et al., 2005; Rosen et al., 2005) and while the outcome of ligation on NK cells is generally accepted to be inhibitory (Aldemir et al., 2005; Lanier et al., 1994; Rosen et al., 2005), the effect on T cells is less clear, with reports of both co-stimulatory (Aldemir et al., 2005; Exley et al., 1998) and inhibitory effects

(Le Bourhis et al., 2013; Rosen et al., 2008). Expression of CD161 has been associated with a type 17 phenotype, with CD161 significantly upregulated in Th17 clones compared to those of Th1 and Th2 (Cosmi et al., 2008), and the ability to secrete IL-17 restricted to CD161 positive cells across all T cell lineages (Maggi et al., 2010). MAIT cells also display a type-17 phenotype, including high expression of RORγt and the ability to produce IL-17 (Billerbeck et al., 2010; Dusseaux et al., 2011).

Both CD161 expression and type 17 phenotype appear to be determined early in development. CD161 is expressed on a subset of T cells in the foetal liver and amongst single positive thymocytes (Cosmi et al., 2008; Lanier et al., 1994; Martin et al., 2009). Naïve UCB CD161 positive CD4+, CD8+ and DN TCRγδ+ cells already express mRNA for RORγt and IL-23R (Maggi et al., 2010), and both UCB CD161++ CD8+ (Walker et al., 2012) and CD161+CD4+ (Cosmi et al., 2008) T cells express CCR6 and CXCR6. These naïve, yet pre-programmed, CD161 positive cells are therefore thought to represent the precursors of adult Th17 and MAIT cells. Indeed, microarray analysis demonstrated significant correlation in gene expression between CD161++ CD8+ T cells in UCB with those in the adult, despite only a small proportion expressing the Vα7.2 TCR chain at this stage (Walker et al., 2012). Together, this suggests that CD161 marks cells of a distinct phenotypic pathway of differentiation. Expression of CD161, therefore, may link diverse T cell populations through shared transcriptional profiles, which may correspond to a specific shared function between these otherwise disparate cell types.

3.2 Aims

1. Examine to what extent the MAIT cell phenotype is shared with other CD161++ but Vα7.2– CD8+ T cells
2. Analyse mRNA microarray data from CD161 positive T cell subsets, previously generated within the lab, to identify shared transcriptional signatures
3. Determine the functional significance of shared expression of CD161 across T cell lineages

3.3 Materials and Methods

Chapter-specific materials and methods are detailed below. All other methods and reagents are described in Chapter 2.

3.3.1 Vβ Typing by flow cytometry

PBMC were surfaced stained with T cell receptor Vβ antibodies; Vβ 1, 2, 4, 5.3, 7.2, 8, 9, 11, 13.2, 14, 16, 18, 23-PE, and Vβ 3, 5.1, 5.2, 7.1, 12, 13.1, 13.6, 14, 16, 17, 20, 21.3, 22-FITC (Beckman Coulter). Data were acquired on a MACSQuant (Miltenyi Biotec) and analysed on FlowJo software (Treestar, Inc.).

3.3.2 TCR sequencing

Vα7.2+ and Vα7.2– CD161++CD8+ T cells were sorted (MoFlo, Beckman Coulter) as single cells into wells of a 96 well plate containing 2.5μl of iScript cDNA Synthesis reaction mixture (Bio-Rad) with 0.1% Triton X-100. TCR transcripts for each cell were amplified by multiplex nested polymerase chain reaction (PCR) using 1 unit of Platinum Taq DNA polymerase High Fidelity, 10X PCR Buffer, 2mM magnesium sulphate and 0.2mM deoxynucleotide triphosphate (Invitrogen), 2.5pmol of each external TRAV and TRBV primer and 10pmol of each external TRAC and TRBC in the first round. Products were then split and amplified for either alpha or beta TCR chains, using the same concentration of either internal TRAV and TRAC or internal TRBV and TRBC primers in the second round (primers as detailed in Appendix III.i). The PCR conditions were 95°C for 2min, followed by 35 cycles of 95°C for 20s, 52°C for 20s, 72°C for 45s, followed by 1 cycle of 72°C for 7min (Wang et al., 2012). PCR products were identified by visualization on a 1% agarose gel with SYBR green (Invitrogen), run for approximately 45min at 110V, 400mA in 1X TBE Buffer. PCR

products were purified from PCR reactions by DNA precipitation. In brief, 10μl of water, 2μl of 3M sodium acetate and 50μl 100% Ethanol was added to each well and incubated at room temperature for 15min. Plates were then centrifuged for 60mins at 4000rpm at 4°C. Afterwards, wells were blotted and pulsed to dry. 200μl of 70% ethanol was subsequently added to each well and centrifuged at 4000rpm for 15mins. This was repeated. Finally, the plate was heated to 95°C for 1min to evaporate remaining ethanol. Products were sequenced by Sanger sequencing (Department of Zoology) with the corresponding TRAC or TRBC primer.

3.3.3 CyTOF

For a detailed description of stimulation and staining of cells see Chapter 2 Materials & Methods. Data was analysed by principal component analysis (PCA), which is a mathematical algorithm that reduces the dimensionality of the data yet retains the information from the variation in the data set. It does this by identifying directions, or principal components, in which the variation in the data is the greatest; principal components are therefore linear combinations of the original variables. Samples can then be represented by these summary principal component values, instead of individual values for each of the markers assayed, aiding the visualisation of the data. The principal components can be expressed in terms of the original variables: the component loading value, giving a weight to each marker (Ringnér, 2008). Each cell is given a value for a particular principal component, which represents the sum of the expression levels of each marker (equivalent of the geoMFI) multiplied by its component loading value. To perform PCA, live CD8+ T cell events were exported and analysed with scripts written in Matlab. Matlab scripts produced text files that were converted back to FCS files for further analysis on FlowJo software (Treestar, Inc.).

3.3.4 Microarrays

Microarrays of CD161 subsets within CD8+ T cells were obtained from the publication by Billerbeck et al. (2010). Briefly, sorted CD8+ T cell subsets from 4 adult donors were lysed and homogenized using an RNeasy Mini Kit (Qiagen) according to the manufacturer's instructions. cDNA was synthesized and cRNA was amplified and purified using Illumina TotalPrep RNA amplification kit (Ambion). cRNA was hybridized to Illumina Sentrix Human Whole Genome 6 BeadChips (Illumina) and scanned with an Illumina BeadArray Reader. *Performed by Yu-Hoi Kang.*

For CD161+CD4+ T cell microarray, CD4+ T cells were isolated from 3 adult donors by magnetic bead enrichment (EasySep, Stemcell Technologies), and CD161 subsets selected by staining anti-CD161-PE (Beckman Coutler) followed by purification with anti-PE MicroBeads (Miltenyi Biotec). Purity, as determined by flow cytometry, was >95% for all samples. Total RNA was extracted using an RNeasy Mini Kit (Qiagen) and quality measured using the ND 1000 Spectrophotometer (Saveen Werner, Sweden). cRNA was amplified and purified using Illumina TotalPrep RNA amplification kit (Ambion) and hybridized to the Illumina HumanWG-6 v3.0 Expression BeadChip (Illumina). *Performed by Vicki Fleming.*

For gene expression profiling of TCR$\gamma\delta$+ T cell subsets, T cells were enriched from PBMC from 4 adult donors as per the manufacturer's instructions (EasySep T-cell enrichment kit, Stemcell Technologies). CD3+TCR$\gamma\delta$+CD161+ or CD161− were sorted using a FACSAria (BD Biosciences). Cell pellets were snap frozen and sent to Miltenyi Biotec Genomic Services (Bergisch Gladbach, Germany) for RNA extraction and hybridization to Agilent Whole Human Genome Oligo Microarray. *Performed by Neil Rajoriya.*

Microarray features in all microarrays were normalized using variance stabilising normalisation (vsn) (Huber et al., 2002) using R (http://cran.r-project.org/) and Bioconductor (bioconductor.org) packages. Gene lists of interest were generated from those genes >2-fold up/down-regulated and with a $p<0.05$ for comparison using the Venn diagram module of GenePattern (Gould et al., 2006). Heat maps were generated using GENE-E (http://www.broadinstitute.org/cancer/software/GENE-E/index.html). Gene set enrichment analysis was performed using GSEA version 2.0.14 (Subramanian et al., 2005). GSEA generates a ranked list of genes, and calculates a normalized enrichment score (NES) for a particular gene set by 'walking' down the ranked list of genes, increasing a running-sum statistic when a gene is in the gene set and decreasing it when it is not (represented by the green line, below). The NES is the maximum deviation from zero encountered in 'walking' the list. The leading edge subset of a gene set is the subset of members of that gene set that contribute most to the enrichment score.

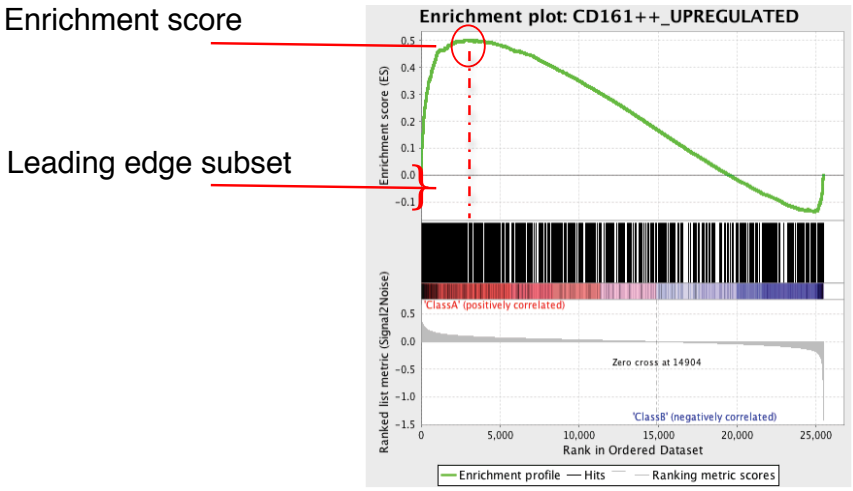

3.4 Results

3.4.1 CD161++ CD8+ T cells are composed of both Vα7.2+ MAIT and Vα7.2– cells

MAIT cells express an invariant TCR α chain (Vα7.2) together with high levels of CD161 (Dusseaux et al., 2011) and the majority express the CD8 co-receptor (>90%) (Walker et al., 2012). While Vα7.2+ MAIT cells represent the vast majority of the CD161++ CD8+ T cell population (<95%) in adult blood, a population of CD161++CD8+ T cells that are Vα7.2– is also evident (Figure 3-1A), comprising an average of 11.41% of CD161++CD8+ T cells in healthy adults. The identity of this additional CD161++CD8+ T cell population in relation to MAIT cells was investigated. Interestingly, in UCB, where CD161++CD8+ T cells are already pre-programmed to a MAIT-like, type-17 phenotype (Walker et al., 2012), this Vα7.2– population comprised the major proportion of CD161++CD8+ T cells (84.69%). After birth, Vα7.2+ MAIT cell expansion drives the MAIT cell domination of the CD161++ population (Gold et al., 2013; Leeansyah et al., 2014), and a corresponding reduction in the proportion of Vα7.2– cells was seen. This was evident as early as 24 months where the MAIT cell population represented nearly 75% of the CD161++CD8+ T cell population (Figure 3-1).

3.4.2 Unlike Vα7.2+ MAIT cells, the Vα7.2– subset is polyclonal

In addition to invariant expression of Vα7.2, MAIT cells display semi-invariant TCR β usage (Figure 3-2A) with predominant use of Vβ2 and Vβ13.2, as previously described (Reantragoon et al., 2013; Walker et al., 2012). In contrast, a panel of Vβ antibodies revealed non-discriminate Vβ usage by Vα7.2– CD161++CD8+ T cells (Figure 3-2B). The TCR repertoire of this population was further investigated by TCR

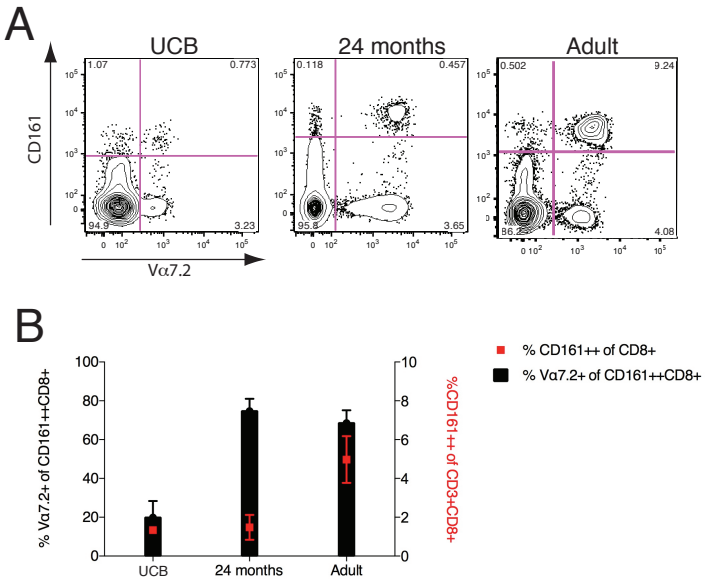

Figure 3-1: CD161++ CD8+ T cells are comprised of both Vα7.2– and Vα7.2+ populations. A) Representative flow cytometry plots of CD161 and Vα7.2 expression by CD8+CD3+ lymphocytes in UCB, 24 month and adult blood. **B**) Percentage Vα7.2+ of CD161++CD8+ T cells (histogram) and percentage CD161++ of CD8+ T cells (red point) in cord (n=3), 24 month (n=8) and adult blood (n=8). Flow cytometry staining of PBMC from 24 month old donors was performed by Sophia Bjorkander.

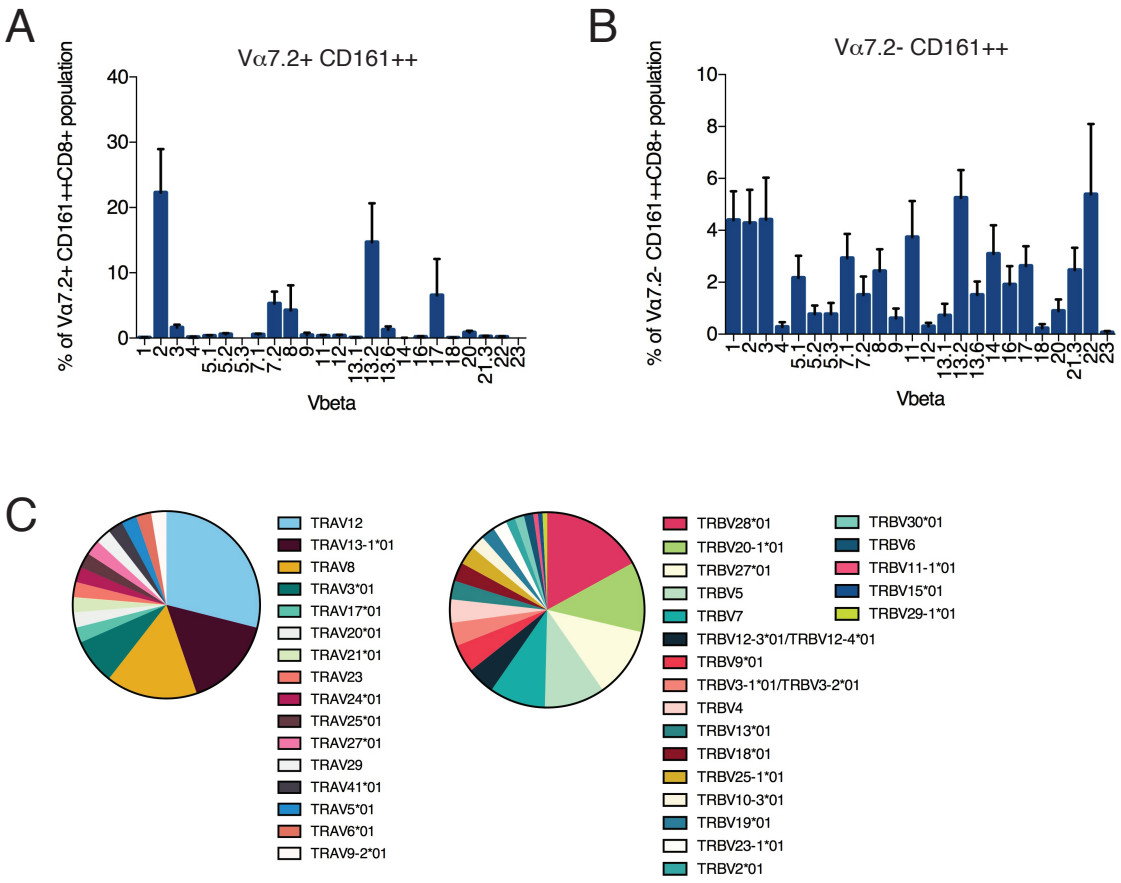

Figure 3-2: Polyclonal TCR usage by Vα7.2– CD161++ CD8+ T cells. PBMC were stained with a TCR Vβ antibody panel. Histograms show the percentage of Vα7.2+ (**A**) and Vα7.2– (**B**) CD8+ T cells using each Vβ. **C**) Proportional Vα (38 sequences) and Vβ (129 sequences) usage by Vα7.2– CD161++CD8+ T cells as determined by single cell TCR sequencing (n=3). TCR sequencing was performed in collaboration with Ruth Simmons.

sequencing, performed on single cells, as described (see 3.3.2., Wang et al. 2012). This confirmed Vβ usage by Vα7.2− CD161++CD8+ T cells to be polyclonal. Furthermore, polyclonality within α chain usage was also evident (Figure 3-2C). Although there may be some bias, with TRAV12 expressed by all three donors, these were paired with multiple J regions and displayed non-canonical CDR3 sequences (Appendix III.ii), indicating diversity in recombination unlike the invariant MAIT Vα7.2-Jα33/12/20 TCR.

3.4.3 Vα7.2−CD161++ CD8+ T cells are not activated in an MR1-dependent manner but, like MAIT cells, respond to stimulation by IL-12+IL-18

The semi-invariant MAIT cell TCR recognises bacterially-derived riboflavin precursors presented by the antigen presenting molecule MR1 (Corbett et al., 2014; Kjer-Nielsen et al., 2012). MHC-tetramer positive populations against various viral epitopes are rarely CD161++ (Chapter 4, Figure 4-1). Therefore, to establish the MR1-responsiveness of Vα7.2− CD161++CD8+ T cells a 5hr co-culture assay, previously described to activate MAIT cells via the TCR to produce IFNγ (Ussher et al., 2014), was used. Here, THP1s were incubated with fixed *Escherichia coli* (*E. coli*) overnight and then cultured with sort-purified Vα7.2+ or Vα7.2− CD161++CD8+ T cells. As expected, CD161++Vα7.2+ MAIT cells produced IFNγ in response to *E. coli*-pulsed THP1s, and these responses were blocked by addition of an anti-MR1 antibody (Figure 3-3A). While in two donors a limited MR1-mediated response by Vα7.2− CD161++CD8+ T cells to *E.coli* was apparent, the majority of donors did not respond to bacteria. This was reflected in 24 month old donors where no response was observed from Vα7.2− CD161++CD8+ T cells when PBMC were incubated for 5hr with *E. coli*-loaded THP1s (Figure 3-3B).

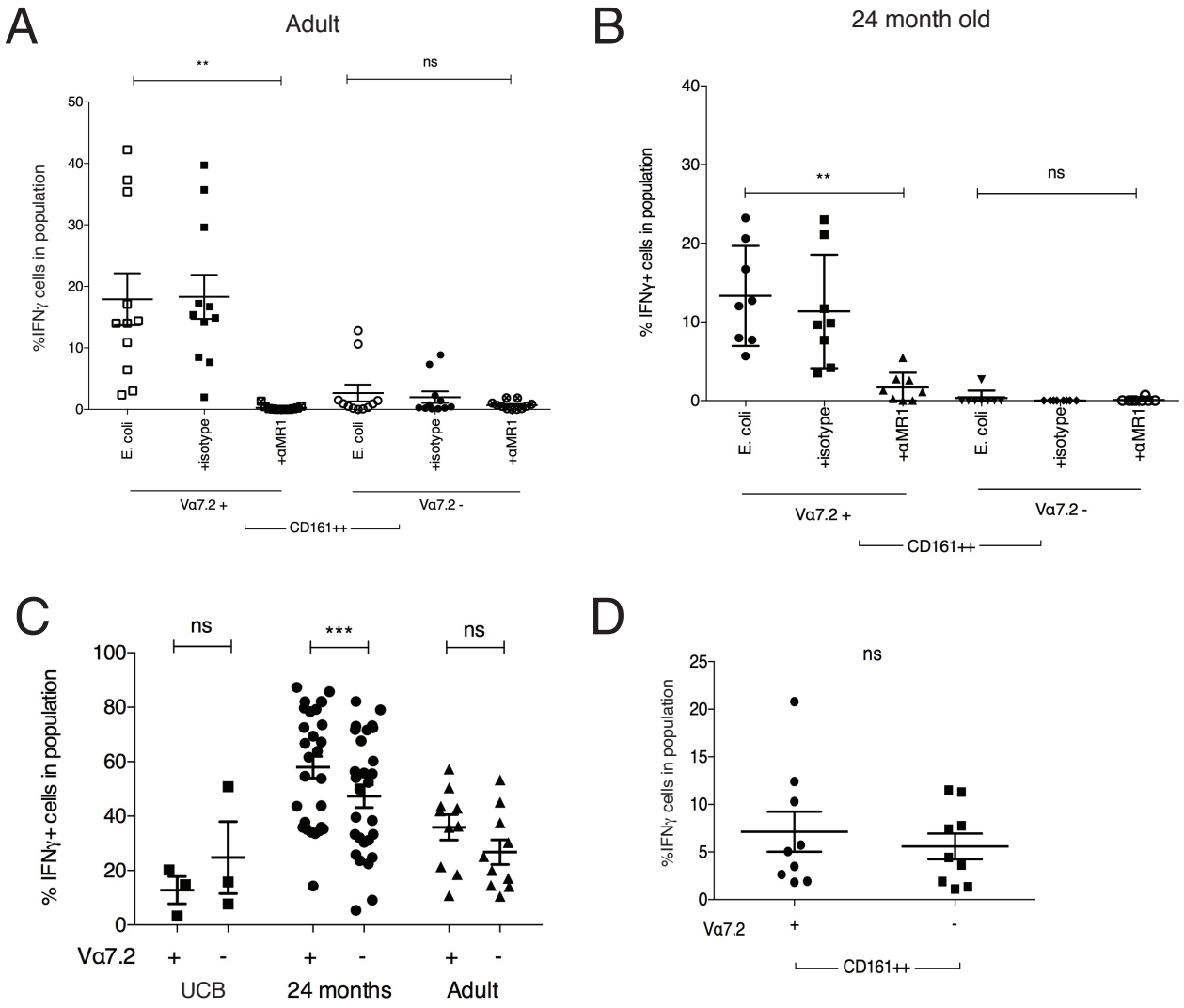

Figure 3-3: Vα7.2– CD161++ CD8+ T cells are not activated in an MR1-dependent manner but, like MAIT cells, respond to stimualtion by IL-12+IL18. **A**) Percentage of IFNγ expression by adult sorted Vα7.2+ or Vα7.2– CD161++ CD8+ T cell subsets co-cultured with THP1 cells exposed to *E. coli* in the presence or absence of anti-MR1 antibody (10μg/ml), or corresponding isotype control (n=11). **B**) PBMC from 24 month old donors were co-cultured with THP1s exposed to *E. coli* for 5hr in the presence or absence of anti-MR1 antibody or isotype control (10μg/ml). Data shows percentage IFNγ expression from gated subsets. (n=8). ** p<0.01 One-way ANOVA with Dunnett's multiple comparisons test compared to *E. coli* alone. **C**) Percentage IFNγ expression of PBMC cultured overnight with IL-12 + IL-18 (50ng/ml each) from UCB (n=3), 24 month (n=28) and adult (n=10) blood. ***p<0.001, ns= not significant by paired t-tests. **D**) Percentage of IFNγ expression by sorted adult Vα7.2+ or Vα7.2– CD161++CD8+ T cells incubated overnight with IL-12 + IL-18 at 50ng/ml each (n=9). ns = not significant by paired t-test. Experiment B was performed by Sophia Bjorkander. IL-12+18 stimulation of PBMC from 24 month old donors (C) was performed by Christian B. Willberg.

In addition to MR1-mediated stimulation through the TCR, MAIT cells have also been described to be activated by a combination of IL-12 plus IL-18 in a TCR-independent, innate manner; a characteristic that was shared by other CD161++CD8+ T cells (Ussher et al., 2014). Gating of both CD161++CD8+ T cell populations in adult, 24 month old and cord blood again showed that both Vα7.2+ and Vα7.2− portions were capable of IFNγ production (Figure 3-3C). This was confirmed in sorted adult populations, where both Vα7.2+ and Vα7.2− CD161++CD8+ T cells produced IFNγ in response to cytokine stimulation (Figure 3-3D), confirming this as a feature of CD161++CD8+ T cells as a whole.

3.4.4 Vα7.2−CD161++ CD8+ T cells mirror the Vα7.2+ MAIT cell phenotype

Next, it was asked whether Vα7.2− CD161++CD8+ T cells shared the characteristic transcription factor expression of MAIT cells, namely expression of RORγt, associated with the type-17 profile of MAIT cells (Billerbeck et al., 2010; Dusseaux et al., 2011) and PLZF, related to the innate-like effector differentiation of MAIT and NKT cells (Savage et al., 2008). Expression of these transcription factors by Vα7.2− CD161++CD8+ was significantly ($p<0.01$) higher than in conventional CD8+ T cells, but expressed on average at slightly lower levels than MAIT cells (Figure 3-4A&B). This was true of many other MAIT cell markers including IL18R, CCR6 and CXCR6 (Appendix III.iii). Vα7.2− CD161++CD8+ T cells also principally displayed an effector memory (CD62L−CD45RA−) phenotype, as seen in Vα7.2+ MAIT cells (Figure 3-4C).

Together, these results illustrate that despite different TCR expression and restriction, both Vα7.2+ MAIT and Vα7.2− CD161++CD8+ T cells share a pre-programmed phenotype and an innate ability to respond to cytokine stimulation, and can therefore be viewed as a common population related through high expression of CD161.

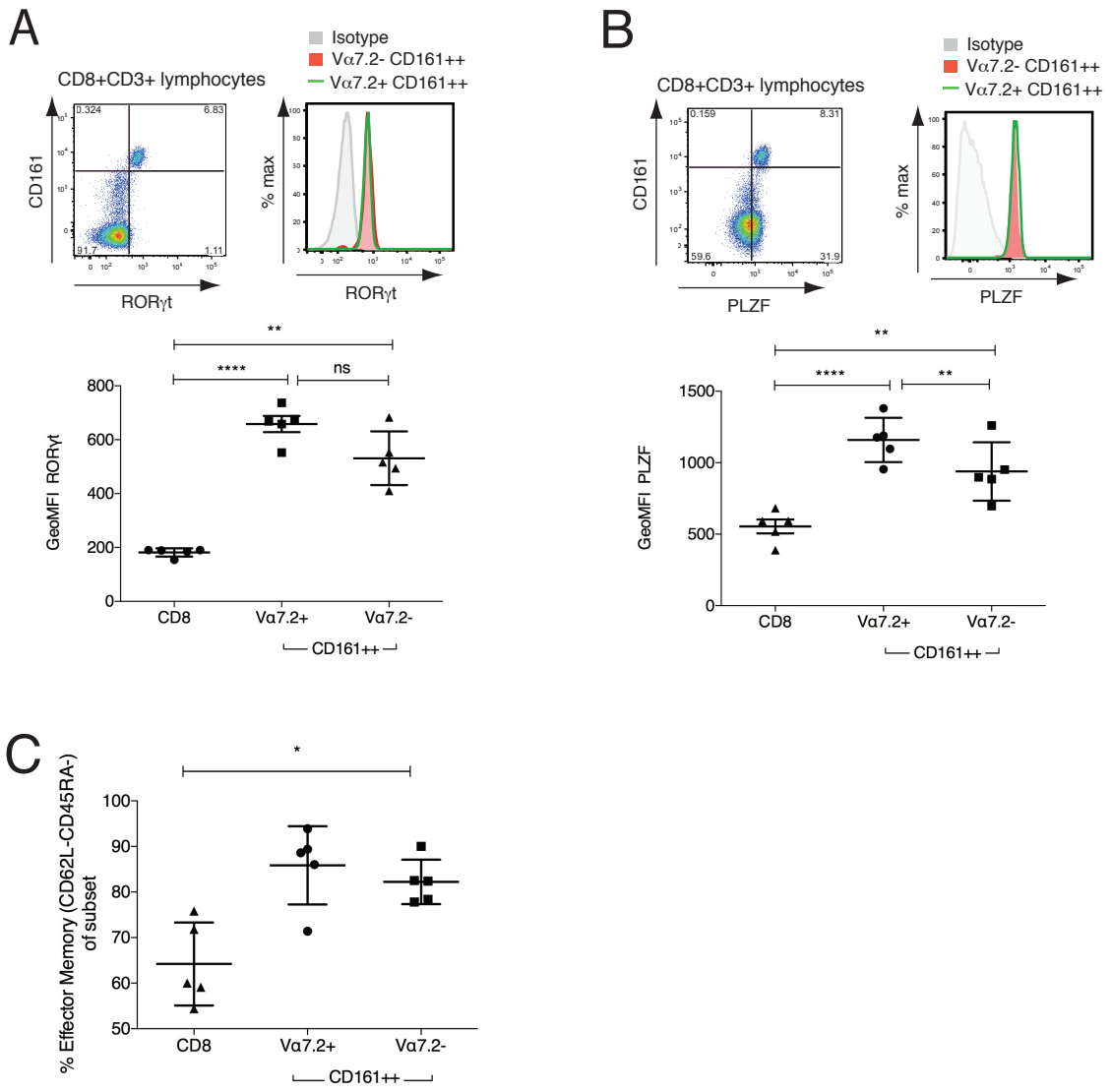

Figure 3-4: Vα7.2– CD161++ CD8+ T cells reflect the phenotype of Vα7.2+ MAIT cells. **A-B**) Transcription factor expression as determined by flow cytometry. Graphs show GeoMFI of RORγt (**A**) and PLZF (**B**) by conventional CD8+ T cells (CD3+CD8+ cells excluding CD161++), Vα7.2+ or Vα7.2– CD161++ CD8+ T cells (n=5). ****p<0.0001, **p<0.01 One-way ANOVA with Tukey's multiple comparison test. Representative flow cytometry plots and histograms show isotype (grey), Vα7.2+ (green line) and Vα7.2– (red) for each transcription factor. **C**) Percentage of Vα7.2+ and Vα7.2– CD161++ CD8+ T cells displaying an effector memory (CD62L–CD45RA–) phenotype compared to conventional (non-CD161++) CD8+ T cells, (n=5). *p<0.05, ** p<0.01 by one-way ANOVA with Dunnett's multiple comparisons test.

3.4.5 Analysis of CD161-expressing CD8+ T cells by CyTOF

As CD161++CD8+ T cells displayed a common phenotype across Vα7.2+ and Vα7.2− subsets, it was hypothesised that expression of CD161, and specifically different levels of expression (as illustrated in Figure 3-5A), defined distinct CD8+ T cell phenotypes. To test this hypothesis expression of 23 markers (see Table 2-2) was assayed simultaneously across PMA plus ionomycin-stimulated CD8+ T cells by mass cytometry (CyTOF). Principal component analysis (PCA) was then used as a means of integrating the patterns of expression of all markers into a smaller number of summary values (Newell et al., 2012). PCA looks for directions, or components, that cumulatively account for the variation contained within the dataset (see 3.3.4), with the first four components here accounting for >60% of the total variation (Figure 3-5B). This analysis allowed the patterns of expression of all 23 markers to be summarised for each cell, which can then be viewed on a 2D or 3D plot, thereby allowing the different CD8+ T cell populations to be viewed in relation to one another.

When stimulated CD8+ T cells were plotted upon the first three components, CD161++ cells occupied a distinct niche compared to the other CD8+ T cell subsets (Figure 3-5C). Similarly, when plotted in 2D on component 1, which accounts for the most variation, and component 4, to which CD161 contributed the most to the variation described (component loading, Fig 3-5B), CD161++ cells again occupied a distinct niche amongst the spectrum of CD8+ T cell phenotypes (Figure 3-5D). In addition to CD8+ T cells that express high levels of CD161, a population of CD8+ T cells that express low, or intermediate, levels of CD161 is also apparent in the circulation (CD161+; Figure 3-5A). These cells displayed an overlap with the phenotypic niche of CD161++ cells (Figure 3-5D).

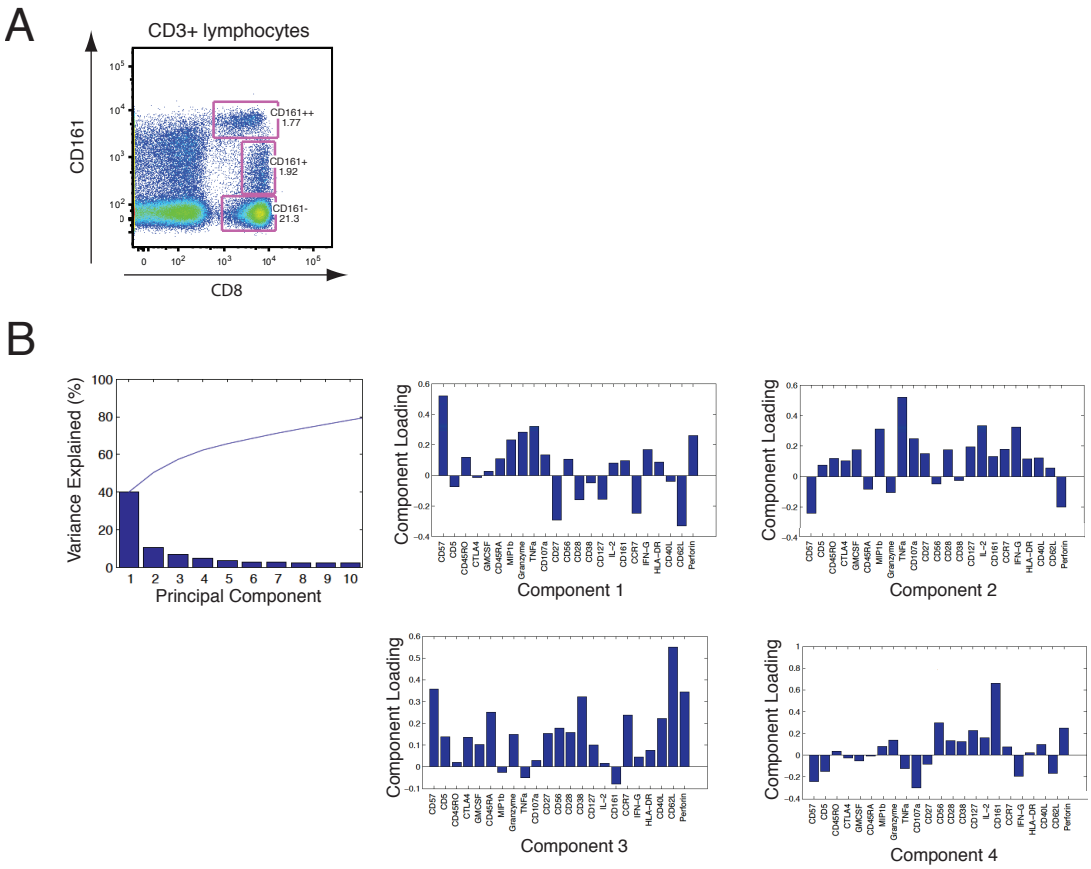
A
CD3+ lymphocytes
CD161
CD8
CD161++
1.77
CD161+
1.92
CD161-
21.3
B
Variance Explained (%)
Principal Component
Component Loading
Component 1
Component 2
Component 3
Component 4
C
Bulk CD8+ T cells
PC2
PC3
PC1
CD161++
CD161+
CD161-
D
CD161++
CD161+
CD161-
PC1
PC4

Figure 3-5: CyTOF and principal component analysis (PCA) reveals CD161++ cells to be unique amongst CD8+ T cells. A) Representative flow cytometry plot of the division of CD8+ T cells into 3 subsets based upon expression of CD161. **B)** Data generated for PMA + ionomycin stimulated CD8+ T cells was analysed by PCA. The percent variation explained is plotted for each component (bars) and cumulatively (line) and the parameter loadings (weighting coefficients) for the first four components are shown. **C)** Stimulated CD8+ T cells from one representative donor are plotted on the first three components as a bulk population (black) and for the three subsets; CD161++ (green), CD161+ (blue) and CD161− (red). **E)** Density plots of bulk stimulated CD8+ T cells are plotted on component 1 and component 4, and are overlaid with contour density of plots of CD161++ (green), CD161+ (blue) and CD161− (red) cells. Principal component analysis was performed by Evan Newell.

3.4.6 The phenotypic and transcriptional profile of CD161+CD8+ T cells overlaps with CD161++CD8+ T cells

To explore in more depth the phenotypic overlap of CD161+ and CD161++/MAIT CD8+ T cells, genome-wide mRNA expression of these CD8+ T cell populations was probed by microarray. Previously, Billerbeck *et al.* (2010) identified a set of genes differentially expressed by CD161++CD8+ T cells compared to CD161− CD8+ T cells (Figure 3-6A). This included the upregulated expression of RORγt, CXCR6, and IL18R. Given the dominance of MAIT cells within the CD161++CD8+T cell population, these markers are consequently thought to be descriptive of the MAIT cell subset as well. Similarly, microarray analysis was performed on CD161+CD8+ T cells in comparison to CD161−CD8+ T cells in the same donors (Figure 3-6B), and identified 544 differentially expressed genes. When compared with the CD161++/MAIT cell transcriptional signature, 79% of those genes significantly differentially expressed by CD161+CD8+ T cells were shared by CD161++CD8+ T cells (Figure 3-6C, Appendices III.iv & v). Although the majority of shared genes were downregulated, among the 107 shared upregulated genes were those characteristic of MAIT cells, including *CCR6*, *CXCR6*, *ABCB1* (encoding MDR1) and *IL18R* (Billerbeck et al., 2010; Dusseaux et al., 2011).

Next, the gene expression data was analysed as a whole using gene set enrichment analysis (GSEA) (Subramanian et al., 2005), rather than limiting analysis to significant genes only, which may miss relevant biological differences or pathway effects. GSEA orders the genes into a ranked list according to their differential expression between CD161+ and CD161− CD8+ T cells. The location of the CD161++CD8+ T cell associated genes, divided into upregulated (those upregulated within CD161++CD8+ T cells) or downregulated (upregulated within CD161−CD8+ T cells; Figure 3-6A) genes, within this ranked list was then identified. Significant enrichment of genes upregulated in CD161++ CD8+ T cells was observed in CD161+CD8+ T cells (Normalised Enrichment Score (NES) =3.79, $p<0.001$), and corresponding enrichment of downregulated genes with those genes more associated with a CD161− phenotype (NES=-3.12, $p<0.001$; Figure 3-6D).

The correlation in CD161 expression with a number of "MAIT cell markers" identified amongst the shared upregulated genes was then investigated at the protein level using flow cytometric analysis. To prevent skewing by the differing proportions of each subset, defined as CD161++, CD161+ and CD161− (Figure 3-5A), individual subsets were gated, and the expression levels of each marker at the population level (taken as geometric mean fluorescence intensity (geoMFI)) were plotted in relation to that of CD161 expression (Figure 3-7). This revealed a highly significant correlation ($p<0.0001$) between the levels of CD161 expressed and the expression of CCR6 ($r^2 = 0.9143$), CXCR6 ($r^2 = 0.9258$), MDR1 ($r^2 = 0.9322$) and IL18Rα ($r^2 = 0.9554$) (Figure 3-7A-D). Therefore, expression of CD161 by CD8+ T cells correlates with a phenotypic signature that includes a distinct set of chemokine and cytokine receptors.

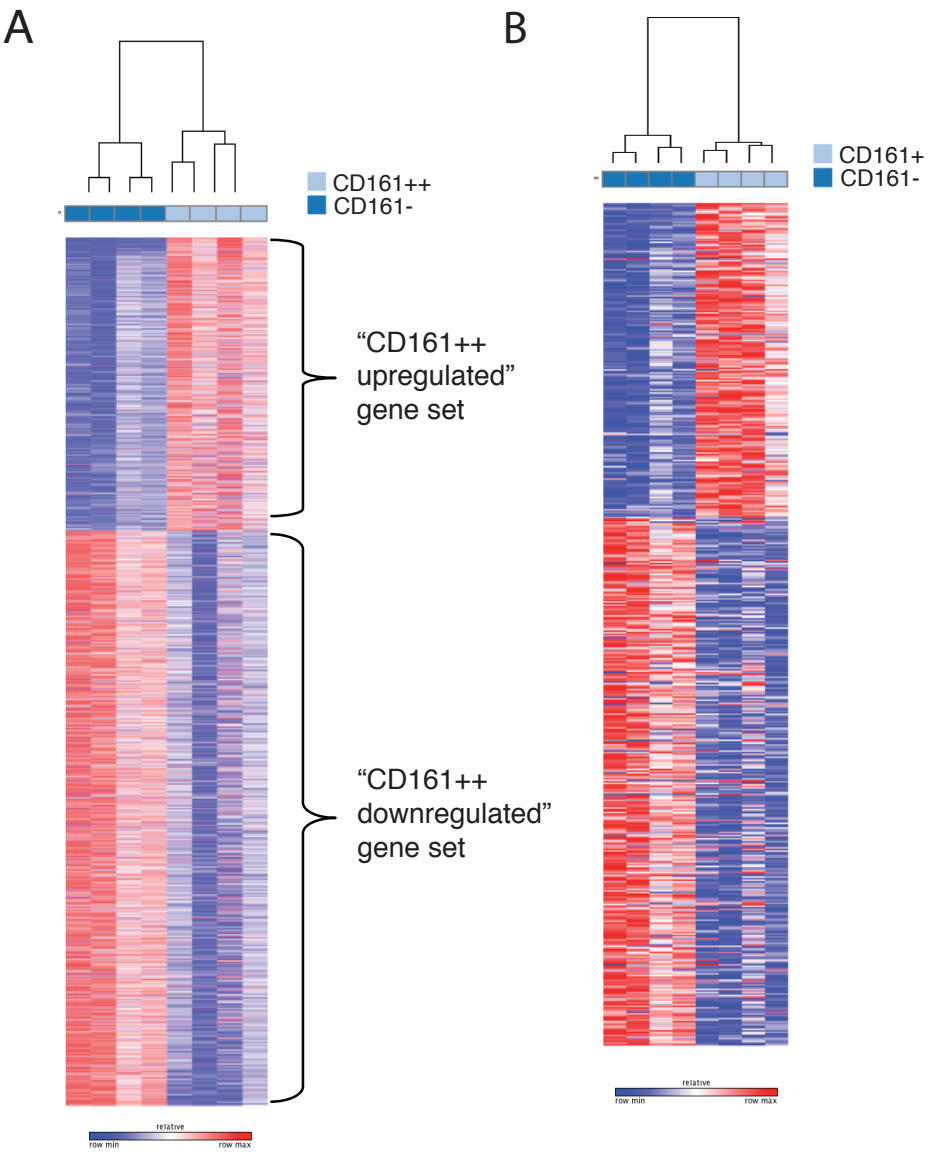
A
CD161++
CD161-
"CD161++ upregulated" gene set
"CD161++ downregulated" gene set
relative
row min
row max
B
CD161+
CD161-
relative
row min
row max

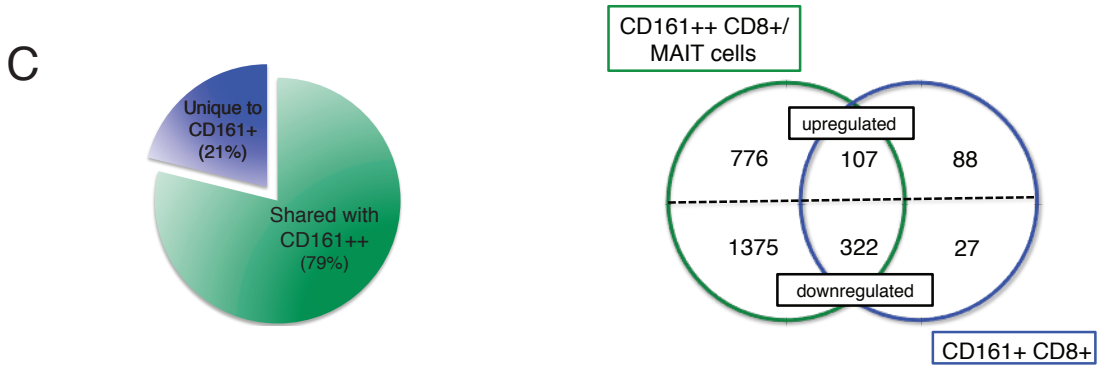
C
Unique to CD161+ (21%)
Shared with CD161++ (79%)
CD161++ CD8+/ MAIT cells
upregulated
776
107
88
1375
322
27
downregulated
CD161+ CD8+

D

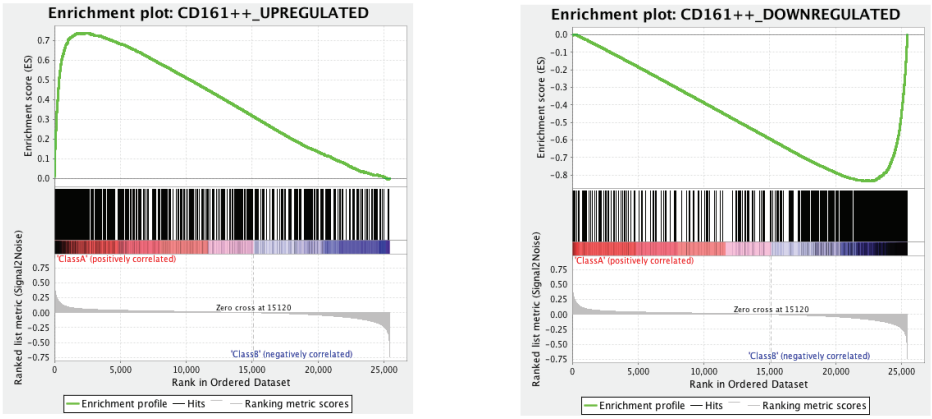

p<0.001
NES = 3.79

p<0.001
NES = -3.12

Figure 3-6: CD161+CD8+ T cells share a CD161++ transcriptional signature and phenotypic profile. **A**) Heat map showing 3025 significantly (p<0.05) differentially expressed transcripts between CD161++ and CD161– CD8+ T cells in 4 donors. Subsets clustered by one minus Pearson correlation. **B**) Heat map showing 544 significantly differentially expressed genes between CD161+ and CD161– CD8+ T cells in the same 4 donors. Subsets clustered by one minus Pearson correlation. **C**) Pie chart shows proportion of genes differentially expressed by CD161+ that are shared with CD161++ (79%), when compared to CD161– CD8+ T cells. Venn diagram shows breakdown of upregulated and downregulated genes unique to or shared by each subset. **D**) Gene set enrichment summary plots for vsn-normalised CD161+ vs CD161– CD8+ T cell ranked genes, and CD161++ upregulated (top) and downregulated (bottom) gene sets. Normalised enrichment score (NES) = 3.79, p<0.001 upregulated genes, NES = -3.12, p<0.001 downregulated genes. Microarray sample preparation was performed by YuHoi Kang.

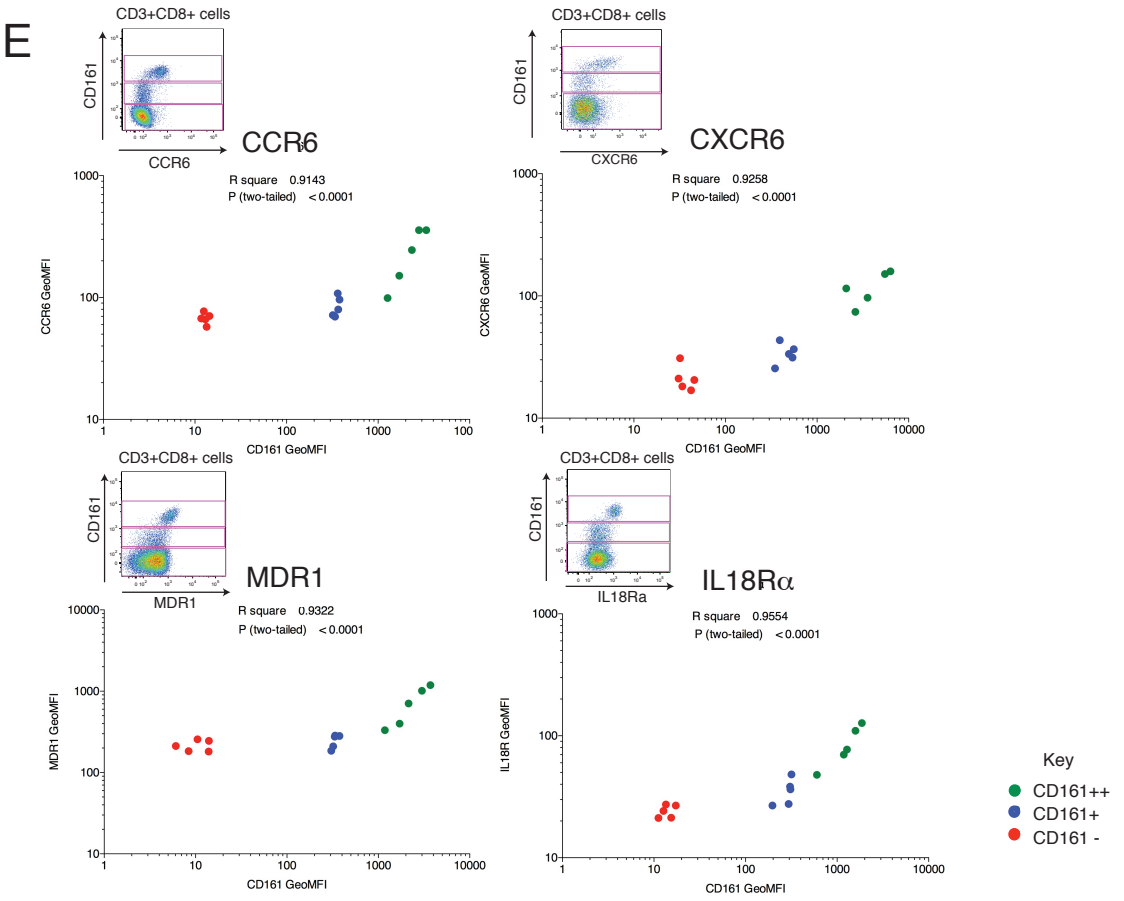

Figure 3-7: Expression of CD161 correlates with that of "MAIT cell" markers. GeoMFI of CD161 for CD161++ (green), CD161+ (blue) and CD161– (red) CD8+ T cell subsets correlated with geoMFI of CCR6 (r^2= 0.9143, p<0.0001) (**A**), CXCR6 (r^2= 0.9258, p<0.0001) (**B**), MDR1 (r^2= 0.9322, p<0.0001) (**C**) and IL18Rα (r^2= 0.9554, p<0.0001) (**D**), (n=5). Representative flow cytometry plots shown for each.

3.4.7 Conserved transcriptional changes in CD161-expressing CD4+ and TCRγδ+ T cells

A population of CD4+ T cells expressing CD161 is also apparent in the adult circulation and UCB (Figure 3-8A). Both CD161+CD4+ T cells (Cosmi et al., 2008; Maggi et al., 2010) and CD161++ CD8+/MAIT cells (Billerbeck et al., 2010; Dusseaux et al., 2011) have been associated with a type 17 phenotype. Therefore, the phenotypic overlap between these populations was investigated on a global scale by performing gene expression profiling of adult CD161+CD4+ T cells by microarray. Genes significantly differentially expressed compared to CD161−CD4+ T cells were identified and compared to the CD161++CD8+ gene dataset (Figure 3-8B). CD161+CD4+ T cells shared a third of distinguishing genes with CD161++CD8+ T cells, including *IL18RAP* (Figure 3-8C, Appendices III.vi & vii). Again, GSEA demonstrated significant enrichment ($p<0.001$) of those genes upregulated in CD161++CD8+ T cells in the CD161+CD4+ transcriptional profile (NES=2.45), and downregulated genes with the CD161−CD4+ phenotype (NES=-3.04; Figure 3-8D), demonstrating concordance of transcriptional profiles, independently of co-receptor expression amongst T cells.

To investigate whether the CD161++/MAIT phenotype was also enriched in T cells expressing a different TCR, the analysis was extended to T cells expressing TCRγδ. Again, both CD161+ and CD161− TCRγδ+ T cells are evident within the adult circulation and UCB (Figure 3-9A). Gene expression analysis was performed on sorted adult CD161+ and CD161− TCRγδ+ T cells and those genes significantly differentially expressed identified (Figure 3-9B). Approximately a fifth of these were again shared with the CD161++CD8+ gene dataset, including *IL18R1* and *ABCB1*, which encodes MDR1 (Appendices III.viii & ix). As seen for CD8+ and CD4+ T cells, GSEA revealed the CD161++CD8+ gene set to be significantly enriched ($p<0.001$) in CD161+TCRγδ+ T cells, corresponding to both upregulated (NES=2.78) and downregulated (NES=-2.62) genes (Figure 3-9D), despite a reduced number of

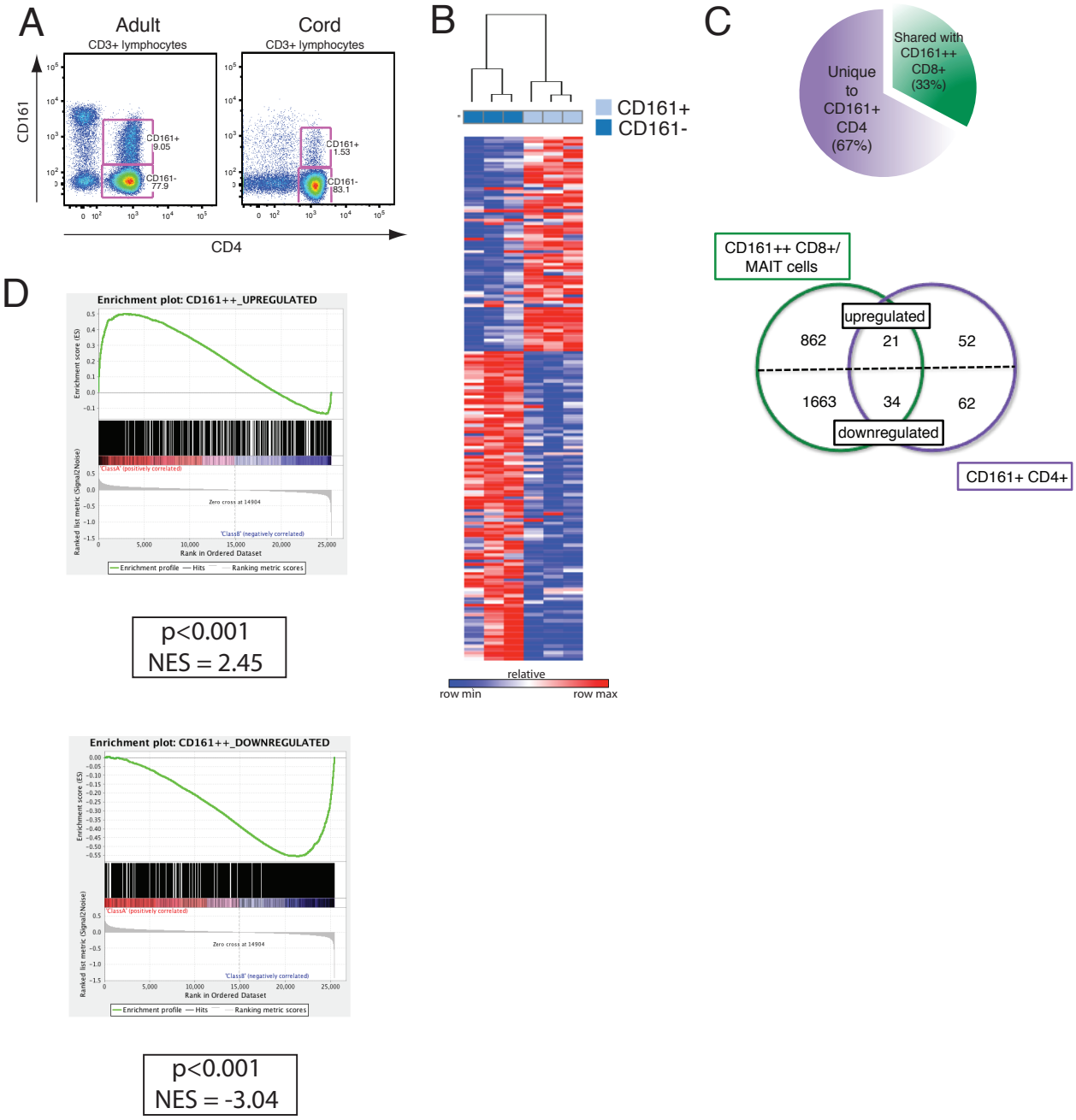

Figure 3-8: CD161+CD4+ are enriched for the CD161++CD8+/MAIT transcriptional signature. **A**) Representative flow cytometry plot showing CD161+CD4+ T cells within the adult circulation and UCB. **B**) Heat map showing 169 significantly differentially expressed genes between CD161+ and CD161– CD4+ T cells in 3 donors. Subsets clustered by one minus Pearson correlation. **C**) Pie chart shows proportion of genes differentially expressed by CD161+CD4+ that are shared with CD161++CD8+ (33%), when compared to their CD161– counterparts. Venn diagram shows breakdown of upregulated and downregulated genes unique to or shared by each subset. **D**) Gene set enrichment summary plots for vsn-normalised CD161+ vs CD161– CD4+ T cell ranked genes, and CD161++CD8+ upregulated (left) and downregulated (right) genes. NES = 2.45, p<0.001 upregulated genes, NES = -3.04, p<0.001 downregulated genes. Preparation of microarray samples was performed by Vicki M. Fleming.

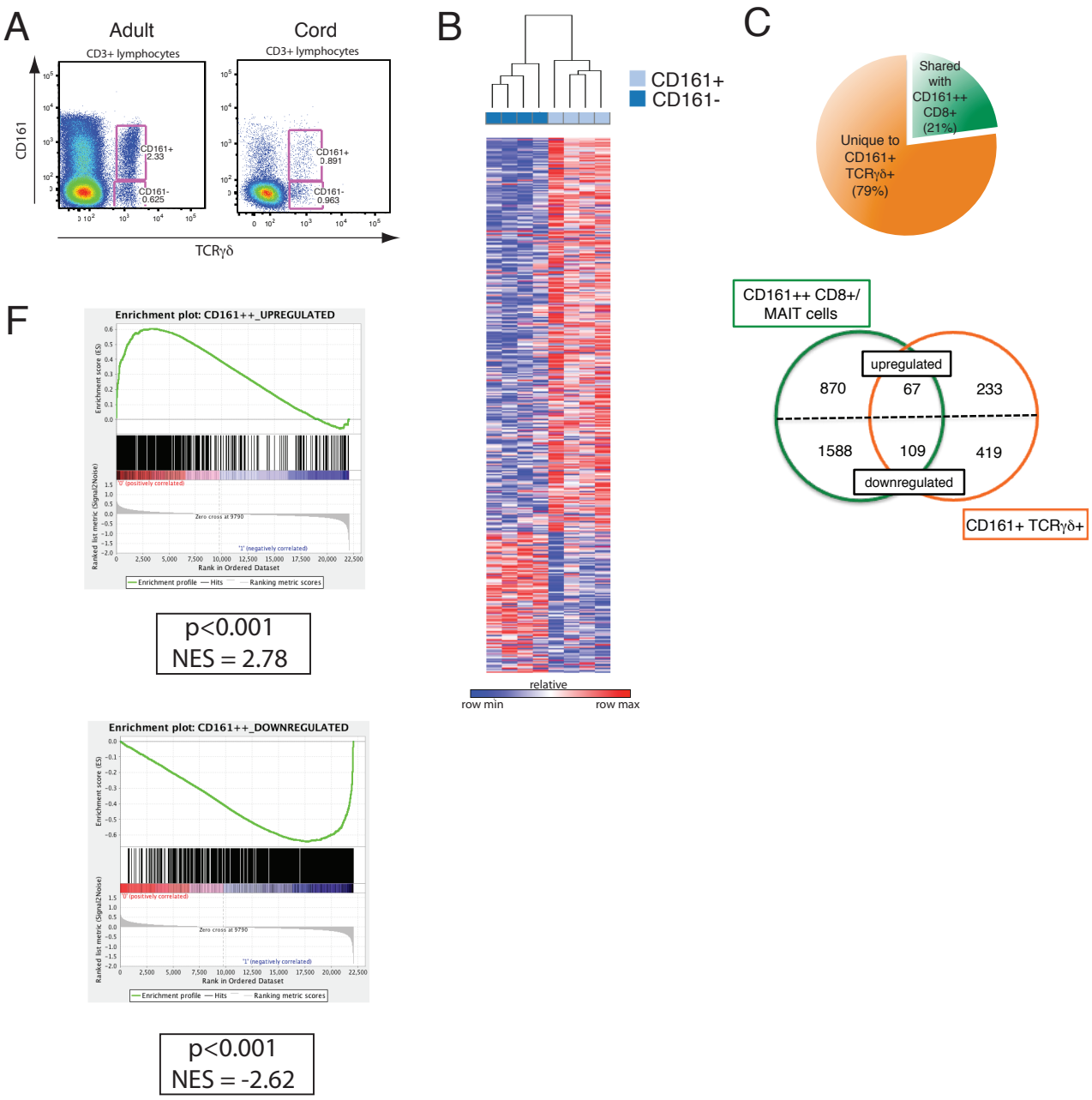

Figure 3-9: CD161+TCRγδ+ T cells are also enriched for the CD161++CD8+/MAIT transcriptional signature. **A**) Representative flow cytometry plot showing CD161+TCRγδ + T cells within the adult circulation and UCB. **B**) Heatmap showing 828 significantly differentially expressed genes between CD161+ and CD161– TCRγδ+ T cells in 4 donors. Subsets clustered by one minus Pearson correlation. **C**) Pie chart shows proportion of genes differentially expressed by CD161+TCRγδ+ that are shared with CD161++CD8+ (23%), when compared to their CD161– counterparts. Venn diagram shows breakdown of upregulated and downregulated genes unique to or shared by each subset. **D**) Gene set enrichment summary plots for vsn-normalised CD161+ vs CD161– TCRγδ+ T cell ranked genes, and CD161++CD8+ upregulated (left) and downregulated (right) genes. NES = 2.78, p<0.001 upregulated genes, NES = -2.62, p<0.001 downregulated genes. Preparation of microarray samples was performed by Neil Rajoriya.

genes being shared. For comparisons with CD161+CD8+ T cells please see Appendix III.x.

Overall, CD161 expression can distinguish distinct populations of T cells within each T cell lineage, whether CD8+, CD4+ or TCRγδ+, with a defined CD161++/MAIT cell –associated transcriptional signature enriched within these CD161 positive subsets. Moreover, comparison of the leading edge gene set (the core set of genes that account for this enrichment) from each T cell population distinguished a core of 124 upregulated (Table 3-1) and 199 downregulated (Table 3-2) genes commonly enriched in all CD161 positive T cells, and which therefore defines the CD161-associated transcriptional signature. This included upregulated expression of *ABCB1* (MDR1), *RORC* (RORγ), *ZBTB16* (PLZF), *IL12RB2* and *IL18R1*.

3.4.8 A common functional correlate of CD161-expression in all T cell subsets

IL18R was one of the defining components of the leading edge gene set associated with CD161 expression. The receptor is composed of two subunits, IL18Rα and IL18RAP. *IL18R1* (IL18Rα) was significantly upregulated in CD161-expressing TCRγδ+ ($p<0.01$) and both populations of CD8+ ($p<0.0001$) T cells, and *IL18RAP* significantly upregulated in all CD161-expressing T cell subsets ($p<0.0001$; Figure 3-10A). Expression was confirmed at the protein level by flow cytometry, which also revealed a previously unappreciated CD161++IL18Rα++ subset amongst CD4+ and TCRγδ+ T cells (Figures 3-10B). Gating of these three subsets (CD161++, CD161+ and CD161–) revealed a significant correlation between CD161 expression and IL18Rα expression (Figure 3-10C) amongst CD4+ ($p<0.0001$) and TCRγδ+ ($p=0.0001$) T cells, as for CD8+ T cells (Figure 3-7).

ABCA2	*CTNNA1*	*IGFBP4*	*MYO1F*	*SESN1*
ABCB1	*CTSH*	***IL12RB2***	*NADK*	*SIPA1L2*
ACTN4	***CXCR6***	*IL15*	*NBEAL2*	*SLAMF1*
ADCY9	*CXXC5*	***IL18R1***	*NETO2*	*SLC1A5*
ADRB2	*CYB561*	***IL18RAP***	*NPC1*	*SLC2A8*
AGPAT4	*CYFIP1*	*IL23R*	*PBX4*	*SLC7A5*
ALCAM	*DENND3*	*IRAK2*	*PERP*	*SLCO3A1*
ARNTL	*DUSP5*	*JSRP1*	*PHACTR2*	*SMAD3*
AUTS2	*EIF2C4*	*KIAA1539*	*PHLDA1*	*SMAD7*
B4GALT1	*ELOVL4*	*KIF5C*	*PIK3AP1*	*SNAI3*
CACNA2D2	*ELOVL6*	***KLRB1***	*PLCB1*	*SYNE2*
CACNA2D4	*ERN1*	*KLRG1*	*PLEKHG3*	*SYTL2*
CAMTA1	*FAM43A*	*LAG3*	*PLXNC1*	*THBS1*
CAPN12	*FAS*	*LATS2*	*PODXL*	*TLE1*
CCR2	*FOSL2*	*LONRF3*	*PRDM1*	*TNF*
CD58	*GALM*	*LTB4R*	*PRDM8*	*TNFRSF18*
CD72	*GBP5*	*LTK*	*PRF1*	*TNFSF14*
CERK	*GFPT2*	*MAFF*	*PTGDS*	*TPM2*
CFH	*GPR65*	*MAP3K5*	*PTPRM*	*VCL*
CLCF1	*GPR68*	*MAP3K8*	*RAB11FIP1*	*VLDLR*
CLIC5	*GTF3C1*	*MATK*	*RASD1*	*WNT1*
COL5A1	*GZMA*	*ME1*	*RHBDF2*	*YPEL1*
COL5A3	*GZMK*	*METRNL*	*RORA*	***ZBTB16***
COLQ	*IFI44*	*MICALCL*	***RORC***	*ZDHHC14*
CREB3L2	*IFNGR1*	*MYO1D*	*RPPH1*	

Table 3-1: Core transcriptional signature of CD161-associated upregulated genes. Leading edge analysis was performed on the enriched CD161++CD8+ T cell upregulated gene set in all T cell subsets. The leading edge gene set was compared from each T cell population and a core set of 124 genes identified and listed in alphabetical order. Those referred to in the text are highlighted in bold.

ABCD2	*COQ6*	*LEPROTL1*	*PKIA*	*SNPH*
ACCN2	*CRLF3*	*LIMS2*	*PLAG1*	*SNRPN*
ACSM3	*CYP2J2*	*LOC338799*	*PLEKHB1*	*SOX8*
ACTN1	*DSC1*	*LOC388588*	*PPAP2A*	*SPINK2*
AEBP1	*EFHD1*	*LOC401431*	*PPAPDC2*	*SPINT2*
AGMAT	*EPHX2*	*LOC641518*	*PPP1R3E*	*SRPK2*
ALKBH7	*ERLIN2*	*LRRN3*	*PRIM1*	*STAT1*
ANAPC13	*ESD*	*LYPD3*	*PRKACB*	*SUCLG2*
APBA2	*ETS1*	*MAD1L1*	*PRKAR1B*	*SULT1B1*
APEX1	*FAM55C*	*MAD2L1*	*PRKCA*	*SUMF2*
ARHGEF4	*FBLN5*	*MAGEF1*	*PSAT1*	*SUSD3*
ARMCX1	*FBXO15*	***MAL***	*PSIP1*	*SYPL1*
ARMCX2	*FCGBP*	*MAN1C1*	*PTPRK*	*TAF4B*
ATG9B	*FHIT*	*MARCKSL1*	*PTTG2*	*TATDN1*
AXIN2	*GCET2*	*MMP11*	*RAB30*	*TBXA2R*
BANF1	*GJB6*	*MPP6*	*RAB33A*	*TCEA3*
BCAS4	*GLS2*	*MRPL52*	*RAB3GAP1*	*TCF7*
BCL9	*GP5*	*MTA3*	*RAB43*	*TGIF2*
BEX1	*GPC2*	*MTUS1*	*RALA*	*THOC3*
BEX2	*GRAP*	*MYB*	*RANBP6*	*THYN1*
BIRC2	*GSTM2*	*N6AMT1*	*RBM11*	*TMEM123*
BZW2	*GTF2IRD2*	*NAP1L3*	*RGMB*	*TMEM69*
CAMSAP1L1	*H2AFY2*	*NDFIP1*	*RPIA*	*TMEM97*
CASP6	*HEMGN*	*NECAP2*	*RPL22*	*TNFRSF10D*
CBR3	*HERC3*	*NELL2*	*SAE1*	*TOP1MT*
CCDC25	*HIRIP3*	*NET1*	*SAP18*	*TSGA10*
CCNG1	*HKDC1*	*NGFRAP1*	*SCML1*	*TSNAX*
CCR7	*HPCAL1*	*NOG*	*SDCCAG8*	*TSPAN3*
CD248	*HSD17B8*	*NOSIP*	*SDK2*	*VIPR1*
CD55	*HSPB1*	*NPM3*	*SELL*	*VNN2*
CDCA7L	*ICOS*	*NRCAM*	*SERPINE2*	*VPS24*
CHI3L2	*IL6ST*	*NSMCE1*	*SERTAD2*	*YPEL2*
CIAPIN1	*IMPDH2*	*NUCB2*	*SETMAR*	*ZNF101*
CITED4	***ITK***	*OR2A9P*	*SFXN4*	*ZNF154*
CLEC11A	*KBTBD11*	*P2RY10*	*SH3YL1*	*ZNF181*
CLN5	*KCNMB4*	*PCSK5*	*SIRPG*	*ZNF200*
CMTM7	*KRT18*	*PDE9A*	*SLC16A10*	*ZNF415*
CNN3	*LAMC3*	*PECAM1*	*SLC22A17*	*ZNF439*
CNOT7	*LDLRAP1*	*PHGDH*	*SLC24A6*	*ZNF671*
COL18A1	*LEF1*	*PIGC*	*SLC25A26*	

Table 3-2: Core transcriptional signature of CD161-associated downregulated genes. Leading edge analysis was performed on the GSEA of CD161++ downregulated genes in all T cell subsets. The leading edge gene set was compared and a core set of 199 genes identified and listed in alphabetical order. Those referred to in the text are highlighted in bold.

It was recently described that elevated expression of IL18R enables CD161++CD8+/MAIT cells to be activated by IL-12+IL-18 in a TCR-independent manner (Ussher et al., 2014). As genes encoding both subunits of the IL-18R and *IL12RB2* were contained within the core leading edge set of CD161-associated upregulated genes (Table 3-1), IFNγ production in response to overnight stimulation with IL-12+IL-18 was assayed in CD8+, CD4+ and TCRγδ+ T cells. IFNγ production was apparent by intracellular cytokine staining in all three T cell lineages, and particularly apparent within the CD161++ population of each (Figure 3-10D). Although CD4+ MAIT cells do exist (Reantragoon et al., 2013), IFNγ responses were not restricted to Vα7.2+CD4+ T cells (Appendix III.xi). This response to IL12+IL18 was correlated to the levels of CD161 expressed by gating on the three CD161 populations (CD161++, CD161+, CD161−) within each T cell lineage, as previously (Figure 3-7). As expected, there was a significant correlation between levels of CD161 expressed by each population and the percentage of that population expressing IFNγ in response to IL-12+IL-18 (Figure 3-10E), with the greatest responses seen by the CD161++ population in each.

Together, these results demonstrate T lymphocytes expressing CD161 to be related both in terms of gene expression and function, including elevated expression of IL18R in the resting state. This is linked to their shared ability to make an innate response to cytokine stimulation by IL-12+IL-18, which is independent of the TCR, yet correlated to expression of CD161.

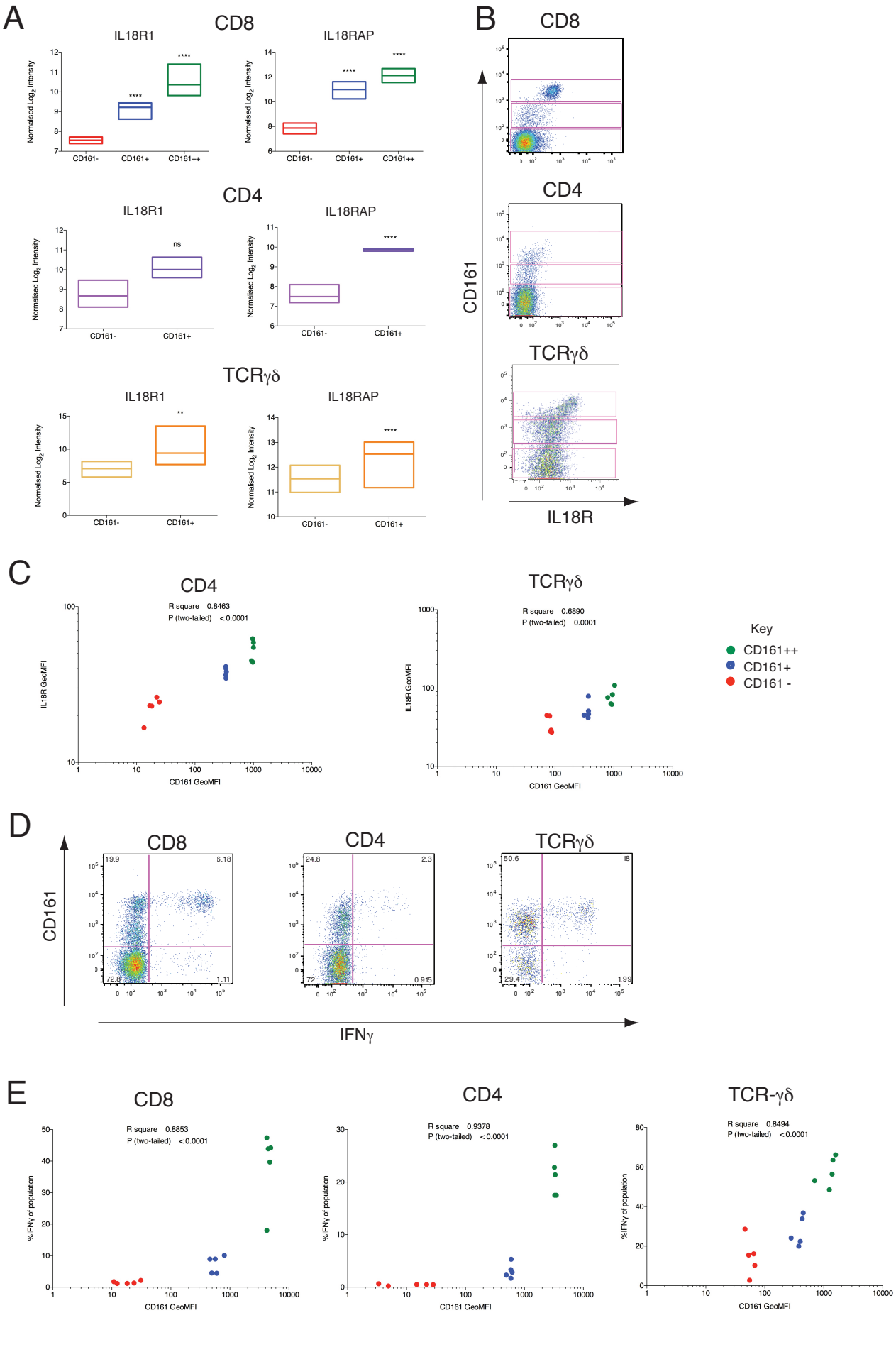
A
CD8
IL18R1
IL18RAP
Normalised Log2 Intensity
CD161-
CD161+
CD161++
****
CD4
ns
TCRγδ
**
B
CD8
CD4
TCRγδ
CD161
IL18R
C
CD4
R square 0.8463
P (two-tailed) <0.0001
TCRγδ
R square 0.6890
P (two-tailed) 0.0001
IL18R GeoMFI
CD161 GeoMFI
Key
CD161++
CD161+
CD161 -
D
CD8
CD4
TCRγδ
19.9
8.18
72.8
1.11
24.8
2.3
72
0.915
50.6
18
29.4
1.99
CD161
IFNγ
E
CD8
R square 0.8853
P (two-tailed) <0.0001
CD4
R square 0.9378
P (two-tailed) <0.0001
TCR-γδ
R square 0.8494
P (two-tailed) <0.0001
%IFNγ of population
CD161 GeoMFI

Figure 3-10: CD161-expressing T cell subsets express elevated levels of IL18Rα and respond to stimulation by IL-12+IL-18. A) Relative expression levels of IL18R subunits by CD161 positive and CD161 negative sorted T cells and statistical significance from mRNA expression analyses after normalization and correction for multiple testing. ns= not significant, ** p<0.01, **** p<0.0001. **B)** Representative flow cytometry plots for IL18Rα expression in each T cell lineage, revealing CD161++, CD161+ and CD161− subsets in each (gated). **C)** GeoMFI of CD161 for CD161++ (green), CD161+ (blue) and CD161− (red) subsets in CD4+ and TCRγδ+ T cells correlated with geoMFI of IL18Rα. CD4 r^2=0.8463, p<0.0001, TCR-γδ r^2=0.6890, p<0.0001 (n=5). **D)** PBMC were stimulated overnight with 50ng/ml IL-12+IL-18. Representative flow cytometry plots for IFNγ expression by gated CD8+, CD4+ and TCRγδ+ CD3+ live lymphocytes. **E)** GeoMFI of CD161 for CD161++ (green), CD161+ (blue) and CD161− (red) subsets in CD8+, CD4+ and TCRγδ+ T cells correlated with percentage of each subset expressing IFNγ in response to overnight stimulation with IL-12+IL-18. CD8 r^2=0.8853, p<0.0001, CD4 r^2=0.9378, p<0.0001, TCRγδ r^2=0.8494, p<0.0001 (n=5). Correlations include data generated by Ayako Kurioka and Christian B. Willberg.

3.5 Discussion

MAIT cells are an innate-like T cell subset, unique both in terms of TCR expression and function. They uniformly express an invariant TCR Vα chain and respond to a bacterially-derived ligand presented on an evolutionary-conserved antigen presenting molecule (Reantragoon et al., 2013). Here, however, MAIT cells were shown to be related to other T lymphocytes through expression of the C-type lectin receptor CD161.

Previously, the CD161++CD8+ T cell population, predominantly comprised of Vα7.2+ MAIT cells, was found to possess a unique transcriptional profile related to a type 17 phenotype (Billerbeck et al., 2010). This genetic signature was predefined and apparent within naïve CD161++CD8+ T cells from UCB (Walker et al., 2012); this was despite the presence of minimal Vα7.2+ MAIT cells and a predominance of Vα7.2− cells at this age. Moreover, these CD161++CD8+ T cells already displayed a distinct pattern of chemokine receptors (eg. CCR6), cytokine receptors (eg. IL18R) and transcription factors (eg. RORγt). This suggests that a phenotypic/transcriptional signature, which is shared by the CD161++ Vα7.2− CD8+ T cell subset, primarily

defines the MAIT cell phenotype, rather than a specific TCR. This was highlighted by the fact that the Vα7.2− CD161++CD8+ T cell population was found to be heterogeneous in terms of both TCR α and β chain expression. Although there appeared to be an indication of bias in TCR expression, this would require a greater depth of sequencing – across more donors – to confirm.

NKT cells, like MAIT cells, are an innate-like T cell subset which express an invariant TCR recognising a non-peptide antigen presented by conserved antigen presenting molecules, such as CD1d (Bendelac et al., 2007). Furthermore, NKT cells with diverse TCR expression, but which are restricted by CD1d, have been identified and referred to as type II NKT cells (Gadola et al., 2002; Godfrey et al., 2004). Here, it was investigated whether diverse Vα7.2− cells represented an analogous type II MAIT cell subset. It appeared that Vα7.2− CD161++CD8+ T cells were not MR1 responsive in the majority of donors, however this does not rule out the possibility that this population may by reactive to other non-classical ligands, and warrants further investigation.

Despite differing ligand specificities, Vα7.2+ and Vα7.2− subsets display common characteristics. Both CD161++ subsets express elevated levels of the polarising transcription factors RORγt and PLZF. The central role of PLZF in directing the innate-like functions of NKT and MAIT cells (Savage et al., 2008), and other innate lymphocytes (Constantinides et al., 2014) has recently been revealed. The shared expression by Vα7.2− CD161++CD8+ T cells suggests that these cells may also display innate characteristics. Indeed, this transcription factor was expressed early during development of this population (Walker et al., 2012). Furthermore, both CD161++ populations express high levels of the IL18R (Ussher et al., 2014) and respond to innate stimulation by cytokines, specifically a combination of IL-12 and IL-18. It would be of interest to identify the location of the Vα7.2− CD161++CD8+ T cell population within the spectrum of CD8+ T cell phenotypes identified by mass

cytometry, particularly their position in relation to MAIT cells, which was precluded here by the absence of an isotope-tagged Vα7.2 antibody.

In addition to a shared phenotype across Vα7.2+ CD161++CD8+ MAIT and Vα7.2– CD161++CD8+ T cells, transcriptional analysis revealed CD161++CD8+ T cell differential transcripts to be enriched within other CD161 positive T lymphocytes, both amongst other CD8+ T cells and across T cells of different lineages. While the fact that microarrays were performed on different platforms and at different times prevents direct comparison of expression levels due to differences in microarray probes and sampling effects, raw data were normalised to allow comparison of ranked lists. Thus, leading edge analysis by GSEA identified a CD161-associated transcriptional signature that was differentially expressed in all CD161 positive T cells.

By focusing on significantly differentially expressed genes, the IL18R was found to be significantly upregulated in all CD161 positive T cells, with the levels expressed correlating with levels of CD161. Further, this was related to their ability to produce IFNγ in response to a combination of IL-12 and IL-18, in a TCR-independent manner. The combination of IL-12 and IL-18 has long been known to induce IFNγ production by NK cells (Chaix et al., 2008; Lauwerys et al., 1999), an innate cell type capable of making an early response to infection. Previously this was also identified to be a feature of MAIT cells (Ussher et al., 2014). Here other CD161 expressing, particularly CD161++, T lymphocytes were found to show a similar propensity to respond to cytokine stimulation by IL-12 and IL-18. This ability to respond to cytokine production by APCs (Bachmann et al., 2006; Rintahaka et al., 2008) suggests a means by which these cells could function in a range of diseases, including both infectious (Billerbeck et al., 2010; Chua et al., 2012; Fagundes et al., 2011; Kang et al., 2012) and autoimmune (Annibali et al., 2011; Kleinschek et al., 2009; Miyazaki et al., 2011; Poggi et al., 1999b), with expression of receptors for IL-12 and IL-18 being specifically implicated in the pathogenesis of rheumatoid arthritis (Aita et al., 2004).

CD161 expression has previously been associated with the ability to produce IL-17 across T cell lineages (Maggi et al., 2010) and here CD161 was found to mark cells with high expression of IL18R and capable of making innate-type responses to cytokine stimulation. CD161 is expressed early in development, being expressed on CD3+ thymocytes (Lanier et al., 1994; Martin et al., 2009), and CD4+ (Cosmi et al., 2008) and CD8+ T cells (Walker et al., 2012) expressing CD161 present in UCB. Furthermore, these cells already bear the hallmarks of their adult counterparts, suggesting that CD161 marks cells of a pre-committed phenotype. Therefore, CD161 marks a distinct phenotype which is independent of lineage, and identifies a family of related lymphocytes with innate characteristics that includes MAIT cells.

3.6 Summary

- CD161 expression defines specific T cell subsets, including CD8+, CD4+ and TCR$\gamma\delta$+
- T lymphocytes which express CD161 are enriched for a conserved transcriptional signature
- CD161 positive lymphocytes share an innate response to stimulation by IL-12+18

Appendix III.i: Table of Primers for TCR Sequencing, referring to section 3.3.3

TCR gene	External primer sequence		Internal primer sequence	
TRAV1	5′ AACTGCACGTACCAGACATC 3′		5′ GCACCCACATTTCTKTCTTAC 3′	
TRAV2	5′ GATGTGCACCAAGACTCC 3′		5′ CACTCTGTGTCCAATGCTTAC 3′	
TRAV3	5′ AAGATCAGGTCAACGTTGC 3′		5′ ATGCACCTATTCAGTCTCTGG 3′	
TRAV4	5′ CTCCATGGACTCATATGAAGG 3′		5′ ATTATATCACGTGGTACCAACAG 3′	
TRAV5	5′ CTTTTCCTGAGTGTCCGAG 3′		5′ TACACAGACAGCTCCTCCAC 3′	
TRAV6	5′ CACCCTGACCTGCAACTATAC 3′		5′ TGGTACCGACAAGATCCAG 3′	
TRAV7	5′ AGCTGCACGTACTCTGTCAG 3′		5′ ACAATTTGCAGTGGTACAGG 3′	
TRAV8-1	5′ CTCACTGGAGTTGGGATG 3′		5′ GTCAACACCTTCAGCTTCTC 3′	
TRAV8-2,8-4	5′ GCCACCCTGGTTAAAGG 3′		5′ AGAGTGAAACCTCCTTCCAC 3′	
TRAV8-3	5′ CACTGTCTCTGAAGGAGCC 3′		5′ TTTGAGGCTGAATTTAAGAGG 3′	
TRAV8-6	5′ GAGCTGAGGTGCAACTACTC 3′		5′ AACCAAGGACTCCAGCTTC 3′	
TRAV8-7	5′ CTAACAGAGGCCACCCAG 3′		5′ ATCAGAGGTTTTGAGGCTG 3′	
TRAV9-1, 9-2	5′ TGGTATGTCCAATATCCTGG 3′		5′ GAAACCACTTCTTTCCACTTG 3′	
TRAV10	5′ CAAGTGGAGCAGAGTCCTC 3′		5′ GAAAGAACTGCACTCTTCAATG 3′	
TRAV12-1, 12-2, 12-3	5′ CARTGTTCCAGAGGGAGC 3′		5′ AAGATGGAAGGTTTACAGCAC 3′	
TRAV13-1	5′ CATCCTTCAACCCTGAGTG 3′		5′ TCAGACAGTGCCTCAAACTAC 3′	
TRAV13-2	5′ CAGCGCCTCAGACTACTTC 3′		5′ CAGTGAAACATCTCTCTCTGC 3′	
TRAV14	5′ AAGATAACTCAAACCCAACCAG 3′		5′ AGGCTGTGACTCTGGACTG 3′	
TRAV16	5′ AGTGGAGCTGAAGTGCAAC 3′		5′ GTCCAGTACTCCAGACAACG 3′	
TRAV17	5′ GGAGAAGAGGATCCTCAGG 3′		5′ CCACCATGAACTGCAGTTAC 3′	
TRAV18	5′ TCCAGTATCTAAACAAAGAGCC 3′		5′ TGACAGTTCCTTCCACCTG 3′	
TRAV19	5′ AGGTAACTCAAGCGCAGAC 3′		5′ TGTGACCTTGGACTGTGTG 3′	
TRAV20	5′ CACAGTCAGCGGTTTAAGAG 3′		5′ TCTGGTATAGGCAAGATCCTG 3′	
TRAV21	5′ TTCCTGCAGCTCTGAGTG 3′		5′ AACTTGGTTCTCAACTGCAG 3′	
TRAV22	5′ GTCCTCCAGACCTGATTCTC 3′		5′ CTGACTCTGTGAACAATTTGC 3′	
TRAV23	5′ TGCTTATGAGAACACTGCG 3′		5′ TGCATTATTGATAGCCATACG 3′	
TRAV24	5′ CTCAGTCACTGCATGTTCAG 3′		5′ TGCCTTACACTGGTACAGATG 3′	
TRAV25	5′ GGACTTCACCACGTACTGC 3′		5′ TATAAGCAAAGGCCTGGTG 3′	
TRAV26-1	5′ GCAAACCTGCCTTGTAATC 3′		5′ CGACAGATTCACTCCCAG 3′	
TRAV26-2	5′ AGCCAAATTCAATGGAGAG 3′		5′ TTCACTTGCCTTGTAACCAC 3′	
TRAV27	5′ TCAGTTTCTAAGCATCCAAGAG 3′		5′ CTCACTGTGTACTGCAACTCC 3′	
TRAV29	5′ GCAAGTTAAGCAAAATTCACC 3′		5′ CTGCTGAAGGTCCTACATTC 3′	
TRAV30	5′ CAACAACCAGTGCAGAGTC 3′		5′ AGAAGCATGGTGAAGCAC 3′	
TRAV34	5′ AGAACTGGAGCAGAGTCCTC 3′		5′ ATCTCACCATAAACTGCACG 3′	
TRAV35	5′ GGTCAACAGCTGAATCAGAG 3′		5′ ACCTGGCTATGGTACAAGC 3′	
TRAV36	5′ GAAGACAAGGTGGTACAAAGC 3′		5′ ATCTCTGGTTGTCCACGAG 3′	
TRAV38-1, 38-2	5′ GCACATATGACACCAGTGAG 3′		5′ CAGCAGGCAGATGATTCTC 3′	
TRAV39	5′ CTGTTCCTGAGCATGCAG 3′		5′ TCAACCACTTCAGACAGACTG 3′	
TRAV40	5′ GCATCTGTGACTATGAACTGC 3′		5′ GGAGGCGGAAATATTAAAGAC 3′	
TRAV41	5′ AATGAAGTGGAGCAGAGTCC 3′		5′ TTGTTTATGCTGAGCTCAGG 3′	
TRAC	5′ GACCAGCTTGACATCACAG 3′		5′ TGTTGCTCTTGAAGTCCATAG 3′	
TRBV2	5′ TCGATGATCAATTCTCAGTTG 3′		5′ TTCACTCTGAAGATCCGGTC 3′	
TRBV3-1	5′ CAAAATACCTGGTCACACAG 3′		5′ AATCTTCACATCAATTCCCTG 3′	
TRBV4-1, 4-2, 4-3	5′ TCGCTTCTCACCTGAATG 3′		5′ CCTGCAGCCAGAAGACTC 3′	
TRBV5-1, 5-3, 5-4	5′ GATTCTCAGGKCKCCAGTTC 3′		5′ CTTGGAGCTGGRSGACTC 3′	
TRBV5-5, 5-6, 5-7, 5-8	5′ GTACCAACAGGYCCTGGGT 3′		5′ TCTGAGCTGAATGTGAACG 3′	

TRBV6-1, 6-2, 6-3, 6-5, 6-6, 6-7, 6-8, 6-9	5′	ACTCAGACCCCAAAATTCC	3′	5′	GTGTRCCCAGGATATGAACC	3′
TRBV6-4	5′	ACTGGCAAAGGAGAAGTCC	3′	5′	TGGTTATAGTGTCTCCAGAGC	3′
TRBV7-1, 7-2, 7-3	5′	TRTGATCCAATTTCAGGTCA	3′	5′	TCYACTCTGAMGWTCCAGCG	3′
TRBV7-4, 7-6, 7-7, 7-8, 7-9	5′	GSWTCTYTGCAGARAGGCC	3′	5′	TGRMGATYCAGCGCACA	3′
TRBV9	5′	GATCACAGCAACTGGACAG	3′	5′	GTACCAACAGAGCCTGGAC	3′
TRBV10-1, 10-2, 10-3	5′	TGTWCTGGTATCGACAAGACC	3′	5′	TCCYCCTCACTCTGGAGTC	3′
TRBV11-1, 11-2, 11-3	5′	CGATTTTCTGCAGAGACGC	3′	5′	GACTCCACTCTCAAGATCCA	3′
TRBV12-3, 12-4, 12-5	5′	ARGTGACAGARATGGGACAA	3′	5′	CYACTCTGARGATCCAGCC	3′
TRBV13	5′	AGCGATAAAGGAAGCATCC	3′	5′	CATTCTGAACTGAACATGAGC	3′
TRBV14	5′	CCAACAATCGATTCTTAGCTG	3′	5′	ATTCTACTCTGAAGGTGCAGC	3′
TRBV15	5′	AGTGACCCTGAGTTGTTCTC	3′	5′	ATAACTTCCAATCCAGGAGG	3′
TRBV16	5′	GTCTTTGATGAAACAGGTATGC	3′	5′	GAAAGATTTTCAGCTAAGTGCC	3′
TRBV17	5′	CAGACCCCCAGACACAAG	3′	5′	TGTTCACTGGTACCGACAG	3′
TRBV18	5′	CATAGATGAGTCAGGAATGCC	3′	5′	CGATTTTCTGCTGAATTTCC	3′
TRBV19	5′	AGTTGTGAACAGAATTTGAACC	3′	5′	TTCCTCTCACTGTGACATCG	3′
TRBV20-1	5′	AAGTTTCTCATCAACCATGC	3′	5′	ACTCTGACAGTGACCAGTGC	3′
TRBV23-1	5′	GCGATTCTCATCTCAATGC	3′	5′	GCAATCCTGTCCTCAGAAC	3′
TRBV24-1	5′	CCTACGGTTGATCTATTACTCC	3′	5′	GATGGATACAGTGTCTCTCGA	3′
TRBV25-1	5′	ACTACACCTCATCCACTATTCC	3′	5′	CAGAGAAGGGAGATCTTTCC	3′
TRBV27, 28	5′	TGGTATCGACAAGACCCAG	3′	5′	TTCYCCCTGATYCTGGAGTC	3′
TRBV29-1	5′	TTCTGGTACCGTCAGCAAC	3′	5′	TCTGACTGTGAGCAACATGAG	3′
TRBV30	5′	TCCAGCTGCTCTTCTACTCC	3′	5′	AGAATCTCTCAGCCTCCAGAC	3′
TRBC	5′	TAGAACTGGACTTGACAGCG	3′	5′	TTCTGATGGCTCAAACACAG	3′

TRAV family	# of sequences	# of donors (out of 3)	TRAJ	# of sequences	# of donors (out of 3)	CDR3
TRAV12	11	3	TRAJ12*01	1	1	YLCVVNAWMDSSYKLIFGSG
			TRAJ17*01	1	1	YLCAMSKAAGNKLTFGGG
			TRAJ20*01	1	1	YLCAVLSNDYKLSFGAG
			TRAJ27*01	1	1	YLCAVTTNAGKSTFGDG
			TRAJ31*01	1	1	YLCVVNRNNNARLMFGDG
			TRAJ33*01	1	1	YLCVVDVXDSXYQLXWGXG
			TRAJ43*01	2	1	YLCAVNEDDMRFGAG
						YLCAVNDMRFGAG
			TRAJ44*01	1	1	YLCAVTGRGGTASKLTFGTG
			TRAJ57*01	1	1	YLCAMDGSEKLVFGKG
			TRAJ6*01	1	1	YLCVVRLASGGSYIPTFGRG
TRAV13-1	5	2	TRAJ26*01	1	1	YFXADRVHGQNFVFGPG
			TRAJ28*01	1	1	YFCAENMGDSGAGSYQLTFGKG
			TRAJ44*01	1	1	YFCAENMKDTGTASKLTFGTG
			TRAJ49*01	2	2	YFCAEPGYTGNQFYFGTG
						YFCAASKGNTGNQFYFGTG
TRAV8	4	2	TRAJ13*01	1	1	YFXXXNARSGGYQKVTFGIG
			TRAJ20*01	1	1	YFCAVSN*RSNDYKLSFGAG
			TRAJ36*01	1	1	YFCAVSLRRGANNLFFGTG
			TRAJ48*01	1	1	YFCAVSENFGNEKLTFGTG

Appendix III.ii: Predominant alpha chains detected to be expressed by Vα7.2$-$ CD161++ CD8+ T cell populations in 3 donors, the J regions they were paired with and the corresponding complementarity determining region (CDR) 3 amino acid sequence. * indicates a stop codon.

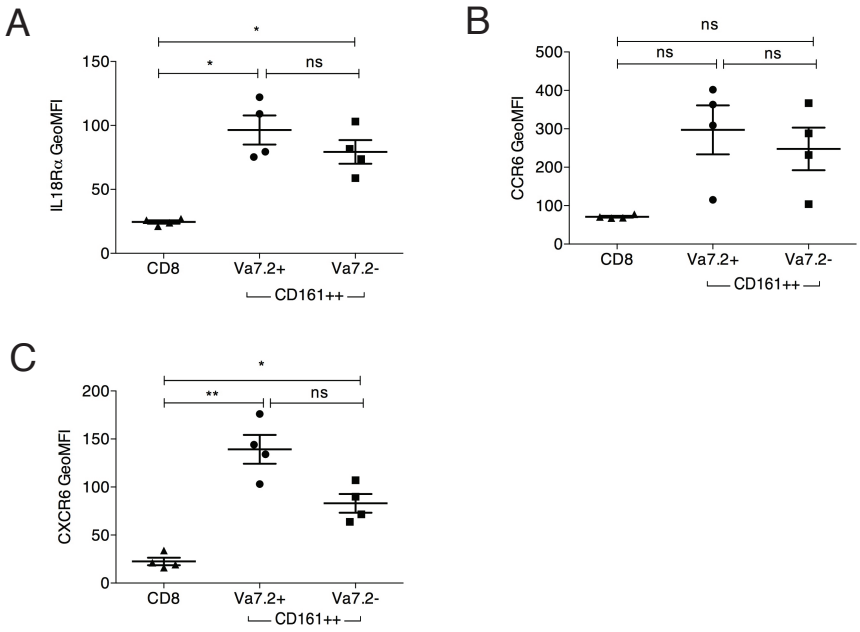

Appendix III.iii: Vα7.2- CD161++ CD8+ T cells reflect the phenotype of Vα7.2+ CD161++ MAIT cells. GeoMFI of IL18Ra (**A**), CCR6 (**B**) and CXCR6 (**C**) by Va7.2+ and Va7.2- CD161++ subsets, compared to conventional (non-CD161++) CD8+ T cells, as detected by flow cytometry, (n=4). **p<0.01, *p<0.05 and ns = not significant by one-way ANOVA with Tukey's multiple comparisons test.

Appendix III.iv: Transcriptional comparison of CD161+ vs CD161- CD8+ T cells, upregulated genes shared or unique from CD161++ CD8+ T cells

Upregulated in both			Upregulated in CD161+CD8+ only		
Symbol	logFC	P.Value	Symbol	logFC	P.Value
ABCA2	1.404479835	0.01706444	AKR1C3	2.833808162	0.00252577
ADAM19	1.574390852	0.031828302	ANXA1	0.913256936	0.046793684
ADAM8	1.557668293	0.01520899	ANXA4	1.742091633	0.015198587
ADRB2	1.872160779	0.004392261	ARP10	1.702049361	0.045622303
AGPAT4	1.624739706	0.0208177	ASCL2	1.771939079	0.005682058
AHNAK	1.240505241	0.027996503	B3GAT1	1.947445869	0.007082106
ANXA2	0.93762162	0.048203297	BFSP1	1.507269536	0.048781677
ANXA2P1	0.9383045	0.04607879	C1orf21	1.790809344	0.006913213
ANXA2P3	1.62525215	0.00360344	CD226	1.237781421	0.03095305
ATP2B4	1.242701513	0.02190406	CD300A	1.74640419	0.00631972
AUTS2	1.636112123	0.01520899	CLDND2	1.672651524	0.018102195
B4GALT5	1.184171901	0.031721084	CLIC3	1.278102574	0.025250616
BHLHB2	1.986259629	0.034095133	CMKLR1	1.676658662	0.025055635
C17orf58	1.362642187	0.025055635	CTSC	0.959752903	0.046240124
C1orf24	1.576235341	0.043778859	CX3CR1	1.488130894	0.007082106
C6orf59	1.949005152	0.02480654	DLEC1	1.400197978	0.039388222
CACNA2D2	1.715054265	0.00491685	DRD3	1.252542536	0.031736342
CACNB3	1.014201991	0.045622303	EFHD2	1.125897152	0.035909939
CAMK2N1	1.40287717	0.018387903	ENPP5	1.436847707	0.031815777
CCR6	2.033019254	0.00252577	ERBB2	1.745142778	0.018387903
CD58	1.651902548	0.006862275	FASLG	1.697985575	0.00819438
CENTD3	1.857650535	0.039686951	FCGR3A	2.28033217	0.005267527
CENTG2	2.09218944	0.008989262	FCRLM2	1.161228878	0.032564299
CLCF1	1.446784342	0.018903951	FLJ11783	1.399825567	0.044221766
CMTM1	1.005659409	0.046797786	FLJ14213	1.613615537	0.023521582
COLQ	1.863481125	0.009369868	FLJ20699	1.708404606	0.006742411
CST7	1.585350304	0.003847419	FOXD1	1.767260255	0.017436593
DFNB31	1.037761458	0.045658065	FOXD2	1.186240141	0.025168686
DMN	1.91801301	0.011102488	GARNL4	1.548633166	0.039388222
DNAPTP6	1.620880828	0.032791563	GNLY	1.515553246	0.039386732
DPY19L1	1.457670487	0.012225015	GPR56	1.730975916	0.00360344
EDG8	1.796096416	0.006742411	GZMB	1.853318763	0.007082106
ELOVL6	1.680399646	0.020423533	GZMH	1.460846213	0.013070832
FAM91A2	1.279110425	0.037817073	HRASLS3	1.078797422	0.031828302
FCHO2	1.761155685	0.039388222	IQGAP2	1.041509203	0.035608593
FEZ1	2.606791529	0.008157996	ITGAM	1.611332181	0.017825433
FHOD1	1.198421706	0.038557526	JAZF1	1.368695135	0.039388222
FLJ20245	1.58398446	0.036305935	KATNAL1	1.347568089	0.025055635
FLJ46831	1.574532358	0.012739225	KIAA1817	1.23520456	0.01554345
GDPD5	1.573265229	0.013434245	KIF19	2.015133889	0.030851507
GPR114	1.733393794	0.01002322	KLRD1	1.694843222	0.010069226
GZMA	1.214958951	0.035738478	KSP37	2.055946771	0.00252577
HOP	1.687485886	0.018387903	LGALS1	1.384874853	0.018739764
IGSF4	2.549866843	0.00252577	LILRB1	1.626971002	0.031828302
IL12RB2	1.189657381	0.017574336	LOC197135	1.322204678	0.017299474
IL18R1	2.093860916	0.00491685	LOC440910	2.141282827	0.039945923
IL18RAP	3.424322876	0.001662571	LOC642233	1.369380898	0.028520631
KIAA1754L	1.624205659	0.031828302	LOC645442	1.423344138	0.020485733
KIF5C	1.216050429	0.027853914	LOC647326	0.956741153	0.039388222
KLRB1	4.36933104	6.95E-07	LOC647881	1.530434325	0.010069226
KLRC1	2.905259059	0.001662571	LOC648517	2.327164161	0.020797181

KLRG1	1.588450836	0.010069226	MGC4677	1.89810664	0.031721084
LAG3	1.591204532	0.010069226	NKG7	1.128662537	0.029070215
LATS2	2.423596292	0.003280223	OSBPL5	1.205551835	0.029851116
LIM2	2.337872672	0.001662571	OTOF	1.557776903	0.031828302
LOC644846	1.477396047	0.024053558	PAK6	1.507733594	0.025857821
LOC648470	1.332348768	0.031828302	PALLD	2.664599388	0.003297131
LPAL2	1.551429758	0.008264591	PAM	1.44391955	0.029531263
LTK	1.917798982	0.015040792	PDGFRB	2.576344051	0.003216793
MAF	2.034297383	0.027146389	PHLDB2	1.67683315	0.029851116
MATN2	1.273919912	0.025609928	PITX2	1.103367543	0.049292003
ME1	2.241784095	0.009954379	PODN	2.211998942	0.00252577
METRNL	1.496761941	0.024401138	PPP1R14C	1.84629953	0.031943618
MGC34830	2.171773576	0.00252577	PPP2R1B	1.434356566	0.012298847
MGC52282	1.998438683	0.017240888	PRSS23	2.121096741	0.006357028
MPST	1.096759088	0.021935627	PYHIN1	1.497444263	0.017436593
MYO1F	1.43165323	0.039388222	RGS17	1.398349037	0.010438248
NMUR1	1.992406161	0.002228176	RHOBTB3	2.255585049	0.010069226
NPC1	1.180650736	0.031565979	ROPN1L	1.216668118	0.032900483
NTN4	1.629196868	0.028712431	RUTBC2	1.434695547	0.025916371
PCP4	3.247484069	0.001621429	SATB2	1.767349688	0.021951786
PDZD4	2.196167065	0.00585741	SIGLECP3	1.69692044	0.010069226
PLCB1	1.710464806	0.024179602	SLC15A4	1.397269429	0.016894731
PLEKHF1	1.341732371	0.013070832	SLC1A7	2.77675284	0.013155904
PLEKHG3	1.880748224	0.010069226	SLCO4C1	1.514402803	0.041701571
PPP2R2B	1.352725715	0.025168686	SPON2	2.365356319	0.010069226
PRDM1	1.941415174	0.004861389	SSTR1	1.251431161	0.028998896
PRF1	1.471403538	0.008989262	SUSD1	1.293121816	0.030741205
PTGDR	1.703778948	0.007082106	TBKBP1	1.432514081	0.02375288
PTGDS	2.435404248	0.007082106	TGFBR3	1.52056519	0.014677227
PTMS	1.776513812	0.007766331	TM4SF19	2.658852606	0.006742411
RASSF4	1.473130524	0.044229163	TMCC3	1.549192174	0.035849278
RHOC	1.393975808	0.021037339	TTYH2	1.268926592	0.025250616
RORC	1.970073457	0.008157996	TXNDC3	2.239588145	0.015040792
RPS24	1.974642119	0.01520899	WIPI1	1.546177631	0.017828543
RTKN	1.222490853	0.03045571	ZFHX1B	1.66811531	0.037503742
SLAMF1	1.258572797	0.045782839	ZNF365	1.447169124	0.045225704
SLAMF7	2.14370193	0.018124657	ZNF537	2.282010026	0.001662571
SLC4A4	1.761748892	0.017436593			
SMAD3	1.145362008	0.039650452			
SMAD7	1.623519206	0.028520631			
SNTB2	0.997900545	0.041982159			
STOM	1.186707177	0.047414491			
SYNE2	1.287508252	0.035738478			
SYTL2	1.875696493	0.007503273			
TFEB	1.344653925	0.010069226			
TNFRSF1B	1.56112119	0.035473431			
TNFRSF4	1.54621269	0.031828302			
TNFSF14	1.676029635	0.009071286			
USP54	1.426698557	0.034742318			
UST	1.122061091	0.035999545			
VCL	1.335655412	0.024478999			
VLDLR	1.293941597	0.017574336			
WDR67	1.018842732	0.041435151			

YPEL1	1.408239633	0.008552024
ZBTB16	2.615628753	0.002228176
ZFYVE28	1.674949777	0.019882847

Appendix III.v: Transcriptional comparison of CD161+ vs CD161- CD8+ T cells, downregulated genes shared or unique from CD161++ CD8+ T cells

Downregulated in both			Downregulated in CD161+CD8+ only		
Symbol	logFC	P.Value	Symbol	logFC	P.Value
15E1.2	-1.266552182	0.032153432	ABCG1	-1.242882705	0.042360837
ABCD2	-1.150788799	0.041544357	ANAPC2	-1.4288945	0.031828302
ABLIM1	-2.160275896	0.0119721	ARID5A	-1.441151596	0.02466312
ACCN2	-1.899378008	0.012109755	C10orf35	-1.094489087	0.038168793
ACTN1	-2.041190403	0.031386961	C5orf13	-2.027750675	0.039610335
AEBP1	-2.184230597	0.039610335	ERGIC1	-2.186202686	0.0119721
AES	-1.443939107	0.036923854	GOSR1	-0.94730483	0.047414491
AGMAT	-2.610574157	0.001662571	HK1	-1.718058466	0.013047474
AK5	-1.635677949	0.024725197	KBTBD9	-1.164679693	0.041598639
ALDH6A1	-1.322559156	0.031815777	KCNQ1	-1.677448167	0.024397141
ALDH7A1	-1.556745762	0.016635671	LASS6	-1.611588068	0.017436593
ALS2CR13	-1.383937182	0.035348737	LOC550112	-1.096316856	0.043778859
AP1G1	-1.247791836	0.047588859	MARCH3	-1.969296566	0.004668412
AP1GBP1	-1.216486402	0.039388222	MDN1	-1.191514131	0.044561661
APBB1	-1.805520955	0.007082106	OPA3	-1.296804698	0.045622303
APOBEC3F	-2.254802046	0.020127145	OPLAH	-1.179475473	0.029386475
APPBP2	-1.442647059	0.031828302	PADI4	-2.032414969	0.005103581
ARHGAP25	-1.650559489	0.028998896	PAG1	-1.040956976	0.047588859
ARHGAP30	-2.293992294	0.032114038	POMT1	-1.506944564	0.035738478
ARMCX1	-2.111039835	0.032721954	RPS6KA3	-1.197383601	0.039768851
ARMETL1	-1.089988394	0.045546952	SCARB1	-0.954160669	0.040165212
ASB7	-1.684164017	0.02897066	SRP54	-1.004660139	0.045622303
ATP5G2	-1.492966691	0.018116368	TCF8	-1.542551081	0.010069226
ATP8B2	-1.118240027	0.043409004	THAP5	-1.349362252	0.031828302
BRWD1	-1.182659956	0.045622303	UBE1	-1.194457777	0.047048869
C11orf31	-1.133607908	0.025250616	UBE2E2	-1.612855322	0.010352417
C14orf101	-1.532480744	0.030851507	USP21	-1.400128484	0.018093796
C14orf126	-1.718800573	0.033778665			
C14orf46	-1.155239346	0.028712431			
C15orf44	-1.514315725	0.037503742			
C16orf35	-1.923882433	0.003838189			
C19orf48	-1.223719434	0.049990461			
C1orf108	-2.327381056	0.014260707			
C1orf43	-1.935297421	0.033778665			
C1orf80	-1.716355791	0.01890879			
C20orf32	-1.323431157	0.040124313			
C21orf25	-1.228097572	0.01706444			
C21orf56	-1.32781584	0.045225704			
C3orf63	-1.224979751	0.022603382			
C9orf132	-1.446979061	0.025250616			
CACHD1	-1.961215968	0.047013171			
CASC4	-1.401282143	0.024725197			
CASP2	-2.185576857	0.007503273			
CCDC57	-1.473362847	0.013155904			
CD55	-1.202976956	0.046547284			
CD8B	-1.97623754	0.029386475			
CD8B1	-2.080439098	0.023521582			
CDC42	-1.828158941	0.004483616			
CDCA7L	-2.930311009	0.004605112			
CECR1	-1.488729001	0.032900483			
CHI3L2	-1.665061002	0.031828302			

CITED4	-1.567132759	0.007766331
CLEC11A	-2.485111327	0.01520899
CLEC2D	-1.311390266	0.038168793
CNN2	-2.443313128	0.018825312
CNN3	-1.71104392	0.010361815
COG5	-2.121669318	0.033252932
COL6A3	-1.787094496	0.03455457
CPNE1	-1.636853136	0.031019934
CR2	-1.680768368	0.017240888
CRK	-1.263114584	0.039388222
CRLF3	-1.960884205	0.016659918
CTF8	-2.132861006	0.015198587
CXorf34	-1.245303772	0.023236527
DDB1	-1.544941317	0.023236527
DDX31	-1.792251968	0.007082106
DERPC	-1.476490837	0.025250616
DGKA	-1.247106388	0.030911143
DHFR	-1.035869203	0.044001083
DHX9	-1.542254729	0.048965929
DIABLO	-1.419052774	0.016894731
DIDO1	-1.486669452	0.029851116
DKFZp761P042	-1.64803823	0.023977647
DOCK9	-1.584506057	0.033437635
DPH2	-1.910964014	0.016650095
DSC1	-2.518675268	0.005682058
DSCR1L2	-2.305635876	0.00474535
EDAR	-2.757281308	0.027853914
EEF1G	-1.182364765	0.041670788
EI24	-1.189927677	0.040348275
EIF4G2	-1.470809721	0.046668805
ENSA	-1.585104455	0.047414491
EPB41	-2.961944338	0.025612928
ERBB2IP	-1.279998184	0.014527806
ERCC4	-1.259464639	0.043009545
F8A3	-2.55921172	0.012298847
FAF1	-1.624398131	0.030712002
FAM102A	-1.944258194	0.030710295
FAM10A4	-1.367077983	0.032900483
FAM55C	-1.743952778	0.035381712
FASTKD2	-1.136738088	0.032900483
FBLN2	-2.643157221	0.038912184
FBLN5	-1.569789753	0.014677227
FLJ20152	-2.256034039	0.006913213
FLJ20718	-2.01018822	0.018102195
FLJ35801	-3.402830546	0.017436593
FLJ40722	-1.096328995	0.049941003
FLJ45645	-1.735869795	0.012196832
FLNB	-1.629749027	0.01800719
GART	-1.397154057	0.043778859
GCC2	-1.418412346	0.023521582
GIYD1	-1.663773403	0.040165212
GIYD2	-2.005484743	0.031815777
GPR89A	-1.295363465	0.03295169

GRAP	-2.06155789	0.010718928
GTF2I	-1.391306098	0.039388222
GTF2IP1	-1.808675954	0.023553585
GTF2IRD2	-1.269221659	0.01554345
HEXA	-1.344394195	0.039388222
HMGN2	-1.599776176	0.009369868
HNRPA1	-2.437269465	0.00252577
HPCAL1	-2.611292003	0.003280223
HSF1	-1.543688978	0.011748984
HSPD1	-1.458650756	0.048781677
HSU79303	-1.659921828	0.033778665
IFI6	-1.440249876	0.035909939
IGFBP6	-1.206541787	0.039610335
IL6R	-2.566097808	0.010585465
IL6ST	-1.58285832	0.042355788
IPO7	-1.273987943	0.033252932
IRS1	-1.887274817	0.0119721
ITGA6	-2.200799974	0.008914106
KCNMB4	-2.194964888	0.015516946
KENAE	-1.250345275	0.02466397
KIAA0251	-2.401342327	0.00360344
KIAA0265	-1.081684164	0.033778665
KIAA1160	-1.479906298	0.040165212
KIAA1967	-1.454141359	0.03172652
KIAA2010	-1.323679579	0.039388222
LATS1	-2.263229109	0.005628181
LBH	-1.668618118	0.029851116
LCK	-2.436920435	0.005054251
LDLRAP1	-1.588676546	0.041670788
LDOC1	-1.525852613	0.015040792
LETMD1	-1.770096377	0.013174027
LGALS3BP	-1.948865685	0.02201652
LGMN	-2.008629085	0.009817681
LIN7C	-1.472352684	0.031828302
LINS1	-1.845109553	0.006913213
LOC136306	-2.194386128	0.00685181
LOC144983	-1.806852848	0.006913213
LOC147804	-1.711746698	0.046668805
LOC344620	-2.051676981	0.012298847
LOC346950	-1.735205598	0.037503742
LOC399942	-1.760379265	0.0371886
LOC400721	-1.143052998	0.026083955
LOC401431	-1.66469322	0.028998896
LOC402562	-1.796619446	0.032900483
LOC440667	-1.429076817	0.022428474
LOC441032	-1.995685732	0.024725197
LOC642817	-2.247495475	0.020792453
LOC643033	-2.283228271	0.009954379
LOC643300	-1.875104438	0.026248706
LOC643790	-1.264788242	0.025250616
LOC644037	-1.996974471	0.037407982
LOC644134	-1.344417122	0.046668805
LOC644253	-1.468507227	0.039388222

LOC644295	-1.249308178	0.046668805
LOC645001	-1.500200261	0.039610335
LOC645385	-1.67633555	0.024053558
LOC645436	-1.871899158	0.017299474
LOC647615	-1.59815724	0.01918771
LOC648210	-1.865575573	0.020348739
LOC648676	-2.748878735	0.002228176
LOC648763	-1.123596317	0.043778859
LOC649095	-3.301698092	0.012644796
LOC649150	-1.344661039	0.036466983
LOC649270	-1.082652946	0.031815777
LOC650230	-1.528134234	0.039388222
LOC650751	-2.067175108	0.017139824
LOC650795	-2.173008133	0.025168686
LOC651610	-1.318227261	0.027996503
LOC652605	-1.099972314	0.047414491
LOC652615	-1.281978953	0.037184059
LOC653105	-1.968547369	0.006913213
LOC653119	-1.748998056	0.035608593
LOC653133	-1.515351328	0.018093796
LOC653141	-1.812230982	0.032900483
LOC653491	-1.571812561	0.023977647
LOC653542	-2.058042797	0.01520899
LOC653743	-2.352441689	0.005628181
LOC653980	-1.63996127	0.008552024
LOC653994	-1.824916824	0.030712002
LOC654052	-1.307166721	0.028998896
LOC654116	-1.65064338	0.007082106
LOC654189	-1.337163173	0.026083955
LOC90624	-1.261387676	0.037305075
LRRC16	-2.298743524	0.00631972
LYPD3	-1.738559836	0.029851116
MAEA	-1.729875172	0.013434245
MAGED1	-2.328361367	0.003216793
MAGED2	-1.906255219	0.01920988
MAML2	-2.270998254	0.00491685
MAN1C1	-1.806016633	0.036155269
MAP2K6	-1.198715062	0.033778665
MAPK14	-1.541570848	0.023977647
MATR3	-1.941124998	0.037774477
MDM4	-2.800723455	0.006056381
MEIS3P1	-1.703096501	0.0341034
MEST	-2.105016103	0.011102488
MGC17330	-1.20298771	0.047188735
MGC33556	-1.979495668	0.039388222
MMP28	-1.956736371	0.00685181
MTUS1	-1.994606606	0.0119721
MXRA8	-1.946554444	0.003280223
MYB	-2.107960818	0.007082106
N6AMT1	-1.154980387	0.026276026
NBEA	-1.77637993	0.044161383
NDRG3	-2.093324144	0.027964882
NET1	-1.578993011	0.046419498

NGRN	-1.7503563	0.014555636
NOC4L	-1.259847467	0.02656233
NOG	-3.177183649	0.012635234
NOMO2	-1.63758709	0.018102195
NOMO3	-2.472108375	0.003216793
NPAS2	-1.842350513	0.004111137
NRF1	-1.252186858	0.024179602
NUAK2	-2.554720664	0.011677713
NUP50	-1.097398353	0.042958364
OAS2	-1.973505342	0.010069226
OBSCN	-1.330906209	0.046668805
OGFOD1	-1.530883755	0.025179532
OPN3	-1.421208406	0.043812512
ORC5L	-1.384518654	0.025250616
PABPC3	-1.488309526	0.031355885
PATZ1	-2.024546251	0.025916371
PCSK5	-1.406973275	0.018525229
PDE6B	-1.595694152	0.009369868
PDE7A	-1.633097268	0.031721084
PECAM1	-1.566765755	0.045622303
PGPEP1	-1.587276521	0.010069226
PICALM	-1.304281524	0.045807916
PKM2	-1.51605076	0.048279161
PLAG1	-1.757337112	0.033778665
PLD3	-1.981111984	0.007082106
PLEKHB1	-1.628589906	0.020348739
PMS2	-1.60304884	0.028712431
PPAP2A	-1.378871388	0.024705773
PPP2R5D	-2.264260862	0.003216793
PRKAR1B	-2.40468765	0.00252577
ProSAPiP1	-1.166138167	0.016635671
PRRT1	-1.252057653	0.045945527
PSEN1	-1.634556459	0.010069226
PTD004	-1.611890564	0.012631365
RAB11B	-1.784977092	0.02466397
RAB43	-1.333418712	0.035348737
RAB6IP1	-1.303050457	0.035074477
RABL2A	-1.546163571	0.045792769
RABL2B	-1.315945173	0.049842024
RABL3	-1.275016019	0.044626461
RASGRP2	-1.83353097	0.033785011
RASSF5	-1.541044751	0.032502003
REG4	-3.166670945	0.002228176
RNF38	-1.651612265	0.0119721
RNU25	-1.346138687	0.033778665
RPL22	-1.198271411	0.032153432
RPL32	-1.107129594	0.043778859
RTN4	-2.002547815	0.042494231
RUNX3	-1.679949188	0.007082106
SCAND2	-1.158077432	0.02316366
SCML4	-1.518116867	0.04447052
SDCCAG8	-1.165421199	0.025714659
SEC14L2	-1.917838371	0.017252632

SELL	-1.940612213	0.040348275
SERPINE2	-2.208143607	0.010069226
SFI1	-1.417905056	0.034793416
SFRP5	-2.673295663	0.017436593
SFXN1	-1.372999063	0.015366125
SH3MD4	-1.089807581	0.041435151
SIRPB2	-2.425064897	0.017082631
SIRPG	-1.278912649	0.039388222
SLC16A10	-2.012210535	0.016894731
SLC25A15	-0.959630514	0.042530707
SLC25A26	-1.557342548	0.008552024
SLC7A6	-1.325187586	0.033785011
SLC7A8	-2.27393986	0.004991378
SMAP1L	-1.499248981	0.02466312
SNORD107	-1.054338966	0.02466397
SNX14	-1.564473759	0.044566027
SON	-1.860623951	0.04878206
SOX8	-1.921937437	0.017436593
SPG21	-1.687386628	0.02637119
SPINT2	-2.229024199	0.043778859
SPTBN1	-1.342641757	0.040423502
ST3GAL1	-2.437442002	0.017436593
STK16	-2.047441387	0.025179532
SUMF2	-2.440522969	0.004861389
TAPBP	-1.999932449	0.041563621
TCF7	-1.750559779	0.023236527
THAP4	-1.837449527	0.045999049
THAP7	-1.500033783	0.029386475
THEM4	-1.362012085	0.036232944
THOC3	-1.822127066	0.04447052
TMEM46	-2.027161439	0.007503273
TOP1MT	-2.065403212	0.017436593
TPST1	-1.557137839	0.031721084
TRIM14	-1.940520695	0.031943618
TRUB1	-1.128166161	0.027853914
TSC1	-1.824214197	0.034894002
TSGA14	-1.328174345	0.024725197
UBASH3A	-1.771659345	0.006742411
UBE2V1	-1.860581303	0.012298847
USP53	-2.247027287	0.014555636
VASP	-1.235199603	0.042530707
VIPR1	-1.294421721	0.035738478
VNN2	-2.521512944	0.00252577
WBSCR1	-2.343953159	0.038168793
WHSC1L1	-1.45131401	0.028680591
YPEL2	-1.340079052	0.019376307
YWHAZ	-2.423572066	0.006913213
ZC3H11A	-1.369010023	0.024725197
ZIK1	-1.306198623	0.028520631
ZNF135	-1.285669719	0.028839468
ZNF136	-1.633481757	0.004543607
ZNF278	-1.84029579	0.042494231
ZNF285A	-1.356479402	0.045225704

ZNF286	-1.720184291	0.046247121
ZNF471	-1.33602661	0.006913213
ZNF586	-2.080051377	0.022253383
ZNF609	-1.382272278	0.01520899
ZNF611	-1.16092137	0.034557355
ZNF667	-1.366613477	0.025916371

Appendix III.vi: Transcriptional comparison of CD161+ vs CD161- CD4+ T cells, upregulated genes shared or unique from CD161++ CD8+ T cells

Upregulated in both			Upregulated in CD161+CD4+ only		
Symbol	logFC	P.Value	Symbol	logFC	P.Value
AGPAT4	1.518523776	0.045692392	ANKRD44	2.24108164	0.029277867
AIM2	1.760059709	0.0169281	BCYRN1	1.448759124	0.048897511
ATXN2L	2.104766707	0.021499402	BLZF1	1.785661284	0.033275651
AUTS2	1.34943779	0.035429465	C14orf82	1.914877166	0.037731234
CSF2RA	1.556170808	0.03537636	CASP8	2.229926994	0.020327246
ELOVL4	1.339428729	0.045692392	CATSPER2	1.372064532	0.045792521
ELOVL6	1.699282699	0.043720498	CCBE1	1.490356587	0.044728366
FAM38A	1.415877544	0.034935013	CCR9	2.583922086	0.045692392
IL18RAP	2.768928649	0.008596419	CYCSL1	2.255851385	0.012377766
IL4I1	2.387513146	0.045792521	CYTH3	2.337839537	0.04663728
KIT	2.274699832	0.022319103	DDB1	1.510521682	0.044728366
KLRB1	2.313400043	0.006983434	DENR	1.498127699	0.035596958
MAF	2.92591254	0.023942857	ETV3	1.643148216	0.028580792
ME1	2.709008061	0.044620194	EVI5	1.339161983	0.044620194
NLF2	2.329424781	0.010225887	FAM73A	1.595270265	0.036058143
NPC1	1.388556961	0.038424063	FLJ40722	1.420822103	0.04663728
NTN4	2.445229595	0.03537636	GSTTP2	1.720400434	0.045692392
PCP4	1.630996515	0.037771682	HEATR3	1.505809135	0.044728366
PTPN13	2.742228086	0.024010367	HLF	2.466840291	0.021499402
PTPRM	1.56189603	0.039649558	IL10	1.254252584	0.043720498
SIPA1L2	2.003804728	0.020327246	IL17RB	2.652965662	0.023129287
			KIAA0319L	1.821245967	0.027038362
			LEP	1.939560359	0.043720498
			LMOD3	1.756198046	0.038424063
			LOC400304	1.572939332	0.031197999
			LOC642946	1.810981418	0.046761304
			LOC643423	1.418538358	0.040154108
			LOC643882	1.401897163	0.04663728
			LOC644852	2.185203656	0.035884847
			LOC648852	1.880372903	0.025134651
			LOC649181	2.348027762	0.023942857
			LOC649456	2.094671396	0.020327246
			LOC650128	1.664553705	0.030435208
			LOC90586	1.464868096	0.044728366
			LSDP5	2.050832571	0.033454829
			NLRP8	1.593145163	0.04663728
			PCDHB19P	1.768335202	0.045692392
			PCDHB9	1.613236547	0.044728366
			POLR2J4	2.821772978	0.01429944
			PRO1853	1.970892039	0.016463129
			PRRT2	2.632934832	0.045792521
			PTGR2	1.697945237	0.038624996
			RHBDL2	1.780047652	0.038413198
			SCARNA9	1.667627866	0.033275651
			SLC23A3	1.664374036	0.04663728
			SLC25A20	2.490355704	0.035884847
			SLC35E1	1.469006466	0.03813996
			SLC5A8	2.043341061	0.020788821
			TRIM39	1.948736588	0.044728366
			ZNF577	1.539598134	0.04663728
			ZNF682	1.531109478	0.037542373
			ZNF93	2.239366416	0.023942857

Appendix III.vii: Transcriptional comparison of CD161+ vs CD161- CD4+ T cells, downregulated genes shared or unique from CD161++ CD8+ T cells

Downregulated in both			Downregulated in CD161+CD4+ only		
Symbol	logFC	P.Value	Symbol	logFC	P.Value
ACTN1	-1.957048074	0.039649558	AIF1	-3.580963046	0.005960602
AK5	-2.695145157	0.01271847	ARG1	-2.941937355	0.023942857
BCAS4	-1.697009364	0.04663728	AZU1	-4.71200697	0.020788821
BEX1	-2.660739606	0.034935013	BCL11A	-2.312923193	0.011666242
C1orf165	-2.345433926	0.011666242	BPI	-4.908163089	0.030156488
CDCA7L	-2.780965434	0.008596419	C12orf48	-2.126380614	0.027038362
CEACAM1	-1.631730251	0.033909473	C5orf13	-2.883575847	0.026694309
CLEC11A	-3.205292639	0.027446769	C6orf105	-2.30835324	0.010877309
CNN3	-1.564320647	0.035884847	CD24	-4.463852309	0.024010367
COG5	-1.971379386	0.027038362	CD34	-3.273639271	0.043720498
DPH5	-1.69871791	0.018237497	CDC45L	-2.522645837	0.015945932
DSC1	-2.65292114	0.023942857	CEACAM6	-4.847204108	0.031901414
EDAR	-2.487225243	0.006983434	CEACAM8	-4.196819107	0.034935013
ELA1	-2.962334045	0.003476412	CTSG	-5.329121199	0.015563436
FCRL3	-2.911840728	0.009093673	DACT1	-2.355860828	0.024099729
FHIT	-3.370486384	0.020788821	DBH	-3.53554145	0.003971683
FOXP1	-2.678740043	0.040346775	DEFA1	-7.4058445	0.028939981
GPR55	-2.109990268	0.037771682	DEFA3	-7.435437393	0.011450988
GTSCR1	-2.938903572	0.010877309	DEFA4	-6.537996632	0.008596419
KCNMB4	-1.654193034	0.027038362	ELA2	-7.838229013	0.004150057
KRT1	-1.844022652	0.045692392	FCGRT	-1.952921287	0.027038362
LAMC3	-2.031449397	0.030548074	GPR160	-1.517723844	0.032880888
LOC649143	-1.908436357	0.012710388	H1F0	-3.243530125	0.03809006
MMP28	-2.353892515	0.006983434	HLA-DMA	-1.905526506	0.046336855
MYB	-2.579702228	0.01429944	HLA-DPB1	-2.233683695	0.013446927
NET1	-2.723038052	0.020251494	HLA-DQA1	-2.062126752	0.011666242
NOG	-2.821479616	0.008596419	HLA-DRA	-1.643868404	0.035803396
RGS10	-1.435280066	0.037542373	HLA-DRB3	-2.20298635	0.034413911
SDK2	-2.986434323	0.037542373	HLA-DRB6	-2.541459707	0.026245588
SELL	-1.630929844	0.04663728	HSD17B14	-2.365639532	0.0169281
SERPINE2	-3.132954928	0.020327246	IL2RA	-2.1206545	0.037542373
STMN1	-1.597300956	0.032497359	KRT2	-3.302800088	0.003971683
VNN2	-1.46341885	0.030696183	KRT72	-2.674578098	0.01271847
VPS24	-1.64356424	0.01431643	KRT73	-3.720748309	0.008596419
			LCN2	-3.540691142	0.039283917
			LOC648405	-1.935299342	0.044728366
			LOC653600	-6.531582757	0.011666242
			LOC728358	-6.292023291	0.008596419
			MARCKS	-2.733566374	0.023942857
			MPO	-4.587537736	0.002523377
			MPP1	-2.462956713	0.034413911
			MS4A3	-3.822812069	0.044728366
			NAE1	-2.24437929	0.037542373
			NFE2	-2.616303446	0.020327246
			OLFM4	-3.126465847	0.015007818
			OLR1	-2.686638921	0.032880888
			PADI4	-3.179469015	0.027038362
			PLLP	-1.86145956	0.043720498
			PTK2	-1.869287927	0.038624996
			RNASE2	-4.407160061	0.031543409
			RNASE3	-5.473140694	0.026629066

RNF175	-3.684847522	0.008596419
S100A8	-3.376934652	0.04663728
S100A9	-3.420477477	0.026629066
S100P	-3.16993205	0.03048291
SEPT5	-2.98290183	0.030435208
SLC2A5	-2.930485899	0.037771682
TSPAN33	-3.095841125	0.030435208
UBE2E2	-2.343467979	0.034990532
VAV3	-1.731744273	0.031901414
ZNF789	-1.41156819	0.042080679
ZNF789	-1.41156819	0.042080679

Appendix III.viii: Transcriptional comparison of CD161+ vs CD161- TCRγδ+ cells, upregulated genes shared or unique from CD161++ CD8+ T cells

Upregulated in both			Upregulated in CD161+TCRγδ+ only		
Symbol	logFC	P.Value	Symbol	logFC	P.Value
ABCB1	0.31582	3.20E-04	AACSP1	0.45736	0.03264
ADAM12	0.37429	0.01266	ACOXL	0.60078	0.02512
ADRB2	0.42574	2.72E-14	ACSBG2	0.52898	0.00992
AGPAT4	0.31214	0.00119	ADAMTS16	0.68863	0.02847
AUTS2	0.31763	0.0011	ADAMTS2	0.42	0.02044
B3GALT2	1.04492	0.00263	AGAP1	0.32405	0.00899
BCL11A	0.94385	0.0031	AIFM2	0.86296	0.00422
BLK	0.48458	0.0015	AKNA	0.5961	0.04313
BRSK1	0.33939	0.04508	AKR1CL1	0.57667	0.01908
C10orf128	0.62851	0.02739	ANK2	0.91417	0.004
CACNA2D2	0.32849	8.00E-04	ANKRD33B	0.62032	0.0103
CCL20	0.98073	7.88E-08	AP1S3	0.38484	0.00735
CCR1	0.5886	0.00419	AQP4	0.57475	0.04827
CCR2	0.70891	2.50E-04	ATP4B	0.65032	0.02597
CDH2	0.35131	0.00451	B3GNT8	0.40867	6.60E-06
CES1	0.61855	0.02581	C14orf41	0.49055	0.01981
CLIC4	0.33483	0.04417	C1orf227	0.99722	0.00329
COL5A1	0.35932	8.00E-05	C22orf41	0.79033	0.00874
COL5A3	0.6298	0.04754	C2CD4D	0.51362	0.01343
COLQ	0.55214	5.10E-07	C6orf58	0.80635	0.00663
CYBRD1	0.62887	0.01936	C8orf83	0.4649	0.00851
DPP4	0.36469	0.02099	C9orf44	0.56847	0.009
DSC2	0.7051	0.01561	C9orf53	0.39301	0.0025
ELOVL4	0.50582	0.01193	CAPSL	0.97684	0.02792
ERN1	0.37558	0.01651	CASC2	0.55943	0.01078
FAM7A1	0.41666	1.90E-04	CCDC164	0.87792	0.00601
IL12RB2	0.45251	0.02607	CCDC89	0.36874	0.02298
IL18R1	0.37945	0.0061	CCL25	0.52642	0.01954
IL18RAP	0.53506	5.00E-05	CD22	0.63584	0.0158
IL23R	0.76003	0.00255	CDC42EP3	0.33393	0.00924
ITPKA	0.39271	0.00107	CDH20	0.58821	0.0029
KIT	0.37432	0.02977	CHRNA4	0.77423	0.02102
KLRB1	1.80837	7.24E-36	CHST10	0.32185	0.01875
LAMA2	0.59324	1.30E-04	CLMN	1.18635	7.10E-04
LEPREL2	0.30213	6.50E-06	CNTN5	1.03474	1.10E-04
LIM2	0.46134	0.03555	CPNE5	0.34488	0.00279
LOC619207	0.47595	0.00578	CSN3	0.95867	0.01083
LRRC6	0.38398	0.02282	CTRB1	0.99595	2.90E-04
LTK	0.51124	5.30E-04	CYP11B1	0.99799	0.01331
ME1	0.64192	0.00731	CYP4F22	0.67835	5.50E-04
MPPED2	0.6032	0.01486	CYTH3	0.37492	1.15E-07
P2RY14	0.59274	0.00151	DCLK1	0.47974	0.03734
PACSIN1	0.45347	0.00127	DEFB108B	1.14274	5.30E-04
PERP	0.37471	0.00199	DEFB126	0.89422	0.0041
PHACTR2	0.30876	0.00119	DMRTA2	0.73113	0.02184
PLCB1	0.36209	0.0441	DNAJC5G	0.77337	4.00E-05
PLD1	0.61612	0.00545	DSPP	0.5889	0.02275
PLEKHG3	0.32391	0.00513	DTHD1	0.40673	0.01622
PLXDC2	0.8047	1.77E-09	ECM2	0.74053	0.01238
PRSS35	1.11254	1.40E-04	EFS	0.62971	0.0249
QPCT	0.72631	0.00764	FAM135B	1.45997	0.00133
RNASE2	0.75499	0.01262	FAM172BP	0.71932	2.90E-04
ROR2	0.51991	0.00349	FAM197Y2P	0.66564	0.02602
RORA	0.30285	0.00295	FAM20A	1.45515	0.00139
S100A9	0.39305	0.0066	FGD5	0.62536	0.0249
SERPINA1	0.67021	0.02722	FLJ22763	1.37796	9.40E-04

SLC17A3	0.49915	0.02883
SLC22A4	0.53726	0.00868
SLC4A10	0.62291	0.04423
SYTL2	0.40055	2.10E-04
TANC1	0.81761	0.00143
THBS1	0.44889	1.10E-04
TLE1	0.3896	9.00E-05
TSPAN15	0.57153	0.00441
TYRO3	0.39839	0.00302
VLDLR	0.56233	0.00165
ZBTB16	0.38317	0.01961

FLJ40536	1.24985	2.10E-04
FNDC4	0.92809	0.00117
GAGE7	1.34863	0.00256
GALNTL2	1.1798	0.00133
GALR1	1.02522	0.00861
GCM2	0.54063	0.03555
GJA8	0.73902	0.027
GJB7	0.79471	0.0125
GLT1D1	0.5597	0.01567
GOT1L1	1.32955	3.40E-04
GRHL3	0.36065	0.01672
GS85	1.03304	8.50E-04
HAND1	0.39493	0.02391
HEATR4	0.61382	0.04248
HHIPL1	0.81678	0.00963
HIGD1B	0.64975	0.04315
HLX	1.10359	8.04E-06
HOXA11-AS1	0.71881	0.00293
HOXA6	0.56182	0.03822
HSP90AB6P	0.87949	0.00416
IGDCC3	0.78566	0.01209
IGKV1D-13	0.89745	0.00287
IL3	0.77254	0.00155
IL31	0.77862	0.01601
IL5	0.49547	0.01244
INSRR	0.5279	0.04278
IQSEC2	0.30745	2.45E-06
KCNH7	0.7455	0.01906
KCNJ9	0.57969	0.03938
KCNN3	0.46147	0.04335
KIF19	0.32026	0.03924
KIF24	0.43157	0.00351
KLHL23	0.34964	0.03608
KRT13	0.69618	0.03365
KRTAP21-2	0.62095	0.0301
KRTAP4-8	0.80732	0.00482
KRTAP5-8	1.01771	0.01438
L3MBTL4	0.32346	0.04546
LAMB3	0.37728	0.01306
LCE2C	1.08335	7.20E-04
LHFPL2	0.62998	0.02799
LOC100126448	0.58202	0.03416
LOC100128651	0.86028	0.00738
LOC100128668	0.43767	0.00551
LOC100130071	0.8442	8.40E-04
LOC100130540	0.36021	0.01712
LOC100130713	0.45564	0.01154
LOC100130865	0.47725	5.20E-06
LOC100131053	0.80557	0.00355
LOC100133654	1.16884	9.60E-04
LOC100134285	0.47681	0.04391
LOC100507610	0.60652	0.03418
LOC100510678	0.30997	0.02361
LOC254128	0.32232	0.0114
LOC284395	1.18036	4.30E-04
LOC284412	0.89925	0.00792
LOC286189	1.42248	0.00103
LOC388242	0.31628	0.02198

LOC401847	0.33757	0.0242
LOC440117	0.32927	0.04955
LOC440925	1.32709	7.00E-04
LOC728208	0.6674	0.03969
LOC730668	1.22492	0.00201
LOC732455	1.08056	0.00155
LOR	0.73374	0.02235
LRP12	0.51626	0.00927
LRP4	0.92189	0.00389
LY86-AS1	1.0496	1.30E-04
LYPD6B	1.26423	6.40E-04
MAPK15	0.39619	0.00785
MASP1	0.33457	0.02093
MEIS1	0.67067	0.01526
MMRN1	0.56996	0.04458
MPP3	0.49481	5.92E-07
MPV17L	0.507	0.0105
MS4A1	0.31505	3.90E-04
MS4A12	1.20744	2.50E-04
MXRA8	0.62202	0.04065
MYBPC2	0.48339	0.04187
MYCL1	0.56274	0.03451
MYH1	0.77515	0.01222
MYH7	0.76267	0.00651
MYL3	0.64456	0.02668
MYLK	0.64909	0.01693
MYOM3	0.63764	0.02823
N4BP3	0.89641	0.0416
NCRNA00051	0.61405	0.01435
NCRNA00222	0.48785	0.04228
NCRNA00244	0.73257	0.00443
NCRNA00299	0.43317	0.00347
NCRNA00311	0.66794	0.00464
NEFH	0.45398	0.04558
NFIB	0.64262	0.02861
NR0B1	0.65313	0.0257
NR1I3	0.84528	0.01424
NTSR2	0.58311	0.03337
NWD1	1.14793	0.00109
OLFM4	0.63203	0.04237
OOSP1	0.5674	0.04254
OR10A7	0.56784	0.01133
OR2G2	0.61414	0.02824
OR4C6	0.51669	0.03158
OR4D1	0.60269	0.01427
OR4D5	0.51521	0.01884
OR4K13	0.52766	0.01477
OR51A2	1.1709	7.50E-04
OR52L1	1.1192	0.00162
PACRGL	0.78713	0.02733
PAGE3	0.5991	0.00798
PARVA	0.40814	0.00108
PAX6	0.44321	0.01458
PCDH11Y	0.31563	0.04693
PDE6C	0.57885	0.02446
PDZD7	0.99127	0.00323
PKDCC	0.32385	0.02205
PLA2G2F	0.56386	0.04265

PLCD3	0.79237	0.02735
PLIN1	0.95438	0.01691
PLXND1	0.36939	5.60E-04
POTED	0.69111	0.00311
PRDM13	0.69259	3.70E-04
PRDM5	0.694	0.00384
PRH2	0.61861	0.03311
PSMB11	1.13301	0.00286
PTCH1	0.32399	0.00273
PTK6	0.4644	0.01306
PVRL2	0.87871	5.60E-04
PWRN1	0.86976	0.00657
RAB38	0.50788	0.02383
RBFOX1	0.40456	0.00441
RGS3	0.35237	0.02984
RSPH9	0.53254	0.01795
RTP1	0.31235	0.00665
S100A7L2	0.63443	0.02681
SCN1B	0.41111	0.04231
SCN5A	0.99562	0.00822
SERPINB11	1.13389	2.30E-04
SH2D1B	0.57853	0.02644
SIGLEC11	0.61858	0.00825
SLC16A8	0.66806	0.00845
SLC6A10P	0.74324	0.00122
SLC6A8	0.44449	0.04893
SNORA65	1.29699	0.00934
SORCS2	0.54338	0.02225
SPTBN4	0.32504	0.03493
SSX1	0.85708	0.00768
STEAP1	0.64043	0.02407
SULT1C3	0.34742	0.0134
SULT1E1	1.02183	0.00933
SYCE1	0.87588	0.00316
TBX3	0.50331	0.00862
TCEB3B	0.73311	0.02398
TFF3	0.3837	0.01959
TLCD2	0.47468	8.00E-05
TM4SF19	0.48063	0.03024
TMEM163	0.73282	4.00E-05
TMEM171	0.52697	2.70E-04
TNS4	0.39735	4.40E-04
TPBG	0.90829	2.80E-04
TPRG1	0.56981	0.04939
TRIM36	0.63405	0.02038
TRIP10	0.39575	9.00E-05
TRPM3	1.0865	0.00775
TSHR	0.89305	0.0059
TSHZ3	0.73109	0.00306
TUBB6	1.13696	1.53E-06
TXNRD3NB	1.08275	0.00188
UNC5C	0.96274	0.01125
USP2	0.58593	0.01537
VMO1	0.30237	0.02635
VN1R2	1.10999	0.00123
VNN3	1.10047	4.00E-05
WFDC10B	1.18329	9.60E-04
WNK2	0.76222	0.04506

ZNF385B	1.17692	4.50E-04
ZNF532	0.34981	0.01824
ZNF618	1.10748	0.0035

Appendix III.ix: Transcriptional comparison of CD161+ vs CD161- TCRγδ+ cells, downregulated genes shared or unique from CD161++ CD8+ T cells

Downregulated in both			Downregulated in CD161+TCRγδ+ only		
Symbol	logFC	P.Value	Symbol	logFC	P.Value
ACCN2	-0.86039	5.15E-06	ABI3BP	-0.58742	0.03638
ACTN1	-0.95477	2.00E-05	ACTN3	-0.45676	0.02877
AEBP1	-0.62512	0.00193	ACVR1	-0.3525	8.90E-04
AGMAT	-0.38172	2.00E-05	ACVR2A	-0.43524	2.30E-07
AK5	-0.94679	1.87E-17	ADAM21	-0.66332	0.03104
APBA2	-0.6226	2.10E-04	ADAMTS4	-0.72169	2.60E-04
ARHGEF4	-0.3913	3.70E-04	ADD2	-0.6529	0.00161
ARMCX1	-0.59524	0.02791	ADPRH	-0.37131	0.04727
BACH2	-0.36556	0.00353	AFF3	-0.39067	0.00107
BEX1	-0.86552	9.13E-11	AGPHD1	-0.60121	0.02499
C14orf132	-0.94414	0.0064	AGXT2	-0.79328	0.01047
CA6	-0.45066	1.32E-07	AIF1	-0.80725	1.12E-16
CACNA1I	-1.0753	3.13E-13	AKAP12	-0.69634	0.01236
CCR4	-0.72576	6.40E-04	AKR1E2	-0.41428	0.02165
CD248	-0.58202	2.00E-05	ALOX5	-0.53586	0.00384
CD8B	-0.85145	1.00E-05	ALPK1	-0.39625	0.02557
CDCA7L	-0.67937	1.98E-06	AMOTL2	-0.35023	0.04981
CHMP7	-0.39548	0.03419	ANK1	-0.98716	2.00E-05
CLEC11A	-0.82286	1.30E-04	ANKRD57	-0.61488	1.60E-04
CNN3	-0.70899	0.00632	ARHGAP32	-0.48478	0.00209
CPEB1	-0.55635	0.0194	ARHGAP42	-0.63854	0.01997
CR2	-1.17219	5.59E-07	ARHGEF10	-0.51071	5.00E-05
CYP2J2	-0.76208	5.00E-05	ARHGEF11	-0.74658	0.00159
DCBLD2	-0.54324	0.01526	ARRDC4	-0.82136	1.00E-05
DCHS1	-0.47846	0.0012	ARSK	-0.39129	0.03739
DEPDC7	-0.55089	0.01977	ASAP3	-0.30564	0.02719
DLL1	-0.5957	0.00163	ATOH1	-0.71247	0.01598
DLL3	-0.64559	0.00105	ATP13A4	-0.61058	0.03386
DSC1	-0.99906	2.52E-32	ATP5L2	-0.70112	0.02343
DSEL	-0.38107	8.30E-04	ATPBD4	-0.52369	0.03533
EDAR	-0.38679	0.01718	AURKC	-0.39544	0.00482
EPHB4	-0.62248	1.10E-04	BACE1	-0.34489	0.02589
EPHX2	-0.42669	3.44E-06	BCL2	-0.30206	2.20E-04
FBLN2	-0.92594	8.82E-09	BCL7A	-0.48771	0.01298
FHIT	-0.84608	1.58E-06	BEND4	-0.66042	0.00529
FZD6	-0.6944	5.00E-04	BEND5	-1.19935	2.17E-10
GATM	-0.8345	1.40E-04	BTBD3	-0.73862	0.00167
GCET2	-0.63654	0.03065	C10orf25	-0.55898	0.02545
GJB6	-0.67433	0.00215	C12orf66	-0.52202	0.01005
GP5	-0.80447	0.00338	C15orf33	-0.50534	0.0466
GPA33	-0.43523	0.02307	C15orf50	-0.48868	0.03603
GPC2	-0.3497	3.84E-06	C15orf60	-0.45407	0.04764
GPR55	-0.67074	0.00105	C16orf59	-0.47682	0.03402
HAPLN3	-0.45346	0.00212	C16orf74	-0.3912	0.03329
HLA-DOA	-0.35763	7.10E-04	C16orf75	-0.88623	7.50E-06
IL6R	-0.78298	1.00E-05	C17orf99	-0.62482	0.00301
IRS1	-0.54856	0.01791	C2orf40	-0.38553	0.00701
KCNH2	-0.67677	5.00E-05	C2orf89	-0.52253	0.00126
KRT1	-0.81183	6.00E-05	C4orf47	-0.5522	0.01317
KRT18	-0.46858	1.90E-04	C5orf13	-0.73356	0.0019
LAMC3	-0.45738	0.0096	C5orf34	-0.51117	0.04583

LAMP3	-0.39044	1.20E-04	C6orf105	-1.02145	3.26E-11
LEF1	-0.66552	0.00103	C7orf13	-0.55987	0.02245
LGMN	-0.50221	0.01783	C9orf84	-0.88886	0.00363
LIMS2	-0.6734	2.30E-04	CA13	-0.32586	0.03928
LMO7	-0.52813	0.00826	CBX2	-0.73971	4.50E-04
LOC641518	-1.10561	2.00E-05	CCR8	-0.83972	1.60E-04
LRRN3	-0.97173	7.00E-04	CD200	-0.63276	2.12E-06
LYPD3	-0.70703	0.01542	CD9	-0.67843	2.00E-05
MAL	-1.14917	7.05E-12	CDC42BPB	-0.41755	1.09E-10
MARS2	-0.30435	0.02887	CDH1	-0.76988	1.00E-04
MYB	-0.72806	4.58E-07	CDNF	-0.34902	0.03422
NBEA	-0.75726	2.49E-09	CDR2	-0.33937	8.38E-07
NEK11	-0.38513	0.01894	CEBPE	-0.66701	0.03274
NELL2	-0.52164	3.90E-04	CES4A	-0.32625	0.00239
NGFRAP1	-0.99975	8.74E-10	CFP	-0.45623	3.53E-06
NOG	-1.34548	8.46E-14	CHRFAM7A	-0.60163	0.0302
NPAS2	-0.34624	0.00672	CHST2	-0.74464	0.00236
NRCAM	-0.50379	5.00E-05	CKM	-0.68453	0.02725
NT5E	-0.53981	0.00837	CLC	-0.83639	9.00E-05
OR2A20P	-0.55385	0.02161	CNKSR2	-0.30344	0.04623
PASK	-0.95233	5.55E-09	COCH	-0.58797	0.02613
PCSK5	-0.56889	2.75E-08	COL5A2	-0.38822	0.01103
PECAM1	-0.5495	1.65E-15	CPAMD8	-0.69652	5.70E-08
PHC1	-0.89014	0.0053	CR1	-0.92376	1.13E-24
PHGDH	-0.57288	5.87E-06	CR1L	-0.59715	0.00105
PKIA	-0.41243	0.00725	CRB3	-0.37569	3.03E-06
PLCL1	-0.48781	5.00E-05	CREG2	-0.30421	0.00733
PRKAR1B	-0.37255	0.03439	CRHR2	-0.82287	0.01465
PRKCA	-0.35741	0.0034	CRNDE	-0.52996	0.0127
PTCD2	-0.50002	0.01946	CSGALNACT1	-0.58724	0.01683
PTPRK	-0.64749	9.60E-04	CSN1S2BP	-0.49649	0.0041
RBM11	-0.43211	0.00209	CTDSPL	-0.33637	0.03005
REG4	-0.51104	0.00232	CTLA4	-0.42233	2.50E-04
SCML1	-0.47294	0.04562	CTTN	-0.48836	0.0254
SDK2	-1.02019	5.82E-08	CXCL2	-0.93902	6.66E-06
SERINC5	-0.44703	3.00E-05	CXCR5	-0.46698	0.03
SERPINE2	-0.37142	0.00133	CYP24A1	-0.93394	1.30E-04
SLC16A10	-0.95941	1.55E-07	CYSLTR1	-0.57964	3.00E-05
SLC7A8	-0.94922	2.50E-04	DACT1	-0.73739	2.00E-05
SPINT2	-0.69716	2.46E-20	DDX25	-1.02355	0.00308
ST6GALNAC3	-0.9615	0.00193	DENND5A	-0.30648	3.15E-06
STXBP1	-0.47346	0.00982	DGKK	-0.65629	0.02041
SULT1B1	-0.93471	2.60E-13	DHCR24	-0.32394	0.02182
TBC1D4	-0.56309	0.0212	DIP2B	-0.32738	8.20E-06
TCEA3	-0.81551	2.95E-15	DIRC3	-0.93644	6.31E-06
TMEM45B	-1.00777	7.70E-04	DKK3	-0.45903	0.00198
TNFRSF10D	-0.70195	1.10E-04	DNAH11	-0.58139	9.90E-04
VIPR1	-0.51803	5.70E-15	DSCAML1	-0.60362	0.00332
VSIG1	-0.57297	0.00924	E2F5	-0.52257	4.00E-04
WBP5	-0.54883	0.01343	E2F8	-1.06379	5.80E-04
WNT7A	-0.97293	2.92E-16	EDA	-0.5495	0.00905
ZNF135	-1.11657	4.70E-04	EDN1	-0.3392	3.50E-04
ZNF154	-0.38857	0.03179	EDN3	-0.4346	0.00431

ZNF365	-1.00319	1.78E-18	EEPD1	-0.44647	0.0212
ZNF415	-0.91449	0.00102	ELOVL3	-0.61924	0.03622
ZNF662	-0.59585	0.00674	ENTPD1	-0.60508	0.00772
ZNF667	-0.31208	0.03386	EPB41L1	-0.40495	0.04227
ZNF80	-0.77665	2.00E-05	EPHB2	-0.70363	0.01358
			EPS8	-0.33306	0.01921
			F13A1	-0.45454	0.02669
			F2RL1	-0.69146	0.0099
			F5	-0.54245	0.01041
			FAAH2	-0.55369	1.50E-06
			FAM153A	-0.36394	0.03694
			FAM164A	-0.85306	1.15E-09
			FAM184A	-0.32379	0.04813
			FAM19A2	-1.14689	8.00E-05
			FAM55B	-0.93948	0.00112
			FAM69C	-1.20363	1.50E-04
			FAM83E	-0.36044	0.00367
			FAM92A1	-0.40274	0.0363
			FAM95B1	-0.59504	0.03359
			FANK1	-0.58436	3.20E-04
			FBLN7	-0.54701	0.0203
			FCER1A	-0.86073	1.10E-04
			FGD4	-0.52029	0.02468
			FLJ20444	-1.16864	1.80E-04
			FLJ22536	-0.58715	0.00666
			FLJ31945	-0.574	0.03472
			FLJ35390	-0.47799	0.00486
			FLJ35946	-0.35487	0.0319
			FLJ44674	-0.39462	0.04443
			FLJ45983	-0.78733	5.34E-09
			FLT3	-0.53459	0.04615
			FNBP1L	-0.50286	0.0371
			FOXJ1	-0.66509	2.30E-04
			FRY	-0.41639	0.01503
			FST	-1.19919	1.00E-05
			FTCD	-0.55804	0.00247
			GABRD	-0.61061	0.02377
			GALR2	-0.84816	0.00491
			GAS6	-0.6456	0.00557
			GATA2	-0.61971	0.01775
			GCNT4	-0.48872	5.40E-04
			GDF10	-0.5092	0.01603
			GEM	-1.05643	5.00E-04
			GFI1B	-0.31317	0.01387
			GJA9	-0.57143	0.01235
			GJC2	-0.34855	0.01512
			GNAI1	-0.41065	0.02792
			GNG11	-0.45773	0.04071
			GP1BB	-0.96218	8.41E-06
			GPLD1	-0.47289	0.03972
			GPR125	-0.57016	0.01049
			GPR39	-0.68228	0.03822
			GPR44	-0.62938	3.70E-04

GPT2	-0.52746	0.04478
GRB10	-0.72573	2.50E-04
GREB1L	-0.63545	0.04319
GRIK1-AS1	-0.59998	0.00938
GSG1L	-1.05414	0.00456
GTF2IRD1	-0.43837	1.00E-05
GUCY2E	-1.22366	1.70E-04
GYG2	-0.59694	0.03122
GYPE	-0.5481	0.00478
HCG9	-0.74539	0.01077
HCN1	-0.78617	0.00821
HCRP1	-0.38278	0.00769
HDC	-0.70602	0.0184
HEPH	-0.45415	2.90E-04
HGC6.3	-0.52615	0.00382
HHEX	-0.65962	0.00226
HMOX1	-0.42411	0.0017
HPSE2	-0.6807	4.50E-04
HSD17B3	-0.4882	0.01355
HSPG2	-0.63356	5.27E-06
HTR7P1	-0.32039	6.26E-06
IFFO1	-0.37943	0.04641
IFNGR2	-0.60509	0.00469
IKZF2	-0.56806	1.90E-04
IL1R1	-0.98817	1.50E-04
IL2	-0.4632	0.01709
IL5RA	-0.39348	0.02422
INF2	-0.7613	6.89E-14
INMT	-0.46523	5.60E-04
INPP4B	-0.62941	0.01814
IQCA1	-0.57161	0.00585
IQSEC3	-0.46943	0.00792
IRF4	-0.36992	0.01895
ITGB3	-0.49088	0.04556
JPH2	-0.30769	0.0488
KALRN	-0.48885	0.01204
KANK1	-1.07789	1.37E-08
KATNAL2	-0.91641	1.30E-04
KCNJ12	-0.53984	0.01478
KCNN4	-0.30457	0.04955
KCNQ1	-0.73615	6.35E-07
KCTD12	-1.2211	5.28E-15
KIAA0125	-0.92432	5.68E-10
KIAA0408	-0.33021	0.00751
KIAA1257	-0.54431	0.04546
KIAA1958	-0.34186	0.00725
KLF5	-0.49984	9.00E-04
KLF7	-1.16187	3.28E-22
KLHL14	-0.61963	0.01887
KLHL29	-0.46299	1.22E-13
KLHL34	-0.47696	0.01877
KRT2	-0.67477	4.00E-05
KRT72	-0.88518	2.40E-04

LARGE	-0.46196	1.50E-04
LAT2	-0.44671	0.00807
LAYN	-0.99157	1.00E-04
LIMCH1	-0.92138	0.00285
LOC10012825	-1.16242	1.81E-06
LOC10012888	-0.66136	0.02232
LOC10013023	-0.40172	0.02828
LOC10013154	-0.56861	6.00E-04
LOC10013158	-0.58609	0.03738
LOC10013166	-1.09781	9.00E-05
LOC10013234	-0.44598	0.00211
LOC10013252	-0.48475	0.04028
LOC10013350	-0.37672	0.0362
LOC10050580	-0.67183	0.0182
LOC10050717	-0.44031	0.03398
LOC10050901	-0.42395	0.00185
LOC121456	-0.31301	0.0483
LOC254896	-0.50328	0.04709
LOC283050	-0.30531	0.0463
LOC284798	-0.78677	0.00318
LOC285441	-1.37371	1.90E-04
LOC285456	-0.61207	0.03157
LOC339788	-0.49396	0.01889
LOC388780	-0.70978	8.60E-04
LOC389332	-0.85032	8.10E-04
LOC400622	-0.86216	0.00196
LOC401220	-0.39309	0.03058
LOC439949	-0.37365	3.20E-04
LOC440131	-0.49017	0.01549
LOC440910	-0.76952	0.002
LOC641510	-0.44593	0.00116
LOC642776	-0.54368	0.04102
LOC642781	-0.63041	0.02271
LOC645586	-0.3445	0.04968
LOC647020	-0.91633	0.00171
LOC650293	-0.36973	0.02018
LOC729680	-0.49757	0.00251
LOC729911	-0.56874	0.03075
LOC729970	-0.4501	0.02735
LRRC32	-0.47166	0.00751
LRRC34	-0.53687	0.01699
LRRC8B	-0.34728	7.50E-08
LRRN1	-0.84598	0.00239
LY96	-0.71855	5.10E-04
LYL1	-0.50185	0.01079
MALL	-1.06453	0.0018
MAOA	-0.5853	0.00409
MAP3K1	-0.34761	3.20E-04
MB21D2	-0.75622	1.02E-06
MCM10	-0.5608	0.03679
MDS2	-0.81248	3.56E-07
MEGF6	-0.30104	0.00422
METTL11B	-0.59246	0.00147

MFGE8	-0.30598	0.0083
MGAT3	-0.72333	0.00122
MGC15705	-0.44927	0.00302
MGP	-0.30626	0.01612
MLF1	-0.63409	0.01057
MME	-0.77991	4.00E-04
MOXD1	-0.87184	0.00159
MRC2	-0.44115	0.00316
MSH4	-0.87835	0.00552
MSL3	-0.526	0.00415
MTHFD1L	-0.30348	0.01737
MTHFD2L	-0.35911	0.01636
MTSS1	-0.3372	0.02462
MYH4	-1.24481	1.10E-04
MYO1E	-0.79449	0.00533
MYO7A	-0.45004	0.01863
MYOM2	-0.50588	0.00199
NANOS2	-1.21694	3.40E-04
NAT8L	-0.55749	0.04593
NBEAP1	-0.42843	0.02669
NCF2	-0.38059	0.04001
NCRNA00173	-0.56885	5.00E-04
NCRNA00282	-0.7317	0.00557
NHLRC4	-0.45417	0.02157
NIPAL2	-0.37337	0.01866
NKD2	-0.45814	0.01231
NLN	-0.53761	0.03166
NOX3	-0.83322	0.00258
NPCDR1	-0.57475	0.00463
NRGN	-0.52565	0.0465
NUP62CL	-0.51589	0.04722
OIP5	-0.45838	0.03649
OR9H1P	-0.49455	0.0302
OTOL1	-0.97569	0.00154
P2RY2	-0.78112	0.00842
PBK	-0.5404	0.02626
PDE7B	-0.80365	0.00439
PDLIM1	-0.50487	0.01376
PDZK1	-0.38071	0.0113
PER4	-0.91061	0.00316
PF4	-0.51308	0.02615
PHLPP1	-0.32058	0.03002
PKIG	-0.31779	0.02136
PLEKHH2	-0.63529	0.00226
PLXNA4	-0.66892	5.38E-06
PLXNB2	-0.90759	2.50E-04
POU2AF1	-0.50868	0.03988
PP12613	-0.46449	0.03751
PPARGC1B	-0.30667	0.00798
PPBP	-0.61022	0.00254
PRKAR2B	-0.50628	0.00317
PTGER3	-0.77785	0.01035
PTK2	-0.5698	0.00497

PTPRO	-0.51698	0.04073
PVT1	-0.33445	2.78E-09
PXDN	-0.69784	0.00758
QRSL1	-0.55304	0.01973
RAB32	-0.55235	0.03848
RAB34	-0.65912	4.61E-06
RALGPS2	-0.37762	0.03018
RASGRP3	-0.34159	9.90E-04
RBM20	-0.87204	1.00E-04
RCAN2	-0.67312	0.00237
RCAN3	-0.38096	9.14E-06
RECQL5	-0.39068	0.02788
RFPL2	-0.59308	9.40E-04
RIMKLB	-0.49009	0.00701
RIPK4	-0.6156	0.01204
RNF144B	-0.6443	0.00568
RNF157	-0.50951	0.00284
RNF17	-0.33838	0.02677
RNF216	-0.44277	0.02415
RTN4RL1	-0.66025	0.00145
SDPR	-0.50755	0.04568
SEC14L3	-0.90025	0.00386
SELP	-0.3593	0.0451
SEMA5A	-0.55927	3.00E-04
SEMA5B	-0.56187	0.00641
SEPT10	-0.74692	6.90E-04
SERP2	-0.4974	0.0335
SERPINA10	-0.79303	0.00896
SERPINF1	-0.30663	0.00388
SESN3	-0.5776	3.18E-07
SESTD1	-0.59859	0.01919
SGPP2	-0.86625	3.00E-05
SH3RF3	-0.97431	8.40E-04
SHISA2	-0.55284	0.03352
SLC10A7	-0.40725	0.01882
SLC22A23	-1.12955	1.00E-34
SLC40A1	-1.03824	1.15E-09
SLC7A4	-0.43562	0.02296
SLC9A7	-0.38269	7.40E-04
SMYD1	-0.77895	0.01254
SNTG2	-0.65899	0.00236
SNX7	-0.63804	0.0273
SOD3	-0.58897	0.0307
SORBS2	-0.79292	1.50E-04
SOX5	-0.69944	0.00683
SOX9	-0.39656	0.0133
SPATA6	-0.53974	4.50E-04
SPIN3	-0.59766	0.0057
SPINK5	-0.8407	0.00801
ST6GALNAC1	-0.36272	0.04667
SUOX	-0.62787	0.01756
SVOPL	-0.53409	0.00364
SYCE1L	-0.36705	0.0251

TCF7L1	-0.34058	0.00624
THNSL2	-0.46093	0.0077
TIAM1	-0.48883	9.50E-04
TIMP2	-0.65032	4.40E-04
TJP3	-0.30322	0.02774
TLR2	-0.50969	0.0011
TLR5	-0.43067	0.04682
TLR7	-0.77032	0.01242
TMEM196	-0.70249	0.01961
TMEM22	-0.40735	0.04202
TMIE	-0.67947	1.80E-06
TMPRSS4	-0.54885	0.01966
TOP2A	-0.34583	0.03066
TOX	-0.35296	7.80E-04
TP53I3	-0.43537	0.03206
TP73	-0.45696	0.03489
TRIM58	-0.36525	5.00E-05
TRPV6	-0.37881	0.02517
TSHZ2	-0.90635	7.80E-04
TSKS	-0.44629	0.02147
TSPAN33	-0.36909	6.13E-06
TTLL10	-0.76904	0.01046
TTN	-0.52515	0.01587
TUBB1	-0.56163	0.01196
TUSC3	-0.91244	0.00594
TXNRD3	-0.58809	2.00E-05
UBE2E2	-0.80619	9.00E-04
UFSP1	-0.31163	0.0245
UNC5B	-0.56666	0.01296
UNQ6494	-0.74028	0.01555
USP6NL	-0.74263	9.00E-05
VIT	-0.44412	0.03837
VSIG2	-0.36578	0.03451
VSIG4	-1.05267	5.06E-08
WDFY4	-0.53488	7.00E-05
WNT7B	-0.82383	8.00E-05
WWC1	-0.55461	0.01837
ZAR1L	-0.46993	0.00734
ZC3H12D	-0.60463	1.90E-04
ZDHHC23	-0.3028	0.00283
ZNF114	-0.79913	0.00349
ZNF233	-0.53478	0.02503
ZNF285	-0.86169	5.20E-06
ZNF334	-0.85347	0.00129
ZNF516	-0.35535	0.03349
ZP1	-0.80303	7.39E-07
ZP3	-0.33381	0.00978
ZSCAN12	-0.39852	0.0152
ZWINT	-0.4955	0.00201
ZYG11A	-1.00226	7.20E-04

A

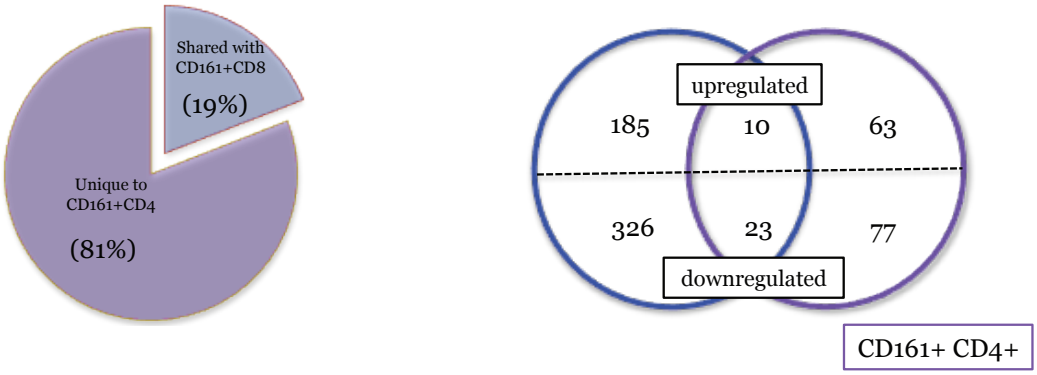

B

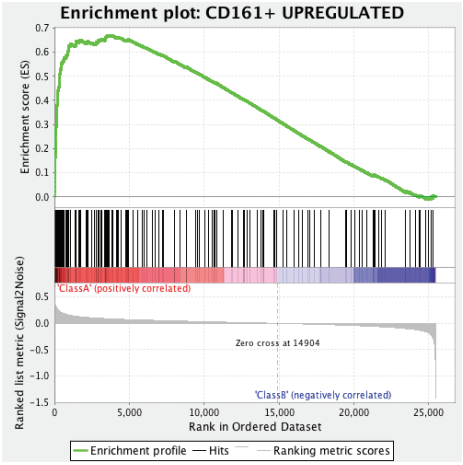

p<0.001
NES = 2.85

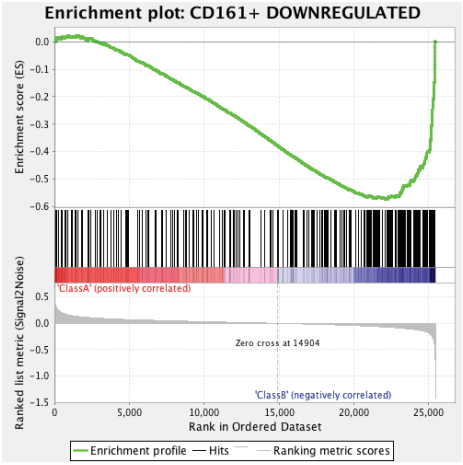

p<0.001
NES = -2.8

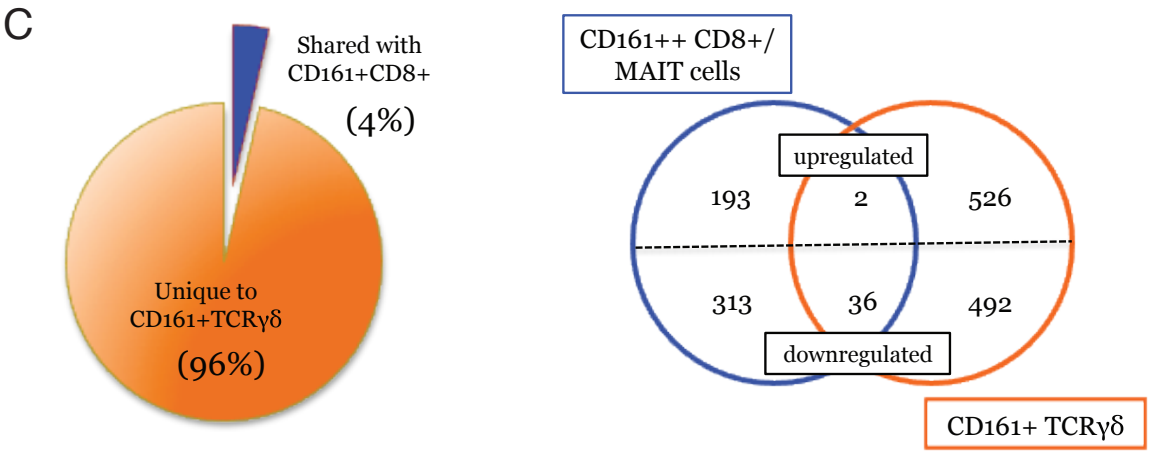

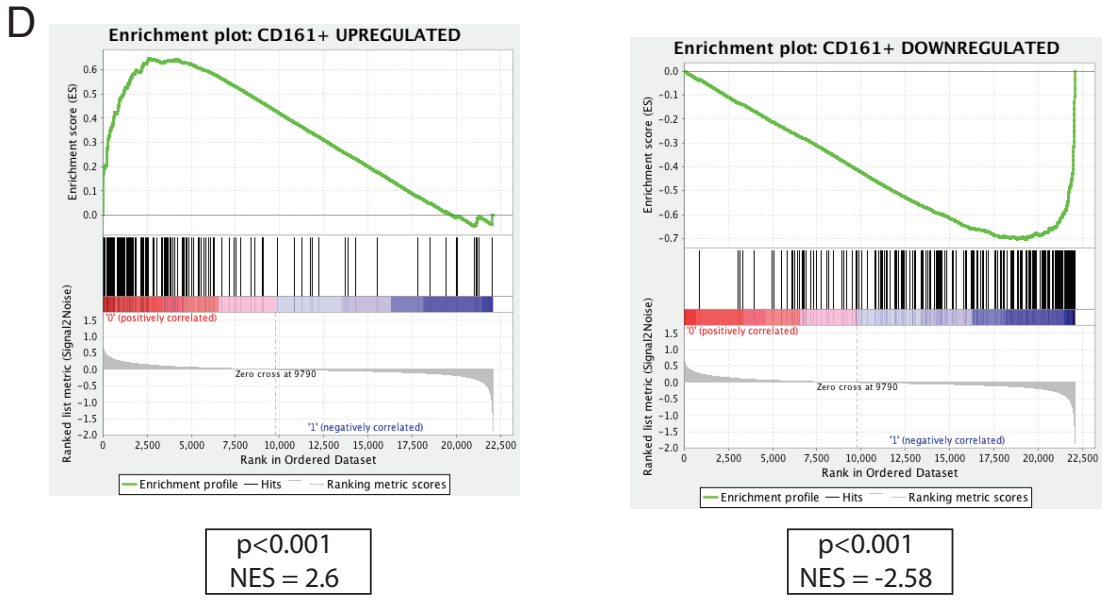

p<0.001
NES = 2.6

p<0.001
NES = -2.58

Appendix III.X: Comparison of CD161+ CD4 and TCRγδ T cells with CD161+CD8+ T cells. Pie charts show proportion of genes differentially expressed by CD161+CD4 (**A**) and CD161+TCRγδ (**C**) that are shared with CD161+CD8+, when compared to their CD161– counterparts. Venn diagrams shows breakdown of upregulated and downregulated genes unique to or shared by each subset. **B** & **D**) Gene set enrichment summary plots for vsn-normalised CD161+ vs CD161– CD4+ T cells (**B**) and CD161+ vs CD161- TCRγδ T cells (**D**) ranked genes, and CD161+ upregulated (left) and downregulated (right) gene sets. NES = normalised enrichment score, vsn = variance stabilizing normalisation, see 3.3.5.

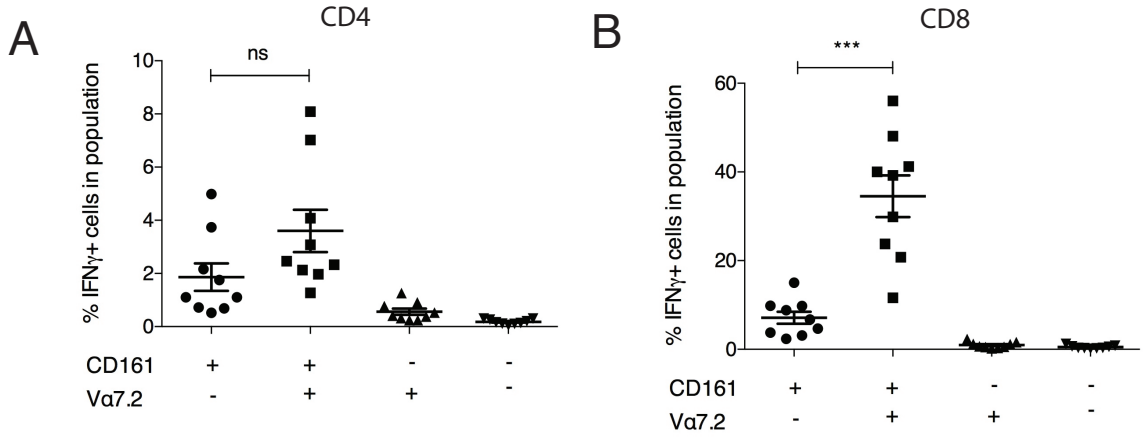

Appendix III.Xi: IL-12+IL-18 induces responses from Vα7.2+ and Vα7.2- CD161+ T cells. PBMC were incubated overnight with 50ng/ml each of IL-12 + IL-18 and IFNγ production assayed by intracellular cytokine staining. Percentage IFNγ-producing cells of CD161+/CD161- and either Vα7.2+/Vα7.2- populations was calculated and plotted for CD4+ (**A**) and CD8+ (**B**) T cells. *** $p<0.001$, ns = not significant with Tukey's multiple comparisons test (n=9).

4. CD161+ CD8+ T cells: Phenotype and Function

4.1 Introduction

The T lymphocyte lineage incorporates a variety of phenotypes, including division of subtypes based on co-receptor expression, namely CD4+ and CD8+, and various differentiation phenotypes, as T cells develop from naïve to memory, either T_{EM} or T_{CM} (see Chapter 1: Introduction). However, examples are now appearing which blur these divisions. The presence of memory cells in peripheral tissues, a feature of T_{EM}, but which do not recirculate, led to the categorisation of a further memory subset termed "tissue-resident" memory (Jiang et al., 2012). Study of T cells that are neither CD4+ or CD8+ (the DN population) also revealed the existence of T cells with restricted TCR β and invariant TCR α expression (Porcelli et al., 1993). T cells that express an invariant Vα7.2-Jα33 T cell receptor (TCR) were subsequently identified as MAIT cells, which are in fact predominantly CD8+ and comprise around 15% of the CD8+ T cell pool (Walker et al., 2012). However, although CD8+, MAIT cells express low levels of granzyme B and perforin (Billerbeck et al., 2010; Kurioka et al., 2014), and are not restricted by classical MHC class I molecules (Tilloy et al., 1999). Instead, MAIT cells are characterised by anti-bacterial activity through restriction to the non-classical antigen presenting molecule MR1 (Le Bourhis et al., 2010), in addition to expression of IL18Rα and MDR1 (Dusseaux et al., 2011), and high levels of CD161 (Dusseaux et al., 2011; Martin et al., 2009).

CD161 expression is associated with a memory phenotype within the adult circulation, with CD161++ MAIT cells uniformly expressing a T_{EM} phenotype (Martin et al., 2009). A number of other CD161 positive T cell subsets including CD4+ (Annunziato et al., 2007; Cosmi et al., 2008; Kleinschek et al., 2009; Takahashi et al., 2006), CD8+ (Maggi et al., 2010; Takahashi et al., 2006), DN TCRαβ+ and TCRγδ+ T cells (Maggi et al., 2010) also display a memory phenotype. CD161 expression

has also been associated with homing to distinct tissues. CD161 positive T cells, of both CD4+ and CD8+ subtype, make up more than half of T cells in the healthy human intestine (O'Keeffe et al., 2004) and T cells expressing CD161 home to the liver (Ishihara et al., 1999). CD161++ MAIT cells, specifically, have been described to be enriched with the gut (Treiner et al., 2003) and liver (Dusseaux et al., 2011). This may be associated with expression of CCR6 and CXCR6 by these cell subsets (Cosmi et al., 2008; Dusseaux et al., 2011). Consequently, CD161 positive lymphocytes appear to represent a unique type of tissue resident memory.

Expression of CD161 has further been associated with a type 17 phenotype. In all T cell subsets, the ability to secrete IL-17 was virtually restricted to those cells expressing CD161 (Maggi et al., 2010), and CD161 was significantly upregulated in Th17 clones compared to those of Th1 or Th2 (Cosmi et al., 2008). MAIT cells also express IL-17 and the type-17 transcription factor RORγt (Dusseaux et al., 2011). Amongst CD8+ T cells IL-17 secretion was restricted to the CD161++ MAIT cell subset and was not seen from the CD161+ CD8+ T cell population (Billerbeck et al., 2010).

In a study by Billerbeck *et al.* (2010) these IL-17-secreting CD161++CD8+ T cells were described to be enriched within the HCV-infected liver, suggesting a role for these cells in this disease. Furthermore, CD8+ T cells specific for epitopes from HCV and HBV in infected donors, as identified by fluorescent MHC-multimers, are enriched for CD161 expression (Northfield et al., 2008). As CD161++ MAIT cells are anti-bacterial, rather than anti-viral, and do not bind MHC (Dusseaux et al., 2011; Tilloy et al., 1999), it follows that those HCV-specific CD8+ T cells identified by MHC-multimers are not CD161++ MAIT cells, but rather CD8+ T cells expressing lower levels of CD161; the CD161+CD8+ T cell population. CD8+ T cell responses are important in viral control, with the specific T cell phenotypes induced impacting disease progression and outcome (Appay et al., 2008). However, the phenotype of this CD161+CD8+ T cell subset, both in comparison to MAIT cells with which they

share expression of CD161, and conventional CD161–CD8+ T cells, has not yet been explored.

4.2 Aims

1. Describe the phenotype of CD161+CD8+ T cells, including any similarities to CD161++MAIT cells (as indicated in the previous chapter) and any differences from the CD161– population
2. Investigate the function of CD161+CD8+ T cell population
3. Identify the tissue location of CD161+CD8+ T cells
4. Investigate the phenotype of CD161+CD8+ T cells in Hepatitis C, and hence the significance of enrichment in CD161 expression on HCV-specific cells identified by Northfield *et al.* (2008)

4.3 Materials and Methods

Chapter-specific materials and methods are detailed below. All other methods and reagents are described in Chapter 2.

4.3.1 Study Subjects and Cells

PBMC from healthy adults, 24 month olds and UCB were isolated as per 2.1.1. Liver-associated mononuclear cells were collected from non-pathological liver grafts preceding liver transplantation, and kindly provided by Antonio Bertoletti. Lymphocytes were isolated from the colon of patients with IBD, either inflamed or non-inflamed, or with Diverticular disease. Healthy control lamina propria lymphocytes were isolated from adjacent non-involved tissue of patients with colorectal cancer. These were kindly provided by the Powrie lab.

Peripheral blood samples were obtained from patients with chronic HCV infection who were enrolled in the study after informed consent and in accordance with the local ethics committee. Patient details are shown in Table 4-2. Cells were isolated as detailed in Chapter 2, frozen and stored in liquid nitrogen until use. After thawing, cells were rested overnight before functional and phenotyping assays were performed. Patients were typed for HLA-A2 type by surface staining with HLA-A2 PE (clone BB7.2; BioLegend).

HCV vaccinated patients were recruited and vaccinated as described (Barnes et al., 2012). Briefly, healthy volunteers were vaccinated intramuscularly with adenoviral vectors encoding the NS3-5B region of HCV. Anti-viral responses were detected by pentamers loaded with HCV NS3 1406 (KLSALGINAV; HLA-A*0201) and HCV NS3 (ATDALMTGY; HLA-A*0101). All volunteers gave written informed consent prior to enrolment. PBMC were extracted from peripheral blood, frozen and thawed before phenotyping by flow cytometry, as described in Chapter 2.

4.3.2 Quantitative (q)PCR

Thawed PBMC were rested overnight before CD8+ T cells were enriched using CD8 Microbeads (Miltenyi Biotec) following the manufacturer's protocol, and as detailed in Chapter 2. Enriched CD8+ T cells were split equally and stimulated with PMA + Ionomycin in R10, for lengths of time ranging from 0-6 hours. Stimulation was stopped by washing the cells in PBS and total RNA was subsequently extracted using RNeasy Micro or Mini RNA extraction Kits (Qiagen) as per manufacturer's instructions, and according to cell number. RNA concentration and quality was assessed by ND-100 Spectrophotometer (NanoDrop Technologies). cDNA was then synthesised from 70-100ng of RNA using Superscript III Reverse Transcriptase (Invitrogen, Life Technologies), following the manufacturer's protocol. The resulting cDNA was then mixed with Faststart universal probe master (Roche), sterile distilled water, 0.5μM forward and reverse primers for either IFNγ or the housekeeping gene HPRT, and the corresponding probe from the Roche universal probe library as detailed in Table 4-1. Samples were loaded in triplicate into a 96-well Lightcycler 480 multiwell plate (Roche) and run on the Lightcycler 480 96 well block (Roche) on the following cycle: 95°C for 10 min, 45 cycles of 95°C for 5min, 60°C for 30 seconds, 72°C for 10 seconds, and one cycle of 40°C for 10 seconds. Fold change was normalised to expression of the housekeeping gene HPRT using the $2^{-\Delta\Delta CT}$ method (Livak and Schmittgen, 2001) and calculated relative to unstimulated samples.

Gene	Probe number	Primers
HPRT	#73	3'-tgaccttgatttattttgcatacc-5'
		5'-cgagcaagacgttcagtcct-3'
IFNγ	#21	3'-tggaaagaggagagtgacagaaa-5'
		5'-ttggatgctctggtcatcttt-3'

Table 4-1: qPCR primers and probes

4.3.3 mRNA Microarray

CD8+ T cells were enriched from PBMC using CD8 Microbeads (Miltenyi Biotec) and sorted on a MoFlo Legacy or MoFlo XDP (Beckman Coulter). Sorted CD161+ and CD161- subsets were either snap frozen immediately (unstimulated array, Figure 4-3) or stimulated for 4hrs (determined optimal see Figure 4-11) with cell stimulation cocktail (eBioscience) prior to snap freezing (stimulated array, Figure 4-12). Frozen cell pellets were sent to Miltenyi Genomic Services (Bergisch Gladbach, Germany) for RNA extraction and hybridization to Agilent Whole Human Genome Oligo Microarray. The Agilent Feature Extraction Software was used to read out and process the microarray image files, which were further analysed using the Rosetta Resolver gene expression data analysis system (Rosetta Biosoftware). Genes considered to be significantly differentially expressed were those genes with a fold change >2 and p-value <0.01.

Cord blood microarray analyses were performed as previously described (Walker et al., 2012). Briefly, cells were sorted by CD8 enrichment (Miltenyi Biotec) and fluorescence activated cell sorting. Total RNA was extracted using an RNeasy mini kit (Qiagen) and cDNA amplified using the Ovation Pico WTA System (NuGEN). cDNA was fragmented and labelled using the Encore Biotin Module kit (NuGEN) before hybridization to GeneChip Human Genome U133 Plus 2.0 arrays (Affymetrix) using the hybridization, wash and stain kit (Affymetrix), and scanned with the GeneChip scanner 3000 7G (Affymetrix). *Performed by Lucy Walker.*

4.4 Results

4.4.1 CD161 is expressed by a subset of anti-viral CD8+ T cells

CD161 expression defines three populations of CD8+CD3+ lymphocytes within the circulation of healthy adults: CD161++ (of which the majority are Vα7.2+ MAIT cells), CD161+ and CD161– (Figure 4-1A), with on average equal percentages of CD161++ and CD161+ (mean 10.60% and 11.68%, respectively), and the vast majority being CD161– (mean 76.09%). However, proportions vary widely between individuals, as illustrated by the flow cytometry plots shown in Figure 4-1B. Anti-viral CD8+ T cells specific for epitopes from cytomegalovirus (CMV), Epstein Barr virus (EBV) and influenza (FLU) were identified using MHC class I-dextramers and were present in both CD161+ and CD161– populations, but were rarely, if ever, CD161++ (Figure 4-1B). This fits with CD161++ MAIT cells being restricted by the MHC class Ib molecule MR1, and reactive against a range of bacteria rather than viruses (Le Bourhis et al., 2010). Approximately 15% of anti-viral populations expressed CD161 (Figure 4-1B) for all three viruses, suggesting that expression is not associated with either acute (FLU) or chronic (CMV, EBV) infection. Furthermore, although the majority of anti-viral CD8+ T cells were CD161–, there was no significant difference in terms of frequency, when the proportions of each bulk population were taken into account (Figure 4-1C).

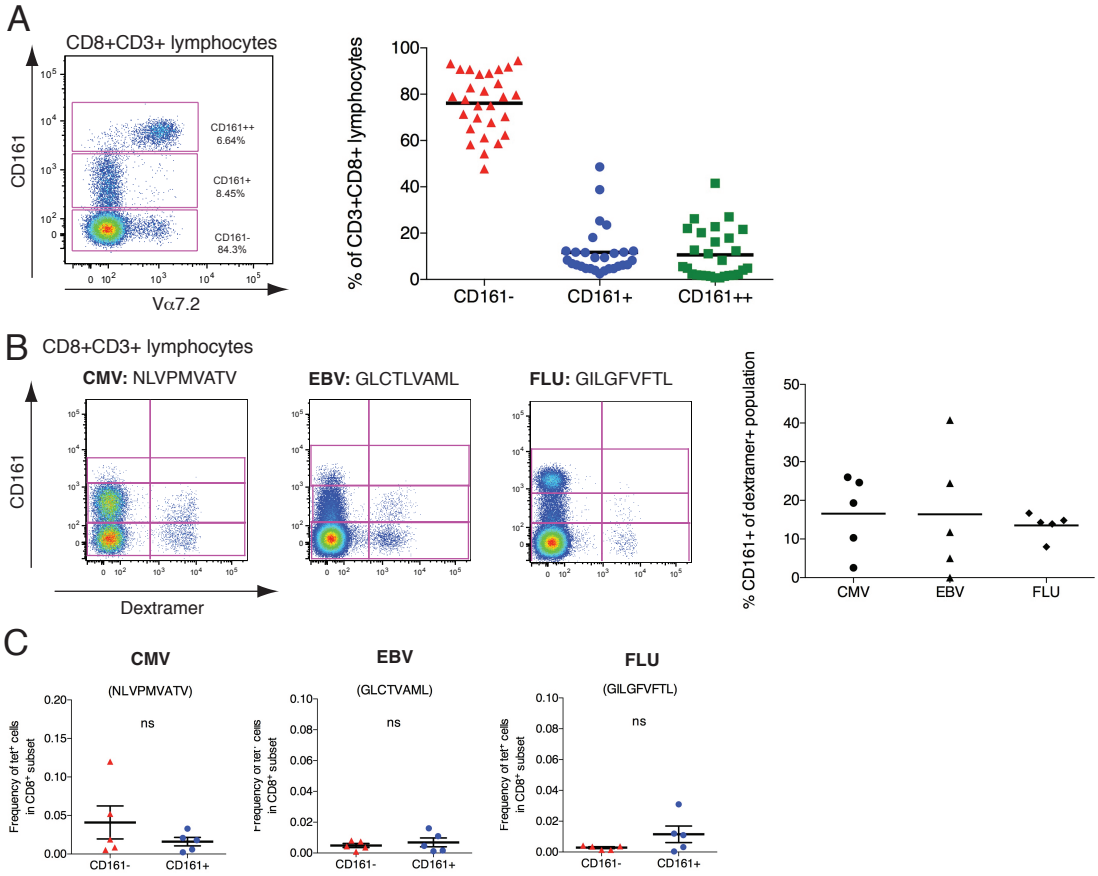

Figure 4-1: A subset of anti-viral CD8+ T cells express CD161. **A**) Representative flow cytometry plot of CD8+CD3+ lymphocytes from a healthy adult divided into three subsets based upon expression of CD161 (left panel), and cumulative data for percentage of each subset (right panel). CD161++ MAIT cells can be distinguished by expression of Vα7.2. Horizontal bars represent mean values, (n=28). **B**) Representative flow cytometry plots showing CD161 expression by CD8+ T cells specific for epitopes from CMV (NLVPMVATV), EBV (GLCTVAML) and influenza (FLU; GILGFVFTL) as distinguished by dextramer staining (left panel), and cumulative data (right panel). Horizontal bars represent mean values, (n=5). **C**) Frequency of anti-viral T cells specific for epitopes from CMV, EBV and influenza from either the CD161- or CD161+ population. ns = not significant by paired t-test, (n=5).

4.4.2. CD161 expression on CD8+ T cells is largely restricted to memory cells

CD161++ MAIT cells uniformly express an effector (CCR7−CD45RA−) memory phenotype (Martin et al., 2009). Therefore, the differentiation phenotype of bulk CD161+ CD8+ T cells from healthy adult donors was investigated, using the markers CCR7 and CD45RA to divide T cells into naïve (T_N: CCR7+CD45RA+), terminally differentiated memory (T_{EMRA}: CCR7−CD45RA+), effector memory (T_{EM}: CCR7−CD45RA−) and central memory (T_{CM}: CCR7+CD45RA−) subsets (Sallusto et al., 1999), as shown in Figure 4-2A. While approximately a quarter of CD161− cells displayed a naïve phenotype, only a very small percentage (mean 3.59%) of CD161+ were CCR7+CD45RA+, with the vast majority displaying a memory phenotype, as with CD161++CD8+ T cells (Figure 4-2B). To investigate the division of memory phenotypes, naïve cells were excluded as CCR7+CD45RA+ cells and memory cells gated only. Few T_{CM} cells were identified within peripheral blood, which may reflect their expression of CD62L and homing to the lymph node (Sallusto et al., 1999). Therefore, analysis was restricted to the division of CD161 populations between T_{EM} and T_{EMRA} memory subsets (Figure 4-2C). As expected, CD161++ CD8+ T cells displayed an almost uniform T_{EM} phenotype, while both T_{EM} and T_{EMRA} subsets were found in the CD161+ and CD161− populations. Furthermore, there was no significant difference in the percentage of either T_{EM} or T_{EMRA} subsets between the CD161+ and CD161− populations, suggesting that expression of CD161 (or loss of expression) is not associated with differentiation state. A variety of phenotypic and functional characteristics are associated with differentiation from a naïve to memory phenotype (Appay et al., 2008). As the majority of CD161+ CD8+ T cells display a memory phenotype, while the CD161− CD8+ T cell population contains a mixture of naïve and memory cells, future analyses excluded naïve cells unless otherwise stated, to ensure a fair comparison between populations.

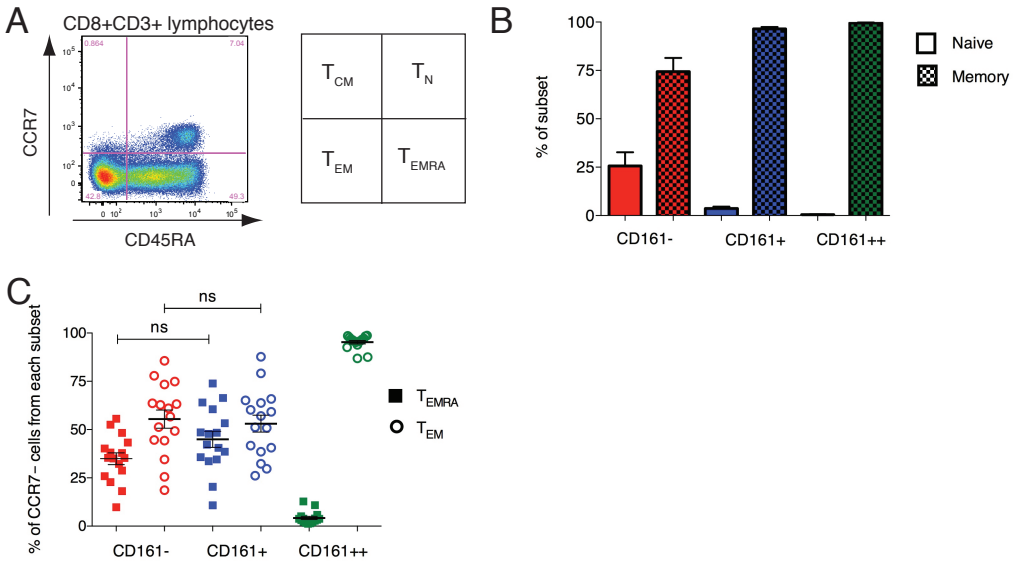

Figure 4-2 CD161 expression on CD8+ T cells in adults is largely restricted to memory cells. **A**) Representative flow cytometry plot showing CD8+CD3+ lymphocytes subgated into memory subsets based upon expression of CCR7 and CD45RA: Central memory (T_{CM}) = CCR7+CD45RA–; effector memory (T_{EM}) = CCR7–CD45RA–; terminal effector memory (T_{EMRA}) = CCR7–CD45RA+ and Naïve (T_N) = CCR7+CD45RA+, (n=11). **B**) Cumulative data for percentage of each subset displaying a naïve or memory (including T_{CM}, T_{EM} and T_{EMRA}) phenotype. **C**) Percentage of memory cells from each subset displaying a T_{EM} or T_{EMRA} phenotype, (n=16). Few T_{CM} cells are found in the peripheral circulation, so were not included in this analysis. ns = not significant by one-way ANOVA with Tukey's multiple comparisons test. Data are represented as mean ± SEM.

4.4.3. Microarray analysis of CD161+ CD8+ T cells reveals a MAIT cell-like profile

To further explore the CD161+CD8+ T cell phenotype, and to take into account the presence of naïve cells within the CD161– population, mRNA microarray analysis was repeated on sorted CD161+ and CD161– CD8+ T cell populations following the gating strategy shown in Figure 4-3A, in which naïve cells were excluded (in contrast to the microarray described in Chapter 3). Comparison of CD161+ to CD161– CD8+ T cells revealed a number of differentially expressed transcripts, including both upregulated and downregulated genes (Figure 4-3B). Of these, 952 were identified to be significantly differentially expressed ($p<0.01$, >2-fold change), illustrated by the heatmap in Figure 4-3C (Appendix IV.i). These transcripts included genes for both subunits of the IL18R (*IL18R1* and *IL18RAP*), CXCR6, MDR1 (*ABCB1*) and PLZF (*ZBTB16*). Expression was probed at the protein level by flow cytometry, and confirmed significant upregulation in expression of IL18Rα ($p<0.05$), CXCR6 ($p<0.01$), MDR1 ($p<0.01$) and PLZF ($p<0.05$) within the CD161+, when compared to the CD161–, CD8+ T cell population. For levels of expression in CD161++ CD8+ T cells please see Appendix IV.ii, and a more detailed analysis of the function of MDR1 on both CD161+ and CD161++ CD8+ T cells is described in Chapter 6. This result reflects that of Chapter 3 (Figure 3-6), in which CD161+ CD8+ T cells can be seen to mirror a CD161++/MAIT-cell phenotype, both in terms of transcriptional profile and protein expression. Indeed, GSEA analysis again showed enrichment of the CD161++/MAIT transcriptional signature within CD161+ CD8+ T cells, when compared to CD161– CD8+ T cells excluding naïve cells (Appendix IV.iii).

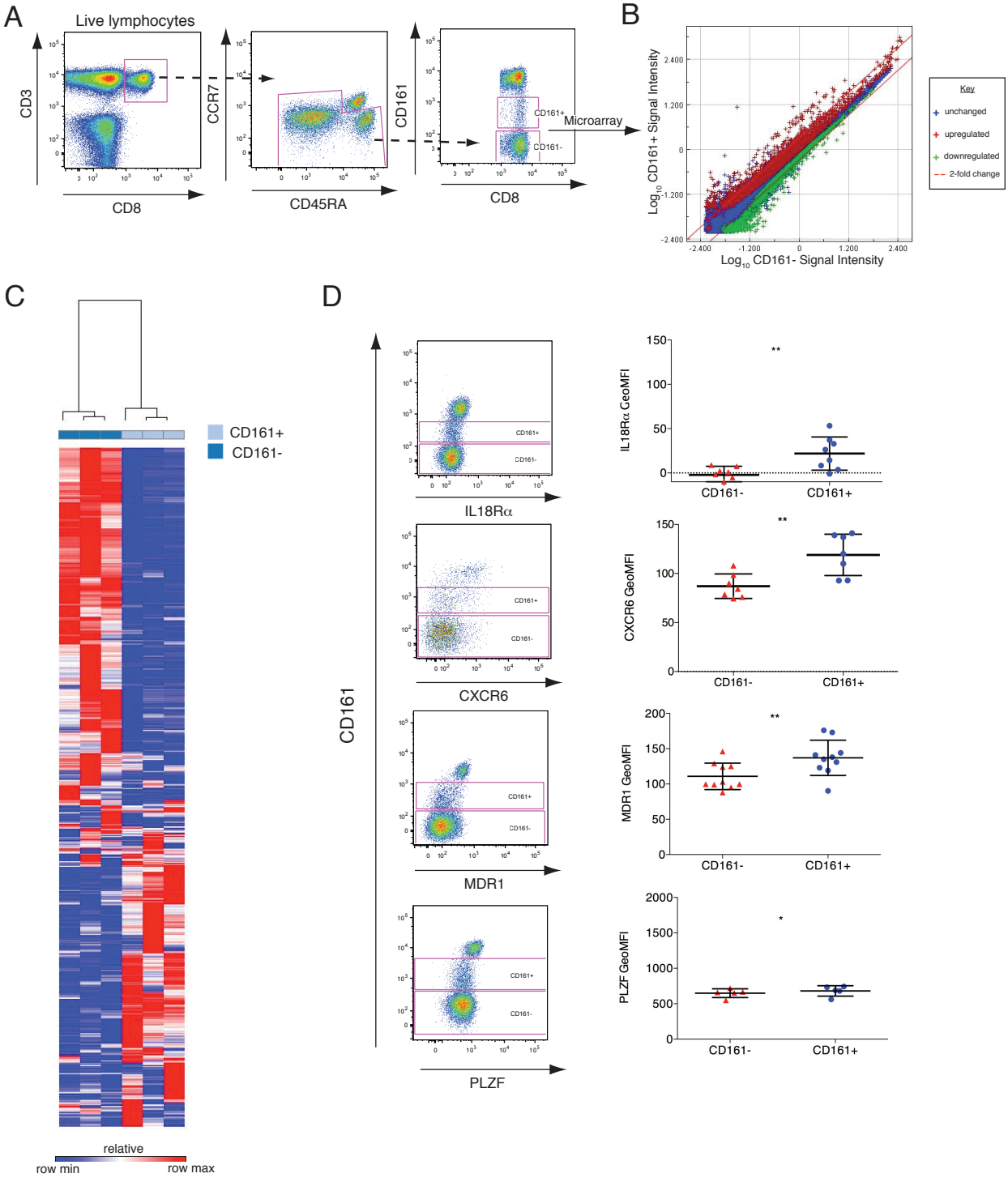

Figure 4-3: Microarray analysis of CD161+ CD8+ T cells. **A**) Gating strategy for sorting of CD161+ and CD161– subsets of CD8+CD3+ lymphocytes from 4 healthy donors for microarray analysis. **B**) Scatter plot of signal intensities of all mRNA probes. The signal intensities of each probe represented by a dot are shown in double logarithmic scale. Red diagonal lines define the areas of 2-fold differential signal intensities. Blue cross: unchanged genes, red cross: significantly upregulated genes ($p<0.01$), green cross: significantly downregulated genes ($p<0.01$). **C**) Heatmap illustrating the 952 significantly ($p<0.01$) differentially expressed transcripts between CD161+ and CD161– CD8+ T cells in 4 donors. Subsets clustered by one minus Pearson correlation. **D**) GeoMFI for IL18Rα (n=8), CXCR6 (n=7), MDR1 (n=10) and PLZF (n=5) for both CD161+ and CD161– subsets, as determined by flow cytometry, and representative flow cytometry plots for each. **$p<0.01$, *$p<0.05$ by paired t-test. Data are represented as mean ± SEM. Microarray preparation performed by James E. Ussher.

4.4.4. Expression of further NK cell receptors by CD161+ CD8+ T cells

CD161 was initially identified as a marker of NK cells (Lanier et al., 1994; Yokoyama and Seaman, 1993), and CD161 is encoded within the NK gene complex (Iizuka et al., 2003). Therefore, surface expression of various other NK cell markers within the CD161+ CD8+ T cell population was investigated by flow cytometry. NK cells are conventionally divided into functional subsets based upon the expression of CD56, the function of which is not fully understood, and CD16, the FcγIII receptor associated with antibody dependent cellular cytotoxicity (Caligiuri, 2008). CD161+ CD8+ T cells showed no significant expression of either marker in comparison to CD161– CD8+ T cells, which both showed low levels of expression. In comparison, the CD161++ CD8+ T cell population displayed significantly ($p<0.05$) higher levels of expression of CD56 than both populations, and no expression of CD16 (Figure 4-4A & B).

In addition, NK cells express a variety of activating and inhibitory receptors that regulate their activity (Bryceson et al., 2006). CD160 and CD244 are activating receptors expressed on the majority of resting NK cells. There was no significant difference in the expression of CD244 between any of the CD8+ T cell populations (Figure 4-4C), however, CD244 was expressed by significantly more CD161 positive CD8+ T cells (both CD161+ and CD161++) than CD161– ($p<0.01$, Figure 4-4D). NKp80 is an activating receptor expressed by virtually all NK cells (Vitale et al., 2001) and recently described to be functionally expressed on a subset of T cells (Kuttruff et al., 2009). This receptor was expressed by significantly ($p<0.05$) more CD161+ than CD161– CD8+ T cells (Figure 4-4E). KLRG1 is also expressed by a subset of NK cells and T cells (Butcher et al. 1998; Voehringer et al. 2002). However, there was no significant difference in the expression of this receptor by CD161+ CD8+ T cells, which was expressed by the majority of all memory CD8+ T cell subsets (Figure 4-4F).

A preliminary look at the expression of further NK receptors, namely NKG2, natural cytotoxicity receptors and killer cell immunoglobulin-like receptors (KIRs), was taken in 3 donors only due to a limit in antibody available (kindly provided by P. Borrow). CD8+CD3+ T lymphocytes in one of these donors are shown in Figure 4-5 (upper panels), with CD3– lymphocytes containing CD56+ NK cells as a comparison (lower panels). This included analysis of expression of NKG2 receptors NKG2D, NKG2C (activating), NKG2A (inhibitory), and CD94 (Figure 4-5A). NKG2C and NKG2A, and to a lesser extent CD94, were expressed by a small fraction of all CD8+ T cells, while NKG2D was not expressed by CD161++ CD8+ T cells. Natural cytotoxicity receptors NKp46, NKp30 and NKp44 were also analysed (Figure 4-5B), with minor expression of NKp46 and no expression of NKp30 by all CD161 positive CD8+ T cells. Although NKp44 appeared to be expressed by all NK cells and in all CD8+ T cell subsets, NKp44 expression has previously been described by IL-2 activated NK cells only (Vitale et al., 1998) and expression has not been found on T cells (Vitale et al., 1998), therefore this requires further investigation. The expression of various KIRs – where the antibody does not distinguish between the activating or inhibitory isoform – was also investigated, with no substantial expression by CD8+ T cells, irrespective of CD161 expression.

Together, these results indicate that CD161 positive CD8+ T cells can express further NK receptors, such as CD244 and NKG2C, but only expression of NKp80 is specifically enriched within the CD161+ CD8+ T cell population, compared to CD161– CD8+ T cells.

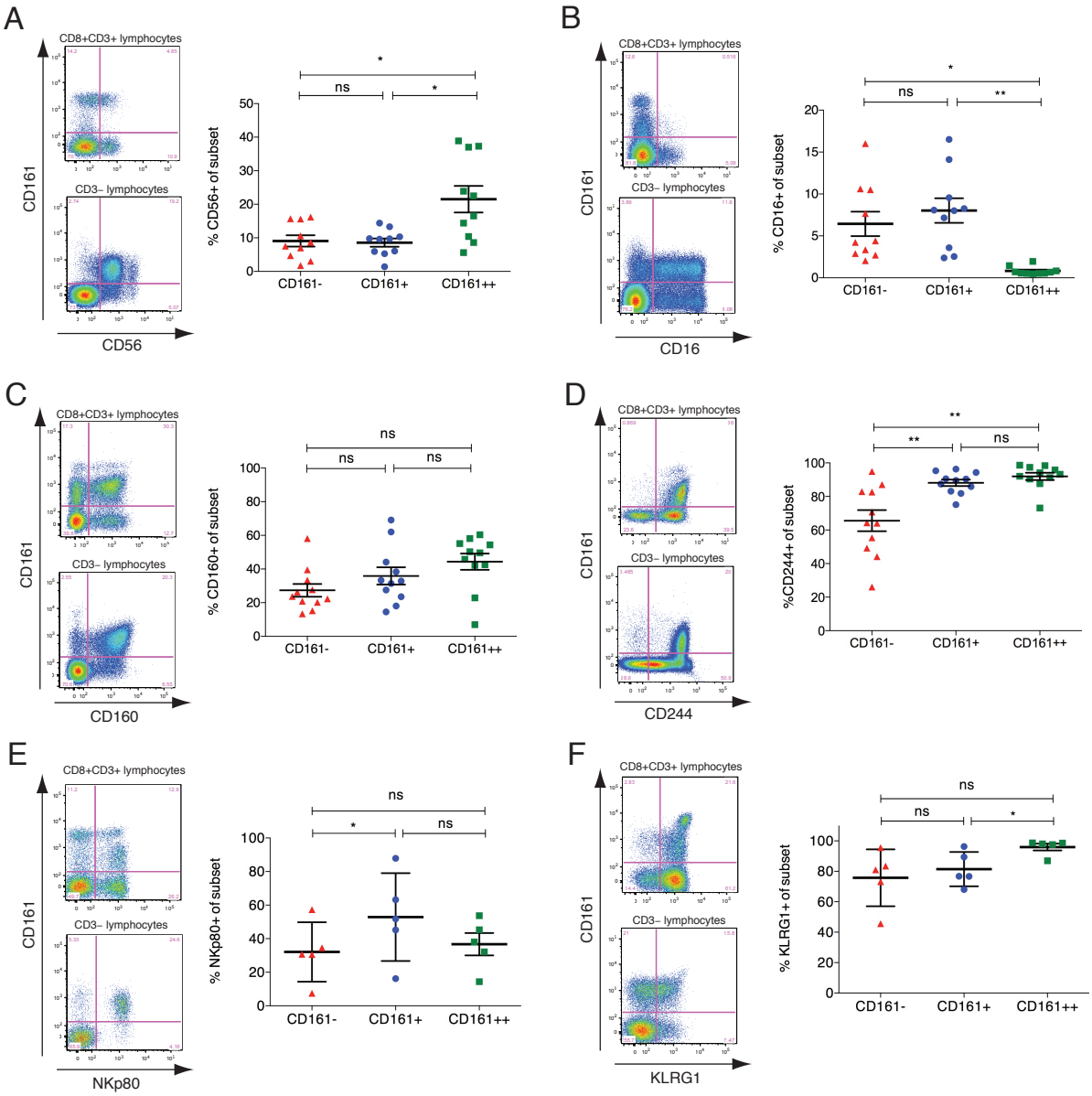

Figure 4-4 Expression of further NK cell markers by CD161+CD8+ T cells. Representative flow cytometry plots and cumulative data for percentage of CD8+CD3+ lymphocytes, excluding CCR7+CD45RA+ naïve cells, expressing CD56 (**A**) (n=10), CD16 (**B**) (n=10), CD160 (**C**) (n=11), CD244 (**D**) (n=11), NKp80 (**E**) (n=5) and KLRG1 (**F**) (n=5) in each CD161 subset. A representative plot of CD3– lymphocytes, including CD161+ NK cells, is shown for comparison. Gates were set according to the corresponding isotype or fluorescence minus one (FMO) sample. **p<0.01, *p<0.05, ns = not significant by one-way ANOVA with Tukey's multiple comparisons test. Data are represented as mean ± SEM.

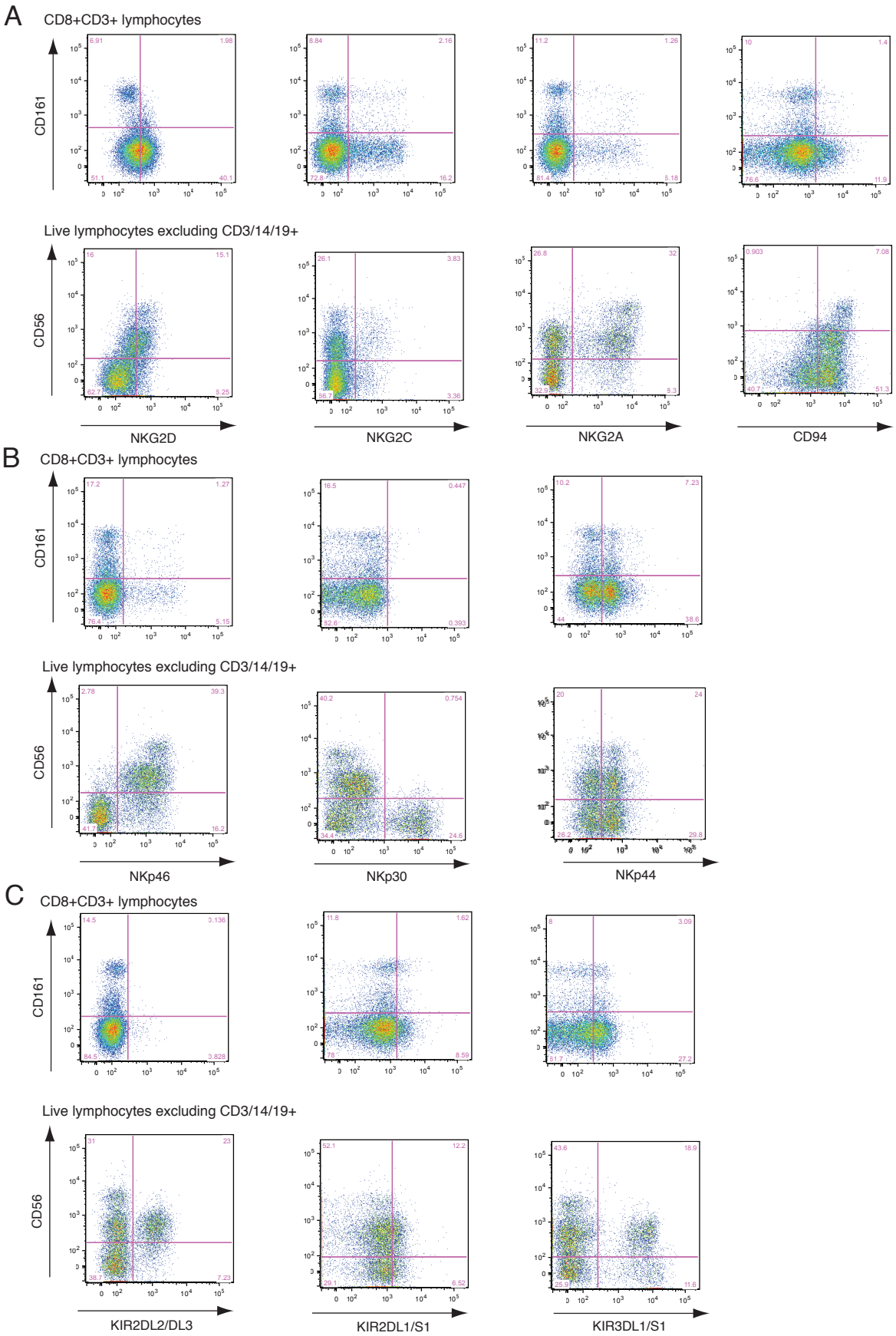

Figure 4-5: Expression of NK cell activating, killer cell immunoglobulin-like (KIRs) and natural cytotoxicity (NCRs) receptors by CD161+ CD8+ T cells. Representative flow cytometry plots show CD8+CD3+ lymphocytes (top panels) and CD3– lymphocytes, including CD56+ NK cells (bottom panels), stained for expression of NK cell activating receptors NKG2D, NKG2C, NKG2A and CD94 (**A**), NCRs NKp46, NKp30 and NKp44 (**B**) and KIRs KIR2DL2/DL3, KIR2DL1/S1 and KIR3DL1/S1. Gates were set according to the corresponding isotype or fluorescence minus one (FMO) sample.

4.4.5. CD161+ CD8+ T cells are potent effector cells

CD8+ T cells and NK cells are both cytotoxic and cytokine-producing effector cells, with the expression of NK cell receptors acting to regulate these responses. Cytotoxicity against target cells is mediated through perforin and granzyme B, pre-formed and held within intracellular vesicles. The expression of these cytotoxic effector molecules was investigated by flow cytometry. The expression pattern of perforin by CD161 subsets renders it difficult to define 'positive' and 'negative' populations, even with an isotype or fluorescence minus one (FMO) control sample, and therefore perforin expression was defined by geometric mean fluorescence intensity (geoMFI). While CD161++ CD8+ T cells are granzyme B negative and perforin low in the resting state (Billerbeck et al., 2010; Kurioka et al., 2014), a significantly larger proportion ($p<0.0001$) of the CD161+ CD8+ T cell population expressed granzyme B (mean 60.74%) compared to the CD161– CD8+ T cell population (Figure 4-6A). Moreover, CD161+ CD8+ T cells expressed significantly higher levels of perforin ($p<0.001$) than CD161– CD8+ T cells (Figure 4-6B), rendering these cells potently equipped for cytotoxic killing of target cells.

CD8+ T cells are also potent cytokine-producing cells, releasing effector cytokines such as IFNγ and IL-2 upon stimulation (Paliard et al., 1988). Therefore, expression of these cytokines was assayed by intracellular cytokine staining (ICS) after stimulation with PMA + ionomycin for 3hrs in the presence of the protein transport inhibitor Brefeldin A. A significantly larger proportion ($p<0.0001$) of CD161+ CD8+ T cells produced IFNγ upon stimulation than either CD161++ or CD161– CD8+ T cells (Figure 4-6C). More CD161+ CD8+ T cells produced IL-2 than CD161++ CD8+ T cells, although not significantly more than by the CD161– CD8+ T cell population. However, CD161+CD8+ T cells were significant ($p<0.01$) dual-producers of a combination of IFNγ and IL-2, with a mean of 22.29% of the population producing both cytokines after 3hrs (Figure 4-6D). Unfortunately, due to technical difficulties, the production of IL-17 could not be assayed by ICS. However, it has previously

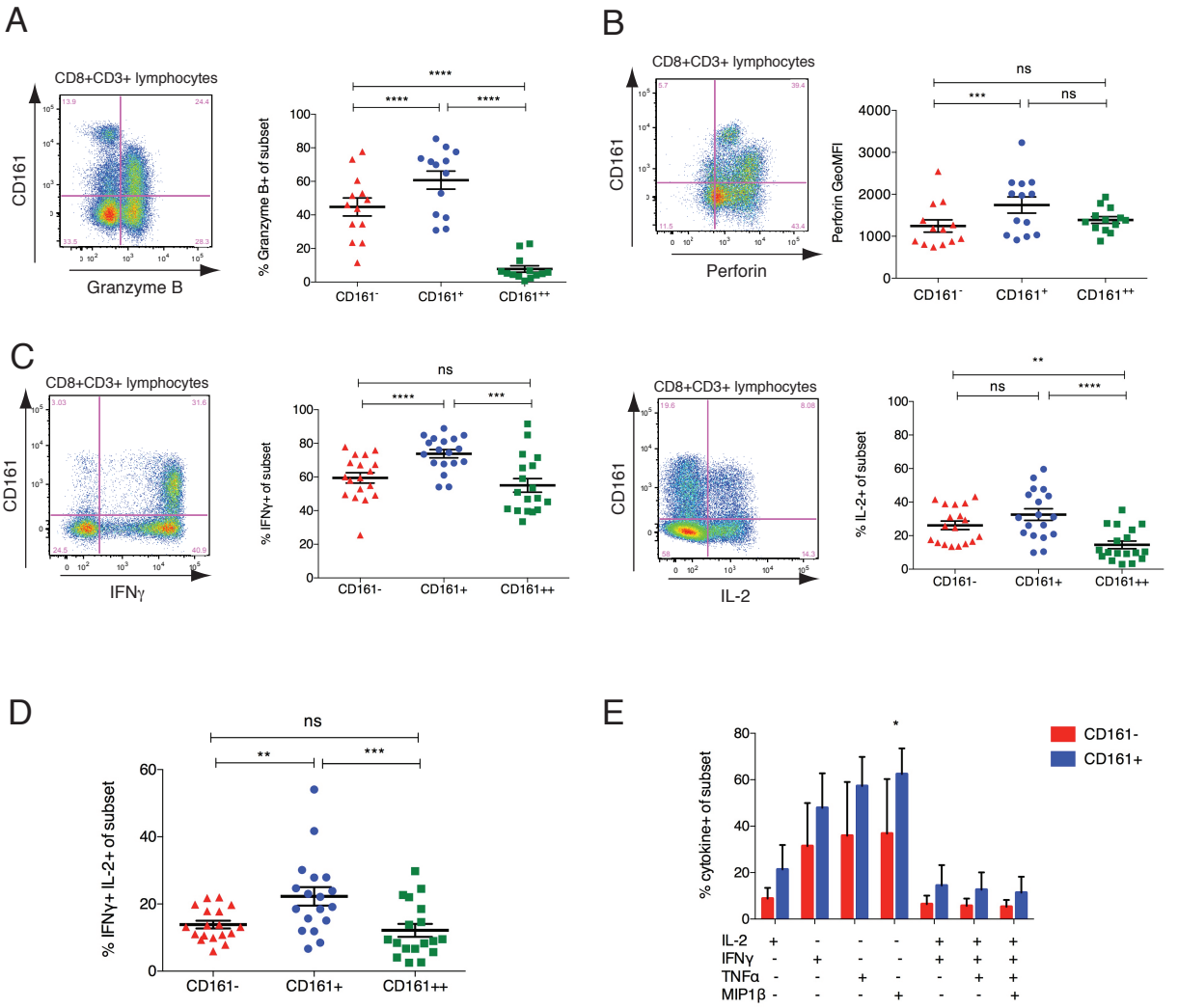

Figure 4-6: High expression of cytotoxic effectors and cytokines by CD161+ CD8+ T cells. **A**) Representative flow cytometry plot and cumulative data for percentage of CD8+CD3+ lymphocytes, excluding CCR7+CD45RA+ naïve cells, expressing granzyme B in each CD161 subset (n=13). Gates were set according to the corresponding FMO. **B**) Representative flow cytometry plot and cumulative data for geometric mean fluorescence intensity (geoMFI) of perforin expression in each CD161 subset of CD8+CD3+ lymphocytes, excluding CCR7+CD45RA+ naïve cells (n=13). **C**) Percentage of each CD161 subset expressing IFNγ (left) and IL-2 (right) upon stimulation with PMA + ionomycin for 3hrs (n=18), and representative flow cytometry plots for each. **D**) Percentage of each CD161 subset expressing both IFNγ and IL-2 upon stimulation with PMA + ionomycin for 3hrs (n=18). **E**) Percentage of each CD161 subset expressing each cytokine (IL-2, IFNγ, TNFα and MIP1β) alone or in combination as assayed by CyTOF upon PMA + ionomycin stimulation for 3hrs (n=4). ****p<0.0001, ***p<0.001, **p<0.01, *p<0.05, ns = not significant by one-way ANOVA with Tukey's multiple comparisons test. Data are represented as mean ± SEM.

been shown that IL-17 secretion amongst CD8+ T cells is restricted to the CD161++ subset (Billerbeck et al., 2010).

Cytokine production was also probed by mass cytometry (CyTOF), which allows the production of multiple cytokines, in this case IL-2, IFNγ, TNFα and MIP1β, to be assayed simultaneously. A larger percentage of CD161+ CD8+ T cells produced each of the four cytokines singly, and in combination, than CD161– CD8+ T cells (Figure 4-6E), demonstrating the CD161+CD8+ T cell population to be polyfunctional.

In sum, these data show CD161+CD8+ T cells to be potent effector cells, expressing more granzyme B, perforin, cytokines and chemokines than the CD161– CD8+ T cell population.

4.4.6. CD161+ CD8+ T cells are the major CD161 positive CD8+ T cell subset in the gut, but not the liver

Analyses so far have phenotyped CD161+ CD8+ T cells from the peripheral blood of healthy adults. However, CD161 positive T cells have been found in healthy tissues, including the gut (O'Keeffe et al., 2004) and liver (Ishihara et al., 1999). Expression of CD103 ($\alpha_E\beta_7$) has been associated with retention of T cells within epithelial tissues (Cepek et al., 1994) and with resident CD8+ memory cells of mucosal tissues including the intestine (Sathaliyawala et al., 2013). Although it has been reported that only 4% of circulating CD8+ T cells bear the CD103 molecule (Uss et al., 2006), this expression appeared to be relatively enriched within the CD161+CD8+ T cell fraction in peripheral blood (Figure 4-7A).

CD161++Vα7.2+ MAIT cells were originally described to be preferentially located in the gut lamina propria of humans (Treiner et al., 2003), related to their expression of $\alpha_4\beta_7$ integrin, however the major CD161+ T cell population within the gut here was

Vα7.2– (Figure 4-7B). Lymphocytes were taken from non-involved colon sections of 11 colorectal cancer patients and divided based upon expression of CD161 and Vα7.2 as determined by flow cytometry (with expression of CD161 alone making it difficult to distinguish three CD8+ T cell populations, such as seen within the blood). CD161 was expressed by an average of 36.06% of memory (CD45RO+) CD8+ T cells, with only a minor proportion of these expressing the Vα7.2 TCR. Furthermore, CD103 expression was enriched within CD161+ CD8+ T cells from the colon (Figure 4-7C, left). CD161+CD8+ T cells are therefore a prominent tissue resident memory population within the gut.

Next, the composition of intestinal T lymphocyte populations during inflammation was investigated. An increase in CD161– cells was evident within the gut during inflammatory bowel disease (IBD) (Figure 4-7C, right). This was reflected by a significant reduction ($p<0.05$) in CD103+ memory (CD45RO+) CD8+ T cells in inflamed tissue from patients with IBD, and a corresponding decrease in the percentage of memory CD8+ T cells expressing CD161 (Figure 4-7D). This was not the case in non-inflamed IBD gut, or in diverticular disease. Analysis of populations expressing both these markers revealed an increase of CD161–CD103– CD8+ T cells in IBD, which resulted in the specific dilution of CD103+CD161+ memory CD8+ T cells (Figure 4-7E). This suggests, therefore, that CD161+ CD8+ T cells, enriched in expression of CD103, represent a resident memory population within the gut, with an increase in CD103–CD161– CD8+ memory T cells associated with inflammation in IBD. As expression of CD103 is thought to result from TGFβ signalling within the gut (Mackay et al., 2013; Masopust et al., 2006b), CD103–CD161– cells enriched during IBD likely represent influxing cells.

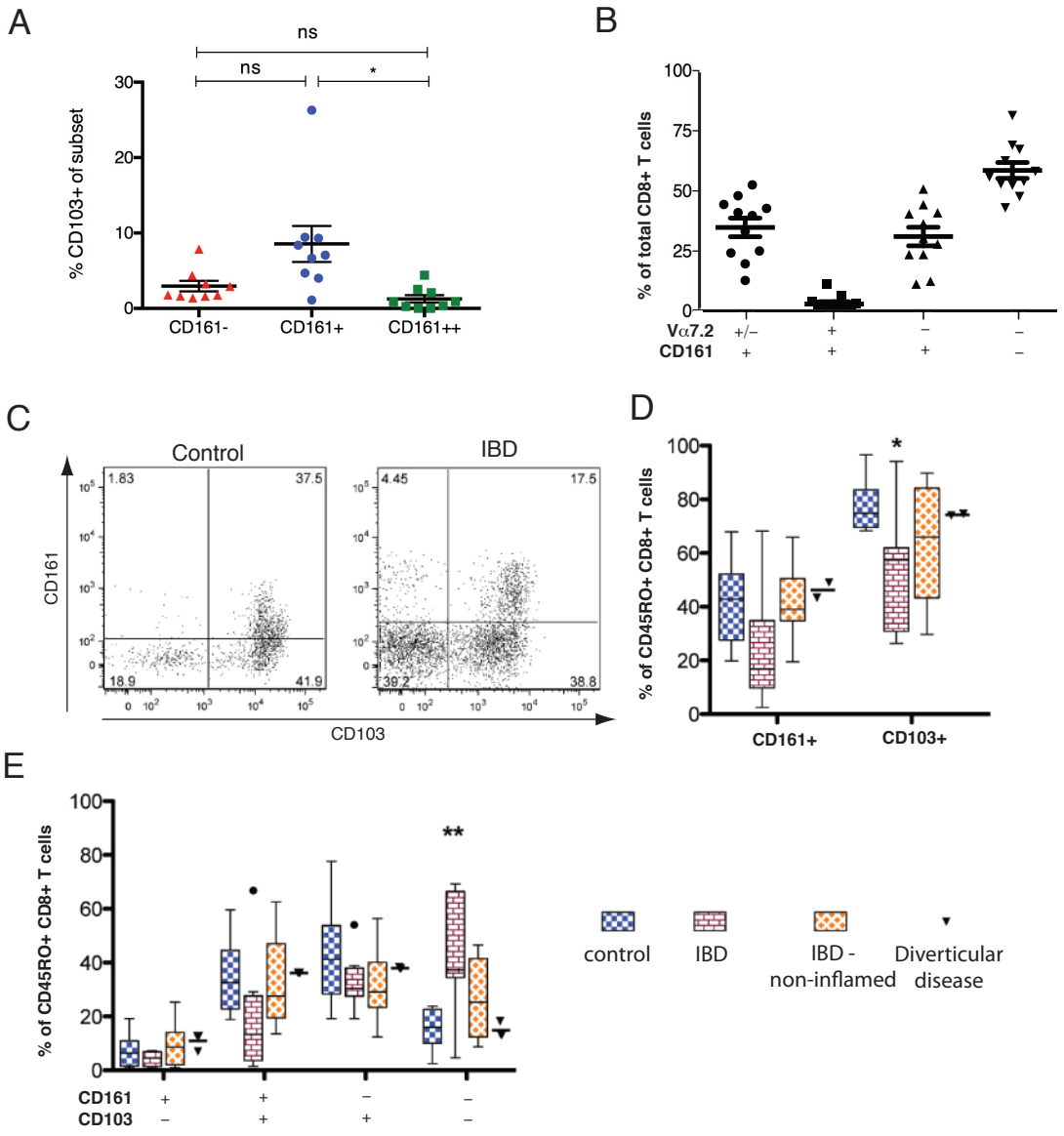

Figure 4-7: CD161+ CD8+ T cells are enriched in the non-inflamed gut. **A**) Percentage of each CD161 subset expressing CD103 in peripheral blood (n=9). *p<0.05, ns = not significant by one-way ANOVA with Tukey's multiple comparisons test. **B**) Percentage of total CD8+ T cells expressing Vα7.2 and/or CD161 amongst lamina propria leukocytes from non-inflamed colon (n=11). **C**) Representative flow cytometry plot of expression of CD103 and CD161 by CD8+CD3+ lamina propria leukocytes from either healthy control (left) or an IBD patient (right). **D** and **E**) Percentage of CD45RO+ memory CD8+ T cells expressing CD161 or CD103 (**D**) or combinations of both (**E**) in healthy control (blue hatch; n=6), IBD (maroon hatch; n=8), IBD non-inflamed gut (orange; n=12) or diverticular disease (triangle; n= 2). Data are represented as mean ± SEM. *p<0.05 by Friedman test with Dunn's multiple comparisons test (**D**) or two-way ANOVA with Bonferroni multiple comparisons test (**E**). Data are represented as mean ± SEM. Data in panels B-E were performed and analysed by, and presented here by kind permission of, Michael Huhn (F. Powrie lab).

CD161++Vα7.2+ MAIT cells have also been described to be enriched within the human liver (Billerbeck et al., 2010; Dusseaux et al., 2011), as have CD103-expressing T cells (Shimizu et al., 2003), with hepatocytes expressing the CD103 ligand E-cadherin (Ashida et al., 1998). A similar analysis of intrahepatic lymphocytes from healthy livers of four donors was performed, to determine if CD161+ CD8+ T cells are similarly enriched within the liver as for gut. Again, division between CD161+ and CD161++ CD8+ T cell subsets is difficult within these tissue lymphocytes, as illustrated by Figure 4-8A, and therefore CD8+ T cells were divided simply as CD161+/– and Vα7.2+/–, as previously (Figure 4-7B). It should be noted that naïve cells were not excluded from this analysis. In contrast to the gut, the majority of CD8+ T lymphocytes expressed CD161 (mean 62.35%) and of those the majority were also Vα7.2+, identifying MAIT cells as the major population within the healthy liver.

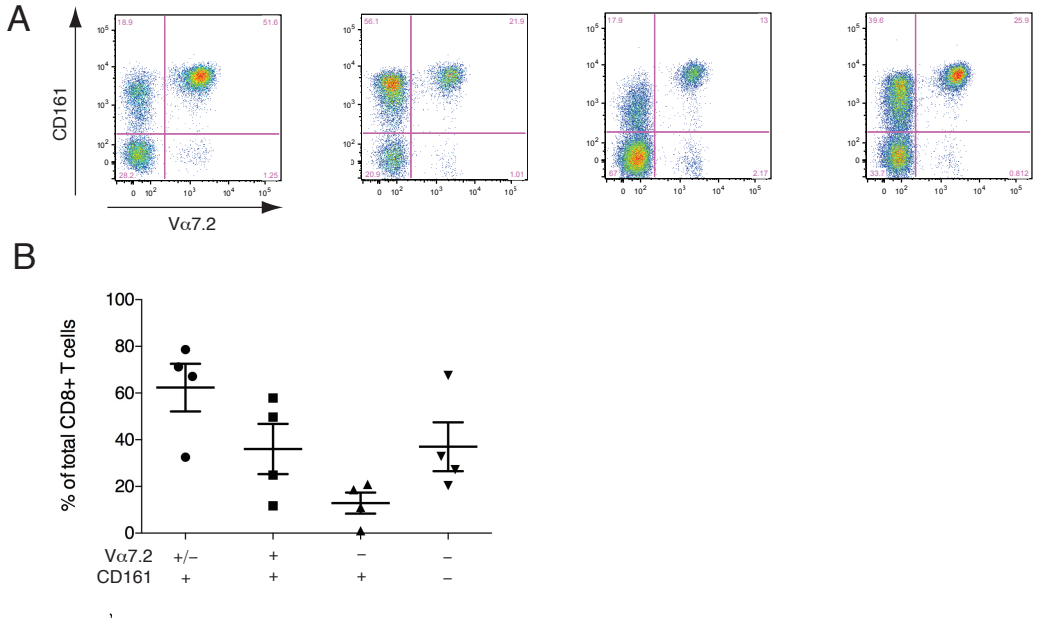

Figure 4-8: MAIT cells are the major CD161 positive CD8+ T cell population in the healthy liver. **A**) Flow cytometry plots of CD161 and Vα7.2 expression by CD8+CD3+ intrahepatic lymphocytes. **B**) Percentage of total CD8+ T cells from intrahepatic lymphocytes from healthy donors expressing Vα7.2 and/or CD161 (n=4). Staining performed by James E. Ussher.

4.4.7. Phenotype of CD161+ CD8+ T cells in peripheral blood of Hepatitis C-infected patients

CD161 is reported to be significantly enriched on CD8+ T cells specific for Hepatitis C virus (HCV) compared to CD8+ T cells specific for human immunodeficiency virus (HIV), CMV or FLU in peripheral blood (Northfield et al., 2008). The majority of CD161++ CD8+ T cells are MR1-reactive MAIT cells, while CD161+CD8+ T cells are identifiable by MHC class I multimers (Figure 4-1). Therefore enrichment of CD161 on HCV-specific CD8+ T cells is likely descriptive of an enrichment in CD161+ CD8+ T cells. Consequently, a comprehensive phenotypic analysis of CD161+ CD8+ T cells in peripheral blood of patients with chronic Hepatitis C infection was undertaken. The clinical attributes of patients included in the study are shown in Table 4-2. All patients were infected with genotype 1 and were treatment naïve. PBMC from HCV patients were phenotyped by flow cytometry, and were stained alongside healthy controls for comparison. Few HCV-tetramer positive populations were detected, and therefore analysis was performed on bulk populations. Naïve cells were excluded from analyses.

Firstly, the proportions of each subset were compared. This demonstrated a significant decrease in CD161++ CD8+ T cells in HCV infection, with a corresponding increase in the proportion of CD161– CD8+ T cells (Figure 4-9A). This confirms previous reports in which CD161++ CD8+ T cells were lost from the blood and enriched within the liver of HCV patients (Billerbeck et al., 2010), indicating a redistribution of this cell subset. The proportion of CD161+ CD8+ T cells was unchanged.

As CD161+ CD8+ T cells in healthy blood are significantly enriched for expression of cytotoxic molecules granzyme B and perforin, compared to other CD8+ T cell subsets (Figure 4-6A &B), the expression of these molecules in the blood of patients

Patient ID	M/F	A2?	Treatment	Genotype	ALT
119	M	y	None	1	99
126	M	y	None	1	88
131	M	y	None	1	118
144	F	y	None	1	57
156	M	y	None	1	37
180	M	n	None	1a	n.d.
181	F	y	None	1b	123
197	F	y	None	1	27
201	M	y	None	1	64
205	M	y	None	1	28
208	M	y	None	1	72
251	F	y	None	1a	36
342	F	y	None	1b	27
354	M	y	None	1a	23
577	M	n	None	1a	24
615	M	n	None	1	77
633	F	y	None	1a	50
641	F	y	None	1	26
671	M	y	None	1a	14
675	M	y	None	1a	71
727	F	n	None	1b	37
765	M	n	None	1	n.d.
836	M	y	None	1b	175
843	M	y	None	1a	n.d.
873	F	y	None	1a	142
875	M	n	None	1a	54
913	F	y	None	1a	166
921	M	n	None	1	49
934	F	n	None	1	70
940	M	y	None	1b	64
945	M	n	None	1a	196
954	M	n	None	1a	54
957	F	n	None	1a	24
960	M	n	None	1a	72
963	M	y	None	1a	56
966	M	y	None	1a	62
972	F	y	None	1a	183

Table 4-2 Hepatitis C-infected patient details. Patients were A2 typed by flow cytometry using an anti-HLA-A2 fluorochrome-tagged antibody. All patients were treatment naive at the time of PBMC sampling. n.d. = not determined.

with HCV infection was investigated. While a significant reduction ($p<0.05$) in the percentage of CD161– CD8+ T cells expressing granzyme B was apparent, no significant difference in the CD161+ CD8+ T cell population was seen (Figure 4-9B), demonstrating that CD161+ CD8+ T cells maintain their granzyme B expression in chronic infection. A significant reduction in perforin expression in bulk CD8+ T cells in HCV patients compared to healthy controls, and not seen in spontaneous resolvers, has been previously described (Lucas et al., 2004). In this patient cohort, a reduction in perforin was seen in both CD161+ and CD161– subsets, but was only significantly reduced ($p<0.01$) within the CD161– CD8+ T cell population (Figure 4-9C), indicating that CD161+ CD8+ T cells also maintain their perforin expression to a better level than CD161– CD8+ T cells.

CD8+ T cell responses during acute HCV infection are important in determining progression to chronic infection over spontaneous resolution (Folgori et al., 2006; Lauer et al., 2004; Spada et al., 2004). Further, polyfunctionality of CD8+ T cells has been associated with differing patient outcomes, particularly with regard to HIV infection (Betts et al., 2006). The CD161+ CD8+ T cell population contains a higher proportion of IL-2 and IFNγ dual-producing cells than within the CD161– CD8+ T cell population (Figure 4-6C). Again, a reduction in dual-producers was seen in both CD161+ and CD161– CD8+ T cell populations. However, cytokine production was significantly ($p<0.05$) reduced within the CD161+ CD8+ T cell population only (Figure 4-9D), demonstrating a more profound loss of polyfunctionality within this population.

Next, the question of whether vaccination could induce CD161 positive anti-viral T cells, and whether these cells mirrored this phenotype, was investigated. A novel vaccination strategy using two adenoviral vectors expressing non-structural proteins from HCV genotype 1B has been shown to be immunogenic in healthy donors, priming sustained CD8+ T cells specific for HCV (Barnes et al., 2012). Of these HCV-specific CD8+ T cells, approximately 18% expressed CD161 (Figure 4-10A). This is in comparison to a median of 16.8% described in natural chronic infection

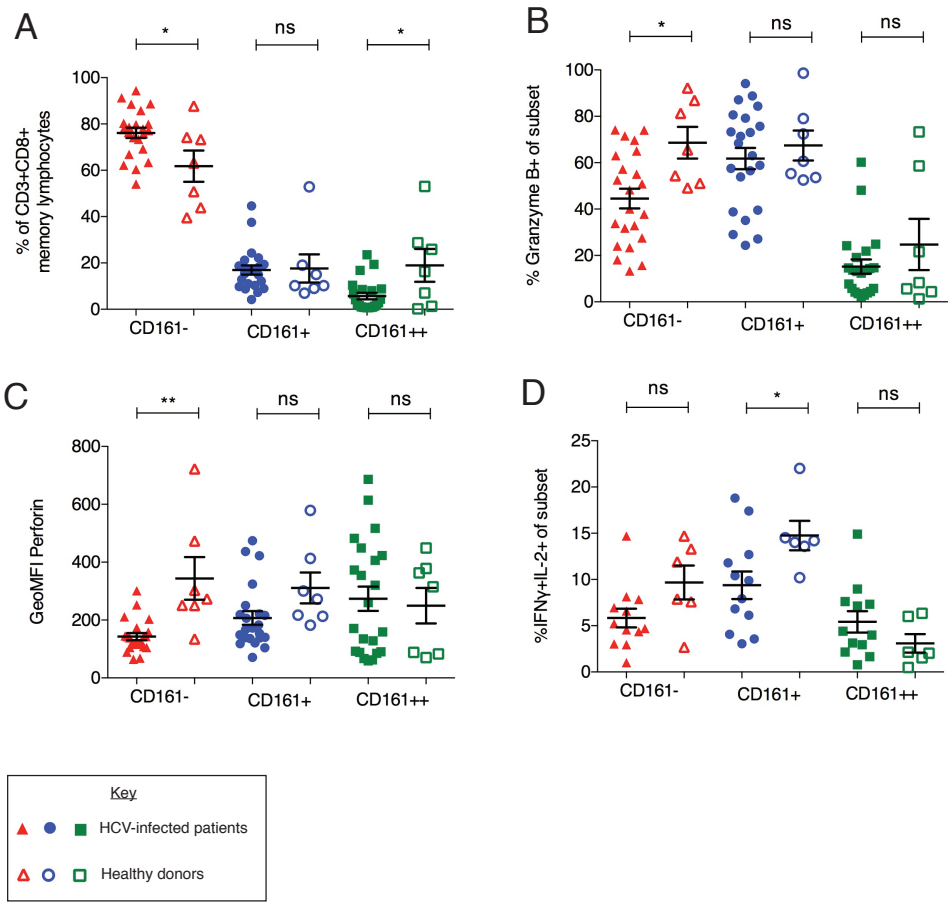

Figure 4-9: Cytotoxic profile, but not cytokine production, is maintained in CD161+ CD8+ T cells of treatment naive Hepatitis C (HCV)-infected patients. **A**) Percentage of each CD161 subset amongst CD8+CD3+ lymphocytes in PBMC of HCV-infected patients (n=22) or healthy donors (n=7). **B** and **C**) Percentage granzyme B positive (**B**) and geoMFI of perforin (**C**) in each CD161 subset in HCV-infected patients (n=22) or healthy donors (n=7). **D**) Percentage of each CD161 subset expressing a combination of IFNγ and IL-2 upon stimulation with PMA + ionomycin for 3hrs in HCV-infected patients (n=12) or healthy donors (n=6). HCV-infected are represented by closed symbols, healthy donors by open symbols. Data are represented as mean ± SEM. **p<0.01, *p<0.05 and ns = not significant by one-way ANOVA with Sidak's multiple comparisons test.

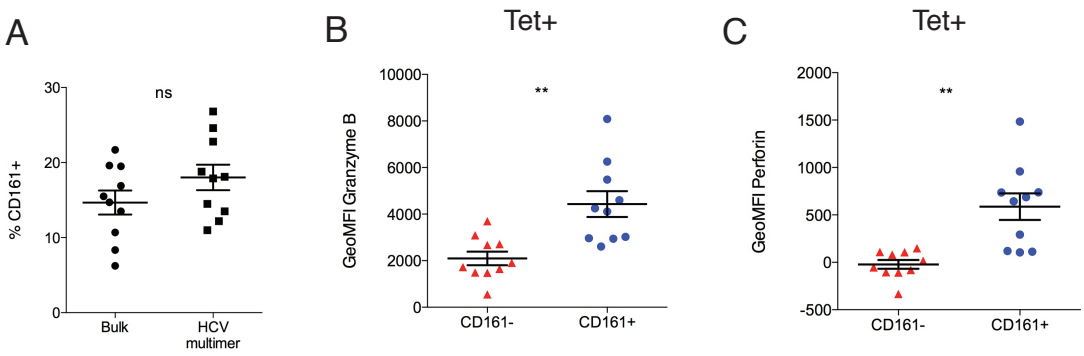

Figure 4-10: CD161 expression defines potent cytotoxic anti-viral responses in hepatitis C vaccinated healthy donors. Vaccine-induced responses were measured at the end of study timepoints (weeks 36 or 52) after vaccination with adenovirus vectors encoding the NS3-5B region of HCV genotype 1B as described (Barnes et al., 2012) **A**) Percentage of bulk CD8+ and vaccine-induced HCV (KSLGLGINAV)-specific CD8+ T cells expressing CD161 as identified by pentamer staining (n=10). **B** and **C**) GeoMFI of granzyme B (**B**) and perforin (**C**) by CD161+ and CD161– subsets of HCV (KSLGLGINAV)-specific CD8+ T cells (Tet+) (n=10). **p<0.01 and ns = not significant by paired t-test. Staining and flow cytometry analysis performed by Leo J. Swadling.

(Northfield et al., 2008). Expression of granzyme B and perforin by the CD161+ and CD161– subsets of the pentamer cloud was also determined, using geoMFI as a readout for expression due to the small number of cells being analysed. This showed significantly ($p<0.01$) higher expression of both granzyme B and perforin by CD161+ CD8+ T cells compared to CD161– (Figure 4-10B&C). Therefore, vaccination can induce a fraction of CD161 expressing HCV-specific T cells that are enriched for both granzyme B and perforin expression.

4.4.8. Analysis of stimulated CD161+ CD8+ T cells by microarray

To further investigate the functional potential of CD161+CD8+ T cells, a hypothesis-free approach was used by which the transcriptional profile of these cells after short-term stimulation was examined by microarray. Firstly, the appropriate time course and stimulant for analysis was determined. PBMC were stimulated for various lengths of time (ranging from 2 to 6 hours) with either PMA plus ionomycin, or CD3/2/28 activation beads, and cytokine production assayed by intracellular cytokine staining. Brefeldin A was added for the last hour of stimulation. CD3/2/28 activation induced little production of cytokine at any of the short timepoints measured (Figure 4-11A-C). In contrast, stimulation with PMA plus ionomycin induced high levels of cytokine. The proportion of cells producing IFNγ peaked at 4hrs and was maintained to 6hrs (Figure 4-11A) and TNFα production increased with time (Figure 4-11B). However, production of IL-2 peaked at 4hrs and was lost by 6hrs (Figure 4-11C). PMA plus ionomycin is a strong stimulus, and high levels of cytokine production are balanced by activation induced cell death. Therefore, the percentage of dead lymphocytes after each timepoint was also analysed, and found to be below 10% at the 4hr timepoint, increasing to approximately 20% by 6hrs.

To confirm peaks in cytokine protein production were reflected at the mRNA level (measured by microarray), IFNγ mRNA levels were measured by quantitiave RT-PCR (qRT-PCR) at 2, 4 or 6hrs of stimulation with PMA plus ionomycin. Expression

of IFNγ mRNA also peaked at 4hrs within 3 donors, and therefore 4hr stimulation with PMA plus ionomycin was chosen to proceed.

PMBC from the same three donors were sorted into CD161+ and CD161− CD8+ T cell subsets (excluding naïve cells) as previously (Figure 4-3). Sorted populations were then stimulated for 4hrs with PMA plus ionomcyin before being snap frozen for microarray analysis. Comparison of transcripts of stimulated CD161+ and CD161− CD8+ T cells to their unstimulated counterparts (data from Figure 4-3) showed an explosion of upregulated and downregulated transcripts upon stimulation (Figure 4-12A) including upregulated expression of the expected genes including IFNγ and IL-2 (Appendix IV.iv). However, when stimulated CD161+ CD8+ T cells were compared to stimulated CD161− CD8+ T cells few significantly differentially expressed transcripts for known chemical mediators (ie. cytokines or chemokines) were found (Figure 4-12B, Appendix IV.v). Of the few transcripts significantly upregulated more than 2-fold, one of the only cytokine genes was *IFNA6*, encoding Interferon (IFN)α-6. The interferon α family is a highly homologous family of cytokines, whose 13 members bind the same receptor and therefore possess the same antiviral properties (Platanias, 2005). Production of this cytokine at the protein level was assayed by flow cytometry, using an antibody recognising multiple isoforms including IFNA6, after 4hr stimulation of PBMC with PMA plus ionomycin. However, no IFNα production was observed by either CD161+ or CD161− CD8+ T cell populations, while CD14+ monocytes, which have previously been described to produce IFNα (Hansmann et al., 2008) produced low levels. Microarray analysis, therefore, demonstrates CD161+ and CD161− CD8+ T cells to have largely identical transcription patterns, at least in terms of cytokine and chemokine production, after 4hr stimulation with PMA plus ionomycin.

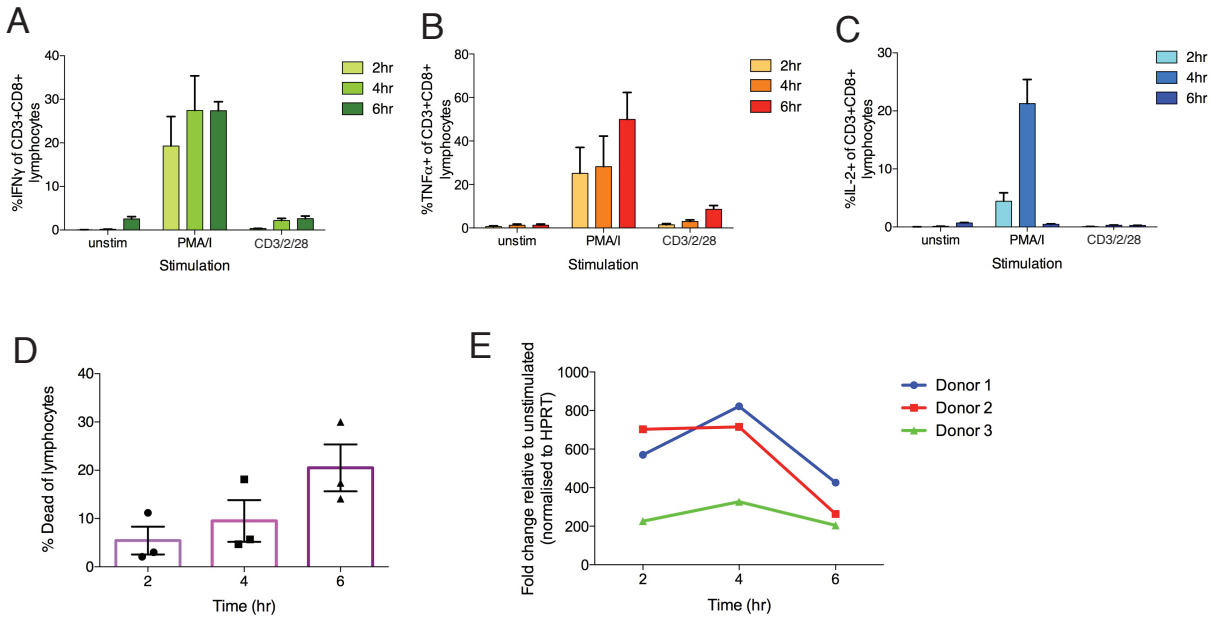

Figure 4-11: Stimulation with PMA + ionomycin for 4hrs was optimal for analysis of cytokine production by microarray. Percentage of CD8+ T cells expressing IFNγ (**A**), TNFα (**B**) and IL-2 (**C**) upon stimulation with either PMA + ionomycin or CD2/3/28 activation beads for either 2, 4 or 6hrs (n=3). Data are represented as mean ± SEM. **D**) Percentage of lymphocytes dead after PMA + ionomycin stimulation after 2, 4 or 6hrs as determined by staining with live/dead dye (see Chapter 2) (n=3). Histograms show the mean and error bars represent SEM. **E**) Relative expression of IFNγ by CD8+ T cells stimulated with PMA + ionomycin for 2, 4 or 6hrs compared to unstimulated controls in 3 donors. Expression was normalised to that of HPRT in all samples. Each donor is represented by a separate line, with each data point displaying the average of triplicate wells.

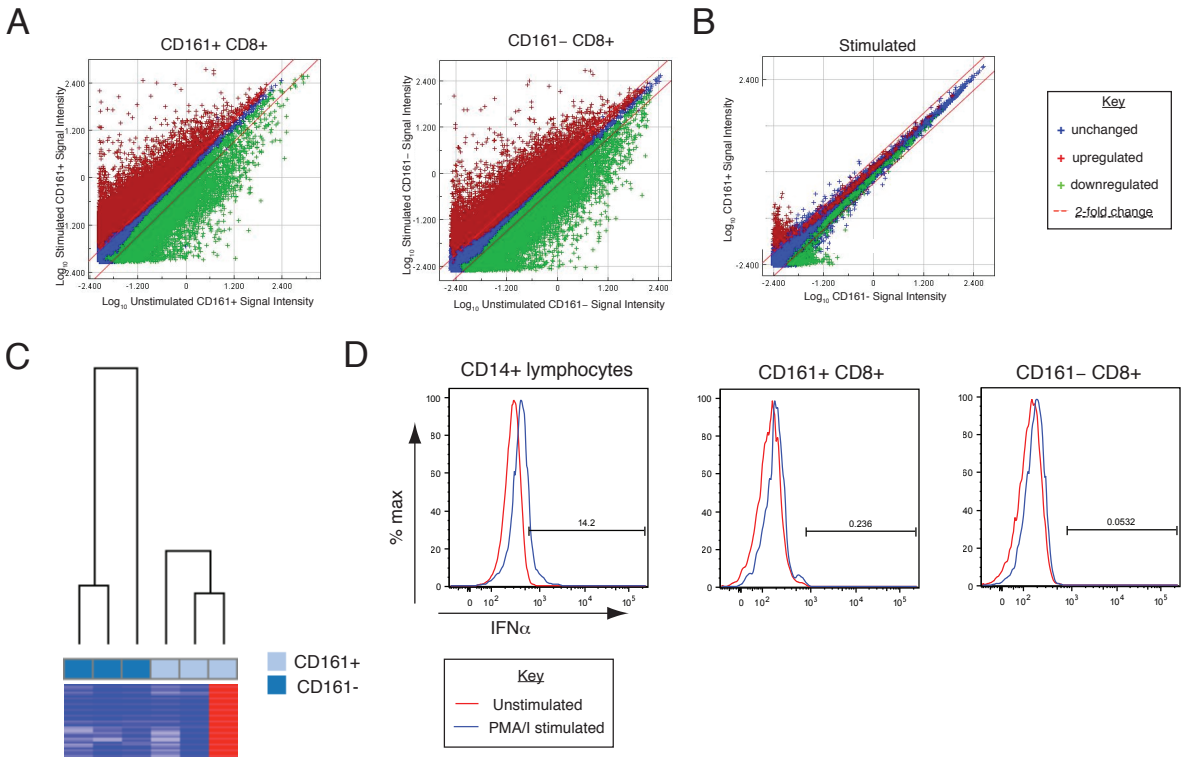

Figure 4-12: Microarray analysis reveals few uniquely expressed cytokines by stimulated CD161+, compared to CD161–, CD8+ T cells. **A**) Scatter plots of signal intensities of all mRNA probes in stimulated (y-axis) vs. unstimulated (x-axis) CD161+ (left) and CD161– (right) CD8+ T cells. **B**) Scatter plot of signal intensities of all mRNA probes in stimulated CD161+ (y-axis) vs. stimulated CD161– (x-axis) CD8+ T cells. The signal intensities of each probe represented by a dot are shown in double logarithmic scale. Red diagonal lines define the areas of 2-fold differential signal intensities. Blue cross: unchanged genes, red cross: significantly upregulated genes ($p<0.01$), green cross: significantly downregulated genes ($p<0.01$). **C**) Heatmap illustrating the 433 significantly ($p<0.01$) differentially expressed transcripts between stimulated CD161+ and CD161– CD8+ T cells in 3 donors. Subsets and genes clustered by one minus Pearson correlation. **D**) Representative histograms from one donor showing IFNα expression by CD14+ monocytes, and both CD161+ and CD161– CD8+ T cells unstimulated (red line) or upon stimulation with PMA + ionomycin for 4hrs (blue line).

4.5 Discussion

CD161+CD8+ T cells mirror many of the characteristics of CD161++ MAIT cells, in addition to their shared expression of CD161. Indeed, the overlap in phenotypes identified during transcriptional analyses in the previous chapter was retained even with the exclusion of naïve cells, which predominate within the CD161– population and could, therefore, accentuate differences between the populations. Here, comparison of memory cells showed CD161+ T cells to express elevated levels of IL18Rα, CXCR6, MDR1 and PLZF in comparison to CD161–CD8+ T cells, albeit at low levels. These are markers characteristic of MAIT cells (Dusseaux et al., 2011), expressed at high levels by these CD161++ cells. Both CD161 positive CD8+ T cell subsets show elevated expression of PLZF, a transcription factor associated with the innate-like function of MAIT and iNKT cells (Kovalovsky et al., 2008; Savage et al., 2008), and may suggest similar innate-like characteristics within the CD161+ population, although levels detected by flow cytometry are very low. However, the type-17 transcription factor RORγt is expressed at high levels by the CD161++ cell subset only (Billerbeck et al. 2010; Dusseaux et al. 2011, Figure 3-4), and was not significantly upregulated by CD161+CD8+ T cells. This excludes, together with a strict gating strategy, the possibility of an influence from CD161++ contamination in the gene expression analyses. The specific expression of RORγt by CD161++CD8+ T cells is likely related to the fact that IL-17 secretion is restricted to this CD8+ subset (Billerbeck et al., 2010; Ivanov et al., 2006). It is potentially the shared expression of PLZF that bestows the similarities between the two CD161 expressing CD8+ T cells, with RORγt accounting for many of the differences.

The CD161+CD8+ T cell population is enriched for expression of cytotoxic effectors perforin and granzyme B, in contrast to CD161++ MAIT cells which lack granzyme B and express low levels of perforin in the resting state (Billerbeck et al., 2010; Kurioka et al., 2014). Whether this translates to increased cytotoxic activity requires further

investigation, for example by performing redirected killing assays with sorted populations. Furthermore, MAIT cells have been found to express granzyme A and K, and exchange these for granzyme B upon activation (Kurioka et al., 2014). It would also be of interest, therefore, to investigate the expression of these non-conventional granzymes, and the affect of activation on granzyme expression and cytotoxicity, in the CD161+CD8+ T cell population.

While CD161+CD8+ T cells lack IL-17 secretion (Billerbeck et al., 2010), CD161+CD8+ T cells were here demonstrated to have increased ability to produce cytokines than either CD161++ or CD161− subsets, particularly in regards to IL-2 and IFNγ production. Secretion of IL-2 and IFNγ by virus-specific T cells has long been used as a functional readout, due to the correlation between polyfunctioin IL-2 and IFNγ secretion and viral control, and the lack of correlation with IFNγ secretion alone (Harari et al., 2006). In HIV, for example, long term non-progressors (LTNPs) maintain highly functional CD8+ T cells (including those secreting IL-2 and IFNγ, in addition to other cytokines) which are lost in progressors, and inversely correlate with viral load (Betts et al., 2006). The presence of IFNγ plus IL-2-secreting CD8+ T cells has also been shown to support CD8+ T cell proliferation in CD4 depleted populations (Zimmerli et al., 2005), with a greater proliferation capacity in CD8+ T cells again associated with viral control (Migueles et al., 2002). Interestingly, this was also linked to increased perforin expression. While here these characteristics were demonstrated within bulk, and not viral-specific, populations, it does suggest that a greater proportion of viral-specific cells expressing CD161 would be linked to an increased presence of these characteristics.

Furthermore, high production of IL-2 and IFNγ, together with expression of CD103, has been described to identify a subset of CD4+ T regulatory cells (Lehmann et al., 2002), with CD103 also a marker of regulatory CD8+ T cells (Uss et al., 2006). It would be of interest, therefore, given the relative enrichment of CD103 on CD161+CD8+ T cells, to investigate the expression of immunosuppressive cytokines

such as IL-10, expression of CTLA4 and potential suppressive function by this population. However, mRNA microarray analysis did not indicate CTLA4 or IL-10 to be significantly differentially expressed by this population when derived from blood. Yet, neither upregulated expression of perforin/granzyme in the resting state nor upregulated expression of IL-2/IFNγ upon stimulation was detected by microarray. This may be because levels were not sufficiently different at the mRNA level between CD161+ and CD161– CD8+ T cells to reach significance, especially with the vigorous multiple hypothesis corrections applied in this type of analysis. Furthermore, comparison of stimulated populations did not reveal the expression of any unique cytokines or chemokines by the CD161+, compared to the CD161– population. Changing the duration of stimulation and/or stimulus, eg. a more physiological stimulus such as CD3/2/28 stimulation over a longer time period, may have allowed more subtle differences to have been detected.

In addition to CD161, the CD161+CD8+ T cell population also expresses various other NK cell receptors, including specific enrichment of NKp80. NKp80 is expressed by virtually all NK cells and stimulates both cytotoxicity and cytokine release (Welte et al., 2006). Like CD161, NKp80 is a type II transmembrane, homodimer C-type lectin-like receptor encoded within the same gene complex as its ligand, Activation-Induced C-type Lectin (AICL). Expression of NKp80 was also recently described on a subset of CD8+ T cells, acting as a costimulatory receptor to enhance anti-CD3-induced degranulation and cytokine release (Kuttruff et al., 2009), as has been suggested for CD161 (Exley et al. 1998). These NKp80+ T cells, although consisting of both CD161+ and CD161– cells, share many characteristics with CD161+CD8+ T cells, including the expression of high levels of perforin and granzyme B, polyfunctionality and a memory phenotype. Indeed, like both MAIT cells (Martin et al., 2009) and CD161+CD4+ T cells (Maggi et al., 2010; Takahashi et al., 2006), CD161+CD8+ T cells display a memory phenotype in the vast majority. These memory cells are heterogeneous, as for NKp80+CD8+ and CD161+CD4+ T cells,

comprising both T_{EM} and T_{EMRA} phenotypes, while MAIT cells are uniformly T_{EM} in phenotype.

MAIT cells were originally described, and consequently named, as enriched within the gut – at least in comparison to skin, related to their expression of the gut-homing integrin α4β7. However, here Vα7.2+ T cells were found to be a minor population of CD8+ T cells within the healthy colon. CD161 positive T cells make up more than half of T cells within the healthy human intestine, the majority of which were TCRαβ+ including both CD4+ and CD8+ subsets, and did not express the iNKT cell receptor Vα24 (O'Keeffe et al., 2004). CD161+CD4+ Th17 cells also express high levels of integrin α4β7 and were found in significant proportions in healthy colonic tissue (Kleinschek et al., 2009). Similarly, here, a significant proportion of memory CD8+ T cells within the healthy colon were found to express CD161 (and lack Vα7.2). However, in contrast to Th17 cells which increase 20-fold in the inflammatory infiltrates of Crohn's Disease and represent the predominant subset of infiltrating CD4+ T cells, the major influxing population in IBD were CD161– (and CD103–) CD8+ T cells. This reflects the result of O'Keeffe *et al.* (2004) who showed that proportions of T cells that expressed CD161 were significantly reduced in colonic carcinoma compared to adjacent uninvolved tissue, while absolute numbers did not differ significantly. This suggests that CD161+CD8+ T cells represent a relatively stable gut-resident population. This tissue location, together with their memory phenotype and expression of CD103, identifies CD161+CD8+ T cells as a population of T_{RM}.

On the other hand, within the liver CD161+CD8+ (Vα7.2–) T cells comprised a minor population of CD8+ T cells, with the predominant population being Vα7.2+CD161+CD8+ T cells. CD161 positive T cells, which were not iNKT cells, have been described to preferentially accumulate within the human liver (Ishihara et al., 1999). This is specifically true of MAIT cells, which are enriched within the liver in HCV infection (Billerbeck et al., 2010) and are found at log-fold higher frequencies in

the healthy liver than the gut (Dusseaux et al., 2011). Together, this data suggests a situation whereby CD161+CD8+ T cells represent the true "mucosal-associated" CD161 positive CD8+ T cell population, while MAIT cells predominantly home to the liver. However, this analysis was of CD8+ T cells only, and does not exclude the possibility that MAIT cells may comprise a more major fraction of DN T cells in the gut.

A role for CD161+CD8+ T cells in liver diseases has been suggested by the enrichment of CD161 expression on T cells specific for HCV and HBV in comparison to those for HIV, CMV or influenza (Northfield et al., 2008). As the quality of the CD8+ T cell response in HCV infection is important in determining disease outcome (Folgori et al., 2006; Lauer et al., 2004; Spada et al., 2004), the phenotype of these enriched CD161+CD8+ T cells in disease may be important. Therefore, the phenotype of CD161+CD8+ T cells was investigated in chronic HCV infection. As few patients had readily detectable tetramer-positive populations (data not shown), this analysis was performed on bulk populations. This demonstrated that the CD161+CD8+ T cell population maintained expression of cytotoxic effectors granzyme B and perforin, previously described to decrease in HCV infection (Lucas et al., 2004), to a better degree than the CD161– population, yet polyfunctionality (assayed by dual IL-2 and IFNγ production) was reduced. As polyfunctionality of CD8+ T cells has previously been associated with patient outcome in HIV infection (Betts et al., 2006), it would be interesting to investigate the affect of this loss within the CD161+CD8+ T cell population to HCV disease progression. If found to be important, vaccination strategies that induce a high proportion of both polyfunctional and cytotoxic CD161+CD8+ T cells should be pursued.

4.6 Summary

1) CD161+CD8+ T cells shared some characteristics with CD161++CD8+ T cells, including elevated expression of IL18Rα, CXCR6, MDR1 and PLZF compared to CD161−CD8+ T cells, albeit at much lower expression (gMFI) levels
2) CD161+CD8+ T cells were potent effector cells, displaying high levels of perforin and granzyme B in the resting state, and multi-cytokine release following stimulation, including a high proportion of IL-2/IFNγ-producing cells
3) CD161+CD8+ T cells were found within the healthy liver, and to a much greater degree within the healthy gut, where they were a stable population during inflammation
4) Tissue location and the expression of both CD103 and memory markers identified CD161+CD8+ T cells as a population of tissue-resident memory (T_{RM}) cells
5) CD161+CD8+ T cells maintain expression of cytotoxic effectors, but display reduced polyfunctionality, in chronic HCV infection

Appendix IV.i: Genes significantly (p<0.01) differentially expressed by CD161+ compared to CD161−, excluding naive, CD8+ T cells

Name	Log(Ratio)	Fold Change	P-value
LOC154449	1.5674	36.93178	7.90E-04
LOC10012939	1.5189	33.02915	0.0016
KIF12	1.40917	25.65476	0.00102
C4orf38	1.39545	24.85694	8.30E-04
KLRB1	1.38407	24.21392	1.27E-35
PRSS41	1.31658	20.72901	1.90E-04
ZNF334	1.25254	17.88716	7.40E-04
CKAP2L	1.15318	14.22915	0.00195
SPTB	1.1363	13.68688	1.30E-04
PANX2	1.1359	13.67427	0.0011
CYLC1	1.10491	12.73236	0.00227
LOC440173	1.09857	12.54791	0.00275
SCGB1D1	1.07624	11.919	0.00433
C8orf48	1.07569	11.90405	0.00263
C14orf162	1.07023	11.75519	2.29E-08
PROKR1	1.00939	10.21865	9.30E-04
KIF6	1.00835	10.19418	0.00357
C1orf185	1.00729	10.16932	0.00775
BIRC8	1.00033	10.00753	0.00193
CTTNBP2NL	0.98936	9.75799	0.00886
PATE2	0.9871	9.70726	0.00586
TMEM178	0.9804	9.55866	0.00283
IL16	0.96773	9.28391	0.00169
CKMT1A	0.96613	9.24976	0.00354
GPR158	0.95515	9.01891	4.60E-04
PTCHD3	0.93862	8.68205	6.69E-06
LOC10012890	0.93801	8.66986	0.00943
ATP13A4	0.93052	8.52158	0.00155
ADAM32	0.92413	8.39702	0.00441
LETM1	0.91559	8.23355	4.86E-09
LOC653203	0.91285	8.18174	5.40E-04
ZSCAN2	0.90342	8.00616	2.27E-10
IGFBP5	0.89929	7.93028	0.00495
C19orf30	0.89232	7.80409	3.04E-11
TTC28	0.88297	7.63782	1.65E-07
ZDHHC20	0.87152	7.43914	2.83E-07
POM121L2	0.86811	7.38095	0.00233
C21orf82	0.8656	7.33838	0.00491
POLR2J2	0.86447	7.3193	2.97E-08
FAM118A	0.84937	7.06926	9.53E-08
PRSS35	0.84807	7.04801	2.60E-04
LOC283335	0.84792	7.04567	1.09E-07
LOC10012985	0.8463	7.01936	0.00299
RAB3B	0.82609	6.70029	0.00348
VNN3	0.822	6.63745	0.00388
LOC284454	0.81642	6.55273	6.85E-08
PARD3B	0.8155	6.53877	0.00724
TBXA2R	0.80864	6.4364	2.99E-07
TBXA2R	0.80864	6.4364	2.99E-07
GBP6	0.79739	6.27174	2.88E-08
ACBD7	0.79553	6.24495	5.12E-09
KIAA1875	0.78617	6.11187	1.87E-07

KRT23	0.78313	6.06918	3.10E-04
CUX2	0.77457	5.95079	0.0073
DPY19L2P1	0.77174	5.9121	0.00937
ZNF2	0.76997	5.88806	4.62E-08
ZNF713	0.765	5.82107	2.54E-08
ZNF713	0.765	5.82107	2.54E-08
COX6B2	0.74906	5.61126	2.46E-07
HYAL4	0.74218	5.52305	9.81E-08
GS85	0.74076	5.50508	0.00715
LOC401233	0.72701	5.33343	5.58E-06
IL4I1	0.72043	5.25323	8.00E-05
SLC4A10	0.71384	5.17412	0.00453
PABPC1L2A	0.71114	5.14204	0.00572
VPREB3	0.70418	5.06035	1.40E-04
FAM177B	0.69892	4.99943	3.50E-11
ADCY5	0.69791	4.98776	0.00812
CYP2B6	0.68384	4.82881	2.05E-07
IL18RAP	0.66782	4.65393	3.16E-12
IL18RAP	0.66782	4.65393	3.16E-12
LTK	0.66758	4.65134	4.81E-16
PAK3	0.66149	4.58658	0.00656
B3GALT2	0.6379	4.3441	6.10E-04
PTPN13	0.62393	4.2066	6.00E-05
RN28S1	0.61082	4.08151	6.91E-12
RN28S1	0.61082	4.08151	6.91E-12
NCRNA00165	0.60658	4.04187	0.00813
C8orf83	0.6056	4.03277	0.00741
APOL5	0.60506	4.02772	8.00E-05
BLK	0.60473	4.02465	0.00553
LOC10028731	0.59732	3.9566	2.12E-09
APBA1	0.59603	3.94485	4.80E-04
C7orf51	0.59514	3.93677	0.00109
psiTPTE22	0.58892	3.88082	2.00E-05
FAT3	0.58852	3.87726	8.17E-07
TAT	0.58125	3.81287	6.39E-08
LOC10013313	0.57468	3.75565	2.10E-04
ZNF157	0.56904	3.70715	5.65E-07
LOC143286	0.56603	3.68152	2.00E-05
LOC10013077	0.56477	3.67087	9.52E-07
LOC284379	0.56342	3.65948	1.10E-08
LOC340515	0.5591	3.62324	1.42E-13
ARHGAP40	0.55826	3.61628	1.64E-08
PQLC2	0.54889	3.53907	1.18E-09
LOC619207	0.54852	3.53604	1.00E-05
FAM110B	0.53694	3.44305	3.75E-06
CCR1	0.53694	3.44304	2.50E-04
AMN	0.53507	3.4282	1.41E-06
LRP3	0.52924	3.38251	0.00944
AIF1L	0.51954	3.30779	1.80E-04
DYSF	0.51915	3.30481	5.00E-05
SCRN1	0.51147	3.24693	7.59E-06
TYROBP	0.50911	3.22934	1.18E-13
RASL10B	0.50907	3.22902	1.00E-04

LOC10013423	0.50775	3.21919	6.15E-06
SLC8A1	0.50185	3.17577	0.00151
PIH1D2	0.50023	3.16394	1.00E-05
RBP4	0.4995	3.15865	1.00E-04
C14orf167	0.49855	3.15172	2.67E-08
LCE1D	0.49797	3.14756	1.19E-09
LOC10028938	0.49785	3.14663	6.51E-07
LOC10028938	0.49785	3.14663	6.51E-07
FOXA3	0.49743	3.14364	5.98E-06
IL18R1	0.49637	3.13596	5.06E-22
IL18R1	0.49637	3.13596	5.06E-22
IL18R1	0.49637	3.13596	5.06E-22
LOC145757	0.49494	3.12565	8.59E-08
LCN9	0.49364	3.1163	3.00E-05
COLQ	0.49237	3.10718	4.43E-09
GFRA3	0.48685	3.06793	3.31E-07
KIAA0087	0.4862	3.06339	1.90E-04
LGALS3	0.48534	3.05729	2.00E-05
FAM115C	0.48489	3.05413	1.63E-09
LOC645553	0.48175	3.03212	2.04E-07
LOC10013466	0.4814	3.02973	7.48E-06
ISLR2	0.48137	3.02949	7.90E-04
LOC284263	0.481	3.02694	4.18E-07
LOC728449	0.48067	3.02459	2.49E-06
LOC10013221	0.47889	3.01225	1.36E-06
LOC10013221	0.47889	3.01225	1.36E-06
LOC10013221	0.47889	3.01225	1.36E-06
C17orf54	0.4782	3.00743	1.70E-04
LOC10012866	0.47476	2.98372	0.00324
HRH3	0.47467	2.9831	7.48E-07
NRG4	0.47231	2.96697	2.00E-05
ADAMTS7	0.47212	2.96566	6.59E-09
ZNF865	0.4705	2.95463	8.79E-15
CAMK2A	0.46857	2.94152	0.00422
SOX15	0.46658	2.92805	0.0011
PVRL4	0.46594	2.92375	2.80E-04
LOC146795	0.46292	2.90349	2.91E-10
CXCR6	0.46258	2.90122	1.80E-18
SNAR-G1	0.46179	2.89595	0.00303
MAF	0.46054	2.88763	6.94E-09
CELF3	0.45917	2.87854	1.00E-05
LOC10012834	0.45754	2.86772	4.99E-07
LOC10012834	0.45754	2.86772	4.99E-07
TLE1	0.45746	2.86719	1.08E-09
NR4A3	0.45595	2.85729	0.00156
NYX	0.45559	2.8549	2.75E-10
LOC10013155	0.45437	2.84689	1.51E-06
GPR162	0.45246	2.83437	4.50E-04
LOC10013169	0.45227	2.83316	3.78E-08
REREP3	0.45142	2.82762	2.10E-04
LOC145216	0.4488	2.81062	1.63E-07
HHATL	0.44685	2.79801	0.00266
PSD4	0.44674	2.79728	2.48E-06

PCDHGA7	0.44581	2.79133	8.64E-06
ADAM11	0.44522	2.78751	0.00177
C3orf39	0.44474	2.78447	2.28E-07
LDHAL6A	0.44116	2.7616	4.30E-09
AS3MT	0.43977	2.75274	7.26E-15
IQSEC3	0.43958	2.75157	2.33E-07
PPP1R14A	0.43953	2.75122	2.87E-07
SMR3A	0.43851	2.74478	4.20E-04
OR2H1	0.43639	2.73145	3.33E-08
HRH1	0.43616	2.73	1.16E-06
PAPL	0.43461	2.72027	3.72E-16
TMIGD2	0.43457	2.71999	1.90E-04
LOC10012984	0.43435	2.71861	1.00E-05
LOC10013316	0.43154	2.7011	2.02E-10
KLHL35	0.43095	2.69742	6.00E-05
SLC18A3	0.4297	2.68967	5.99E-10
LMX1B	0.4294	2.68781	8.00E-05
CEACAM18	0.42878	2.68396	4.00E-04
SPRNP1	0.426	2.66686	4.53E-08
C17orf91	0.42568	2.66488	6.96E-08
DTNA	0.42496	2.66046	5.27E-06
MMP15	0.42341	2.65101	8.60E-12
ZDHHC8	0.42332	2.65047	2.40E-04
HCRT	0.42327	2.65014	0.00407
GPR155	0.42311	2.64916	6.22E-13
NUDT8	0.4226	2.64605	3.65E-07
PTAFR	0.42253	2.64564	1.92E-06
FBRSL1	0.42226	2.644	1.46E-06
ADAM12	0.4221	2.64304	4.00E-05
SLC9A4	0.42077	2.63494	1.80E-11
SLC9A4	0.42077	2.63494	1.80E-11
LOC654779	0.41996	2.63001	1.40E-04
IQSEC2	0.41729	2.61392	7.70E-07
FAM21C	0.41487	2.5994	4.81E-06
LOC389033	0.41406	2.59456	1.64E-09
KCNH3	0.41401	2.59426	1.10E-06
ABCC6	0.41285	2.58731	1.00E-04
TFEB	0.41277	2.58686	2.32E-13
LOC400558	0.41255	2.58554	1.00E-05
WFDC3	0.41221	2.58349	1.74E-06
LY6G6D	0.41218	2.58331	4.00E-05
SSX3	0.41167	2.58032	2.70E-09
ADAM33	0.4112	2.57752	1.63E-12
ALDH1L2	0.41086	2.57548	0.00908
COL5A1	0.41072	2.57466	4.00E-04
ZBTB16	0.41006	2.57076	8.73E-08
CHST13	0.40964	2.56826	3.96E-12
HOXA10	0.40959	2.56799	7.18E-07
DOCK3	0.40937	2.56665	0.00253
KIT	0.40921	2.56575	0.00272
HRASLS5	0.40686	2.5519	5.99E-17
ATP6V0A4	0.40609	2.54735	0.00106
MOCS3	0.40552	2.54402	4.00E-05

HMX2	0.40545	2.54363	3.00E-05
LOC10012914	0.40517	2.54197	6.67E-09
PHOSPHO1	0.4041	2.53571	1.50E-06
HMG20B	0.40404	2.53539	5.70E-07
TPSG1	0.40329	2.531	3.39E-12
HSCB	0.40311	2.52992	5.01E-13
DNAH10	0.40306	2.52966	0.00142
FAM74A4	0.40252	2.52653	9.26E-15
PALM	0.40198	2.52339	7.00E-05
GPSM1	0.40159	2.52111	8.78E-09
CLCA1	0.40152	2.52067	2.90E-04
BCORP1	0.40074	2.51614	3.20E-04
RRP7B	0.4004	2.51421	4.00E-13
MPDZ	0.39949	2.50894	0.00907
LOC10013236	0.39842	2.50276	7.99E-09
PRB1	0.39814	2.50115	3.41E-07
LOC399744	0.39782	2.49933	9.13E-06
LIN28A	0.39728	2.4962	2.35E-07
SALL3	0.39717	2.49557	9.20E-07
LOC10012831	0.39713	2.49534	3.00E-05
CNTN4	0.39706	2.49496	8.40E-04
TFE3	0.39666	2.49263	3.93E-10
MEG3	0.39614	2.48968	2.00E-05
LRRC26	0.39488	2.48245	1.30E-07
CDCP2	0.39479	2.48194	3.20E-04
NMU	0.39466	2.48121	0.00943
C8orf58	0.39401	2.47745	1.13E-06
RNU105B	0.39387	2.47668	0.0032
DDX58	0.39375	2.47602	4.00E-05
FEZ1	0.39289	2.47109	0.00237
LOC10050774	0.39147	2.46306	1.54E-09
LOC10012959	0.39088	2.4597	7.26E-07
PRLHR	0.39058	2.45799	2.20E-07
LOC440518	0.3899	2.45414	1.30E-04
KRT7	0.38948	2.4518	2.67E-08
LOC10012833	0.38944	2.45154	1.11E-06
NEUROG3	0.38851	2.4463	3.20E-08
F7	0.38803	2.44361	2.00E-05
CDX1	0.38759	2.44112	1.92E-10
LOC10013028	0.38736	2.43981	4.30E-06
LOC10051001	0.38704	2.43802	1.16E-11
TPP1	0.38656	2.43535	3.46E-06
PLCB1	0.38542	2.42893	0.00232
PLCB1	0.38542	2.42893	0.00232
GPR25	0.38404	2.42127	7.34E-07
LOC10012810	0.38367	2.41919	1.13E-09
WNK4	0.38343	2.41784	3.27E-07
LOC10051065	0.38322	2.41668	0.00153
FAM99A	0.38223	2.41119	2.00E-06
MAP4	0.38215	2.41072	7.64E-13
LONRF3	0.38193	2.40953	1.69E-07
TERC	0.38174	2.40847	9.67E-09
LOC10027068	0.38072	2.40284	5.00E-05

KCNK15	0.38056	2.40192	7.67E-09
COL27A1	0.38029	2.40042	2.31E-07
HOXA9	0.37983	2.39788	5.58E-06
CTRB2	0.37814	2.3886	9.58E-06
ACTRT2	0.37774	2.38641	0.00404
ANKRD33	0.37724	2.38363	8.62E-09
LOC10012972	0.37706	2.38264	3.39E-08
BCL2L11	0.37651	2.37961	2.67E-06
CD4	0.37503	2.37155	3.92E-10
PRKAG3	0.37424	2.36723	4.43E-11
LOC10012897	0.37356	2.3635	8.10E-04
CTXN1	0.37338	2.36252	6.94E-08
FLJ23867	0.3731	2.36101	4.70E-04
APBB2	0.37235	2.35697	2.70E-08
C8orf56	0.37233	2.35685	2.23E-07
LOC10012911	0.37072	2.3481	6.90E-07
LFNG	0.37051	2.34698	2.76E-09
HBZ	0.37037	2.34624	1.80E-12
TNP2	0.37035	2.34613	6.71E-10
KRTAP10-10	0.37012	2.34486	6.74E-07
ACAD10	0.36986	2.34348	1.93E-09
C14orf181	0.36976	2.34295	2.00E-05
PRRC2B	0.3687	2.33725	2.00E-05
LOC10013091	0.36809	2.33396	0.00629
IER5L	0.36752	2.3309	3.00E-05
UTF1	0.36706	2.32839	1.57E-09
ALPPL2	0.36662	2.32608	6.83E-09
B3GNT7	0.36641	2.32494	1.52E-08
ACCN4	0.36624	2.32402	1.13E-06
EMILIN3	0.36603	2.32291	4.00E-05
CCR2	0.3655	2.32005	2.00E-05
CCR2	0.3655	2.32005	2.00E-05
ZC3HAV1L	0.36485	2.31662	7.97E-07
LOC10013296	0.36458	2.31515	1.11E-06
LOC10013296	0.36458	2.31515	1.11E-06
ARAF2P	0.36413	2.31278	7.03E-09
RPH3A	0.36401	2.31211	4.00E-05
LOC388152	0.36341	2.30891	1.14E-09
KRTAP1-3	0.36319	2.30778	0.00102
HSP90AA5P	0.36132	2.29787	4.00E-05
SLC6A10P	0.36131	2.2978	3.89E-07
LOC10012911	0.36041	2.29304	0.00669
CLDN19	0.35876	2.28432	6.39E-06
ACAP3	0.35817	2.28126	5.48E-07
EXOC3L	0.35783	2.27948	9.10E-04
CHRD	0.35757	2.2781	4.50E-04
LOC10013023	0.35718	2.27605	1.74E-06
DIABLO	0.35713	2.2758	4.10E-07
OR5H1	0.35709	2.27555	7.66E-06
VPS53	0.35684	2.27426	7.50E-04
NRG1	0.35673	2.2737	0.00234
LOC10013015	0.35669	2.27347	1.69E-08
USP17	0.35622	2.271	0.00143

GALE	0.35577	2.26869	5.00E-05
KRT78	0.35552	2.26737	0.00228
OR5L2	0.35551	2.26733	9.52E-06
C20orf141	0.35537	2.26656	7.77E-06
MGC4859	0.35527	2.26605	3.00E-11
PCDHB13	0.35513	2.26532	3.60E-04
LOC644277	0.35448	2.26193	1.46E-08
DEGS2	0.35331	2.25585	4.34E-08
OR10H2	0.35326	2.25557	1.30E-04
SPOCK2	0.35199	2.24899	1.29E-12
PDE9A	0.35174	2.24771	8.36E-09
ABCB1	0.3516	2.247	0.00741
DPT	0.35137	2.2458	5.19E-07
LOC10012791	0.35122	2.245	3.96E-08
PRB3	0.35084	2.24306	2.00E-05
HR	0.35063	2.24196	5.00E-05
SPSB4	0.35046	2.24111	1.29E-08
CDH22	0.35015	2.23949	1.65E-10
C9orf173	0.34976	2.23746	7.49E-06
C9orf173	0.34976	2.23746	7.49E-06
NCRNA00106	0.34912	2.23417	1.60E-07
WDR90	0.34834	2.23017	6.00E-05
LOC10051006	0.34778	2.22731	7.82E-08
LAMA4	0.34745	2.2256	9.40E-04
MEFV	0.34656	2.22104	4.00E-05
DPYSL4	0.34638	2.22015	4.95E-13
PRRT4	0.3463	2.21974	0.0078
ZSCAN12P1	0.3462	2.21923	3.00E-05
NCRNA00092	0.34617	2.21905	6.50E-04
LOC283868	0.34596	2.21799	3.85E-07
SPRR2D	0.34575	2.21691	2.58E-09
RARA	0.34558	2.21606	1.42E-11
CDRT3	0.34545	2.21541	4.00E-05
C18orf12	0.34537	2.21497	6.71E-08
SLCO2B1	0.34529	2.21455	0.00587
C3orf43	0.34524	2.21433	0.00188
CDK13	0.34522	2.21423	1.18E-09
MAVS	0.345	2.21309	6.40E-04
LOC283547	0.34498	2.21299	3.17E-10
TBKBP1	0.34496	2.2129	1.30E-10
TYMP	0.34493	2.21274	1.25E-11
MYH14	0.34488	2.21247	1.74E-07
FAM178B	0.34476	2.21188	7.00E-05
PANX3	0.34456	2.21084	0.00907
IL28A	0.34423	2.20919	5.71E-07
KRTAP9-1	0.34403	2.20816	3.06E-08
PRAP1	0.34382	2.20707	7.79E-08
FDX1L	0.34365	2.20623	4.03E-07
LOC402036	0.34338	2.20484	1.00E-05
TSPAN11	0.34336	2.20476	2.74E-06
LOC10013147	0.34306	2.20321	3.71E-06
LOC284749	0.34189	2.19733	4.00E-05
ACER2	0.34189	2.19731	0.00178

OR1J4	0.34188	2.19725	0.00921
GHSR	0.34178	2.19676	5.68E-16
KRTAP10-8	0.34158	2.19573	1.00E-05
C1orf158	0.34154	2.19554	1.22E-06
KRTAP9L1	0.3415	2.19533	0.00338
LOC728675	0.34145	2.1951	0.00433
NCRNA00253	0.34099	2.19274	8.82E-06
NEDD4	0.3408	2.1918	0.00231
POLR2F	0.33948	2.18515	5.91E-10
KIRREL2	0.33858	2.18063	2.00E-05
SPINK7	0.33849	2.18018	4.71E-09
SAMD11	0.33849	2.18015	1.00E-04
HES6	0.33833	2.17936	2.65E-11
EPS8L3	0.33801	2.17774	1.40E-04
PRO0471	0.33797	2.17757	0.00658
LOC10013045	0.3376	2.17571	2.70E-09
C15orf62	0.3375	2.17521	2.12E-07
RTN3	0.33725	2.17394	3.26E-08
CHST6	0.33598	2.16758	8.70E-07
LOC400968	0.33588	2.16711	1.00E-05
SLC11A1	0.33581	2.16676	3.25E-09
LOC389273	0.33546	2.165	4.90E-04
LOC285095	0.33544	2.16493	0.00406
PHF21B	0.33463	2.16088	1.00E-04
FLJ44385	0.33405	2.15798	5.30E-04
CCDC78	0.33402	2.15784	1.05E-06
UPK3B	0.33352	2.15536	0.00698
ZSCAN30	0.33349	2.15519	2.70E-04
LOC10050659	0.3334	2.15479	7.00E-05
RPL23AP32	0.33297	2.15263	5.00E-05
NOTCH1	0.33286	2.15207	0.00105
NOTCH1	0.33286	2.15207	0.00105
LOC10051000	0.33284	2.15199	2.21E-10
LOC10013043	0.33251	2.15037	9.10E-04
TOR2A	0.3315	2.14537	6.02E-07
STARD8	0.33107	2.14323	0.00316
DSE	0.33106	2.14317	0.00772
LACTBL1	0.33101	2.14293	4.00E-05
NOBOX	0.32913	2.13368	2.89E-08
CORT	0.329	2.13304	5.10E-04
FAM120C	0.32883	2.13219	3.28E-08
LOC10028958	0.32867	2.13144	2.90E-04
CDC14C	0.32856	2.1309	4.18E-06
LOC10050726	0.32851	2.13064	1.36E-06
SPHK1	0.32825	2.12934	1.00E-05
EMX1	0.3277	2.12669	1.30E-07
CBX7	0.32758	2.1261	1.48E-06
C21orf58	0.32638	2.12022	1.40E-04
IL17RE	0.3263	2.11983	8.37E-08
FLJ40606	0.32611	2.11891	2.78E-09
ARHGAP33	0.32608	2.11877	1.00E-04
SOX13	0.32501	2.11352	1.75E-10
TREM1	0.32445	2.11084	5.50E-04

COL11A2	0.3242	2.10959	6.27E-06
ASB10	0.32382	2.10776	1.00E-05
KRT73	0.3231	2.10426	2.94E-07
ATXN2L	0.32257	2.10167	1.40E-07
TNXB	0.32253	2.10152	1.46E-06
OR11A1	0.32226	2.1002	4.00E-05
KCP	0.32116	2.09489	3.26E-07
RAPH1	0.32046	2.0915	3.30E-04
HAR1A	0.32014	2.08998	4.00E-05
KCND3	0.31992	2.08893	2.24E-10
RTBDN	0.31988	2.08872	7.30E-04
EPHB2	0.31891	2.08408	0.00331
ADM2	0.31871	2.08311	6.30E-04
LOC151009	0.31871	2.08309	3.93E-06
CCL24	0.31831	2.08118	4.75E-07
MOS	0.31823	2.08081	3.00E-05
TH	0.31818	2.08055	1.00E-05
C19orf69	0.31801	2.07974	2.62E-08
LHCGR	0.31789	2.07917	0.00592
GPR152	0.31669	2.07343	8.29E-07
DLK1	0.31648	2.07245	2.10E-04
C14orf70	0.31644	2.07224	2.28E-08
SHISA4	0.31641	2.07209	3.30E-06
LOC146429	0.31553	2.06788	0.00696
SEMA3B	0.31546	2.06757	6.00E-05
LOC10021654	0.31538	2.0672	7.00E-05
KRTAP9L2	0.31517	2.06617	1.06E-08
KLHL33	0.31516	2.06614	1.90E-06
LOC149950	0.3151	2.06586	3.55E-09
BTNL8	0.31461	2.0635	3.90E-04
WWOX	0.31428	2.06197	0.00359
EFCAB10	0.31383	2.05982	1.30E-04
SLC17A7	0.31375	2.05944	4.26E-08
SLC16A12	0.31352	2.05835	6.57E-13
KIF17	0.31348	2.05818	0.00418
LOC648044	0.31299	2.05586	0.00604
FIGNL2	0.31282	2.05503	2.20E-04
DERL3	0.31279	2.0549	3.24E-08
LOC10013398	0.31217	2.05199	4.60E-09
TTLL4	0.3121	2.05165	1.30E-06
AXL	0.31183	2.05038	3.00E-04
PLEKHG5	0.31168	2.04964	3.35E-09
FMO6P	0.31164	2.04945	0.00123
SLC6A6	0.31146	2.04862	7.00E-05
FGF5	0.31123	2.04753	0.00206
LOC10012997	0.31101	2.04648	0.00175
CABP5	0.31059	2.04452	1.33E-08
FLJ39632	0.3102	2.04269	4.62E-08
CCL16	0.31007	2.04207	4.08E-07
CD79A	0.30971	2.04039	2.00E-04
LOC10013279	0.30949	2.03935	3.09E-12
C8orf67	0.30894	2.03674	4.90E-04
LOC10012919	0.30886	2.03638	3.40E-04

ESRRG	0.30884	2.03627	7.70E-04
C16orf5	0.30871	2.03568	2.00E-05
PALM3	0.3087	2.03563	9.00E-05
TMEM146	0.30843	2.03439	3.61E-08
FAM71E2	0.30828	2.03368	3.55E-06
ATF3	0.30828	2.03366	1.90E-04
ATF3	0.30828	2.03366	1.90E-04
LOC652119	0.30798	2.03228	2.41E-09
MEF2D	0.3078	2.03144	3.43E-06
WNT3A	0.30746	2.02984	2.89E-06
C9orf71	0.30697	2.02756	0.00111
GNAO1	0.306	2.02303	8.00E-05
LOC731932	0.30527	2.01962	7.46E-09
HGFAC	0.30521	2.01935	1.34E-07
LOC10050718	0.30507	2.0187	5.75E-06
KRT85	0.30487	2.01777	2.00E-05
SCUBE1	0.30485	2.01768	0.001
LRRN2	0.30462	2.0166	7.65E-07
LST1	0.30461	2.01653	0.00206
MEX3D	0.30443	2.01573	1.51E-15
IL17REL	0.30434	2.01529	2.16E-07
KRT81	0.30402	2.01382	5.37E-11
TMEM201	0.30343	2.01109	4.77E-08
PHF16	0.30326	2.0103	5.40E-04
LOC440313	0.30318	2.00991	0.00171
LOC10012838	0.30312	2.00964	0.00838
MT3	0.30288	2.00852	1.03E-06
TAS1R3	0.30268	2.00761	6.00E-05
SLC5A6	0.30238	2.00623	3.72E-11
PITX3	0.30208	2.00484	5.22E-07
NCRNA00260	0.30153	2.0023	5.70E-04
CLN5	-0.30305	-2.00934	0.00508
MPPE1	-0.30364	-2.01204	5.30E-04
TSEN2	-0.3037	-2.01231	7.70E-04
SUPT3H	-0.30372	-2.01243	0.00512
IKBKE	-0.30445	-2.01582	0.00368
PPARGC1B	-0.30538	-2.02013	0.00897
LOC649294	-0.30602	-2.0231	0.00252
FAM117B	-0.30721	-2.02868	1.03E-07
CTSZ	-0.30747	-2.02986	0.00952
CTSZ	-0.30747	-2.02986	0.00952
PRIM2	-0.30802	-2.03245	0.00564
CTPS2	-0.30808	-2.03273	8.70E-04
LOC338620	-0.31101	-2.04647	0.0027
TP53	-0.31139	-2.04827	1.20E-04
TMEM185A	-0.31216	-2.05192	6.20E-04
RDX	-0.3122	-2.0521	0.00759
IFNAR2	-0.31456	-2.0633	0.00346
CRIP2	-0.31687	-2.07427	0.00604
EPHX2	-0.31714	-2.07558	0.00145
EGLN3	-0.31722	-2.07598	0.00159
FANCI	-0.31725	-2.07609	0.00362
LOC727916	-0.31754	-2.07751	0.00884

EGFEM1P	-0.31792	-2.07934	0.00622
LOC257396	-0.31843	-2.08173	0.0017
MCM7	-0.31944	-2.0866	1.00E-05
INF2	-0.31947	-2.08675	7.00E-05
ST8SIA1	-0.31948	-2.08681	0.00147
RTN2	-0.31975	-2.08808	0.00414
MAP3K1	-0.31999	-2.08924	4.94E-07
TMPO	-0.32007	-2.08965	0.00106
IL4	-0.32036	-2.09102	0.00727
SLC7A1	-0.32115	-2.09485	5.30E-04
FCGBP	-0.32211	-2.09947	8.00E-05
TGFB3	-0.32347	-2.10605	6.50E-04
PRKCA	-0.32378	-2.10755	7.60E-04
HSD17B3	-0.32381	-2.1077	0.00461
CCDC134	-0.3244	-2.11059	0.00549
RABIF	-0.32456	-2.11137	0.00385
TTLL13	-0.3249	-2.113	0.00266
LEKR1	-0.32551	-2.11598	0.00358
SC4MOL	-0.32703	-2.1234	3.10E-04
GINS4	-0.32737	-2.12504	2.90E-04
MRC2	-0.32949	-2.13544	0.00264
LYL1	-0.32949	-2.13548	0.00158
SUN3	-0.33059	-2.14088	0.0031
CRTC3	-0.33122	-2.14397	7.00E-05
WDHD1	-0.33147	-2.14523	0.00194
SLC23A3	-0.33171	-2.14637	9.40E-04
SLC1A5	-0.33171	-2.14641	0.00583
CLEC3B	-0.33273	-2.15144	0.00689
INCENP	-0.3329	-2.15228	0.00331
LOC10050938	-0.33431	-2.15927	0.00963
ELL3	-0.33492	-2.1623	0.00367
CCNG2	-0.33599	-2.16765	0.00109
FOXK1	-0.33751	-2.17524	0.00737
IL6ST	-0.33752	-2.1753	1.02E-14
IL6ST	-0.33752	-2.1753	1.02E-14
IL6ST	-0.33752	-2.1753	1.02E-14
WNT10A	-0.33773	-2.17635	0.00202
PLTP	-0.34062	-2.1909	0.00492
ZNF823	-0.3413	-2.19431	0.00909
AMT	-0.34147	-2.19516	0.00281
HNRPLL	-0.34187	-2.19722	0.00947
LHFPL5	-0.34277	-2.20175	4.60E-04
CES4A	-0.34292	-2.20252	0.0015
LOC401037	-0.34569	-2.21662	0.0066
ADCK1	-0.34714	-2.22401	0.00297
GAB2	-0.34774	-2.22712	0.00412
MAL	-0.34832	-2.23009	2.80E-04
HS1BP3	-0.34871	-2.23206	0.00813
HERC2	-0.34879	-2.23247	0.00195
PKIA	-0.34973	-2.23731	7.00E-05
C1S	-0.34992	-2.23829	9.10E-04
FLJ36848	-0.35018	-2.23964	0.00148
MCM4	-0.35118	-2.2448	0.0098

MAGED2	-0.3528	-2.25319	0.00542
GREB1L	-0.35396	-2.25924	0.00118
CASS4	-0.35429	-2.26095	0.00171
TMEM194A	-0.35436	-2.26133	0.00107
LOC10013399	-0.35439	-2.26148	0.00671
GHITM	-0.35539	-2.26669	0.00936
C1R	-0.35757	-2.27807	0.00361
FGD4	-0.35849	-2.28291	0.00631
E2F2	-0.36014	-2.29158	5.00E-05
ZNF433	-0.36098	-2.29604	0.00856
OR2A1	-0.36179	-2.30031	0.00268
C2orf89	-0.3618	-2.30036	0.00461
SFXN1	-0.36184	-2.30058	0.00888
TRIB1	-0.36249	-2.30405	5.70E-04
NCRNA00162	-0.36416	-2.31294	0.00284
ADORA2A	-0.36488	-2.31677	0.00979
CCDC19	-0.36507	-2.31779	0.00996
APP	-0.36509	-2.31788	0.00102
KIF20B	-0.36698	-2.328	4.40E-04
C1orf228	-0.36796	-2.33324	3.40E-04
MURC	-0.36813	-2.33417	0.00881
FBXO15	-0.37009	-2.34472	0.00224
LOC643783	-0.37226	-2.35646	1.00E-04
ZNF488	-0.37358	-2.36363	0.00577
RGS16	-0.37591	-2.37636	6.60E-04
ADAMTS6	-0.37618	-2.37784	0.00799
SESN3	-0.37687	-2.38159	0.00476
BCL7A	-0.3772	-2.38341	0.00921
FCHSD1	-0.37897	-2.39317	0.00858
BICD1	-0.38202	-2.40999	0.00551
MLF1IP	-0.38207	-2.41029	0.00863
USP21	-0.3828	-2.41435	0.00808
MYEF2	-0.38692	-2.43734	9.20E-04
RPL32P3	-0.38759	-2.44111	8.00E-05
BTBD8	-0.38831	-2.44519	0.00368
HCRP1	-0.38925	-2.45046	0.00307
LASS6	-0.39082	-2.45933	7.00E-05
LASS6	-0.39082	-2.45933	7.00E-05
ZNF35	-0.39175	-2.46462	0.00194
MEOX1	-0.39301	-2.47176	0.00195
GYPE	-0.39332	-2.47354	0.00745
KCNRG	-0.39351	-2.47461	0.00384
RWDD4	-0.39431	-2.47918	6.20E-04
L3MBTL1	-0.39502	-2.48323	6.10E-04
L3MBTL1	-0.39502	-2.48323	6.10E-04
OSMR	-0.39556	-2.48635	0.00735
SGOL2	-0.39563	-2.48675	0.00371
SLC25A26	-0.3967	-2.49286	0.00325
AKTIP	-0.39681	-2.49348	1.00E-05
CSGALNACT1	-0.39955	-2.5093	6.70E-04
CSGALNACT1	-0.39955	-2.5093	6.70E-04
SEMA5A	-0.39981	-2.51082	0.00763
PPIEL	-0.4003	-2.51362	0.00894

CPLX3	-0.4012	-2.51884	0.00594
NELL2	-0.40157	-2.52096	1.80E-04
TOR3A	-0.40213	-2.52423	1.90E-04
TNNC1	-0.40224	-2.52488	0.00182
CENPE	-0.40255	-2.5267	0.0015
ZFP14	-0.40288	-2.52857	9.70E-04
SLC26A1	-0.40327	-2.53089	0.00313
ZDHHC23	-0.40469	-2.53914	0.002
HSF5	-0.40549	-2.54384	0.0081
IQCA1	-0.40583	-2.54583	0.00704
NUDT7	-0.406	-2.54683	0.00528
LOC643837	-0.40639	-2.54913	0.00888
SPATA24	-0.40667	-2.55077	0.00965
UBTD2	-0.40947	-2.56726	0.00782
LOC729680	-0.4098	-2.5692	0.00311
SORD	-0.41016	-2.57136	0.00884
C1orf162	-0.41107	-2.57674	1.27E-07
ProSAPiP1	-0.41109	-2.57687	4.00E-05
C6orf163	-0.41144	-2.57892	0.00243
RG9MTD2	-0.41227	-2.58387	1.40E-04
FPR2	-0.41232	-2.58413	0.0074
CDCA7L	-0.41363	-2.59196	0.00354
ARHGEF4	-0.41373	-2.59257	2.50E-04
MTHFD1L	-0.41642	-2.60869	2.80E-04
LOC10012911	-0.41643	-2.60872	0.00401
ZNF177	-0.41745	-2.61484	0.00231
CENPW	-0.41937	-2.62645	0.00202
PTPRK	-0.41988	-2.62953	0.00175
SERAC1	-0.42094	-2.63596	0.00531
PRKAR1B	-0.42094	-2.63599	7.10E-04
ZNF273	-0.42145	-2.63908	0.0013
KCTD1	-0.42268	-2.64654	0.00701
CYP2J2	-0.42315	-2.64943	9.72E-08
ARHGEF5	-0.42339	-2.6509	0.00933
KCTD13	-0.4236	-2.65214	0.0027
TCEA3	-0.42378	-2.65327	3.74E-08
PRELID2	-0.42586	-2.666	0.00831
STIL	-0.42595	-2.66657	0.00302
TMEM106A	-0.42632	-2.66884	7.72E-06
IER3	-0.42672	-2.67131	0.00589
FAM106C	-0.43106	-2.69812	0.00733
HMGB3P1	-0.43132	-2.69975	0.0051
ATG9B	-0.43319	-2.71137	0.00204
ZNF850	-0.43387	-2.71563	0.00361
SLC4A8	-0.43405	-2.71674	4.70E-04
MEIG1	-0.43554	-2.72606	0.00161
SNN	-0.43576	-2.7275	1.35E-07
MBP	-0.43581	-2.7278	0.0065
ZNF239	-0.4361	-2.72959	0.00653
RHEB	-0.43722	-2.73667	0.0046
TRIM34	-0.43724	-2.73679	0.00146
KIAA0556	-0.43738	-2.73766	0.00161
DENND5A	-0.43799	-2.74153	3.91E-13

C15orf29	-0.43838	-2.744	0.00278
GGTA1	-0.44186	-2.76607	0.00695
AHI1	-0.44294	-2.77296	4.00E-05
KRTCAP3	-0.44562	-2.79008	5.80E-04
NCRNA00282	-0.44703	-2.79914	0.00341
LOC10013106	-0.44866	-2.80972	0.0014
OR10G9	-0.44954	-2.81539	0.00504
KCNH2	-0.44979	-2.817	9.80E-04
TBC1D3B	-0.4504	-2.82099	8.90E-04
GRB10	-0.45059	-2.82221	5.30E-04
CH25H	-0.45195	-2.83106	0.00892
GALNT2	-0.4525	-2.83465	5.00E-05
RYR1	-0.45259	-2.83525	0.00262
HTR7P1	-0.45262	-2.83546	0.00415
SECISBP2	-0.45278	-2.83649	6.50E-04
LIMS2	-0.45289	-2.83723	0.00722
HLA-DOA	-0.45374	-2.84276	0.00426
DPCR1	-0.45415	-2.84547	2.90E-04
SGPP2	-0.45625	-2.85925	0.00582
C2orf40	-0.45707	-2.86465	0.00323
PTCD3	-0.45741	-2.86686	1.16E-06
RWDD2B	-0.45776	-2.86919	0.00665
GCET2	-0.45848	-2.87396	0.0079
SHMT1	-0.46014	-2.88496	0.00198
FAM126A	-0.46076	-2.88911	6.80E-04
SLC39A9	-0.46201	-2.89743	0.00398
RFPL1	-0.46269	-2.90195	4.80E-04
SEMA4B	-0.46522	-2.91889	0.00239
ZNF202	-0.46613	-2.92505	3.40E-04
FAM169A	-0.46831	-2.93972	5.86E-10
AGBL5	-0.46984	-2.95015	0.00664
HMMR	-0.47211	-2.96558	8.20E-04
ADAMTS4	-0.47215	-2.96586	0.00576
FADS3	-0.47232	-2.96702	2.00E-05
CEP55	-0.473	-2.97165	0.00184
MGP	-0.47662	-2.99656	2.10E-04
KIF11	-0.47705	-2.99951	0.00146
ACTN3	-0.47889	-3.01223	3.40E-04
AXIN2	-0.47947	-3.01628	4.00E-05
B3GNT9	-0.48146	-3.03009	5.70E-06
TMEM184C	-0.4824	-3.03666	0.00176
CCNB1	-0.48325	-3.04261	3.00E-05
POU5F2	-0.48384	-3.0468	0.00415
CEBPE	-0.48595	-3.06163	0.00687
ZSCAN22	-0.48617	-3.06318	0.00181
ZNF284	-0.48688	-3.06819	0.00468
RDH10	-0.48801	-3.07618	0.00402
ZRANB3	-0.48845	-3.0793	2.00E-05
HOXB2	-0.4887	-3.08104	0.00769
SPIN3	-0.48933	-3.08552	0.00135
TIAM1	-0.49117	-3.09862	1.86E-06
RRM2	-0.49143	-3.10048	0.0055
MGC15705	-0.49145	-3.10064	0.00635

ZBTB32	-0.4919	-3.10385	0.00153
GNB4	-0.49316	-3.11288	0.00159
USP46	-0.49332	-3.11398	4.00E-04
IGF1	-0.49402	-3.11907	0.00683
PTGIR	-0.49504	-3.12637	0.00399
GIT1	-0.49555	-3.13006	9.00E-05
COX4I2	-0.49598	-3.13316	0.00845
CDH1	-0.49605	-3.13367	3.00E-05
CDK1	-0.49736	-3.1431	2.70E-04
FLJ22447	-0.49835	-3.15026	6.70E-04
CCDC114	-0.49973	-3.16032	0.00155
ZNF257	-0.4998	-3.16085	7.00E-05
KALRN	-0.50067	-3.16716	6.40E-04
SPHK2	-0.501	-3.16958	0.00691
CCR7	-0.50144	-3.1728	2.95E-10
SLC40A1	-0.50169	-3.17463	5.73E-09
NGFRAP1	-0.50355	-3.18824	6.49E-10
SPDYE8P	-0.50366	-3.18905	0.00928
LOC401431	-0.50396	-3.19127	8.14E-09
BCAT1	-0.50401	-3.19162	0.00638
ZNF827	-0.50592	-3.20566	0.00146
SLC7A14	-0.50798	-3.22093	0.0068
DIO3	-0.50814	-3.22214	0.0032
MYO1E	-0.51009	-3.23663	0.00579
OTUD4	-0.5107	-3.24117	4.34E-06
C20orf177	-0.5108	-3.24192	6.70E-04
MDS2	-0.51752	-3.29245	0.00907
PDE4DIP	-0.51941	-3.30678	0.00359
GAL3ST3	-0.5203	-3.31357	0.00605
EPHA1	-0.52365	-3.33927	6.00E-05
ZNF483	-0.52417	-3.34325	8.40E-04
POU2AF1	-0.52431	-3.34433	0.00291
SELP	-0.52598	-3.35725	0.00551
SELP	-0.52598	-3.35725	0.00551
LEPRE1	-0.52683	-3.3638	1.80E-04
PIGW	-0.52692	-3.36446	0.00708
SNAR-B1	-0.5276	-3.3698	0.00671
S100A14	-0.52895	-3.38024	0.00947
KCNMB4	-0.5307	-3.39394	0.00298
ST6GALNAC3	-0.53075	-3.39431	0.00466
C1orf94	-0.53266	-3.40923	0.00749
LOC148189	-0.53317	-3.41329	0.00142
GRAP	-0.53348	-3.41574	1.00E-05
NKX2-8	-0.53506	-3.42812	0.00884
LEF1	-0.53644	-3.43907	2.60E-22
LAT2	-0.53877	-3.45755	2.00E-05
TJP2	-0.54282	-3.48998	3.00E-05
ZNF836	-0.54323	-3.49324	9.90E-04
VAT1L	-0.54397	-3.4992	0.00874
FOXD1	-0.54416	-3.50075	8.20E-04
CALCR	-0.54705	-3.52412	0.00374
C1QL2	-0.54775	-3.52981	0.00775
ENTPD1	-0.54789	-3.53095	0.0096

BEND7	-0.54842	-3.53524	0.0051
KANK1	-0.54899	-3.53988	0.00216
KANK1	-0.54899	-3.53988	0.00216
LOC10019237	-0.55188	-3.56352	3.60E-04
MAGEB4	-0.55336	-3.57567	0.00644
ZNF404	-0.55396	-3.58062	4.10E-04
LOC284023	-0.5545	-3.58508	0.00489
CAMSAP1L1	-0.55547	-3.59312	3.00E-05
RNASE6	-0.5555	-3.59336	0.00434
SETD5	-0.55727	-3.608	5.00E-05
CXCR5	-0.56119	-3.64072	4.00E-05
IL5	-0.56317	-3.6574	0.0038
HOMER1	-0.5655	-3.67706	0.0049
PLEKHA4	-0.56654	-3.6859	0.00126
LOC729991	-0.56692	-3.68911	1.00E-05
DEFB121	-0.568	-3.69827	0.00947
FHIT	-0.56804	-3.6986	0.00175
LY96	-0.56927	-3.70914	3.00E-05
NEFL	-0.56979	-3.71356	0.00682
FLJ45079	-0.57221	-3.73433	0.00517
PSMC3IP	-0.57355	-3.74582	3.50E-04
CASC5	-0.57383	-3.74822	7.00E-05
ZNF135	-0.57499	-3.75831	0.00679
PXDN	-0.57526	-3.76061	0.00992
PXDN	-0.57526	-3.76061	0.00992
ASB14	-0.57543	-3.76206	0.0033
SLC16A10	-0.57698	-3.77554	8.30E-04
UBD	-0.5771	-3.77659	8.00E-05
MPPED1	-0.57802	-3.78464	0.00143
PLXDC1	-0.57958	-3.7982	2.00E-05
CELF4	-0.58096	-3.81032	0.00525
CYP3A5	-0.58277	-3.82618	0.00126
FREM1	-0.58289	-3.82726	0.00803
SLC24A2	-0.58475	-3.8437	0.00486
ASPM	-0.58776	-3.87041	0.00177
EN1	-0.5881	-3.87344	8.90E-04
CHRNB4	-0.58811	-3.87358	0.00428
SLC22A10	-0.58846	-3.8767	0.00243
FAM74A3	-0.58875	-3.87923	0.00334
LOC440934	-0.59057	-3.89552	0.00357
PARP11	-0.59094	-3.89885	4.45E-06
NCRNA00272	-0.59141	-3.90307	0.00265
ARHGAP21	-0.59197	-3.90815	7.00E-05
LOC10050754	-0.59257	-3.91357	1.90E-04
SPSB1	-0.59569	-3.94178	0.0062
RETN	-0.59648	-3.94895	2.50E-04
LOC90586	-0.59772	-3.96025	0.00247
SELL	-0.59863	-3.96849	1.33E-12
CCR10	-0.60044	-3.98511	6.00E-05
NCKAP5	-0.60124	-3.99247	0.00357
LOC283404	-0.60154	-3.99521	0.00325
LIPH	-0.60343	-4.01262	0.00204
OR4C45	-0.60399	-4.01779	0.00365

TMEM45B	-0.6108	-4.08131	0.00135
CDCA5	-0.61446	-4.11584	8.64E-06
OIP5	-0.61629	-4.13327	0.00473
FLJ45983	-0.61699	-4.13991	0.00422
COL1A1	-0.62206	-4.18854	0.00194
LOC646268	-0.623	-4.19763	0.00255
ACTN1	-0.62376	-4.20495	5.92E-10
SLC22A23	-0.62584	-4.22516	0.00953
NRN1	-0.62797	-4.24592	0.00149
PPFIA4	-0.62885	-4.25448	0.00245
TPST1	-0.63173	-4.28283	0.00136
LOC388630	-0.6339	-4.30426	0.00357
HDGFRP3	-0.63788	-4.3439	5.00E-05
LONRF2	-0.63839	-4.34903	0.00224
GPR44	-0.63957	-4.36086	3.10E-04
ASPN	-0.6407	-4.37215	0.0033
FBLN2	-0.64645	-4.43046	6.50E-04
USP11	-0.65106	-4.47779	2.00E-05
MCTP1	-0.65422	-4.51042	7.90E-04
KRT24	-0.65666	-4.53584	0.00458
MAGED4B	-0.65813	-4.55122	0.00121
E2F1	-0.65834	-4.55345	1.94E-10
DTL	-0.65868	-4.55699	9.00E-05
FLJ22763	-0.66326	-4.60531	0.00199
SH3PXD2A	-0.66618	-4.63634	0.00141
BEND5	-0.66977	-4.67489	3.12E-06
OR51A7	-0.67399	-4.72053	0.00653
MYB	-0.67532	-4.73501	3.00E-05
C3orf14	-0.67682	-4.75135	4.35E-07
LOC729159	-0.67724	-4.75597	0.00149
SLC35F4	-0.68672	-4.8609	0.008
ANO7	-0.69173	-4.91737	6.00E-05
FAM75D3	-0.69333	-4.93548	1.00E-04
NUSAP1	-0.69504	-4.95494	3.20E-04
PDZK1IP1	-0.69531	-4.95804	4.60E-04
WSCD2	-0.6961	-4.96711	9.00E-04
ZWINT	-0.70013	-5.01339	3.40E-04
BIRC5	-0.7006	-5.01879	0.0024
ADAMTSL3	-0.703	-5.04661	0.00104
FLJ46552	-0.70425	-5.0612	0.00514
ADORA1	-0.70575	-5.07865	5.80E-04
SPRY2	-0.70607	-5.0824	1.45E-07
SLC6A13	-0.7085	-5.11088	0.00901
C10orf90	-0.71004	-5.12909	1.80E-04
STS	-0.71265	-5.15999	0.0033
SIRPA	-0.71343	-5.16931	0.00984
C3orf45	-0.71383	-5.17401	0.00364
CCR8	-0.7176	-5.21919	1.24E-08
LOC644662	-0.71968	-5.24417	6.20E-04
FGD5	-0.72133	-5.26417	0.00637
UHRF1	-0.72254	-5.27891	5.00E-04
CDKN3	-0.72867	-5.3539	2.62E-12
C22orf24	-0.72978	-5.36762	0.00756

LOC10013117	-0.73132	-5.38666	0.00273
C19orf77	-0.73206	-5.39587	0.00785
TNNT2	-0.73394	-5.41926	0.00552
CDT1	-0.74155	-5.51511	1.60E-04
PLXNB2	-0.74221	-5.5235	0.00695
FAM71F1	-0.7424	-5.52592	0.00607
FAM55A	-0.74542	-5.56444	0.00422
OR10W1	-0.74843	-5.60307	0.00131
RFPL2	-0.75067	-5.63206	8.52E-06
KIAA0101	-0.75157	-5.64375	0.00109
PCDHA4	-0.75339	-5.66753	5.80E-04
CFB	-0.75582	-5.69929	6.10E-04
LOC440047	-0.75676	-5.71167	0.00134
EEPD1	-0.76266	-5.78973	6.37E-09
IFNA10	-0.76383	-5.80541	0.00164
ALX1	-0.7645	-5.81429	0.00138
KCTD12	-0.77602	-5.97062	4.90E-08
KCTD12	-0.77602	-5.97062	4.90E-08
FCRL2	-0.79202	-6.19475	0.00591
TULP1	-0.7953	-6.24165	2.20E-04
KCNQ1DN	-0.79815	-6.28282	0.00787
INHBE	-0.80284	-6.3509	0.00587
SIGLEC11	-0.8031	-6.35481	0.00827
GAS2L2	-0.80884	-6.43932	0.00354
GINS2	-0.81318	-6.50402	3.94E-09
MXRA8	-0.83209	-6.79346	0.0042
TSPYL5	-0.83883	-6.89974	2.62E-08
PTCRA	-0.83894	-6.90144	0.00321
GCM2	-0.84001	-6.91844	5.70E-04
BDNF-AS1	-0.84808	-7.04825	0.00305
KIAA0125	-0.85683	-7.19167	6.01E-06
FLJ30679	-0.86083	-7.25817	0.00273
BTBD17	-0.86477	-7.32436	0.00427
LOC10013166	-0.8668	-7.3586	1.03E-08
LOC389247	-0.86713	-7.36428	0.00401
AEBP1	-0.87437	-7.48813	3.33E-15
ZNF501	-0.87812	-7.55303	0.00264
TBX3	-0.87856	-7.56074	3.59E-13
LOC10013112	-0.88041	-7.59297	0.00279
RTKN2	-0.88732	-7.71474	9.24E-13
CCNB2	-0.8877	-7.72149	7.28E-06
OR5B17	-0.89367	-7.82831	0.00176
PHGDH	-0.90209	-7.98159	2.13E-11
C5orf13	-0.91129	-8.15249	3.00E-08
KLF7	-0.92632	-8.43959	1.71E-11
AQP4	-0.93397	-8.58958	2.00E-04
CENPF	-0.94603	-8.83147	3.90E-08
CDKN2B	-0.95346	-8.98382	2.00E-04
TRIM71	-1.01828	-10.42979	0.00105
NCRNA00244	-1.07988	-12.01931	3.30E-04
VSIG4	-1.0987	-12.55148	6.49E-13
NOG	-1.12596	-13.36458	1.58E-09

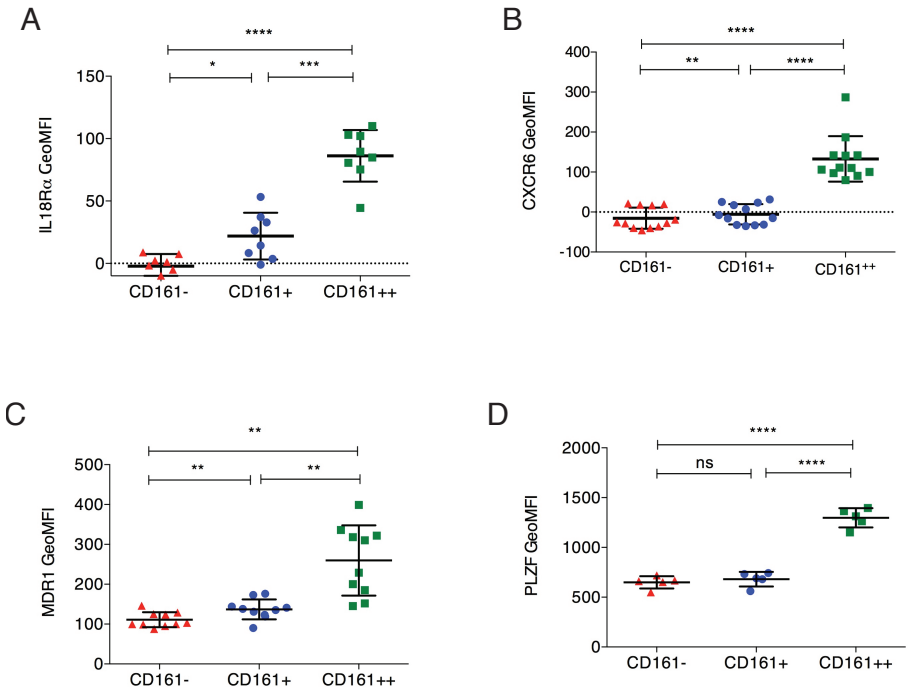

Appendix IV.ii: Microarray confirmation in all CD161 subsets. GeoMFI of IL18Ra (**A**), CXCR6 (**B**), MDR1 (**C**) and PLZF (**D**) in all three subsets of CD8+ T lymphocytes as determined by flow cytometry.

A

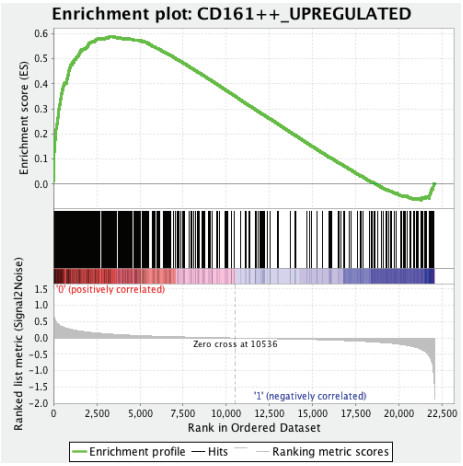

Dataset	CD161+ vs CD161−
GeneSet	CD161++_UP
Upregulated in	CD161+
Enrichment Score (ES)	0.59
Normalised ES (NES)	2.64
Nominal p-value	<0.001

B

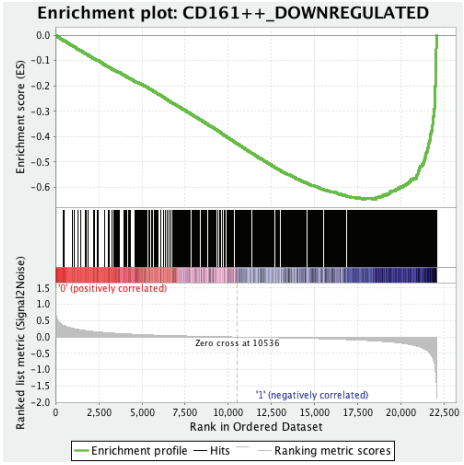

Dataset	CD161+ vs CD161−
GeneSet	CD161++_DOWN
Upregulated in	CD161−
Enrichment Score (ES)	−0.65
Normalised ES (NES)	−2.64
Nominal p-value	<0.001

Appendix IV.iii: Microarray analysis was performed on CD161+ and CD161- CD8+ T cells in adult blood excluding naive cells. Gene set enrichment analysis (GSEA) summary plots comparing gene expression between CD161+ and CD161- CD8+ T cells. Genes significantly upregulated in CD161++ CD8+ T cells were significantly ($p<0.001$) enriched in CD161+ CD8+ T cells (**A**). Genes significantly downregulated in CD161++ CD8+ T cells were significantly ($p<0.001$) enriched in CD161- CD8+ T cells (**B**).

Appendix IV.iv: Genes significantly differentially expressed between stimulated vs. unstimulated CD161+, and stimulated vs. unstimulated CD161− CD8+ T cells. Genes referred to in the text are highlighted in bold.

	CD161+		
Symbol	**Log(Ratio)**	**Fold Change**	**P-value**
CCL20	2	100	0
CCL3L3	2	100	0
IFNG	2	100	0
IL13	2	100	0
IL2	2	100	0
IL21	2	100	0
IL3	2	100	0
IL4	2	100	0
CCL4	1.98057	95.62418	0
IL10	1.89003	77.63063	0
IL31	1.81784	65.74178	0
CCL3	1.73401	54.20181	5.01E-35
IL23A	1.68192	48.07494	0
IL5	1.66374	46.10404	3.41E-14
IL11	1.63913	43.56461	0
IL22	1.63083	42.73958	2.31E-10
IL17F	1.54097	34.75123	1.01E-13
CXCL2	1.5196	33.08287	1.62E-08
IL1B	1.50201	31.76928	1.34E-16
CCL1	1.26355	18.34628	5.60E-07
IFNA6	1.10063	12.60752	0.00003
CXCL3	1.06275	11.55444	1.62E-18
IFNE	0.87249	7.45581	3.64E-15
CCL18	0.86631	7.35035	4.02E-13
IL24	0.86238	7.28423	8.93E-18
IFNAR2	0.75811	5.72938	3.71E-21
IL6	0.68732	4.86764	3.99E-08
IL17D	0.62571	4.22384	7.09E-09
IL28A	0.32429	2.11002	3.95E-08
IL26	0.30181	2.00358	6.83E-06
CXCL16	-0.31988	-2.0887	1.05E-08
IFNA4	-0.40987	-2.56963	2.35E-13
CXCL12	-0.51247	-3.25441	1.97E-11
CCL28	-0.60662	-4.04223	7.09E-10
IL17C	-0.61893	-4.15842	0.00662
IL29	-0.69618	-4.96795	8.88E-06
IL15	-0.84463	-6.99245	1.89E-09
IL32	-0.86591	-7.34361	1.67E-38
CCL23	-1.02478	-10.58709	0.00125
CXCL5	-1.11002	-12.88307	1.86E-43
CCL24	-1.25558	-18.01277	0
IL16	-1.3737	-23.64262	0

Symbol	CD161– Log(Ratio)	Fold Change	P-value
CCL20	2	100	0
CCL3L3	2	100	0
IFNG	2	100	0
IL2	2	100	0
IL3	2	100	0
IL13	1.99905	99.78169	0
IL31	1.99628	99.14742	0
IL21	1.97438	94.27056	0
IL10	1.93585	86.26813	0
CXCL2	1.92853	84.82661	0
IL4	1.92547	84.23036	0
IL11	1.89813	79.09109	0
CXCL3	1.89811	79.08788	0
CCL4	1.86385	73.08866	0
IL22	1.82616	67.01241	2.31E-36
IL5	1.80205	63.39455	4.83E-28
CCL1	1.71716	52.13913	2.18E-10
IL1B	1.65547	45.23426	2.90E-06
CCL3	1.57954	37.97852	2.73E-19
IL23A	1.52115	33.20068	2.38E-44
IL17F	1.47492	29.84858	0
CCL18	1.32723	21.24357	3.37E-10
IL9	1.30126	20.01053	2.79E-18
IL8	1.28335	19.20236	8.48E-15
IL24	1.24926	17.75255	2.86E-11
IL6	1.24587	17.61463	4.38E-08
IL26	1.22463	16.77378	1.96E-10
IFNE	1.21164	16.2795	1.76E-24
CXCL1	0.83586	6.85261	4.04E-11
IL17D	0.76164	5.77623	9.94E-11
IL12A	0.70531	5.07356	1.53E-15
CXCL16	0.58975	3.88825	0.00195
IL28A	0.52041	3.31447	0.00002
CXCL13	0.48054	3.02368	0.00222
CXCL12	-0.41425	-2.59567	0.00005
IL16	-0.44071	-2.75873	0.00054
IFNA4	-0.5126	-3.25534	9.10E-35
IL17C	-0.55126	-3.55842	0.00089
IL15	-0.64435	-4.40907	9.93E-12
IL29	-0.72757	-5.34041	9.14E-08
IL32	-0.7311	-5.38396	0
CCL28	-0.82803	-6.73028	4.52E-17
CCL24	-0.88455	-7.66567	2.92E-32
IL16	-1.20232	-15.93365	4.29E-42
IL16	-1.43147	-27.00685	1.51E-11
CXCL5	-1.54045	-34.70966	0

Appendix IV.v: Genes differentially expressed by stimulated CD161+ vs. stimulated CD161− CD8+ T cells. Genes referred to in the text are highlighted in bold.

Name	Log(Ratio)	Fold Change	P-value
NLRP13	1.47134	29.60327	0.0006
CAMKMT	1.44882	28.10717	0.00011
PLCH1	1.42324	26.49952	0.00014
TCF21	1.41343	25.90762	0.00011
MYO16	1.41276	25.8677	0.00224
LOC339666	1.39821	25.01582	0.00011
ESYT3	1.39433	24.79314	0.00016
GRM5	1.31368	20.59122	0.00005
FLJ35424	1.29998	19.95174	0.00006
NME5	1.29333	19.64845	0.00008
PRO2214	1.27519	18.84458	0.00011
SOHLH2	1.26099	18.23844	0.00011
FOXP2	1.21821	16.52746	0.00003
CYP4A22	1.21616	16.44996	0.00007
PROL1	1.21392	16.36524	0.00012
UCP1	1.2129	16.32678	0.00152
UGGT2	1.16977	14.78313	0.00007
GALNTL6	1.16783	14.71726	0.00076
HERC3	1.16023	14.46217	0.00009
ZNF311	1.15516	14.29424	0.00015
AGXT2L1	1.15196	14.18938	0.00025
CACNA1A	1.15138	14.17031	0.00033
AP4S1	1.13613	13.68151	0.00066
TP73	1.12146	13.22687	0.00018
WFDC13	1.10678	12.78738	0.0004
FAM188B	1.10117	12.62315	0.00044
FRRS1	1.08323	12.11243	0.00044
KRTAP5-3	1.08086	12.04654	0.00058
IFNA6	1.07652	11.92665	0.00003
LOC10028770	1.05996	11.48055	0.0006
SORCS1	1.05721	11.40793	0.00087
LRIG2	1.05001	11.2204	0.00057
OR2T8	1.04465	11.08271	0.00132
XLOC_011510	1.04365	11.0573	0.00126
OOSP1	1.04162	11.00579	0.0009
ZMYND12	1.04151	11.00296	0.00062
C9orf150	1.03747	10.90103	0.00067
GDNF	1.0248	10.58759	0.00337
FOXL1	1.02117	10.49964	0.00101
C8B	1.01237	10.28902	0.00343
ZBTB49	1.00513	10.11892	0.00103
LOC10028776	0.99305	9.84125	0.00068
EXOC6B	0.99021	9.77706	0.00163
DEFB135	0.98027	9.55592	0.0014
CACNA2D3	0.97144	9.3636	0.00127
XLOC_001851	0.97139	9.36255	0.00015
LRFN2	0.95519	9.01975	0.00002
ARHGAP33	0.95295	8.97317	0.00203
TBX22	0.94914	8.89496	0.00094
ZC3H12B	0.94018	8.71324	0.00146
AQP4	0.937	8.64966	0.00192
KIAA0889	0.93544	8.61863	0.00025

LOC10012903	0.93342	8.57873	0.00178
TIFAB	0.9323	8.55658	0.00402
TPRG1	0.91907	8.29983	0.00246
NYNRIN	0.91525	8.22718	0.00263
LOC643037	0.90484	8.03224	0.00311
ADAM20	0.89902	7.92537	0.00018
BACE1	0.89283	7.81319	0.0033
XLOC_000670	0.88978	7.75847	0.00201
LHX9	0.88581	7.68801	0.0031
RALGPS1	0.88545	7.68151	0.00505
IGSF11	0.8835	7.6471	0.00362
BACE1	0.88019	7.58904	0.00996
DPP6	0.87956	7.57806	0.00502
CCDC36	0.87931	7.57374	0.00372
ASCL3	0.87736	7.53983	0.00317
NXN	0.87382	7.47852	0.00406
LOC10019242	0.87306	7.46554	0.00557
LOC285419	0.86811	7.3809	0.00429
C8orf34	0.86789	7.37725	0.00638
ALDH1A2	0.86545	7.3359	0.00468
KC6	0.86544	7.33562	0.00054
SLC17A2	0.86537	7.33448	0.00455
COL5A2	0.864	7.31137	6.55E-07
LOC10029361	0.86251	7.28631	0.00486
IGSF1	0.85511	7.16329	0.00685
LOC10013088	0.85349	7.13651	0.00694
C11orf88	0.85259	7.12182	0.007
MS4A6A	0.85222	7.11568	0.00095
OR5AN1	0.85119	7.09884	0.00516
PPIP5K1	0.84852	7.05535	0.00737
SIX4	0.84805	7.04775	0.00729
MPDZ	0.84603	7.01512	0.00661
SLC6A15	0.84305	6.96704	0.00602
SULT1C2	0.84289	6.96448	3.73E-06
PRAMEF15	0.83704	6.87129	0.00591
Q7VLF4	0.83622	6.85829	0.00276
IPCEF1	0.8358	6.85176	0.00471
ABCG4	0.82733	6.71935	0.00868
OR10J1	0.82725	6.7181	0.00162
ADAM21	0.82593	6.69782	0.00641
LOC286189	0.82299	6.65256	0.00898
LOC643650	0.81766	6.5714	0.00234
KCNG4	0.81624	6.54991	0.00468
ZBTB47	0.81586	6.54419	0.00146
GPR22	0.81124	6.47495	0.00785
CRLF1	0.79679	6.26304	0.00514
KRTAP13-2	0.79117	6.18264	0.00634
PAX3	0.79029	6.17005	0.00032
LOC10012832	0.78475	6.09187	0.00986
PLA2G4F	0.78394	6.08051	0.00018
KPNA7	0.78311	6.06887	0.00595
LOC729178	0.77905	6.01243	0.00119
CYP4A11	0.76897	5.87453	0.00219

LOC729159	0.75832	5.73222	0.00295
STK31	0.75116	5.63845	0.00027
C9orf84	0.74919	5.61294	0.00717
KIF5A	0.74669	5.58067	0.00892
OR10AD1	0.74009	5.49652	0.00702
ARHGEF11	0.73405	5.42059	0.0004
LOC10029268(	0.7293	5.36162	0.00828
CCR9	0.7257	5.31743	0.00238
C9orf172	0.72273	5.2812	0.00288
GPR123	0.71626	5.20305	0.00101
LOC729178	0.71541	5.19286	0.00775
GUSBP1	0.71483	5.18598	0.0012
MMP10	0.71411	5.17739	0.00044
TRMT1L	0.67982	4.78431	0.00145
DOC2A	0.6741	4.72177	0.0026
LOC285191	0.6591	4.56143	0.0065
IGJ	0.65767	4.5464	0.00406
CCDC40	0.65515	4.52013	0.00077
ADAMTSL2	0.65285	4.49621	0.00112
TMEM198	0.61506	4.12156	0.00712
LRRC16A	0.6121	4.09358	0.00366
TRIM46	0.60152	3.99504	0.00841
SLC30A4	0.59975	3.97878	0.00812
TPBG	0.59541	3.93926	0.00092
DIS3L2	0.59302	3.91763	0.00664
LINC00478	0.5823	3.82211	0.0053
MGC11082	0.57822	3.78635	0.00978
HCAR1	0.57134	3.72687	0.00004
PLP1	0.56905	3.70724	0.00561
ITPR2	0.5612	3.64079	0.00273
AMOTL2	0.56002	3.63093	0.00733
SERPINB2	0.54916	3.54126	0.00134
LOC257358	0.53888	3.45845	0.00495
INSR	0.51609	3.28164	0.00963
F3	0.51157	3.24769	0.00152
IDO1	0.49075	3.09564	0.00574
F7	0.48086	3.02597	0.00232
NLRP4	0.47819	3.00738	0.00723
TACR1	0.47326	2.97342	0.00304
FLJ44511	0.46691	2.9303	0.00865
OR8G2	0.46269	2.90195	0.00103
CAV1	0.44125	2.76219	0.00499
IL1RL1	0.44015	2.75519	0.00111
FLJ41423	0.42999	2.69147	0.00021
IGFBP3	0.42449	2.6576	0.00002
KREMEN2	0.39415	2.47829	0.00727
RAPGEFL1	0.39367	2.47555	0.00284
QPCT	0.37517	2.37233	0.00383
CPS1-IT1	0.37377	2.36466	0.00771
LOC338758	0.35514	2.26535	0.00276
SLC2A13	0.34181	2.19689	0.00583
KRTAP5-11	0.32925	2.13426	0.0009
PGF	0.32637	2.12017	0.00884

VSX1	0.31903	2.08463	0.00016
ATP6V0E2	-0.30235	-2.00607	0.00593
DHRS13	-0.30548	-2.0206	0.00596
MMP9	-0.30624	-2.02414	0.00323
ZNF250	-0.30921	-2.03802	0.00017
CNN2	-0.31	-2.04176	0.00022
LOC730961	-0.31638	-2.07194	0.00157
FAM57A	-0.33935	-2.18449	0.00006
NIPSNAP1	-0.3412	-2.1938	0.0013
AIF1	-0.34463	-2.21122	0.00188
AKAP12	-0.34868	-2.23195	2.38E-06
CBFA2T3	-0.35031	-2.24031	0.00921
PLEKHG3	-0.35426	-2.26078	0.0017
SPINT2	-0.3547	-2.2631	0.00071
RPS6KA5	-0.35643	-2.27212	0.00531
HSD17B1	-0.35712	-2.27571	0.00867
BTK	-0.36612	-2.3234	0.00408
JAG2	-0.36638	-2.32479	0.00149
SHMT1	-0.36833	-2.33521	0.00381
LOC10013205	-0.36932	-2.34055	0.00623
SETD1B	-0.37622	-2.37804	0.00033
FAM123B	-0.37779	-2.38667	0.00412
CORO2A	-0.38168	-2.40813	0.00569
TMEM133	-0.38343	-2.41783	0.00844
FLJ42022	-0.38658	-2.43544	0.00048
VPS37A	-0.39745	-2.4972	0.00112
LSS	-0.39931	-2.5079	0.00389
HEATR4	-0.40088	-2.51699	0.00105
FGD4	-0.40564	-2.54472	0.00942
GRIN3A	-0.40677	-2.55138	0.00275
LOC10012827	-0.41196	-2.582	0.00067
BEND5	-0.41521	-2.60139	0.00297
MCAM	-0.41546	-2.60292	0.00029
EDA	-0.41792	-2.6177	0.00381
FMOD	-0.42089	-2.63565	0.00355
SLC2A11	-0.42579	-2.66555	0.00059
RASA2	-0.43422	-2.71781	0.00186
BIRC5	-0.43537	-2.72503	0.00567
LOC10012961	-0.43542	-2.72535	0.0034
NTRK1	-0.43698	-2.73511	0.00009
MYEF2	-0.44698	-2.79885	0.00707
MTUS1	-0.46213	-2.89819	1.27E-12
DACT3	-0.4668	-2.92952	0.0075
XLOC_I2_0079	-0.46946	-2.94753	0.00804
WHSC1	-0.47482	-2.98416	0.00008
ZNF815	-0.48391	-3.04723	0.00722
KAT6B	-0.4894	-3.08606	0.00063
CAPN12	-0.49812	-3.1486	0.00113
IL5RA	-0.50812	-3.22195	0.00337
TYSND1	-0.51191	-3.25019	0.00872
MTCP1	-0.51314	-3.2594	0.00732
CD200R1	-0.51455	-3.27003	0.00026
RNFT2	-0.51544	-3.2767	0.00391

C19orf55	-0.51861	-3.30072	0.00018
KPRP	-0.52118	-3.32033	0.0098
KRT34	-0.52608	-3.35797	0.00535
ZNF710	-0.52919	-3.38216	0.00427
STAC3	-0.53608	-3.43622	0.0093
INSM1	-0.54333	-3.49402	0.00041
TNS1	-0.54768	-3.52922	0.00029
MLL	-0.56668	-3.68707	0.00033
SLC35F3	-0.57023	-3.71729	0.00343
UNC45B	-0.57542	-3.76201	0.00881
LOC10012978	-0.57671	-3.77322	0.00419
CDH2	-0.57719	-3.77739	0.00934
TBXA2R	-0.59227	-3.91085	0.00587
HEATR7A	-0.59545	-3.93954	0.00771
SEPT10	-0.59962	-3.97763	0.00155
MPO	-0.60391	-4.01704	0.00562
LOC10050712	-0.61403	-4.1118	0.00311
LOC388948	-0.61453	-4.11651	0.00506
C17orf104	-0.61529	-4.12373	0.00291
CD79B	-0.63056	-4.27131	0.00367
LOC10050619	-0.63291	-4.29442	0.00019
PIK3R3	-0.63499	-4.3151	0.00091
LRRIQ1	-0.65306	-4.49843	0.00924
GUCY1A3	-0.65624	-4.53148	0.00878
VSIG4	-0.66438	-4.61724	0.00702
KIAA0101	-0.66706	-4.64575	0.00116
CTSZ	-0.67359	-4.71616	0.00293
PARP10	-0.68039	-4.7906	0.00466
TP53I3	-0.682	-4.80837	0.00811
BEGAIN	-0.68525	-4.84449	0.00785
SLC35F1	-0.68668	-4.86047	0.00921
WFDC8	-0.68674	-4.86114	0.00124
XLOC_014103	-0.68936	-4.89056	0.00343
P2RX6	-0.69354	-4.93784	0.00811
FAM83C	-0.69442	-4.94791	0.00244
LHX9	-0.71593	-5.19911	0.00305
ARPP21	-0.71717	-5.21404	0.0005
SLC1A2	-0.72108	-5.2611	0.00565
KLRG2	-0.72493	-5.30801	0.00316
DNAJB7	-0.72565	-5.31679	0.00746
XLOC_006486	-0.72685	-5.33148	0.00433
WDR49	-0.73795	-5.4695	0.00935
GADL1	-0.74081	-5.50571	0.00554
GLT8D2	-0.74133	-5.51221	0.00147
SUFU	-0.74453	-5.553	0.00952
CLRN2	-0.74697	-5.58436	0.00334
ENHO	-0.75109	-5.63749	0.00623
LOC10013108	-0.76091	-5.76642	0.0052
PIRT	-0.7659	-5.83309	0.00518
LOC10050637	-0.7662	-5.8371	0.00307
NEXN	-0.76667	-5.84351	0.001
HCRTR1	-0.76682	-5.84549	0.00788
GABRA5	-0.76961	-5.88308	0.00005

NINJ2	-0.77051	-5.89535	0.00325
LGALSL	-0.77356	-5.93693	0.00111
LRRC3	-0.7779	-5.99656	0.00215
FLJ46257	-0.78087	-6.03772	0.00929
LOC10065284	-0.78337	-6.0725	0.00345
ARHGEF10L	-0.78671	-6.11948	0.00165
CST2	-0.78803	-6.13811	0.00718
LOC10012932	-0.7884	-6.14328	0.00388
LINC00189	-0.78877	-6.14853	0.00325
DPYD	-0.7921	-6.19581	0.00669
ACSS3	-0.79464	-6.23217	0.00497
FAHD1	-0.80036	-6.31482	0.00058
CYCSP52	-0.80651	-6.40482	0.00093
OTOG	-0.81012	-6.45833	0.00493
SAG	-0.81212	-6.48817	0.0067
C21orf58	-0.81278	-6.49803	0.00196
COX15	-0.81506	-6.53222	0.00074
SLC6A20	-0.8162	-6.54943	0.00558
C1orf88	-0.81778	-6.57326	0.00415
LOC10013065	-0.82238	-6.6433	0.00658
DCAF12L1	-0.82495	-6.68268	0.00217
C4orf26	-0.82696	-6.71368	0.00066
ENO4	-0.8274	-6.72044	0.00399
LOC10028732	-0.8327	-6.80303	0.00016
AADAT	-0.83403	-6.82381	0.00455
DIRC3	-0.84104	-6.93492	0.00535
TRIM17	-0.84257	-6.95932	0.00038
CYP26C1	-0.84314	-6.96859	0.00245
LOC10050547	-0.84495	-6.99758	0.00325
TMEM231	-0.84625	-7.01859	0.00417
SLC22A3	-0.85293	-7.12744	0.00725
LINC00482	-0.85465	-7.15575	0.00253
HELT	-0.85516	-7.16403	0.0018
ABCG2	-0.85842	-7.21812	0.00655
LOC653712	-0.86439	-7.31802	0.00144
OR2F1	-0.86668	-7.3566	0.00259
HSFX1	-0.86679	-7.35848	0.00142
VWF	-0.87067	-7.42447	0.00264
NUDT12	-0.87085	-7.42757	0.00372
MARCH1	-0.87315	-7.46711	0.00177
SKOR1	-0.87323	-7.46848	0.00255
CACNA1E	-0.87435	-7.48771	0.00471
FLJ46365	-0.87552	-7.508	0.00392
LOC10050765	-0.88228	-7.62566	0.00064
LRRC4B	-0.88353	-7.64773	0.00326
ADAMTS4	-0.89295	-7.81539	0.00305
APOF	-0.89812	-7.90901	0.00406
ACY3	-0.90525	-8.03991	0.00636
PRAMEF5	-0.90805	-8.09181	0.0027
WNK2	-0.91165	-8.15918	0.00143
CCR2	-0.9126	-8.17715	0.00328
TMEFF2	-0.9144	-8.21105	0.00527
LOC286087	-0.91561	-8.234	0.00011

TPD52	-0.91564	-8.23448	0.00166
KCND3	-0.91647	-8.25032	0.00418
FBXL7	-0.9172	-8.26419	0.00054
CSN1S2AP	-0.92033	-8.32402	0.00333
NETO1	-0.92458	-8.40581	0.0053
AMZ1	-0.92506	-8.41512	0.00147
OR2T10	-0.93206	-8.55181	0.00133
NAALADL2	-0.93997	-8.70908	0.00475
SPINK5	-0.94669	-8.84474	0.00349
CD1E	-0.94998	-8.91206	0.00427
LOC728431	-0.95019	-8.91631	0.00086
C4orf37	-0.9512	-8.93725	0.00054
RPS6KL1	-0.9513	-8.93931	0.00326
PABPC1L2B	-0.96187	-9.15943	0.00103
ARHGEF33	-0.96344	-9.19264	0.00095
SEMG2	-0.96402	-9.20492	0.00469
C6orf38	-0.96639	-9.25536	0.00106
HSPB9	-0.97069	-9.34748	0.00307
LOC10050719	-0.97358	-9.40984	0.00344
OR4C13	-0.98202	-9.59446	0.00301
PAR4	-0.98981	-9.7681	0.00135
PSMB11	-0.99468	-9.8783	0.00003
VWDE	-0.99874	-9.97092	0.00003
ADCY8	-1.00113	-10.02605	0.00363
RGL3	-1.00535	-10.12396	0.00094
SYT8	-1.01212	-10.28291	8.80E-08
OSM	-1.0181	-10.42559	0.00162
GPR128	-1.02619	-10.62158	0.00049
FLJ41455	-1.03142	-10.75025	0.00062
LOC10012988	-1.03232	-10.7727	0.00067
XLOC_011548	-1.04679	-11.1376	0.00047
LHX2	-1.05239	-11.2821	0.00036
DAZ1	-1.05618	-11.38104	0.00038
RNU105B	-1.05697	-11.40167	0.00056
SCG5	-1.06548	-11.6274	0.00604
RIMS1	-1.09534	-12.45492	0.00015
HOXA6	-1.09871	-12.55187	0.00101
LOC10013186	-1.10293	-12.6746	0.00109
C14orf48	-1.10423	-12.71255	0.00039
BOD1P	-1.10791	-12.82075	0.00035
SNX31	-1.12327	-13.28235	0.00086
P39189	-1.13119	-13.52649	0.00044
ZYG11A	-1.13568	-13.66731	0.00244
TRPM8	-1.14264	-13.88786	0.00029
TTLL7	-1.16483	-14.616	0.00029
NTM	-1.16495	-14.61994	0.00073
C16orf47	-1.16995	-14.78949	0.00027
UGT1A6	-1.19742	-15.75496	0.00018
EDDM3B	-1.2504	-17.79919	0.00015
ADAMTSL2	-1.26173	-18.26951	0.00022
OR10H1	-1.26816	-18.54226	0.00025
LOC728093	-1.2702	-18.62947	0.00028
FCAMR	-1.27518	-18.84422	0.00504

ARHGEF4	-1.29497	-19.72275	0.00026
LOC10050617	-1.31325	-20.57087	0.0001
PRAMEF15	-1.32258	-21.01755	0.00016
LOC10012855	-1.32649	-21.20749	0.00048
LOC10050716	-1.32683	-21.22396	0.00158
TTTY18	-1.42431	-26.56514	0.00096
ZNF804B	-1.43288	-27.09422	0.00095
	-1.46445	-29.13754	0.00105

5. Development of CD161+ CD8+ T cells

5.1 Introduction

T lymphocytes mature within the thymus. During this time they undergo V(D)J recombination to express a somatically recombined TCR which is subsequently both positively selected for MHC restriction and negatively selected against self-reactivity. Positive and negative selection is mediated by peptide-presenting MHC molecules expressed by thymic cortical and medullary epithelial cells, as well as medullary APCs, respectively. After release from the thymus, these mature yet naïve T cells circulate between the bloodstream and secondary lymphoid organs in the search for cognate antigen. In response to which, a specific T cell expressing a specific TCR will proliferate to produce a clone of effector cells. Clonal expansion is followed by activation-induced cell death and contraction of antigen-specific T cells, leaving a pool of memory T cells to protect against re-infection.

The pathway of differentiation of T cells from naïve to memory – of both effector (T_{EM}) and central (T_{CM}) memory type – has been contentious, with both linear and independent pathways proposed (see Chapter 1, Figure 1-1). Among the factors suggested to influence the resulting phenotype of the memory T cell pool are antigen load (Papagno et al., 2004), costimulation (Gamadia et al., 2014) and cytokine environment (Alves et al., 2003). One method used in the attempt to distinguish the differentiation pathway of memory cells has been to compare TCR repertoires of T_{EM} and T_{CM} populations by TCR sequencing, with evidence for both pathways emerging. A high degree of overlap between the two populations, with T_{CM} subsets consistently more diverse, seems to support the existence of a linear pathway of differentiation from T_{CM} to T_{EM} (Figure 1-1A; Bouneaud et al. 2005), while comparison of the TCR repertoires shows them to be significantly less similar than would be expected if they had randomly assigned from the same population, conversely arguing for independent and distinct pathways of differentiation (Figure 1-1C; Kedzierska et al. 2006; Venturi et al. 2008).

MAIT cells, on the other hand, display a uniform T_{EM} phenotype in the adult circulation and express a semi-invariant TCR (Dusseaux et al., 2011). Development of MAIT cells, therefore, is somewhat different from that of conventional T cells. Vα7.2+ MAIT cells can be identified within the human thymus (Gold et al., 2013; Leeansyah et al., 2014; Martin et al., 2009). Experiments in mice have identified MAIT cell selection to be dependent on haematopoietic cells, rather than the thymic epithelium (Treiner et al., 2003), and specifically CD4+CD8+ double positive thymocytes (Seach et al., 2013) which express MR1 (Gold et al., 2013). Naïve MAIT cells are also present in UCB, in low numbers which rapidly expand and acquire a memory phenotype after birth (Martin et al., 2009; Walker et al., 2012). Studies in mice transgenic for the murine MAIT cell TCR orthologue (Vα19-Jα33) identified a key role for B cells in this expansion (Martin et al., 2009; Treiner et al., 2003). This is not entirely dependent on MR1 expression by B cells, as MAIT cell expansion was also observed upon adoptive transfer of MR1-deficient B cells into recombination-activating gene (RAG)-knockout mice (Martin et al., 2009). The absence of MAIT cells in germ-free mice also suggested a role for commensal bacteria in this expansion. However, a recent study by Leeansyah et al. (2014) identified the presence of MAIT cells in second trimester foetal tissues and, therefore, before the establishment of the commensal microflora. Interestingly, MAIT cell frequencies were highest in the foetal small intestine, lung and liver (as opposed to the thymus, spleen and mesenteric lymph nodes) where they also displayed the memory phenotype, IL18Rα and PLZF expression characteristic of MAIT cells in the adult (Dusseaux et al., 2011; Savage et al., 2008).

Expression of CD161 is induced early during ontogeny. MAIT cells within the thymus already express CD161 (Leeansyah et al., 2014; Martin et al., 2009) and expression of CD161 by naïve cells within UCB identifies precursors of both CD8+ MAIT cells (Walker et al., 2012) and CD4+ Th17 cells (Cosmi et al., 2008). These cells already express markers such as RORγt and IL23R, also expressed by CD161+CD4+ thymocytes (Cosmi et al., 2008), suggesting that CD161 identifies cells of a pre-committed phenotype. However, whether precursors of CD161+CD8+ T cells are also present, and pre-programmed, during development is not yet known. Alternatively, CD161 expression may be induced during differentiation of memory cells, with factors such as antigen load and cytokine

environment potentially influencing this differentiation, as discussed previously. Modulation of CD161 expression by cytokines has been described for various lymphocytes. Culture of UCB CD4+ T cells with anti-CD3+CD28 stimulation, together with a combination of IL-1β and IL-23 resulted in upregulation of mRNA for CD161 (Cosmi et al., 2008), while NK cells cultured with IL-12 also upregulate CD161 expression (Azzoni et al., 1998; Poggi et al., 1999a). Therefore, although the developmental pathway of CD161++ MAIT cells has begun to be resolved, that of CD161+CD8+ T cells has yet to be investigated.

5.2 Aims of Chapter

1. Investigate if a CD161+CD8+ T cell population exists early in development, as for MAIT cells
2. Determine the phenotype of CD161+CD8+ T cells in early life – are these a pre-committed population?
3. Examine the origin of CD161+CD8+ T cells – could they develop from CD161−CD8+ T cells?

5.3 Materials and Methods

Chapter-specific materials and methods are detailed below. All other methods and reagents are described in Chapter 2.

5.3.1 Cells

Human thymocytes were kindly provided by Georg Holländer.

5.3.2 Vβ Typing and Correlations

PBMC were surfaced stained with T cell receptor Vβ antibodies; Vβ 1, 2, 4, 5.3, 7.2, 8, 9, 11, 13.2, 14, 16, 18, 23-PE, and Vβ 3, 5.1, 5.2, 7.1, 12, 13.1, 13.6, 14, 16, 17, 20, 21.3, 22-FITC (Beckman Coulter). Data were acquired on a MACSQuant (Miltenyi Biotec) and analysed using FlowJo (Treestar, Inc.). Vβ frequencies for CD161+ and CD161− CD8+, and CD8+ and CD8− populations were extracted for each donor. As the frequencies for most donors did not follow a normal distribution, the nonparametric (Spearman rank) correlation coefficient (*r*) between Vβ frequencies for each subset within and between donors was calculated. A modification of the Wilcoxon rank-sum test was subsequently used. Due to the data structure, the 'null hypothesis' was generated by simulation. Therefore, the correlations were arranged in an *n* by *n* matrix, where all diagonal entries were within donor correlation and off-diagonal entries were between donor correlation. A permutation procedure was used were only the rows were shuffled, and ten thousand random shuffles were generated. The median *r* between and median *r* within individuals, or median *r* within donors between CD161+/- and CD8+/-, was compared by two-sample Wilcoxon rank-sum test to determine if they were significantly different. These statistical analyses were performed by Jagadish Kumar, University of New South Wales.

5.3.3 CD161– T cell culture

Naïve T cells were isolated from thawed PBMC using a Naïve Pan T cell Isolation Kit (Miltenyi Biotec) following manufacturer's instructions. This enriched for CD161– cells amongst CD8+ T cells. Approximately 1.5 x 10^6 cells were plated per well of a 96-well round-bottomed plate in R10 with or without CD3/2/28 beads (Miltenyi Biotec) at a bead-to-cell ratio of 1:2. Cells were centrifuged and resuspended in R10 and 50ng/ml of specific cytokines singly or in combination. Cytokines used were IL-2, IL-12 (Miltenyi Biotec), IL-1β, IL-4, IL-6, IL-7, IL-13, IL-15, IL-18, IL-21, IL-23, TGFβ and IFNγ (R&D Systems). Cells were also stimulated with 2μg/ml Phytohemagglutinin (PHA; Sigma) or cell stimulation cocktail (PMA+ionomcyin; eBioscience). For assessment of CD161 expression on NK cells, the column-retained fraction from naïve pan T cell isolation was cultured with or without IL-12 only. Cells were cultured at 37°C, 5% CO_2, and a fraction of cells removed at each timepoint and assessed for CD161 expression by flow cytometry surface staining. Percentage of cells expressing CD161 in the presence of various cytokines was normalised to either cell cultured without cytokine or with activation alone, as detailed in the figure legend, ie. $\frac{\%\ \text{CD161+ with cytokine}}{\%\ \text{CD161+ without cytokine}}$

5.3.4 CMV T cell lines

PBMC from 3 donors with known CMV-dextramer positive responses were thawed and rested for 2hrs in R10. Cells were then counted and resuspended at 4 x 10^6/ml in Rh10. 2 x 10^6 cells of each were then plated into wells of a 12-well plate with 25ng/ml IL-7 (R&D Systems) and either 0.1μg/ml or 1μg/ml CMV peptide NLVPMVATV (ProImmune). Cells were incubated at 37°C, 5% CO_2. On day 3, 25ng/ml IL-2 (R&D Systems) was added. Cells were split between wells and Rh10 plus 25ng/ml IL-2 added as required, when cells were judged to be >90% confluent. At day 0, 7 and 14 cells were removed and stained with MHC class I dextramers with the human CMV pp65 NLVPMVATV peptide (Immudex) and CD161-PE (Miltenyi Biotec) by flow cytometry.

5.4 Results

5.4.1. CD161 is expressed early during development

CD161 expression has previously been described on a subset of T cells in the thymus and foetal liver (Lanier et al., 1994; Martin et al., 2009). Here, CD161 expression was confirmed amongst CD8+ T cells in the thymus and UCB (Figure 5-1A), where Vα7.2+ MAIT cells make up a much smaller percentage of the CD161++ population, making it hard to distinguish CD161+ and CD161++ populations. Unlike the adult circulation (Chapter 4, Figure 4-2) where CD8+ T cells expressing CD161 display a memory phenotype in the majority, CD161+CD8+ T cells in UCB display a naïve (CCR7+CD45RA+) phenotype (Figure 5-1B). By 24 months a CD161+ population, more obviously distinguishable from the CD161++ population, becomes apparent (Figure 5-1A), which is maintained into adulthood, as described in Chapter 4. However, in contrast to UCB, the majority of the CD161+ subset displays a memory phenotype (Figure 5-1C), as in adults (Chapter 4, Figure 4-2). At 24 months, a greater proportion of CD161− T cells are naïve compared to in adults (mean 74.75% vs. 25.62% in adult), likely reflective of reduced antigen exposure at this stage of life. This is true of the CD161+ and CD161++ subsets also, which show a higher percentage of cells displaying a naïve phenotype at 24 months compared to adults (mean CD161+ 10.37% vs. 3.59%; CD161++ 4.64% vs. 0.46%). A further difference is apparent in the comparison of memory phenotypes between CD161+ and CD161− populations, where there was a significant ($p<0.001$) difference in the proportion of T_{EM} cells in CD161+ compared to CD161− CD8+ T cells. In adults, no significant difference was observed (Chapter 4, Figure 4-2). What induces this conversion to memory phenotype after birth, and whether naïve CD161+ CD8+ T cells display a similar or identical phenotype to their adult counterparts is not yet known.

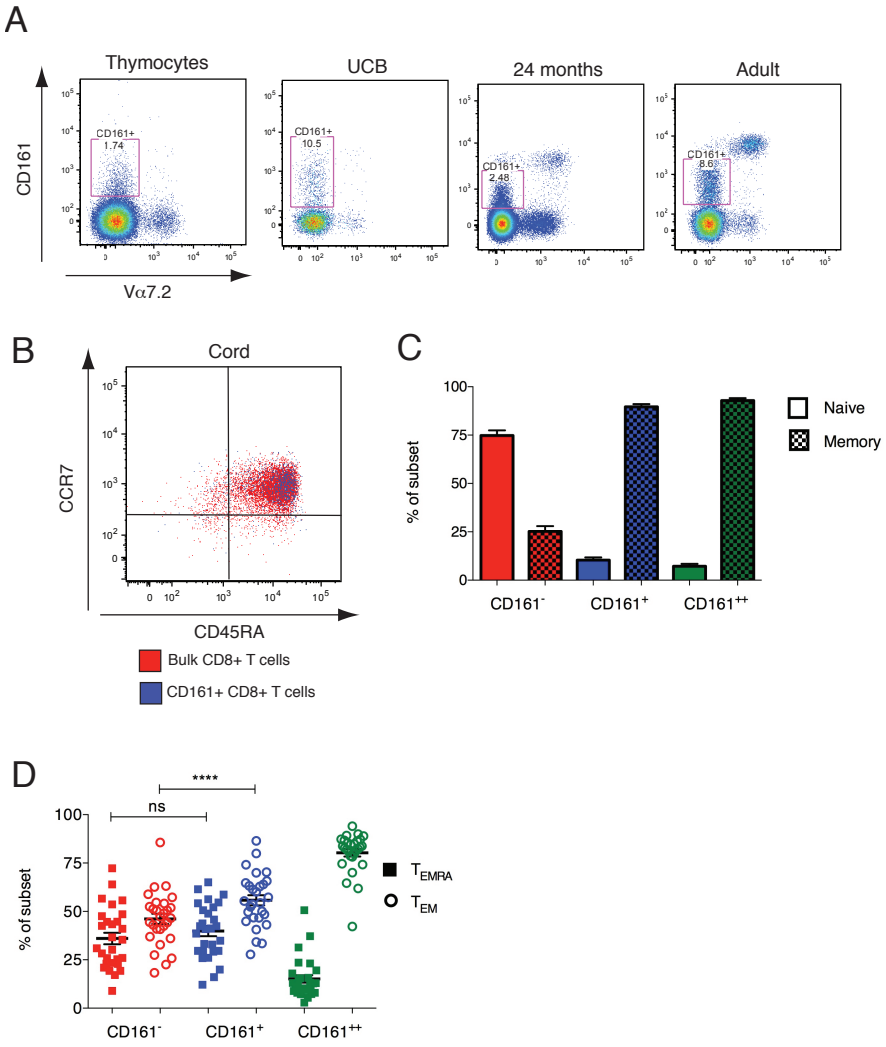

Figure 5-1: CD161 is expressed early during development. **A**) Representative flow cytometry plots showing CD161 expression by CD8+CD3+ lymphocytes in thymocytes, umbilical cord blood (UCB), 24 month old and adult blood. **B**) Representative flow cytometry plot showing naïve phenotype of CD161+CD8+ T cells (blue) overlaid on bulk CD8+ T lymphocytes (red). **C**) Cumulative data for percentage of each CD161 subset displaying a naïve or memory (including T_{CM}, T_{EM} and T_{EMRA}) phenotype in 24 month old donors (n=28). **D**) Percentage of memory cells from each subset displaying a T_{EM} or T_{EMRA} phenotype in 24 month old donors, (n=28). Few T_{CM} cells are found in the peripheral circulation, so were not included in this analysis. ****p<0.0001, ns = not significant by one-way ANOVA with Tukey's multiple comparisons test. Data are represented as mean ± SEM. 24 month old staining performed by Christian B. Willberg.

5.4.2. CD161+CD8+ T cells display a pre-programmed phenotype in cord blood

To determine to what extent naïve CD161+ CD8+ T cells display the phenotype of CD161+ CD8+ T cells in the adult circulation (Chapter 4), CD161 positive subsets in CD8+ T cells from UCB were phenotyped by flow cytometry (Figure 5-2). The three CD161 subsets amongst CD8+ T cells were distinguished by transferring gates from adult PBMC, where the three populations are more easily discernable (Figure 5-2A). Analysis by microarray identified significant upregulation of transcripts for the IL18R, MDR1 and PLZF within the adult CD161+, compared to the CD161−, CD8+ T cell population (Chapter 4, Figure 4-3). Similarly, the CD161+ population displayed significantly higher expression of IL18Rα (Figure 5-2B, $p<0.05$), MDR1 (Figure 5-2C, $p<0.01$) and PLZF (Figure 5-2D, $p<0.01$) than CD161− CD8+ T cells. However, donor numbers studied were small and, therefore, statistical analyses should be approached with caution. The CD161+ CD8+ population was also identified to express higher levels of the cytotoxicity effectors perforin and granzyme B (Chapter 4, Figure 4-6) in the adult circulation. Although not reaching significance, CD161+ CD8+ T cells within UCB also tended towards a higher proportion of perforin and granzyme B expression (Figure 5-2E&F). Furthermore, previous microarray analysis by others within the lab identified a significant correlation between the transcriptional profile of CD161+CD8+ T cells in UCB and adult blood (Appendix V.i). Together, this data demonstrates naïve CD161+ CD8+ T cells in cord blood to reflect many of the characteristics of the CD161+ CD8+ T cell population in the adult circulation, and suggests that they possess a pre-programmed phenotype that is determined early during development.

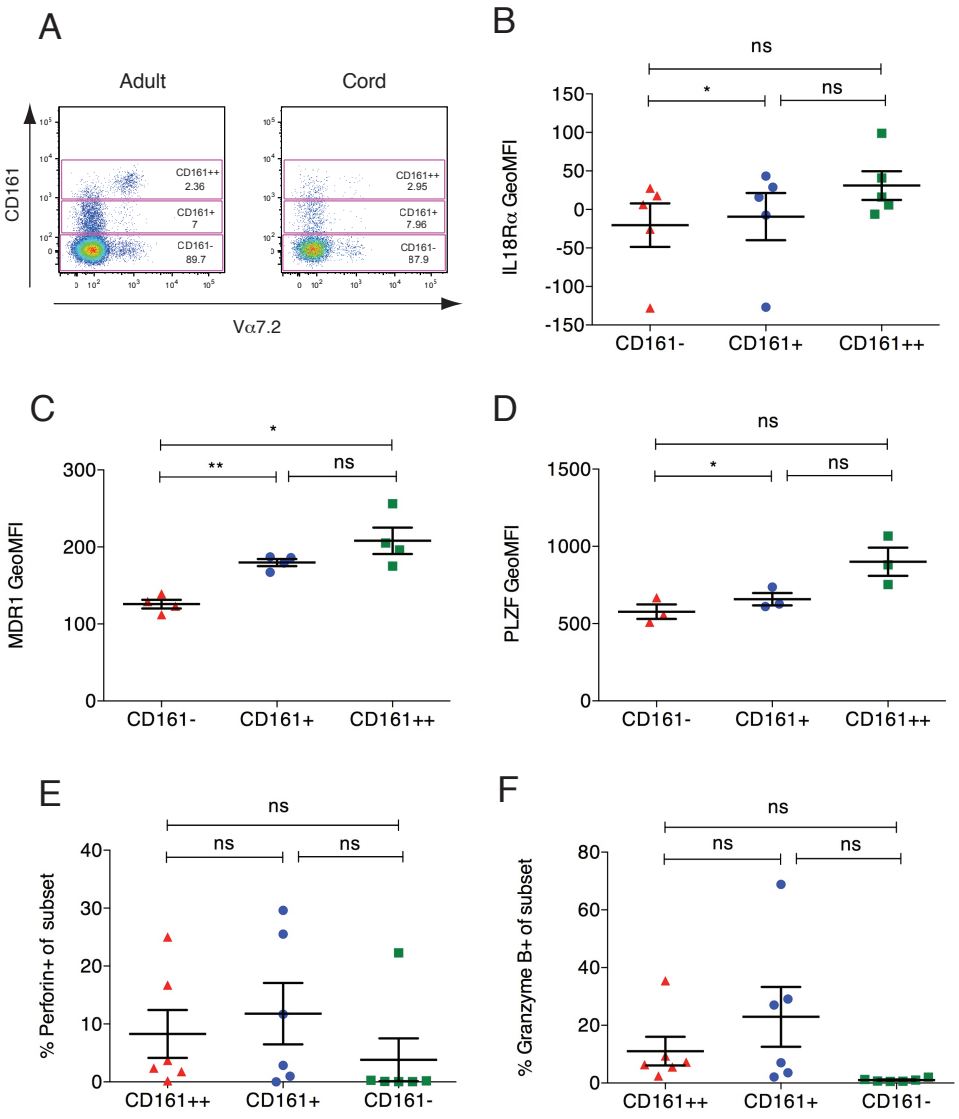

Figure 5-2 CD161+CD8+ T cells display a pre-programmed phenotype in cord blood.
A) Representative gating strategy for CD161 subsets from cord blood. Cumulative data for GeoMFI of IL18Rα (n=5) (**B**), MDR1 (n=4) (**C**) and PLZF (n=3) (**D**) and percentage of each subset positive for perforin (n=6) (**E**) and granzyme B (n=6) (**F**). **p<0.01, *p<0.05, ns = not significant by one-way ANOVA with Tukey's multiple comparisons test. Data are represented as mean ± SEM. Perforin and granzyme B stains performed and analysed by Ayako Kurioka. See also Appendix V.i.

5.4.3. Vβ typing of CD161+ in comparison to CD161− CD8+ T cells

The majority of naïve cells are CD161− (Chapter 4, Figure 4-2), which could suggest therefore that CD161+ cells differentiate from this naïve pool. However, the presence of naïve pre-programmed CD161+ CD8+ T cells in UCB, and a small number of naïve CD161+ CD8+ T cells in adult blood, conversely argues the possibility that CD161+ CD8+ T cells differentiate from a distinct precursor. To investigate this question, the TCR repertoire of both populations was examined by flow cytometry, using a panel of 24 Vβ antibodies covering approximately 70% of the repertoire. It should be noted that due to panel limitations, naïve cells were not excluded from this analysis. Unlike MAIT cells (Chapter 3, Figure 3-2), CD161+CD8+ T cell TCR usage is diverse and comparison of cumulative data of 10 donors shows the repertoire to be largely similar to that of CD161− CD8+ T cell subsets (Figure 5-3A). However, at the individual level considerable differences can be observed, as illustrated by the representative donor in Figure 5-3B.

A statistical approach that determines the correlation in Vβ frequencies between the two populations at the donor level was subsequently used to determine if the populations were clonally related (ie. differentiated from the same source). Correlation in Vβ frequencies between CD161+ and CD161− populations within a donor could suggest clonal relationship, but may also occur due to chance or to Vβ hierarchy effects (Melenhorst et al., 2008). Therefore, the within donor correlation (putative clonal relationship) was compared to that between donors (chance and hierarchy effects) (Figure 5-4). If the within donor correlation is higher than that between donors, then this supports the hypothesis that the two populations arose from the same precursor (see Figure 5-5).

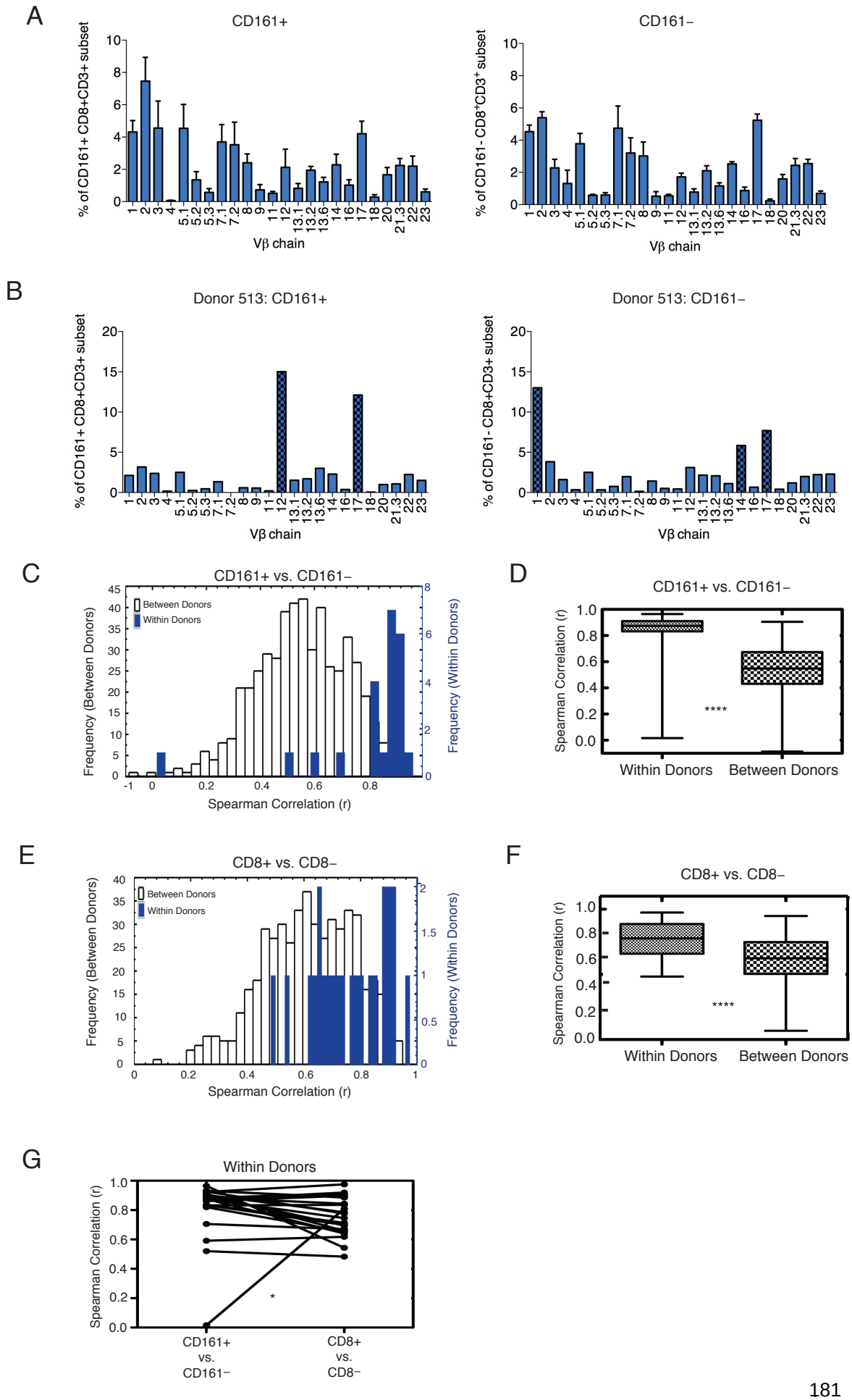
A
CD161+
% of CD161+ CD8+CD3+ subset
Vβ chain
CD161−
% of CD161- CD8+CD3+ subset
B
Donor 513: CD161+
Donor 513: CD161−
C
CD161+ vs. CD161−
Between Donors
Within Donors
Frequency (Between Donors)
Frequency (Within Donors)
Spearman Correlation (r)
D
CD161+ vs. CD161−
Spearman Correlation (r)
****
Within Donors
Between Donors
E
CD8+ vs. CD8−
F
CD8+ vs. CD8−
G
Within Donors
*
CD161+ vs. CD161−
CD8+ vs. CD8−

Figure 5-3 The Vβ usage of CD161+ CD8+ T cells is significantly correlated with that of CD161− CD8+ T cells. **A**) Cumulative data for percentage of each Vβ expressed by the CD161+ (left) or CD161− (right) CD8+ T cell subset as determined by a panel of TCR Vβ antibodies (n=10). **B**) Percentage of each Vβ expressed by the CD161+ (left) or CD161− (right) CD8+ T cell subset in a representative donor (513). All Vβ expressed by >5% of the population are shown in hatch. **C**) The Spearman rank correlation coefficient (r) between Vβ frequency in CD161+ and CD161− CD8+ T cells was calculated within (white bars) and between donors (blue). Bars show the frequency of each value for r for each pair of comparisons (within donors n=23 pairs; between donors n=506 pairs). **D**) Boxes show the median Spearman correlation coefficient (r) between CD161+ and CD161− subsets within and between donors, extending from the 25th to the 75th percentiles. The whiskers extend to the minimum and maximum values of r. **E**) The Spearman rank correlation coefficient (r) between Vβ frequency in CD8+ and CD8− T cells was calculated within (white bars) and between donors (blue). Bars show the frequency of each value for r for each pair of comparisons (within donors n=23 pairs; between donors n=506 pairs). **F**) Boxes show the median Spearman correlation coefficient (r) between CD8+ and CD8− subsets within and between donors, extending from the 25th to the 75th percentiles. The whiskers extend to the minimum and maximum values of r. **G**) Comparison of the Spearman correlation coefficient (r) within donors between CD161+/CD161− CD8+ T cells and CD8+/CD8− T cells (n=23). Each line represents an individual donor. ****p<0.0001 by Wilcoxon rank-sum test, *p<0.05 by Wilcoxon signed rank test where the null hypothesis was generated by random permutation. Statistical analysis performed by Jagadish Kumar, University of New South Wales. See also Appendix V.ii.

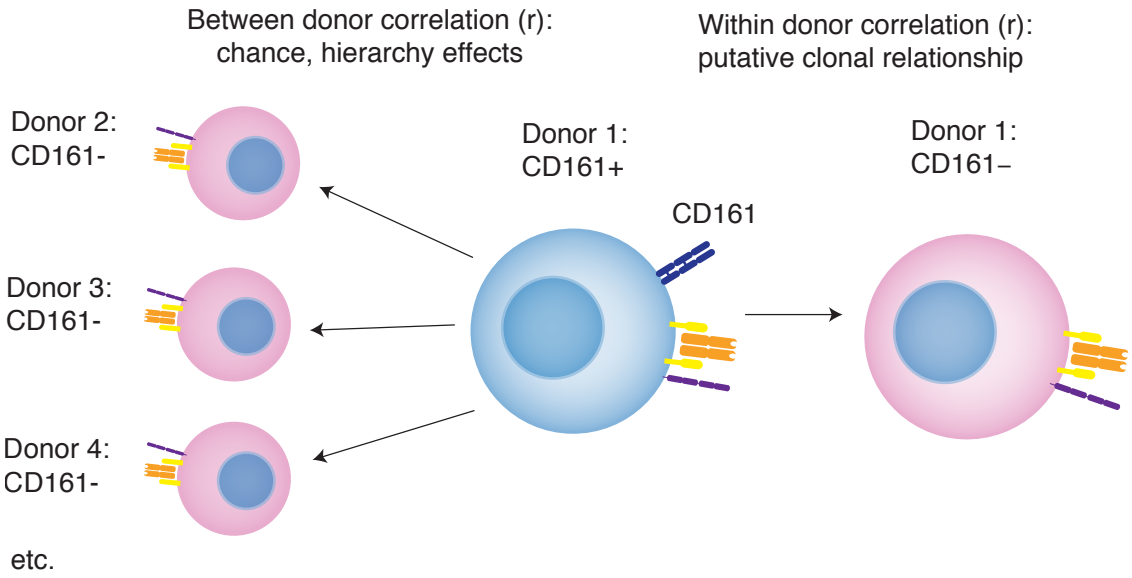

Figure 5-4: Correlation analyses of TCR Vβ expression of CD161+ and CD161– populations. Correlation in TCR Vβ expression within donors suggests a clonal relationship between the CD161+ and CD161– populations. This is compared to the correlation between donors, which can occur as a result of chance or Vβ hierarchy effects.

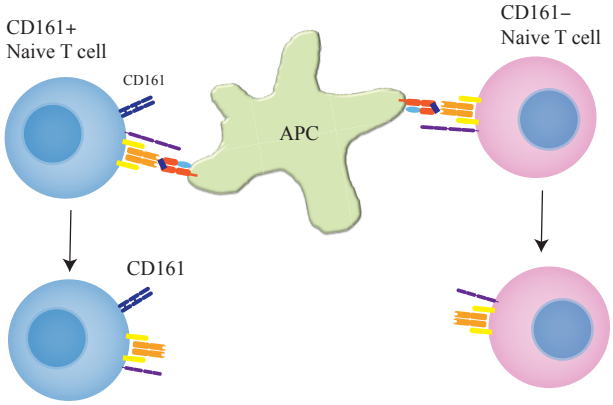

1) Two populations arose from distinct precursors

Result: The correlation between CD161− and CD161+ Vbeta frequencies (within donors) would be lower than expected by chance (ie. between donors)

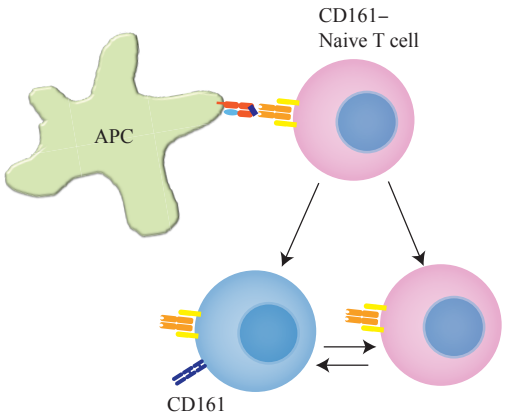

2) Two populations are derived from a common (CD161-) precursor. Cells randomly differentiated into the two compartments.

Result: The correlation between CD161− and CD161+ Vbeta frequencies (within donors) is higher than expected by chance (ie. between donors)

Comparison: CD8+ and CD4+ T cells known to differentiate from different precursors.

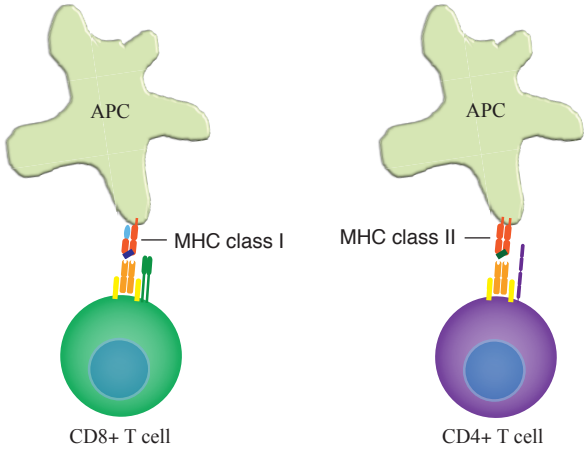

In **1)**: correlation between CD161+ and CD161- populations should be lower than that between CD8+ and CD4+ T cells (within an individual).

In **2)**: correlation between CD161+ and CD161- populations should be higher than that between CD8+ and CD4+ T cells (within an individual).

Figure 5-5: Possible results from Vβ correlation analyses.

A power calculation indicated that a sample size of 23 donors would give 80% power to find a statistically significant difference between the two populations (Appendix V.ii). Therefore, the Vβ frequencies in CD161+ and CD161− CD8+ T cell populations in 23 donors was calculated. As this did not follow a normal distribution in the majority of donors, the nonparametric (Spearman rank) correlation coefficient (r) between Vβ frequency in CD161+ and CD161− T cells, both within and between donors, was calculated (Figure 5-3C). The median value of r within hosts was then compared to that between hosts by the Wilcoxon rank-sum test, where the null hypothesis was generated by random permutation. The median correlation coefficient between individuals was 0.55, indicating that between any two individuals variation in the Vβ hierarchy of CD161+ T cells in one individual would explain ~30% of the variation in the Vβ hierarchy of CD161− in another (r^2) (Appendix V.ii). However, the median correlation within individuals (0.87) was significantly ($p<0.0001$) higher than between individuals (Figure 5-3D).

The same analysis was used to compare CD8+ and CD4+ T cells (Figure 5-3E) which have been selected differently (on MHC class I and II, respectively) and thus develop from distinct precursors (see Figure 5-5). In the absence of CD4 in the antibody panel, CD8− T cells were used as surrogate for CD4+ T cells. Again, and as expected, Vβ frequencies were significantly ($p<0.0001$) more correlated within donors (median r = 0.78) than between donors (median r = 0.62) (Figure 5-3F). Furthermore, comparison to the within donor correlation between CD161+ and CD161− indicates that CD161+ and CD161− are significantly ($p=0.02$) more correlated than CD8+ and CD8− (r = 0.87 vs. 0.78, respectively). This analysis suggests that CD161+ and CD161− CD8+ T cell subsets are more likely to have arisen from the same lineage than CD8+ and CD8− T cells. However, the correlation coefficients are largely similar between the two comparisons, and determination of clonal overlap of CDR3 sequences would be required to more definitively answer this question (see Appendix V.iii).

5.4.4. Can CD161− CD8+ T cells be induced to express CD161?

Given this indication, the possibility that CD161 expression could be induced on CD161− CD8+ T cells was investigated. Addition of various cytokines to culture media has previously been described to modulate CD161 expression on NK cells (Azzoni et al., 1998; Poggi et al., 1998) and CD4+ T cells (Cosmi et al., 2008). Naïve T cells, which are predominantly CD161− (Chapter 4, Figure 4-2), were isolated using a pan naïve T cell isolation kit to gain a population which was >90% CD161− (Figure 5-6A). Firstly, the influence of cytokines alone on CD161 expression was investigated by culturing naïve cells with a panel of cytokines, assessing CD161 expression at days 3 and 5 (Figure 5-6B). The percentage of cells expressing CD161 upon culture with cytokine was normalised to that of cells cultured in the absence of cytokine. PHA and PMA plus ionomycin were added to separate wells as controls for T cell activation. No cytokine alone was sufficient to induce expression of CD161 after 5 days of culture. Indeed, the percentage expressing CD161 decreased under the influence of certain cytokines, including IL-1β, IL-2 and IL-7. In confirmation of previous studies (Azzoni et al., 1998; Poggi et al., 1998), NK cells showed increased expression of CD161 after culture with IL-12 (Figure 5-6C), although this does not necessarily represent a CD161− to CD161+ conversion.

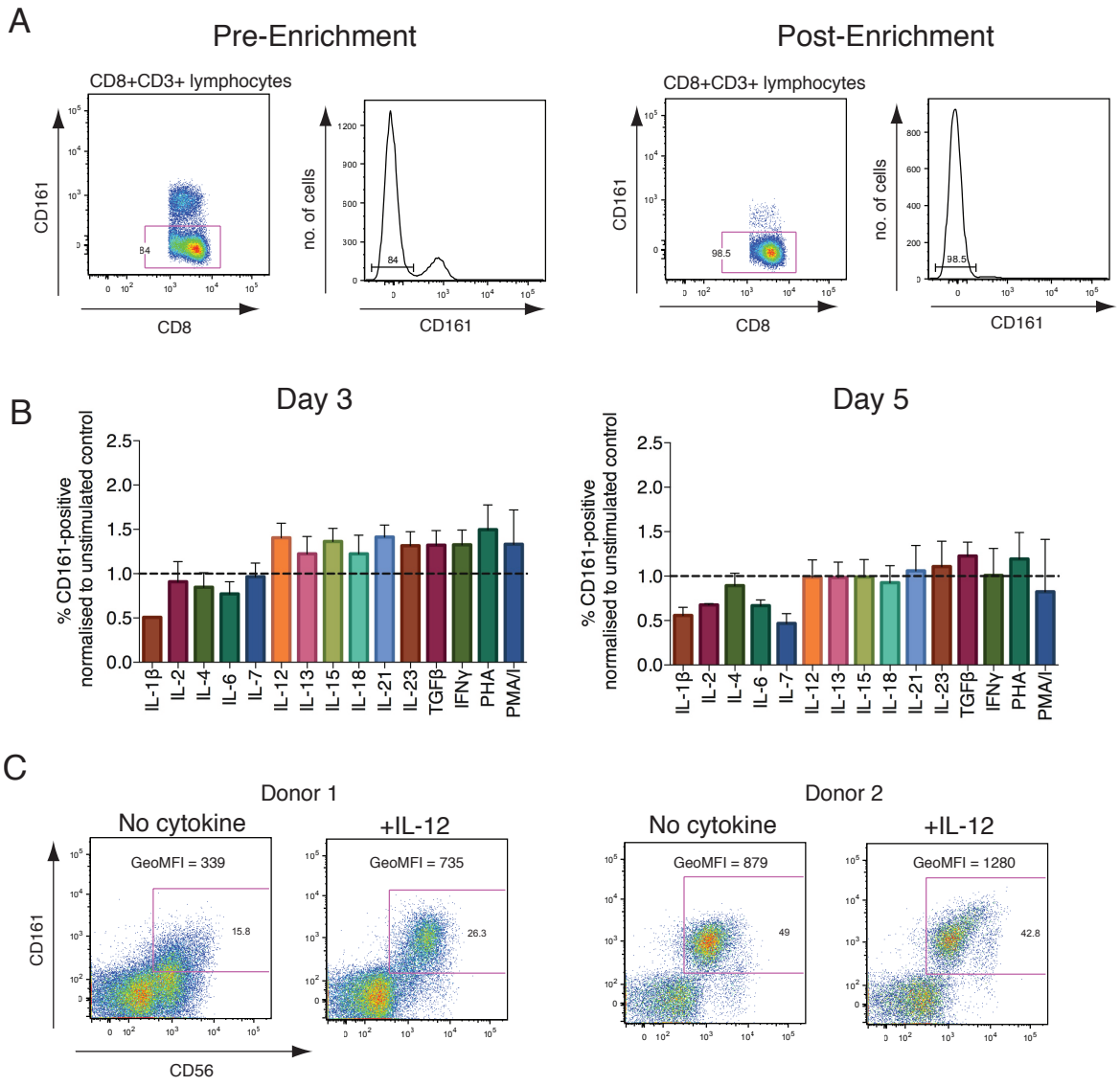

Figure 5-6 Naïve CD161– CD8+ T cells could not be induced to express CD161 by cytokines. **A**) Representative flow cytometry plot and histogram showing percentage of CD161– CD8+ T cells pre- (left) and post- (right) enrichment of pan naïve T cells as determined by flow cytometry. **B**) Percentage of naïve CD8+ T cells expressing CD161 in the presence of various cytokines after 3 (left) or 5 (right) days, normalised to percentage of cells expressing CD161 in the absence of cytokine (n=3). **C**) Representative flow cytometry plots from 2 donors showing CD161 expression at day 5 without cytokine (left) or in the presence of IL-12 (right). The geoMFI is given for CD161 expression.

Next, whether activation of naïve CD161− CD8+ T cells could induce expression of CD161, with or without cytokine, was investigated. Naïve T cells were activated with anti-CD3/2/28 activation beads and CD161 expression assessed at days 3 and 5, as previously (Figure 5-7A), alone or with a more limited panel of cytokines. Activation was observed to decrease expression of CD161, with no cytokine able to maintain or increase expression, although all changes were small as illustrated by the raw data flow cytometry plots (Figure 5.7A, upper panel).

Previously, activation in the presence of a combination of IL-1β and IL-23 for 7 days has been described to upregulate CD161 mRNA in naïve CD4+ T cells (Cosmi et al., 2008). Therefore, a matrix was designed to investigate the effect of combinations of various cytokines on CD161 expression, and the experiment extended to 7 days (Figure 5-7B-D). Additional combinations of cytokines described to have activating effects on CD161 expressing cells were also included, for example IL-12 plus IL-18 (Ussher et al., 2014). While at day 3 (Figure 5-7B) combinations that included TGFβ appeared to increase the percentage of naïve CD8+ T cells expressing CD161 compared to activation alone, these increases were small and were not maintained to day 5 (Figure 5-7C). Indeed, there was a tendency towards a decrease in expression with all cytokine combinations tested by day 7 (Figure 5-7D), even with IL-1β plus IL-23.

From these experiments it can be seen that naïve CD161− CD8+ T cells do not readily express CD161, even upon activation in the presence of various cytokines.

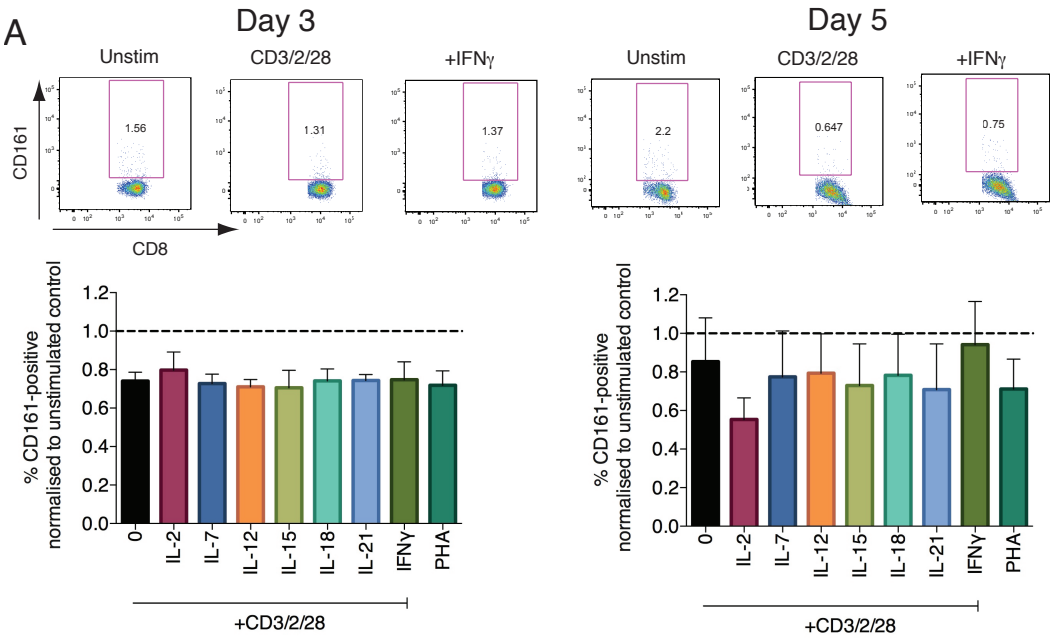
A
Day 3
Day 5
Unstim
CD3/2/28
+IFNγ
CD161
CD8
1.56
1.31
1.37
2.2
0.647
0.75
% CD161-positive normalised to unstimulated control
0
IL-2
IL-7
IL-12
IL-15
IL-18
IL-21
IFNγ
PHA
+CD3/2/28

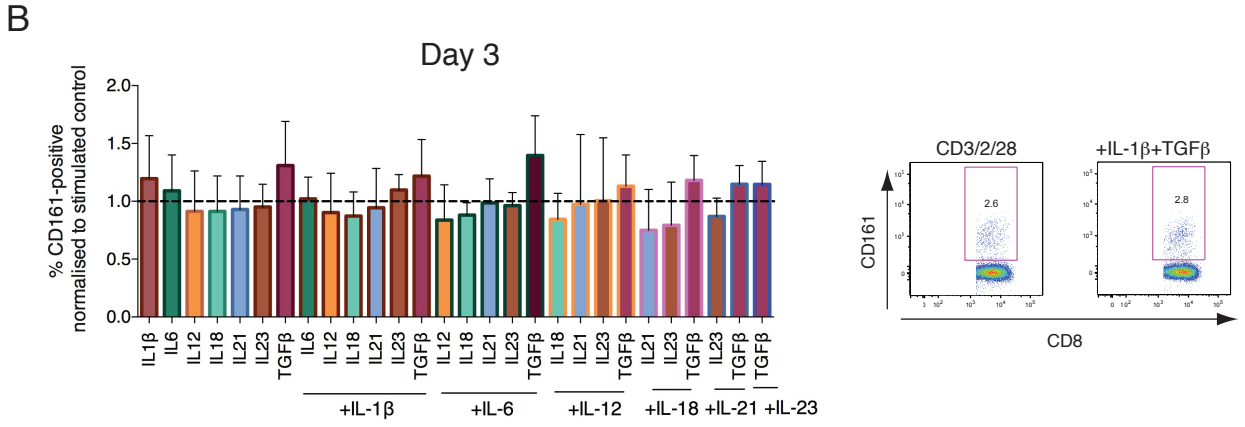
B
Day 3
% CD161-positive normalised to stimulated control
IL1β
IL6
IL12
IL18
IL21
IL23
TGFβ
+IL-1β
+IL-6
+IL-12
+IL-18
+IL-21
+IL-23
CD3/2/28
+IL-1β+TGFβ
2.6
2.8
CD161
CD8

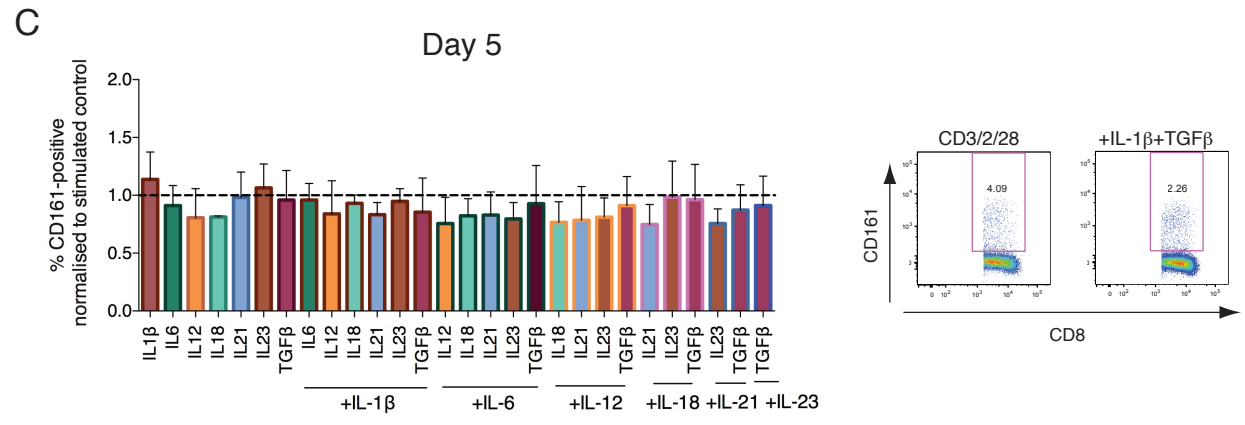
C
Day 5
% CD161-positive normalised to stimulated control
IL1β
IL6
IL12
IL18
IL21
IL23
TGFβ
+IL-1β
+IL-6
+IL-12
+IL-18
+IL-21
+IL-23
CD3/2/28
+IL-1β+TGFβ
4.09
2.26
CD161
CD8

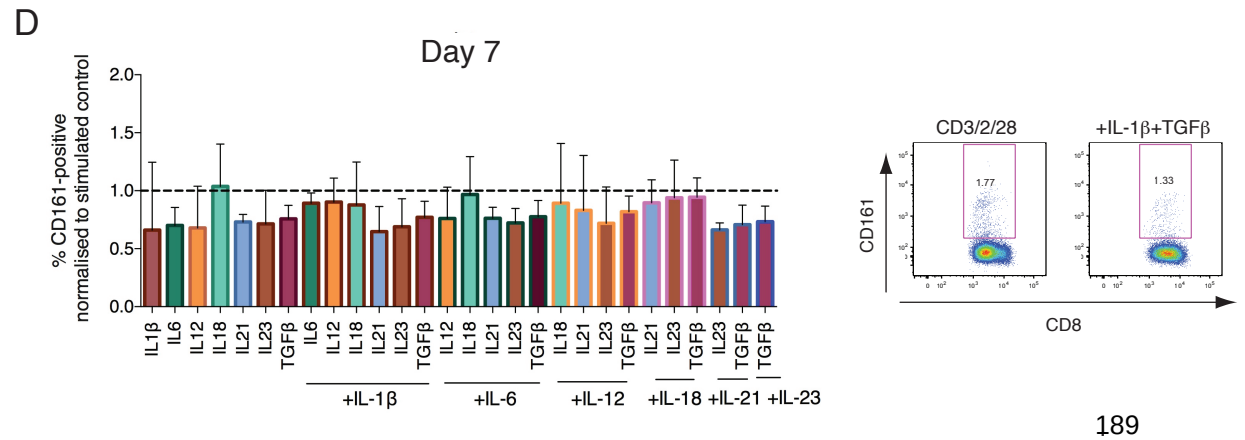
D
Day 7
% CD161-positive normalised to stimulated control
IL1β
IL6
IL12
IL18
IL21
IL23
TGFβ
+IL-1β
+IL-6
+IL-12
+IL-18
+IL-21
+IL-23
CD3/2/28
+IL-1β+TGFβ
1.77
1.33
CD161
CD8

Figure 5-7 Naïve CD161– CD8+ T cells could not be induced to express CD161 by activation in the presence of specific cytokines tested. A) Representative flow cytometry plots for CD161 expression in unstimulated (unstim), CD3/2/28 stimulated alone or plus IFNγ (upper panel) and cumulative data (lower panel) for percentage of naïve CD8+ T cells expressing CD161 at day 3 (left) or day 5 (right) after culture with phytohaemagglutinin (PHA), CD3/2/28 beads alone or in addition to various cytokines, normalised to percentage of cells expressing CD161 in the absence of stimulation (n=3). **B-D**) Percentage of naïve CD8+ T cells expressing CD161 at day 3 (**B**), 5 (**C**) or 7 (**D**) after culture with CD3/2/28 beads plus various cytokines alone or in combination, normalised to percentage of cells expressing CD161 upon activation alone (n=3). Representative flow cytometry plots for percentage of CD3+CD8+ lymphocytes expressing CD161 are shown for CD3/2/28 activated cells alone or plus IL-1β+TGFβ for each timepoint (right panels).

Consequently, modulation of CD161 expression on memory cells was investigated. Three donors were identified with a CMV-specific dextramer-positive CD8+ T cell population composed of both CD161+ and CD161– cells (Figure 5-8A). PBMC from these donors were restimulated with peptide, either at 0.1μg/ml (Figure 5-8B&C) or 1μg/ml (Figure 5-8D&E) as per materials and methods (5.3.4), which induced an expansion of the dextramer-positive CD8+ population to varying degrees between the three donors (Figure 5-8B&D). The percentage of that population expressing CD161 was assessed at baseline (day 0) and at day 7 and 14 following re-stimulation (Figure 5-8C&E). In two donors there was overall no change in the proportion of cells expressing CD161, although percentages did fluctuate at day 7. In contrast donor 1, where expansion of dextramer-positive CD8+ T cells was greatest, a dramatic decrease in the percentage of dextramer-positive cells expressing CD161 was observed. No difference was observed between the two concentrations of peptide, suggesting that antigen load does not influence the resulting phenotype. However, study of a larger number of donors, across a greater range of concentrations, is required to enable any conclusions to be drawn. The sorting of CD161+ and CD161– populations by FACS would also increase confidence in any changes in CD161 expression observed. Nonetheless, these results again suggest that expression of CD161 is not easily induced, with the overall tendency being towards a reduction in CD161 expression as opposed to the contrary.

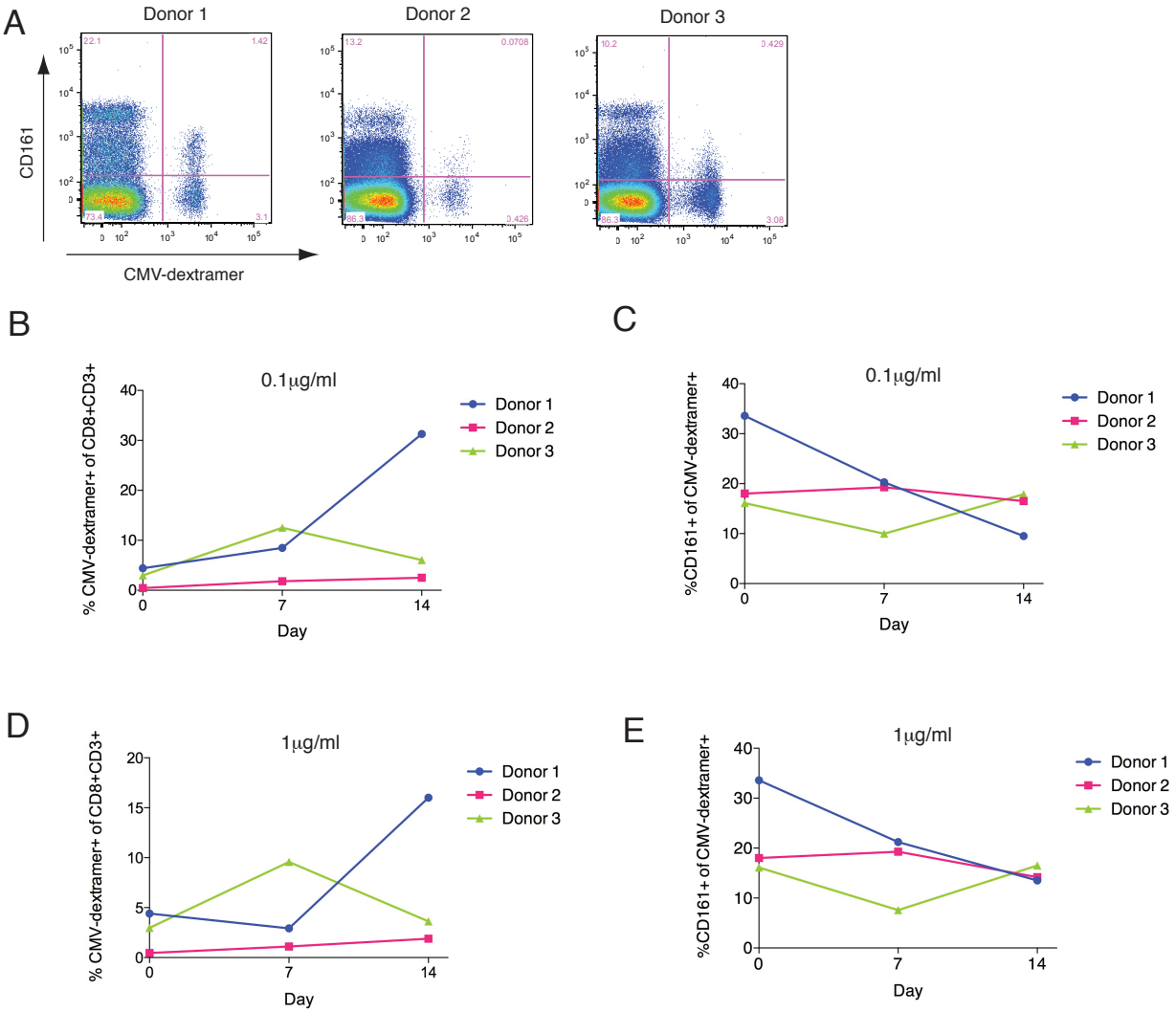

Figure 5-8: Modulation of CD161 expression through activation. A) Flow cytometry plots displaying CD161 expression on 3 donors with a CMV-epitope specific response. Culture of PBMCs from these donors with CMV peptide at either 0.1µg/ml (**B** & **C**) or 1µg/ml (**D** & **E**) and percentage CMV-dextramer+ of CD8+CD3+ lymphocytes (**B** & **D**) and percentage of these CD161 positive (**C** & **E**) assessed at days 7 and 14. Each line represents an individual donor.

5.5 Discussion

Here, CD161 expression in CD8+ T cells within the thymus and UCB is confirmed, where the majority of these cells were Vα7.2−. These, therefore, do not represent precursors of MAIT cells, and instead indicate the presence of a CD161+CD8+ population from the earliest point of T cell development. As with MAIT cells, CD161+CD8+ T cells are naïve within cord blood and acquire a memory phenotype in the majority soon after birth, evidenced by the high percentage of memory cells within this subset at 24 months. What induces this conversion to memory phenotype is not yet known. CD161+CD8+ T cells in UCB, although naïve, already display elevated levels of IL18Rα, MDR1, PLZF, perforin and granzyme B, reflective of their phenotype in the adult circulation. However, the low numbers of donors tested means that statistical analyses should be interpreted with caution. Pre-programming of CD161 positive cells within cord blood has previously been described for both CD161++CD8+ (Walker et al., 2012) and CD161+CD4+ (Cosmi et al., 2008) T cells, which already express markers such as RORγt, IL23R and CCR6. Indeed, CD161+CD4+ thymocytes also constitutively express RORγt and IL23R, and Th17 cells are shown to develop from these CD161+ precursors (Cosmi et al., 2008). As CD161+CD8+ T cells in UCB display characteristics of their adult counterparts, this would seem to suggest that, in a similar manner, CD161+CD8+ thymocytes and UCB T cells represent a pre-committed population which expands, and acquires a memory phenotype, after birth.

Comparison of the TCR repertoires of CD161+ and CD161− CD8+ T cell populations in adult demonstrated these subsets to be highly related, and is suggestive of a common precursor. There are several caveats to this analysis, however. Importantly, it cannot give an outright answer, but only an indication of correlation in repertoires in comparison to another, in this case the between individual or CD8+/CD4+ correlation. This indicated CD161+ and CD161− CD8+ T cell subsets within donors to be more correlated both than that observed between donors, and between CD8+ and CD4+ T cells (which are known to develop from different precursors). This was observed despite the ‘background’

correlation displayed between CD8+ and CD4+ T cells (Melenhorst et al., 2008). A further limitation is that Vβ analysis was performed on bulk populations, including naïve cells. A more focused approach would have been to look at an epitope-specific population, which have developed from specific TCR-bearing precursors and where fewer Vβ families would have been used and, therefore, overlap in usage would be easier to observe. To investigate clonal relationships more comprehensively, the next step would be to sequence (a subset of) each population to determine the overlap in clones shared between the two populations, and therefore the similarity in TCR repertoires (Venturi et al., 2008) (please see Appendix V.iii for optimisation of this strategy). While again this would involve many difficulties in interpretation, including a lack of overlap due to poor recovery of clonotypes, or conversely a high degree of overlap due to 'public' TCRs, this would provide a better indication of the clonal relationship, and hence the developmental relationship, between the two populations.

As a consequence of the indication that CD161+ and CD161− CD8+ T cells developed from a common precursor, the potential for naïve CD161− CD8+ T cells to become CD161+ (Figure 5-5, panel 2) was investigated in a series of preliminary experiments culturing CD161− CD8+ T cells under different conditions. As reported previously, activation alone was not sufficient to induce CD161 expression (Northfield et al., 2008). Further, the addition of various cytokines, either alone or with activation through the TCR, did not cause CD161 upregulation. This is in contrast to NK cells where, as seen here, IL-12 has been reported to induce upregulation in CD161 expression (Azzoni et al., 1998; Poggi et al., 1998). However, this could represent an increase in surface expression of previously CD161+ NK cells. As CD161− CD8+ T cells were isolated for the experiments described here, this was not investigated and would not have been observed. On the other hand, an increase in CD161 expression could also represent a higher proliferation rate amongst the CD161+ population. Although isolation of naïve T cells results in a predominantly CD161− population, a small number of CD161+ T cells were also present. Proliferation of this population may have resulted in a false positive result, and would necessitate cell sorting of pure populations. However, no increase was observed under any of the conditions studied, although this does not preclude the possibility that the correct combination of cytokines was not included.

To investigate potential conversion between CD161+ and CD161− CD8+ memory populations (Figure 5-5 panel 2), CD161 expression was monitored upon restimulation of CMV pp65-specific CD8+ T cells with peptide. In two of the three donors tested, the overall percentage of epitope-specific CD8+ T cells expressing CD161 was unchanged after 14 days, while in one donor expression was decreased. A decrease in CD161 expression has previously been shown upon ligation (Fergusson et al., 2014) and upon TCR stimulation (Turtle et al., 2009). This suggests, therefore, that while it appears difficult to induce CD161 expression, expression may be lost with various stimuli. It would be interesting, therefore, to repeat this experiment with sorted CD161+ and CD161− populations to investigate the modulation of CD161 expression on both populations upon activation or re-stimulation, with or without addition of specific cytokines.

The question of what induces and/or modulates CD161 expression becomes particularly important when considering the enrichment of CD161+ cells amongst HCV-specific CD8+ T cells (Northfield et al., 2008). It may be possible that HCV triggers conversion to a CD161+ phenotype, for example by the cytokines induced upon infection (Nishitsuji et al., 2013; Spanakis et al., 2002). It would be interesting to investigate the effect of these cytokines specifically on CD161 expression. Alternatively, CD161+CD8+ T cells may be ideally located for activation by HCV antigen-bearing APCs and, therefore, by chance CD161+CD8+ T cells are triggered more often than CD161−. Indeed, CD161+CD8+ T cells are present within the liver, (Chapter 4, Figure 4-8). Moreover, given the association of CD161 and CXCR6 (Billerbeck et al., 2010; Northfield et al., 2008), and of CXCR6 and homing to the liver (Sato et al., 2005), this appears a plausible explanation.

5.6 Summary

- A CD161+ (Vα7.2–) CD8+ T cell population is present in both the thymus and UCB, indicating that this population develops early
- Like MAIT cells, CD161+CD8+ T cells acquire a memory phenotype soon after birth (apparent at 24 months)
- UCB naïve CD161+CD8+ T cells already bear many of the characteristics of adult memory CD161+CD8+ T cells
- The TCR repertoire of the CD161+CD8+ T cell population is diverse, and similar to that of the CD161– population
- CD161 expression is not induced upon activation of naïve CD161– CD8+ T cells

A

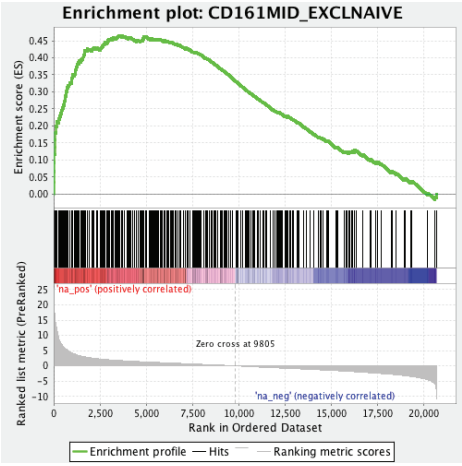

Dataset	Cord CD161+ vs CD161−
GeneSet	Adult CD161+_UP
Upregulated in	Cord CD161+
Enrichment Score (ES)	0.46
Normalised ES (NES)	2.14
Nominal p-value	<0.00001

B

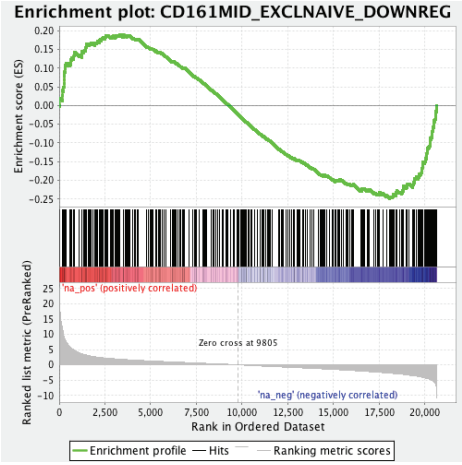

Dataset	Cord CD161+ vs CD161−
GeneSet	Adult CD161+_DOWN
Upregulated in	Cord CD161−
Enrichment Score (ES)	−0.25
Normalised ES (NES)	−1.3
Nominal p-value	0.005

Appendix V.i: The transcriptional phenotype of cord blood CD161+ CD8+ T cells correlates with that in adult. Gene set enrichment analysis (GSEA) summary plots comparing gene expression between CD161+ and CD161− CD8+ T in cord blood. Genes significantly upregulated in adult CD161+ CD8+ T cells were significantly ($p<0.00001$) enriched in cord CD161+ CD8+ T cells (**A**). Genes significantly downregulated in adult CD161+ CD8+ T cells were significantly ($p<0.005$) enriched in CD161− CD8+ T cells in cord blood (**B**). Cord arrays were performed by Lucy J. Walker.

A

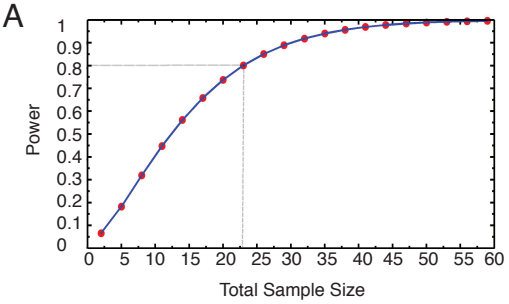

B CD161+ vs. CD161–

Groups	No. of pairs	Median r	p (rank sum)
Within donors	23	0.8740	<0.0001
Between donors	506	0.5487	

	Within donors	Between donors
Minimum	0.01558	-0.08701
Median	0.87402	0.54870
Maximum	0.96493	0.90519
Mean	0.81154	0.54791
Std. Deviation	0.20354	0.16714
Std. Error	0.04244	0.00743
Lower 95% CI	0.72353	0.53331
Upper 95% CI	0.89956	0.56251
p value		<0.0001

C CD8+ vs. CD8–

Groups	No. of pairs	Median r	p (rank sum)
Within donors	23	0.7766	<0.0001
Between donors	506	0.6238	

	Within donors	Between donors
Minimum	0.48311	0.06753
Median	0.77623	0.62337
Maximum	0.97532	0.94805
Mean	0.76318	0.61921
Std. Deviation	0.13162	0.16322
Std. Error	0.02744	0.00725
Lower 95% CI	0.70626	0.60495
Upper 95% CI	0.82010	0.63346
p value		<0.0001

D CD161+ / CD161– vs. CD8+/CD8–

	Within donors CD161+/CD161–	Within donors CD8+/CD8–
Minimum	0.01558	0.48311
Median	0.87402	0.77623
Maximum	0.96493	0.97532
Mean	0.81154	0.76318
Std. Deviation	0.20354	0.13162
Std. Error	0.04244	0.02744
Lower 95% CI	0.72353	0.70626
Upper 95% CI	0.89956	0.82010
p value		<0.0001

Appendix V.ii: Vβ correlation data. A) Line graph shows the statistical power for various values of n. At n=23 there is 80% power to find a statistical significant difference between two groups. Data tables for values corresponding to Spearman correlation coefficient values for CD161+ vs. CD161– (**B**) and CD8+ vs. CD8– (**C**) comparisons where the p value was calculated by Wilcoxon rank-sum test, and for within donor comparisons between CD161+/CD161– and CD8+/CD8– (**D**) where the p value was calculated by Wilcoxon signed rank test.

Appendix V.iii: NextGen TCR Sequencing Optimisation



Due to the variable nature of the 5'end of the TCR transcript, primers cannot be designed which prime synthesis from all V regions



During SMARTer cDNA synthesis (Clontech), a universal primer site is added to the 5' end which allows priming of all V regions for PCR. This can be barcoded to allow sample multi-plexing.

Reaction Mix

	(μl)
Phusion HF Buffer*	5
10mM dNTPs	0.5
Phusion pol.*	0.1
C primer (10uM)	1
UPM	5
cDNA	x
dH_20	up to 25μl

* New England BioLabs
Phusion HF Reaction Buffer #B0518
Phusion Hot Start Flex DNA polymerase #M0535

PCR Programme

98°C	60s	
98°C	10s	x5 cycles
72°C	30s	
98°C	10s	x5 cycles
70°C	15s	
72°C	30s	
98°C	10s	x30 cycles
68°C	15s	
72°C	30s	
72°C	5min	

Firstly, constant primers were designed for both alpha and beta chains using primer3 (simgene.com) such that 250bp sequencing reads from the PCR product would extend into the CDR3 region of the TCR. Four constant beta primers and four constant alpha primers <60bp from the 3' end of J were designed and tested in PCR reactions.

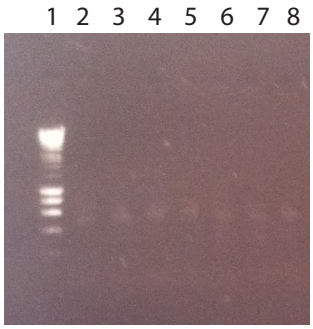

1: Hyperladder I
2: TRAC_2
3: TRAC_22
4: TRAC_58
5: TRAC_59
6: TRBC_29
7: TRBC_28
8: TRBC_50

All constant primers produced a product when run on a 1% agarose gel (110V) (left). Therefore, TRAC_22 and TRBC_29 were chosen to proceed (below). These were then tested in PCRs reactions with each of the barcoded universal primers (kindly provided by A.Smith), to identify primer mixes which were compatible. The suffix _# indicates distance from the 3' end of J.

>TRAC_22	5'-gtctctcagctggtacacgg-3'
>TRBC_29	5'-gatggctcaaacacagcgac-3'

To ensure transcripts amplified were TCR, products were cloned into pCR-Blunt vector, and transformed intoTOP10 *E.coli*. Two clones were sequenced using the TRBC primer. Resulting sequences were run through IMGT V-Quest for TCR identification.

>TCR sequence 152.1

GGGGACTNNTNGGTCTCTAGGAGGAGAGTCGAGTCCCATCACCAAAATGC
TGGGGCTGATTGCTANTCTGTCCCTCTCTAGCACTGCAGATGTAGAAGCT
GCTGTCTTCAGGATGGGCACTGGTCACTGTCAGAGTGGACAAGGTCAGGC
TTGCATGGTTGATGAGAAACTTGTCCTTCTCGACGCCTTGCTCGTATGTG
GCCTTGGAGCCCTCATTGGAAGTTGCCATCAGCATGAGACTCTGTTTCGG
GAACTGACGATACCAAAACATAGTTGTGGCCTGAAAGTCCAGGGAACGGC
ACTCGATCTTCACAGAGGTTCCACTCTTACAGATAACCCTGCTCGGATGT
TGAGAGACGACAGCACCAAGCCCGGAGCCTGGCCCCAGAAGCAGCAGAAG
CAGCAGCATCTTCCGTGATGGCCTCACACCACCTTCTCCCCCATGTACTC
TGCGTTGATACCACTGCTTGCCCTATAGTGAGTCGTATTAGCCTGAATTC
TGCAGATATCCATCACACTGGCGGCCGCTCGAGCATGCATCTAGAGGGCC
CAATTCGCCCTATAGTGAGTCGTATTACAATTCACTGGCCGTCGTTTTAC
AACGTCGTGACTGGGAAAACCCTGGCGTTACCCAACTTAATCGCCTTGCA
GCACATCCCCCTTTCGCCAGCTGGCGTAATAGCGAAGAGGCCCGCACCGA
TCGCCCTTCCCAACAGTTGCGCAGCCTATACGTACGGCAGTTTAAGGTTT
ACACCTATAAAAGAAAGAGCCGTTATCGTCTGTTGTGGATGTACAGAGTG
ATATTATTGACCCCCNGGGCGACGAATGGNGATCCCCTGGCCAGTGCACG
TCTGCTGTCAAANAAGTCTCCNGGAACTTTACCCGGGGNGCATATCGGGA
AGAANCTGNCCAA

TRBV20-1*02	Identity = 100%
TRBJ1-5*01	Identity = 100%
TRBD1*01	In reading frame 2
CDR3	CSAREGQXSNQPQHF

>TCR sequence 152.2

GGGAACNTNNTNGGTCNNCTAGGAGGAGAGTCGAGTCCCATCACCAAAAT
GCTGGGGCTGATCTCTCNAGTAACTGCTGGCACAGAAGTACACAGATGTC
TGGGAGGGAGCAGCCAACTCCAGCCTGAGCGGGAAATCCTCTGTGGTTGA
TCTGGAGACGTTGTAGCCATTCGGGACTTCTCCTTTATCAGTGATACCAG
CACCAACTGAATAATAAATCAGCTTCAGCCCCATGCCTGGGTCTTGTCGA
TACCAGTACATGTAGTTATGGTTCATATCCTGGGTACACTGCAGTGTCAT
GCTCTGTCCTATCTTCAGGATGCGGAATTTTGGGGTCTGAGTGACACCAG
CATTCACTGGACCTGCCCACAGGAGAGGAAAGGCTGCACAGCACAGGAGG
CTGATGCTCATGGCAGGTGCTCCAGGACGGAGGGGTCTTCTGTATCTGTG
CATTGATGAAAGGGGAACAGGCCCCATGTACTCTGCGTTGATACCACTGC
TTGCCCTATAGTGAGTCGTATTAGCCTGAATTCTGCAGATATCCATCACA
CTGGCGGCCGCTCGAGCATGCATCTAGAGGGCCCAATTCGCCCTATAGTG
AGTCGTATTACAATTCACTGGCCGTCGTTTTACAACGTCGTGACTGGGAA
AACCCTGGCGTTACCCAACTTAATCGCCTTGCAGCACATCCCCCTTTCGC
CAGCTGGCGTAATAGCGAAGANGCCCGCACCGATCGCCCTTCCCAACAGT
TGCGCAGCCTATACGTACGGCAGTTTAAGGNTTACACCTATAAAAANAAA
NCNTTATCNTCTGNTTNGTGGATGTACAGAGTGATATNATTGACNCCCCG
GGCGACGNAGGNGATCCCCTGNCAGTNACGTCTGCTGTCAAAAANTCTCC
CGGANCTT

As a practice run to ensure populations with overlapping repertoires could be identified using this approach, naive and memory T cells were isolated from 3 donors by taking the positive and negative fractions after pan naive T cell isolation (Miltenyi Biotec). RNA was extracted using Qiagen RNeasy Mini Kit, 5'-RACE ready cDNA generated and both alpha and beta TCRs amplified (as above) using individual barcodes. Three libraries made up of equal concentrations (23ng) of cDNA from each donor and subset were run on the MiSeq (Illumina; Wellcome Trust Centre for Human Genetics). Samples were run in duplicate libraries, to ensure that in the first instance common clonotypes could be identified between libraries. TCR identificiation was performed by Stephen Preston (A. Smith lab). Analysis is ongoing.

Library 1

Subset/Donor	Chain	Barcode
Naive 169	Alpha	030
Memory 169	Alpha	047
Naive 177	Alpha	045
Memory 177	Alpha	056
Naive 169	Beta	006
Memory 169	Beta	015
Naive 177	Beta	013
Memory 177	Beta	029

Library 2

Subset/Donor	Chain	Barcode
Naive 169	Alpha	030
Memory 169	Alpha	047
Naive 176	Alpha	031
Memory 176	Alpha	052
Naive 169	Beta	006
Memory 169	Beta	015
Naive 176	Beta	007
Memory 176	Beta	016

Library 3

Subset/Donor	Chain	Barcode
Naive 176	Alpha	031
Memory 176	Alpha	052
Naive 177	Alpha	045
Memory 177	Alpha	056
Naive 176	Beta	007
Memory 176	Beta	016
Naive 177	Beta	013
Memory 177	Beta	029

6. MDR1 function in CD161 expressing CD8+ T cells

6.1 Introduction

6.1.1 MAIT cells and chemotherapy

The identity of the enigmatic 'memory stem' cell, able to replenish anti-viral memory T cell pools after chemotherapeutic treatment of haematological malignancies, was recently proposed in a study by Turtle and colleagues (Neuenhahn and Busch, 2009; Turtle et al., 2009). This study described a distinct population of memory CD8+ T cells which preferentially survived chemotherapy, both *in vitro* upon culture with the anthracycline daunorubicin and *in vivo* in acute myeloid leukaemia (AML) patients. Defined by high levels of both CD161 and IL18Rα, these 'memory stem' cells bear striking similarities to MAIT cells (Dusseaux et al., 2011) and likely describe the same population.

Elevated expression of the ATP-binding cassette (ABC)-superfamily multidrug efflux proteins, such as multidrug resistance (MDR) 1 (or P-glycoprotein), can enable malignant cells to acquire resistance to chemotherapeutic agents, such as the MDR1 substrate daunorubicin (Gottesman et al., 2002). Likewise, the CD161++ IL18Rα++ memory population described by Turtle *et al.* expressed high levels of MDR1 which was able to efflux the fluorescent substrate Rhodamine 123 (Rh123), explaining their ability to survive both *in vitro* and *in vivo* exposure to daunorubicin (Turtle et al., 2009). As expression of MDR1 is also a characteristic of stem cells, being described on hematopoietic stem cells within the bone marrow (Chaudhary and Roninson, 1991), this led to their designation as 'memory stem' cells.

MDR1, encoded by *ABCB1*, is the prototypical drug efflux pump mediating multidrug resistance in various cancer cells. It is composed of two homologous halves, each consisting of six transmembrane segments and a nucleotide-binding domain that binds

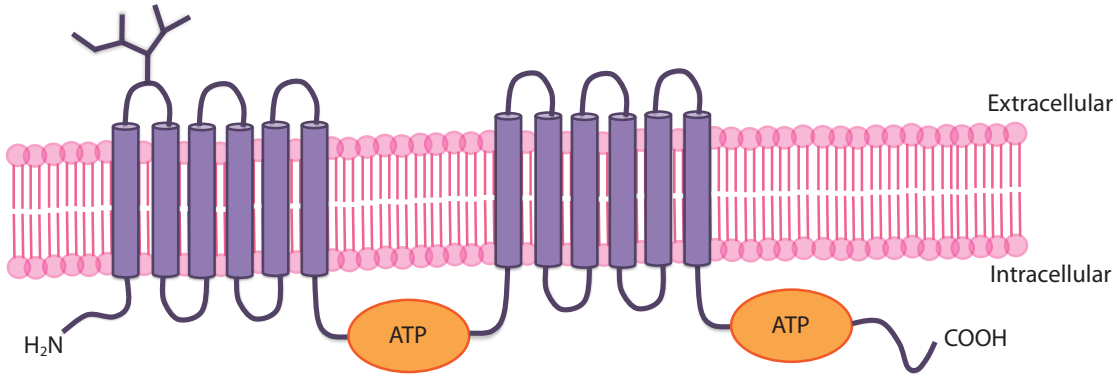

Figure 6-1: Predicted structure of MDR1. MDR1 is composed of two subunits each composed of six transmembrane α helices and a nucleotide (ATP) binding domain. MDR1 is glycosylated at the first extracellular loop. Figure based on *Hoffman & Kroemer, 2004*.

and hydrolyses adenosine triphosphate (ATP) (Figure 6-1). The transmembrane segments are proposed to bind drug substrates from within the lipid bilayer, triggering hydrolysis of ATP by the nucleotide-binding domain and inducing transport of the drug to either the outer leaflet of the membrane or to the extracellular space (Gottesman et al., 2002). MDR1 is a promiscuous transporter with broad specificity for a variety of different substrates, including those that also inhibit transport, such as cyclosporine A (CsA) and verapamil. While much research has been invested in determining the role of MDR1 in the resistance of malignant cells to treatment, less is known about its physiological role. Expression is found in various tissues including the gastrointestinal tract, liver and testes (Borst et al., 1994), with this distribution pattern suggesting a role in protection from xenobiotics or endogeneous metabolites (Gottesman et al., 2002). Expression has also been described on leukocytes (Neyfakh et al., 1989), with a role in secretion of cytokines and cytotoxic mediators within these cells being proposed (Giraud et al., 2010).

Amongst CD8+ T leukocytes, Dusseaux and colleagues (2011) identified MDR1 expression, and the ability to efflux Rh123, to be relatively restricted to CD161++IL18Rα++ MAIT cells. Furthermore, in breast cancer patients MAIT cell numbers were maintained both during and after anthracycline-containing chemotherapy, while numbers of conventional memory cells decreased significantly (Dusseaux et al., 2011). It was therefore suggested that MAIT cells and CD161++ IL18Rα++ 'memory stem' cells represented the same population. However, there is some discrepancy between the findings of the two groups. Turtle et al. (2009) suggested that chemotherapy-resistant CD161++IL18Rα++ 'memory stem' cells provide anti-viral protection during, and replenish anti-viral memory pools after, chemotherapy-induced lymphocytopenia, explaining the low incidence of CMV and EBV-related morbidity in these patients. This was supported by their detection of MHC class I tetramer-binding populations after culture of sort purified Rh123-effluxing populations with peptide-pulsed DCs. However, MAIT cells are not anti-viral (Le Bourhis et al., 2010) and are not stained by fluorescent MHC class I tetramers to CMV, EBV or FLU (Dusseaux et al. 2011; Chapter 4 Figure 4-1). On the other hand, a small proportion of CD161+Vα7.2– cells with the ability to efflux Rh123 were also described (Dusseaux et al., 2011), and as previously demonstrated these memory cells

include anti-viral populations identifiable with MHC class I tetramers (Chapter 4, Figure 4-1), and may represent the true anti-viral 'memory stem' cell population.

6.1.2 MAIT cells and transplantation

In addition to anthracyclines such as daunorubicin, MDR1 substrates include a variety of immunosuppressive drugs, including those used in immunosuppression regimens during transplantation (Fromm, 2002). In allogeneic stem cell transplantation, for example, immunosuppressants are used to prevent the onset of graft-versus-host disease (GVHD). CD161++CD8+ T cells, with their MDR1-related ability to escape inhibition, have previously been implicated in the pathogenesis of GVHD (van der Waart et al., 2012). Immunosuppressive drugs are also used in solid organ transplantation, to prevent tissue rejection by the recipient immune system. Drugs routinely used in immunosuppressive regimens following transplantation include corticosteroids such prednisolone, the calcineurin inhibitor tacrolimus, and mycophenolate mofetil which, once converted into the active compound mycophenolic acid (MPA) within the liver, selectively inhibits *de novo* purine biosynthesis in activated lymphocytes (Taylor et al., 2005). The outcome of treatment with such drugs is therefore the prevention of T cell activation and proliferation. However, the effect of these immunosuppressants on MAIT cells has yet to be investigated, with the ability to efflux such substrates through high expression of MDR1 potentially rendering MAIT cells resistant to inhibition.

6.1.3 Unanswered questions

Defining the ability of particular lymphocytes to resist immunosuppressive drugs is of much importance in determining both treatment outcome and the risk of opportunistic infection during profound immunosuppression. Resistance to chemotherapy conferred by elevated expression of MDR1 has been correlated to expression of CD161, with MAIT (Dusseaux et al., 2011) and 'memory stem' cells (Turtle et al., 2009) – both defined by high expression of CD161 – described to survive chemotherapy through efflux of MDR1 substrates. While these populations are now thought to be one and the same, the provision of anti-viral protection during chemotherapy-induced lymphocytopenia is not

explained by preferential survival of anti-bacterial MAIT cells. This raises the possibility that contamination of anti-viral memory CD8+ T cells that express CD161, the CD161+CD8+ T cell population, may account for many of the results reported by Turtle *et al.* (2009). It therefore becomes important to assess the ability of CD161 positive CD8+ T cells to express and efflux through MDR1, and further to survive exposure to chemotherapy. Furthermore, whereas MAIT cells have been described to survive exposure to cytotoxic anthracyclines (Dusseaux et al., 2011; Turtle et al., 2009), the effect of other MDR1 substrates on this population has not yet been investigated. As these substrates are routinely used in the treatment of various conditions, including in the prevention of tissue rejection during transplantation, determining the effect of these drugs on MAIT cell function is of much interest.

6.2 Aims

1. Determine the expression of MDR1 and consequent efflux capability of CD161 expressing CD8+ T cells
2. Evaluate the potential of CD161+CD8+ T cells to survive chemotherapy, and hence to provide anti-viral protection during lymphocytopenia
3. Investigate the effect of immunosuppressive drugs on MAIT cells

6.3 Materials and Methods

Chapter-specific materials and methods are detailed below. All other methods and reagents are described in Chapter 2.

6.3.1 MDR1 and dextramer staining

MDR1 was stained by ICS using clone UIC2 (BioLegend). Anti-viral T cells were identified using MHC class I dextramers with the human CMV pp65 NLVPMVATV peptide (Immudex).

6.3.2 Efflux Assay

PBMC were loaded with 10μg/ml Rh123 (Sigma) in RPMI + 1% Bovine Serum Albumin (BSA) for 1hr on ice. These were then washed three times in cold R10, setting the centrifuge to 4°C. Cells were resuspended in R10 with or without inhibitors, and either kept on ice (loading control) or cultured at 37°C (efflux) for 30mins. MDR1 inhibitors cyclosporine A (CsA; sigma) and verapamil hydrochloride (verapamil; Sigma) were added at the lowest inhibitory concentration; 0.5μM and 50μM, respectively. In the case of daunorubicin efflux, fresh PBMC were loaded with 2.5μM Daunorubicin hydrochloride (Sigma) for 20mins at 37°C and allowed to efflux for 1hr. After efflux, cells were returned to ice and surface stained for analysis. Rh123 fluorescence was collected at 585/40nm on the MACSQuant, and daunorubicin at 610/20nm on the LSRII. Efflux was calculated as:

$$\frac{(\text{GeoMFI fluorescent substrate})_{\text{Loading control}} - (\text{GeoMFI fluorescent substrate})_{\text{Efflux}}}{(\text{GeoMFI fluorescent substrate})_{\text{Loading control}}}$$

6.3.3 Cytotoxicity Assay

PBMC were cultured with various concentrations of daunorubicin and apoptosis detected by ICS for activated caspase 3 (BD Pharmingen), or by Annexin V (Miltenyi Biotec) surface staining after 24 or 48hrs, respectively. Annexin V staining was performed for

15mins at room temperature in Annexin V binding buffer (Miltenyi Biotec). Verapamil was added at the beginning of culture. For culture of naïve and memory populations, naïve cells were isolated using a naïve pan T cell isolation kit (Miltenyi Biotec), following manufacturer's instructions, and both column-retained (memory) and column-eluted (naïve) fractions cultured with daunorubicin. Percentages expressing Annexin V at each concentration were background subtracted for Annexin V expression in media alone.

6.3.4 Proliferation Assay

PBMC were thawed and washed extensively in PBS before being stained with 2.5μM CellTrace™ Violet (CTV) dye (Invitrogen) for 10mins at room temperature. Ice cold R10 was added to quench the reaction, and cells kept on ice for 5mins. Cells were then washed three times in R10, transferring cells into new tubes between each wash. Finally, cells were incubated at 37°C for 5min, to allow excess dye to diffuse out. Cells were then resuspended at $2x10^6$/ml in Rh10 with anti-CD3/2/28 activation beads (Miltenyi Biotec), as per the manufacturer's instructions, and cultured in 48 well flat bottom plates with or without immunosuppressants Tacrolimus (Sigma), MPA (Sigma) or Prednisolone (Sigma). After 4 days, cells were split and either surface stained for analysis of CTV dilution or assessed for functional activity.

6.3.5 MAIT cell Functional Assay

THP-1 cells (ECACC, UK) were incubated overnight with paraformaldehyde-fixed *E. coli* (DH5α, Invitrogen) at 25 bacteria per cell. Following culture with immunosuppressants, PMBCs were washed extensively then added to washed THP1s for a 5hr co-culture, with Brefeldin A (eBioscience) added after 1hr. IFNγ production was assayed by ICS.

6.4 Results

6.4.1 MDR1 is expressed at elevated levels on CD161++ and CD161+ CD8+ T cells

Expression of the multi-drug efflux pump MDR1 on CD8+ T cell subsets was assessed by flow cytometry. This pump was expressed by the majority of CD161++CD8+ T cells, with an average of 82.17% of this population being MDR1 positive (Figure 6-2A&B). This confirms the results of others (Turtle et al., 2009), including those who have described high expression of MDR1 on MAIT cells (Dusseaux et al., 2011), which make up the majority of the CD161++ population . A proportion of the CD161+CD8+ T cell population (mean 38.9%) also expressed MDR1, significantly ($p<0.05$) more than the CD161– memory subset (mean 27.65%; Figure 6-2B). This was also seen at the cell level (geoMFI) where both CD161+ and, to a greater extent, CD161++ subsets expressed significantly ($p<0.01$) more MDR1 than CD161– memory cells (Figure 6-2C).

6.4.2 CD161 positive CD8+ T cells express functional MDR1

Functional activity of MDR1 can be assayed by measuring efflux of the fluorescent substrate Rh123 (Neyfakh et al., 1989). Cells loaded with the cell-permeant dye can be detected by flow cytometry (Loading control; Figure 6-3A), with efflux determined by a loss in fluorescence (Efflux; Figure 6-3A). By developing a measure of efflux based on the loss in fluorescence relative to the amount of dye loaded, where a value of 1.0 represents complete loss of Rh123 fluorescence (see 6.3.2), both CD161 positive CD8+ T cell populations were found to efflux Rh123 to a significantly ($p<0.0001$) greater degree than the CD161– population (Figure 6-3B). CD161++CD8+ T cells displayed the greatest efflux ability, while CD161+CD8+ T cells demonstrated an intermediate ability to efflux, reflective of their intermediate expression of MDR1.

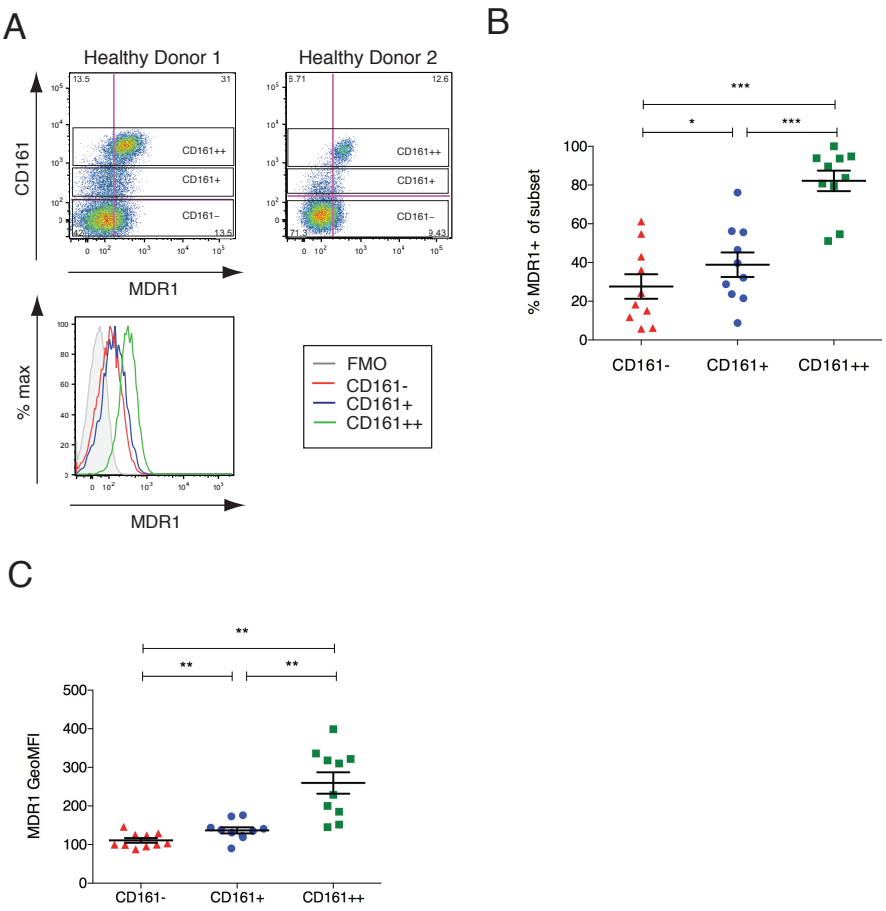

Figure 6-2: CD161-expressing CD8+ T cells express MDR1. **A**) Representative flow cytometry of CD8+CD3+ lymphocytes, excluding CCR7+CD45RA+ naïve cells, from 2 healthy donors, showing expression of MDR1 in relation to CD161. Representative histogram of MDR1 expression by CD161– (red), CD161+ (blue), CD161++ (green) CD8+ T cells, compared to the FMO sample (grey shaded) in healthy donor 1. **B**) Cumulative data for percentage of each memory subset expressing MDR1, (n=10). **C**) GeoMFI for MDR1 on each memory subset as determined by flow cytometry, (n=10). ***p<0.001, **p<0.01, *p<0.05 by one-way ANOVA with Tukey's multiple comparisons test. Data are represented as mean ± SEM.

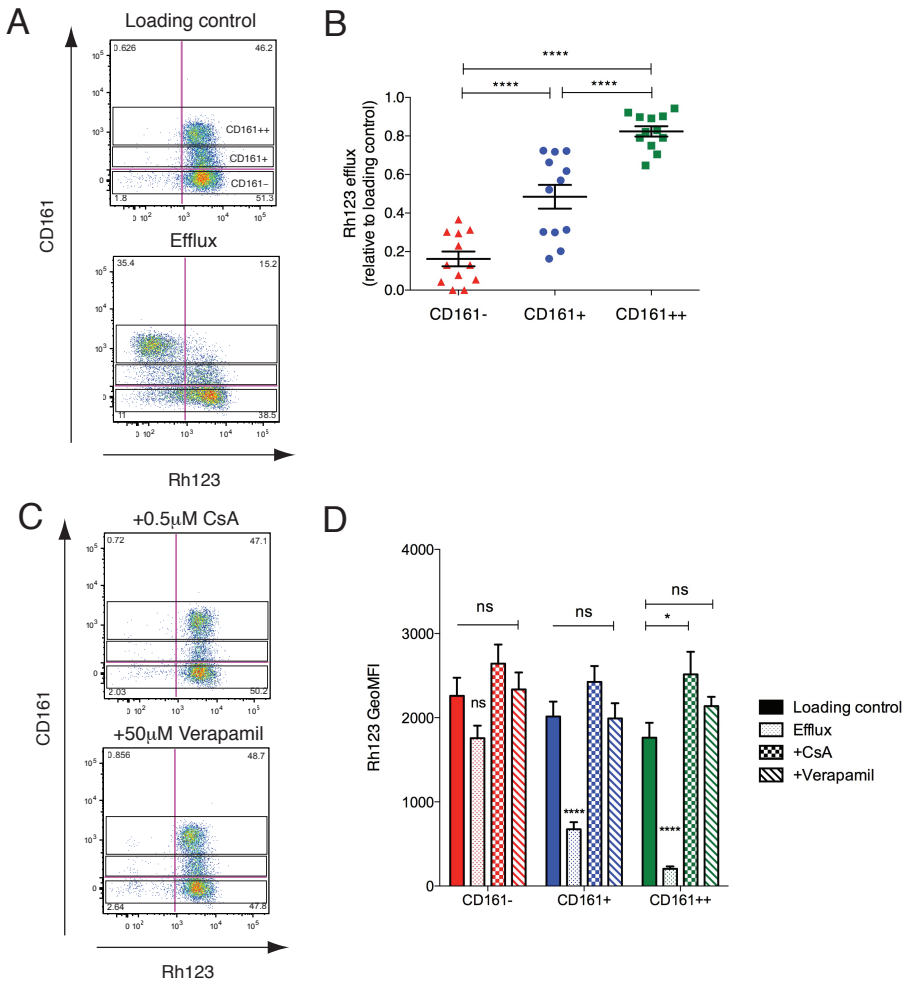

Figure 6-3: CD161-expressing CD8+ T cells rapidly efflux Rh123 through MDR1. **A**) Representative flow cytometry plots of CD8+CD3+ lymphocytes, excluding CCR7+CD45RA+ naïve cells, loaded with Rh123 on ice and either kept on ice (loading control; top) or incubated at 37°C in media (efflux; bottom). **B**) Cumulative data of Rh123 effluxed from each subset calculated as per Materials & Methods (see 6.3.2), (n=12). ****p<0.0001 by one-way ANOVA with Tukey's multiple comparisons test. **C**) Representative flow cytometry plots of the addition of the ABCB1 inhibitors cyclosporine A (CsA) and Verapamil during efflux. **D**) Cumulative data of geoMFI of Rh123 in each subset cultured on ice (loading control), media alone (efflux) or with ABCB1 inhibitors CsA or Verapamil, (n=8). ****p<0.0001, *p<0.05, ns = not significant by two-way ANOVA with Dunnett's multiple comparisons test, compared to the loading control. Data are represented as mean ± SEM.

To confirm efflux was due to activity of MDR1, inhibitors of MDR1 were added during efflux. Cyclosporine A and verapamil are both inhibitors of MDR1,[1] and were added at the lowest inhibitory concentration (Figure 6-3C). While cells cultured in the absence of inhibitors displayed a significant ($p<0.0001$) decrease in Rh123 fluorescence, in CD161 expressing populations, there was no significant difference between cells cultured in the presence of either CsA or verapamil and the loading control, where cells were kept on ice (Figure 6-3D). Inhibition of efflux by CsA and verapamil therefore indicates that the significant efflux activity demonstrated by CD161 positive CD8+ T cells (Figure 6-3B) was related to their elevated expression of MDR1 (Figure 6-2).

6.4.3 MAIT cells are protected from cytotoxicity during exposure to daunorubicin

The ability to efflux Rh123 through MDR1 suggested that CD161 expressing CD8+ T cells may be protected from cytotoxic chemotherapy, as previously described for malignant cells (Gottesman et al., 2002). Therefore, PBMC were exposed to the fluorescent anthracycline daunorubicin and their ability to efflux this drug measured as previously. While efflux was not as marked as for Rh123 (Figure 6-4A), significant ($p<0.0001$) efflux was again demonstrated by the CD161++CD8+ T cell subset compared to the CD161− (Figure 6-4B). In this case no significant difference in efflux was observed between CD161+ and CD161−CD8+ T cells, although it should be noted that naïve cells were not excluded in these analyses due to compensation issues with fluorescent daunorubicin (discussed later).

The ability of these cells to survive exposure to chemotherapeutic drugs was subsequently determined by culture of PBMC with daunorubicin for 48hrs, with apoptosis evaluated by Annexin V staining. Annexin V binds to phosphatidylserine in the outer membrane to identify apoptotic cells (Appendix VI.i). Culture of cells with various concentrations of daunorubicin induced apoptosis in CD8+ T cells (Figure 6-4C). When divided based upon CD161 expression, it could be seen that CD161−CD8+ T cells were highly susceptible to

[1] http://www.fda.gov/drugs/developmentapprovalprocess/developmentresources/druginteractionslabeling/ucm093664.htm#PgpTransport visited 18.09.14

apoptosis when cultured with daunorubicin (Figure 6-4D). CD161+CD8+ T cells also displayed susceptibility to anthracyclines, with no significant difference in the percentage of apoptotic cells between CD161+ and CD161−CD8+ T cells at any concentration of daunorubicin tested. This may be expected given these cells did not display an enhanced ability to efflux daunorubicin (Figure 6-4B). On the other hand, CD161++CD8+ T cells displayed considerable resistance to daunorubicin-induced apoptosis, up to a concentration of 10μM (Figure 6-4D). Therefore, amongst CD8+ T cells the CD161++ subset alone is preferentially protected from anthracycline-induced cytotoxicity. Again, this protection was related to their expression of MDR1, as resistance was abrogated by addition of verapamil as determined by staining for caspase 3, which is activated upon initiation of apoptosis (Appendix VI.i).

To investigate whether MAIT cells remain functional after exposure to daunorubicin, in addition to resisting cytotoxic effects, MAIT cell function was assayed by co-culture with *E.coli*-pulsed THP1s, following 48hr culture with daunorubicin. The percentage of MAIT cells producing IFNγ in response to *E.coli* was reduced upon culture with daunorubicin, particularly at a concentration of 10μM where the response was reduced by over 40% (mean 79.65% vs. 46.10%). A slight reduction in function was also observed at 0.1μM and 1μM, although this was not significant at 1μM (Figure 6-4E).

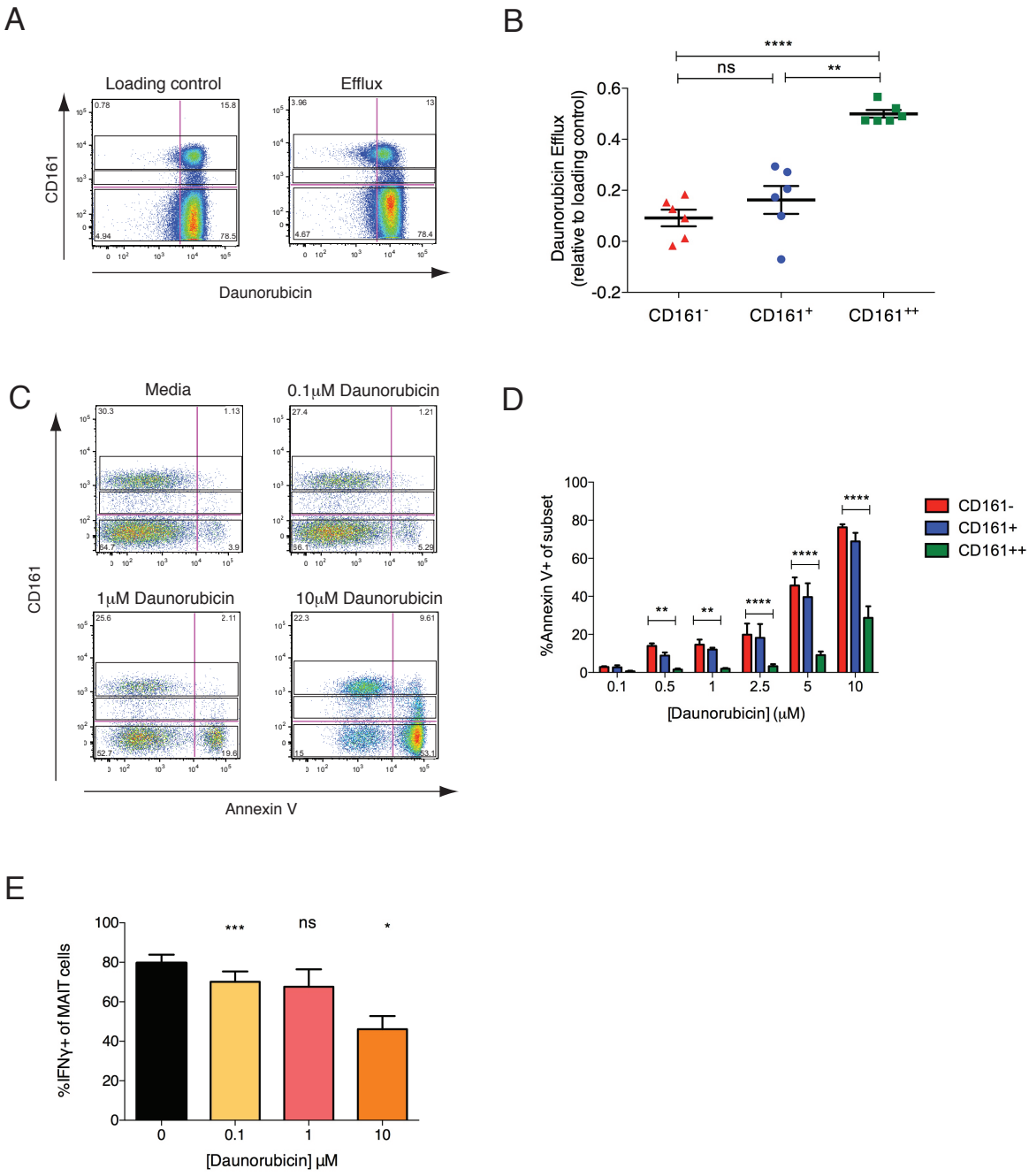

Figure 6-4: CD161++ MAIT, but not CD161+, CD8+ T cells efflux and survive culture with daunorubicin. **A**) Representative flow cytometry plots of CD8+CD3+ lymphocytes loaded with daunorubicin and cultured on ice (loading control; left) or at 37°C (efflux; right). **B**) Cumulative data for daunorubicin effluxed by each subset calculated as for Rh123 (see 6.3.2) (n=6). ****p<0.0001, **p<0.01, ns = not significant by one-way ANOVA with Tukey's multiple comparisons test. **C**) Representative flow cytometry plots of Annexin V staining of CD8+CD3+ lymphocytes cultured for 48hr in media alone or with various concentrations of daunorubicin. **D**) Cumulative data for percentage of CD161– (red), CD161+ (blue), CD161++ (green) CD8+ T cells stained by Annexin V after culture for 48hr with various concentrations of daunorubicin. ****p<0.0001, **P<0.01 by two-way ANOVA with Tukey's multiple comparisons test, all other comparisons were not significant. After culture with daunorubicin, cells were removed and incubated for 5hr with THP1s, preincubated with E.coli as per Materials & Methods. **E**) Cumulative data for percentage of MAIT cells expressing IFNγ in response to E.coli-loaded THP1s after 48hr culture in the presence of various concentrations of daunorubicin (n=6). ***p<0.001, *p<0.05, ns = not significant by one-way ANOVA with Dunnett's multiple comparisons test, compared to untreated cells.

6.4.4 Do anti-viral CD161+CD8+ T cells have the potential to provide protection after ablative chemotherapy?

CD161 was suggested by Turtle *et al.* (2009) to mark anti-viral CD8+ T cells with the ability to survive chemotherapy, and hence provide protection against viruses such as CMV during lymphocytopenia. This was supported by the detection of anti-viral populations upon culture of sort purified Rh123-effluxing CD8+ memory T cells with EBV and FLU peptide-pulsed DCs. Yet MAIT cells are anti-bacterial, rather than anti-viral (Le Bourhis et al., 2010), and do not stain with MHC class I multimers presenting viral peptides (Dusseaux et al. 2011, Chapter 4 Figure 4-1). CD161+CD8+ T cells, on the other hand, include anti-viral cells (Chapter 4 Figure 4-1) and display the ability to efflux Rh123 through MDR1 (Figure 6-3, Dusseaux et al. 2011). Therefore, the presence of these anti-viral tetramer-positive populations may be due to contamination by effluxing CD161+CD8+ T cells, resulting from the sorting strategy employed by Turtle *et al.* (2009). However, this subset did not display a significant ability to survive exposure to the anthracycline daunorubicin, such as demonstrated by CD161++ MAIT cells (Figure 6-4). In this analysis naïve cells, which are predominantly CD161– (Chapter 4, Figure 4-2), were not excluded due to panel and compensation limitations, and may dilute differences between memory CD161+ and CD161– cells. Indeed, there was no significant difference in expression of MDR1 between CD161+ and naïve (CCR7+CD45RA+) CD161– CD8+ T cells, while CD161+CD8+ T cells expressed significantly ($p<0.001$) more MDR1 than their memory CD161– counterparts (Figure 6-5A). To assess whether this translated to better protection of CD161–CD8+ T cells due to inclusion of MDR1-expressing naïve cells in previous assays, naïve and memory T cell fractions were isolated and the levels of apoptosis after 48hr culture with 1μM daunorubicin determined in each fraction separately. These results reflected those observed previously (Figure 6-4) where only CD161++CD8+ T cells were protected, with CD161+CD8+ T cells displaying similar levels of apoptosis to both memory and naïve CD161–CD8+ T cell populations (Figure 6-5B). Furthermore, analysis of MDR1 expression on CD8+ T cells specific for the pp65 epitope from CMV demonstrated no significant difference between those cells expressing CD161 (CD161+) to those that were CD161–. This suggests, therefore, that CD161+CD8+ T

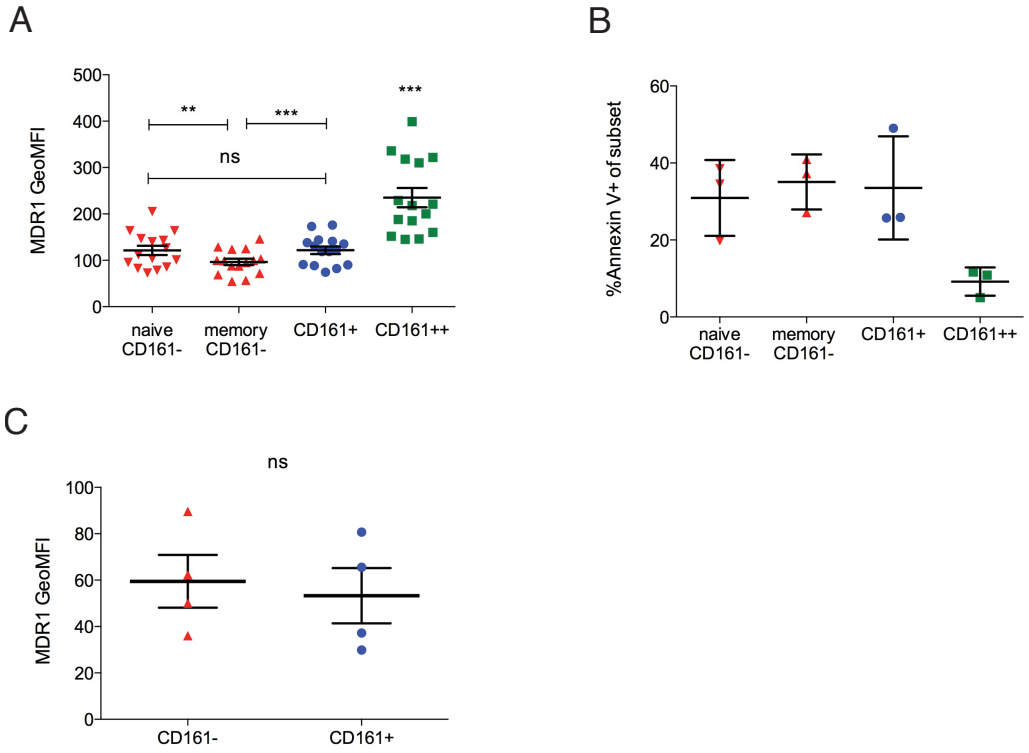

Figure 6-5: CD161+CD8+ T cells are not preferentially protected over CD161–CD8+ T cells by expression of MDR1. **A**) GeoMFI of MDR1 on the different CD161 subsets of CD8+ T cells, including both naïve and memory phenotype CD161–CD8+ T cells (n=15). ***p<0.001, **p<0.01, ns = not significant by one-way ANOVA with Tukey's multiple comparisons test. **B**) Percentage of each subset stained with Annexin V after 48hr culture of sorted naïve or memory cells with 1µM daunorubicin (n=3). **C**) GeoMFI of MDR1 on CD161– or CD161+ CD8+ T cells specific for pp65 from CMV as identified by MHC-dextramer staining, (n=4). ns = not significant by paired t-test.

cells do not possess an enhanced ability to survive chemotherapy and provide anti-viral protection over conventional CD161– CD8+ T cells.

6.4.5 MAIT cells are susceptible to, but remain functional after, exposure to immunosuppressants

The ability of CD161++CD8+ T cells, predominantly composed of the Vα7.2+ MAIT cell population, to survive culture with chemotherapeutic agents through drug efflux by MDR1 suggests that MAIT cells may also possess the ability to efflux, and hence be resistant to, other MDR1 substrates. Such substrates include immunosuppressants such as tacrolimus and MPA, the active form of mycophenolate mofetil, often used in immunosuppression regimens post-transplantation (Taylor et al., 2005). Furthermore, as innate-like lymphocytes, chemotherapy-resistant MAIT cells may represent mediators of early transplant rejection. Therefore, the effect of these immunosuppressants on MAIT cells was investigated. As CD161++ MAIT cells alone had demonstrated resistance to daunorubicin, analysis was confined to this cell subset.

Tacrolimus is a calcineurin inhibitor which hence blocks TCR signal transduction, thereby preventing IL-2 production and T cell proliferation (Taylor et al., 2005). T cell proliferation was assayed by CTV dilution (Lyons and Parish, 1994) upon anti-CD3/2/28 stimulation for 4 days in the presence or absence of physiological concentrations of tacrolimus (Figure 6-6A). The percentage of both MAIT cells and conventional (non-MAIT) T cells ("bulk T cells") that had proliferated was determined by taking cells that had lost CTV fluorescence (CTV^{lo}), representing daughter cells. In the absence of tacrolimus both MAIT and bulk T cells proliferated in response to TCR stimulation (Figure 6-6B). However, both MAIT and bulk T cells were similarly inhibited by tacrolimus, with proliferation inhibited at all concentrations tested. Therefore, MAIT cells do not display preferential protection against tacrolimus-induced inhibition of proliferation, despite expression of MDR1.

After 4-day culture with tacrolimus, MAIT cell activity was assayed by 5hr co-culture with *E.coli*-pulsed THP1s. Activation by *E.coli* was assayed by IFNγ production, as previously

(Figure 6-6C). Despite inhibition of proliferation, there was no difference in the ability of MAIT cells to respond to *E.coli* after culture with tacrolimus, at any concentrations tested, compared to those cultured in media alone (Figure 6-6D).

Similarly, the effect on MAIT cells of exposure to MPA was also investigated. MPA inhibits guanosine nucleotide synthesis in lymphocytes, and hence inhibits T cell proliferation (Taylor et al., 2005). Again, T cell proliferation was assayed by CTV dilution in the presence or absence of MPA (Figure 6-7A), demonstrating that both MAIT and bulk T cells were inhibited to a similar degree by MPA, at all concentrations tested (Figure 6-7B). Yet, similarly to the case with tacrolimus, MAIT cells retained their ability to respond to *E.coli*-loaded THP1s (Figure 6-7C&D).

On the other hand, culture of PBMC with the cortciosteroid prednisolone, used in the prevention of rejection as well as a variety of other conditions, did not affect proliferation of either bulk T or MAIT cells (Figure 6-8A&B). Nor was any significant increase in apoptosis observed in any T cell subset upon culture with prednisolone (Appendix VI.ii). Corticosteroids such as prednisolone may exert immunosuppressive effects through differing mechanisms, including the suppression of cytokine production (Taylor et al., 2005), and therefore immunosuppressive effects would not be detected with these readouts. Nonetheless, MAIT cells exposed to various concentrations of prednisolone again retained their ability to secrete IFNγ upon exposure to *E.coli* (Figure 6-8C&D).

Together, these data demonstrate that while MAIT cells are susceptible to the anti-proliferative action of immunosuppressants tacrolimus and MPA, they retain their functional activity upon exposure to these immunosuppressants, and to the corticosteroid prednisolone – at least in regards to IFNγ response to *E.coli*.

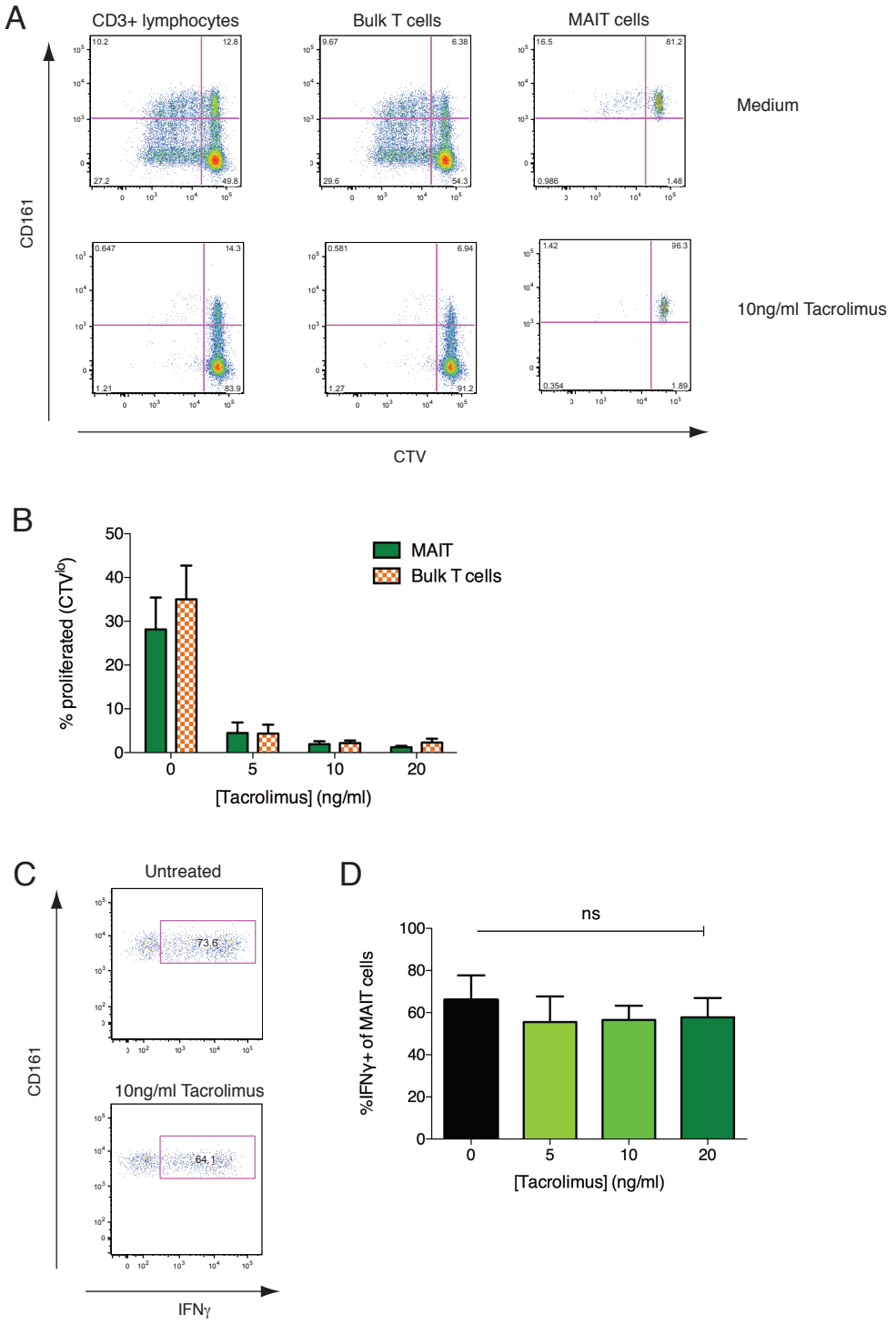

Figure 6-6: MAIT cells are inhibited by, but remain functional after exposure to, tacrolimus. **A**) Representative flow cytometry plots of either CD3+ lymphocytes, non-MAIT bulk T cells (CD3+ lymphocytes, excluding CD161++Vα7.2+) or MAIT cells (CD161++Vα 7.2+CD3+) after activation with anti-CD3/2/28 beads cultured in medium alone (top panel) or with 10ng/ml tacrolimus (bottom panel), showing dilution of CTV dye upon proliferation after 4 days. Gates were set according to unstimulated controls. **B**) Cumulative data for the percentage of either MAIT (green) or non-MAIT bulk T cells (orange hatch) proliferated (CTVlow) after activation for 4 days in the presence of media alone or various concentrations of tacrolimus, (n=6). **C**) After culture with tacrolimus, cells were removed and incubated for 5hr with THP1s, preincubated with E.coli as per Materials & Methods. Representative flow cytometry plots of percentage of MAIT cells producing IFNγ. **D**) Cumulative data for percentage of MAIT cells expressing IFNγ in response to *E.coli*-loaded THP1s after 4 day culture in the presence of various concentrations of tacrolimus, (n=5). ns = not significant by one-way ANOVA with Dunnett's multiple comparisons test, compared to untreated cells.

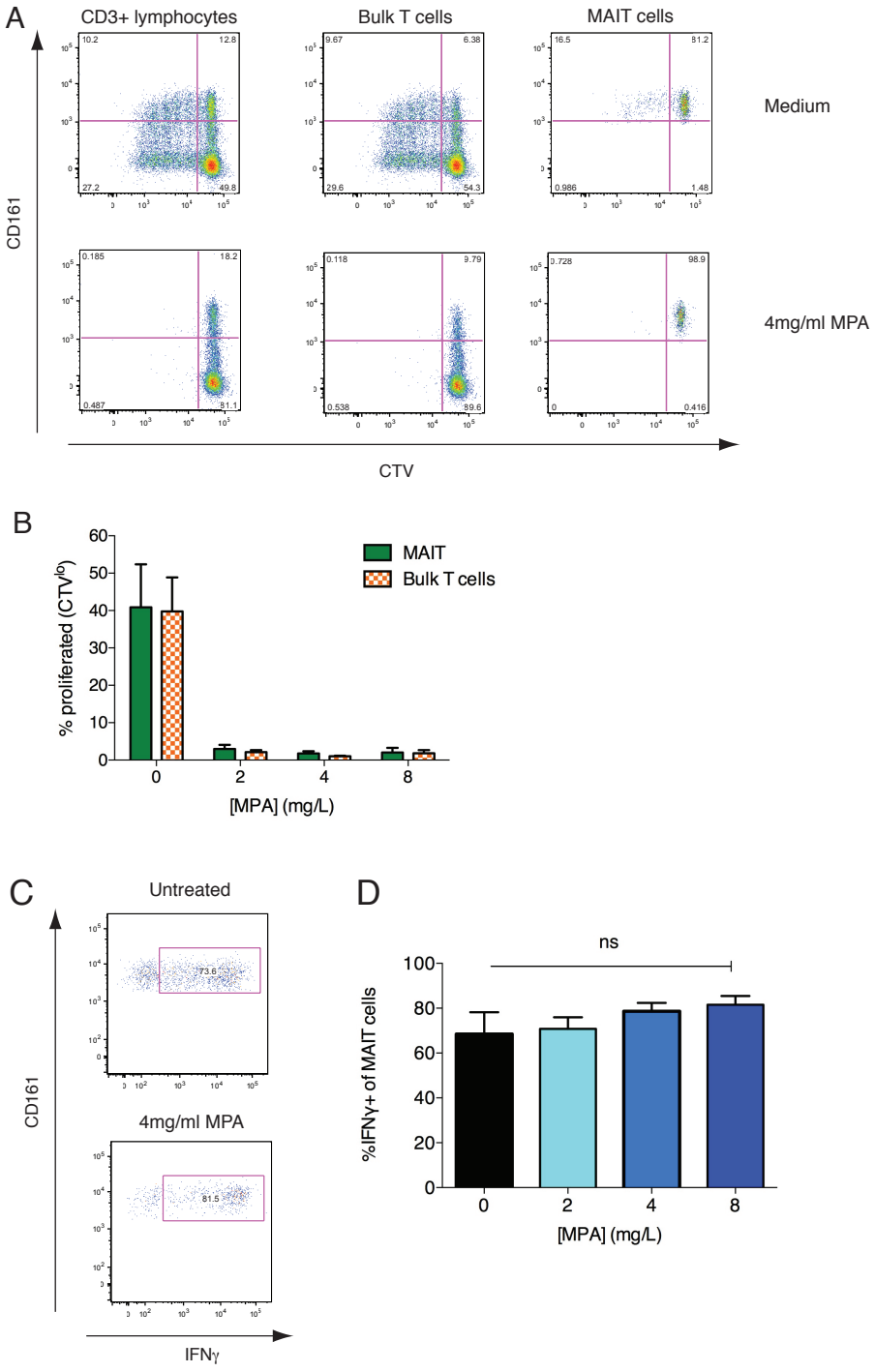

Figure 6-7: MAIT cells are also inhibited by, but remain functional after exposure to, Mycophenolic acid. **A**) Representative flow cytometry plots of either CD3+ lymphocytes, non-MAIT bulk T cells (CD3+ lymphocytes, excluding CD161++Vα7.2+) or MAIT cells (CD161++Vα7.2+CD3+) after activation with anti-CD3/2/28 beads cultured in medium alone (top panel) or with 4mg/ml Mycophenolic acid (MPA) (bottom panel), showing dilution of CTV dye upon proliferation after 4 days. Gates were set according to unstimulated controls. **B**) Cumulative data for the percentage of either MAIT (green) or non-MAIT bulk T cells (orange hatch) proliferated (CTVlow) after activation for 4 days in the presence of media alone or various concentrations of MPA, (n=6). **C**) After culture with MPA, cells were removed and incubated for 5hr with THP1s, preincubated with E.coli as per Materials & Methods. Representative flow cytometry plots of percentage of MAIT cells producing IFNγ. **D**) Cumulative data for percentage of MAIT cells expressing IFNγ in response to *E.coli*-loaded THP1s after 4 day culture in the presence of various concentrations of MPA, (n=6). ns = not significant by one-way ANOVA with Dunnett's multiple comparisons test, compared

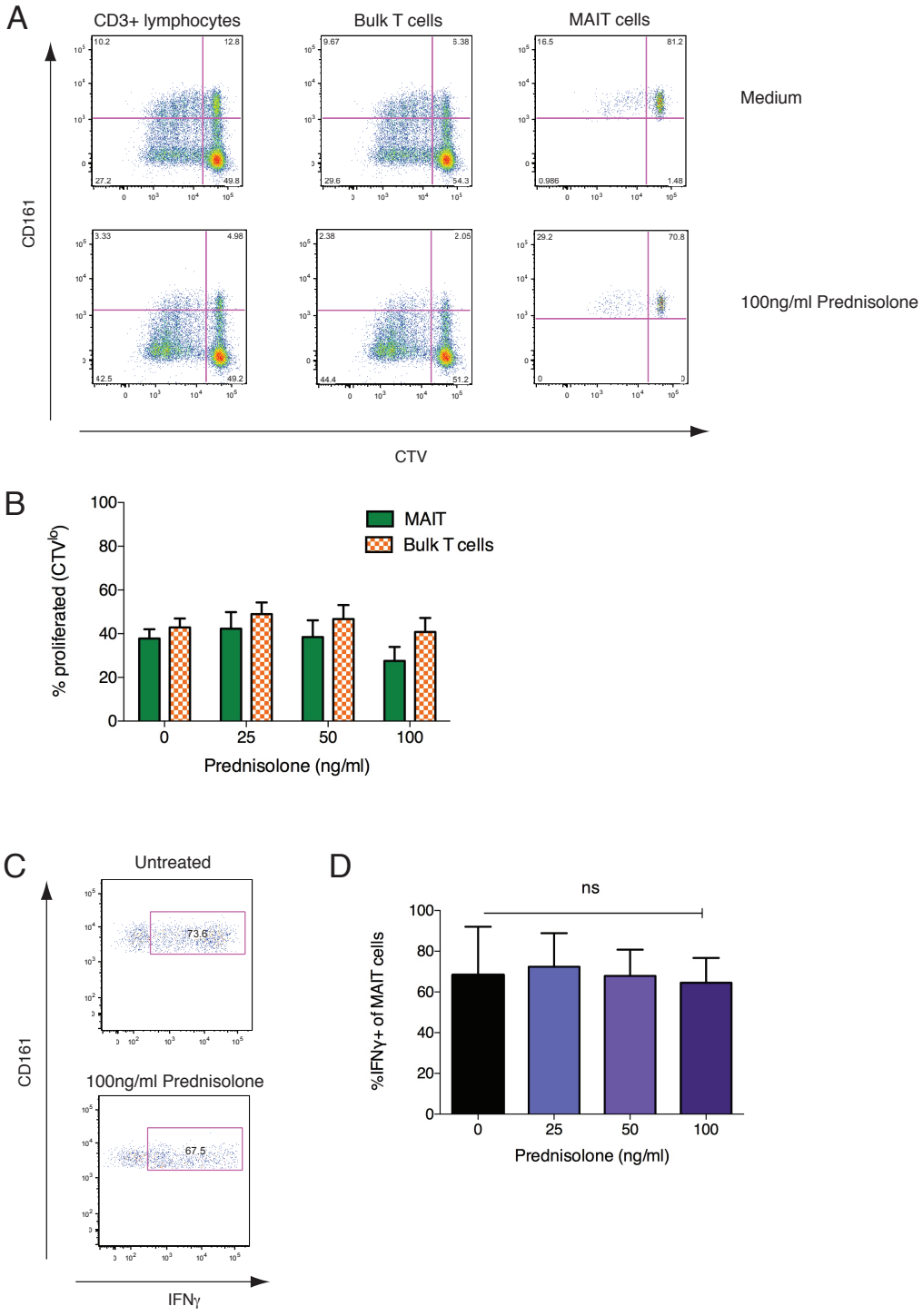

Figure 6-8: MAIT cells also remain functional after exposure to prednisolone. **A**) Representative flow cytometry plots of either CD3+ lymphocytes, non-MAIT bulk T cells (CD3+ lymphocytes, excluding CD161++Vα7.2+) or MAIT cells (CD161++Vα7.2+CD3+) after activation with anti-CD3/2/28 beads cultured in medium alone (top panel) or with 100ng/ml prednisolone (bottom panel), showing dilution of CTV dye upon proliferation after 4 days. Gates were set according to unstimulated controls. **B**) Cumulative data for the percentage of either MAIT (green) or non-MAIT bulk T cells (orange hatch) proliferated (CTVlow) after activation for 4 days in the presence of media alone or various concentrations of prednisolone (n=6). **C**) After culture with prednisolone, cells were removed and incubated for 5hr with THP1s, preincubated with E.coli as per Materials & Methods. Representative flow cytometry plots of percentage of MAIT cells producing IFNγ. **D**) Cumulative data for percentage of MAIT cells expressing IFNγ in response to *E.coli*-loaded THP1s after 4 day culture in the presence of various concentrations of prednisolone, (n=6). ns = not significant by one-way ANOVA with Dunnett's multiple comparisons test, compared to untreated cells.

6.5 Discussion

It has previously been shown that MAIT cells express high levels of MDR1, efflux Rh123 and preferentially survive chemotherapy (Dusseaux et al., 2011). This was confirmed here, and extended to demonstrate significant expression of MDR1 and efflux of Rh123 in the CD161+CD8+ T cell population (Figures 6-2 & 6-3). The existence of a chemotherapy-resistant CD8+ T memory population, identified by Turtle *et al.* (2009), was suggested to provide a pool of cells protective against viral infection during lymphocytopenia. Sort purification of these highly-effluxing cells and culture with viral peptide-pulsed DCs resulted in the appearance of anti-viral CD8+ T cell populations. This sorting strategy, based on the ability to efflux Rh123, may, however, lead to the inclusion of T cell populations other than MAIT cells, including CD161+ and CD161−, a small proportion of which also efflux Rh123 (Figure 6-3). This is supported by further experiments performed by Turtle *et al.* in which culture of these highly-effluxing populations with CMV-infected fibroblasts resulted in populations of CD161+ and CD161−, but not CD161++, cells which produced IFNγ in response to viral peptide. The authors suggested this to result from CD161 downregulation amongst effluxing CD161++ cells, however as it occurred in a small fraction of cells only (unlike population-wide downregulation described previously: Fergusson et al., 2014) it is more likely indicative of contamination and proliferation of other T cell subsets. The elevated MDR1 expression and efflux capability of the CD161+CD8+ T cell population (Figures 6-2 & 6-3) suggested that this population may instead represent the CD161 positive memory CD8+ population with preferential resistance to chemotherapy and ability to provide the anti-viral protection described during lymphocytopenia. However, expression of MDR1 and efflux of Rh123 by the CD161+CD8+ T cell population did not translate into a preferential ability to survive exposure to the chemotherapeutic agent daunorubicin in experiments described here, with CD161++ MAIT cells alone displaying almost complete resistance to this cytotoxic drug (Figure 6-4). However, this efflux capability may be sufficient to provide resistance of CD161+CD8+ T cells against other therapeutic MDR1 substrates.

The detection of anti-viral responses during chemotherapy-induced lymphocytopenia (Turtle et al., 2009) therefore remains unexplained. While CD161+CD8+ T cells do not show advanced ability to survive chemotherapy over CD161–, perhaps those memory cells with capacity to efflux through MDR1 in both CD161+ and CD161– populations are sufficient to provide protection against latent infections. Alternatively, CD161++ non-MAIT (Va7.2–) cells (described in Chapter 3), which contain a higher proportion cells expressing MDR1 than the CD161+CD8+ population (Appendix VI.iii), may prove to be anti-viral and display sufficient efflux capacity to survive exposure to chemotherapy. In the absence of *ex vivo* phenotyping of the anti-viral responses detected in chemotherapy patients, this question is difficult to answer. Human memory stem-cells (T_{SM}) with the self-renewal and multipotent potential of stem cells have also been recently described, which were distinct from MAIT cells and did not express CD161 (Gattinoni et al., 2011).

Nonetheless, MAIT cell survival during chemotherapy, in addition to potentially affording the patient some residual anti-bacterial protection, may also provide anti-viral protection; single-stranded RNA stimulation of Toll-like receptor (TLR)8 induced IL-12 and IL-18 production by APCs, which in turn induced innate IFNγ production from MAIT cells (Ussher et al., 2014). However, MAIT cell function against *E.coli*-loaded THP1s was impaired following *in vitro* culture with daunorubicin, particularly at high concentrations. Furthermore, the resistance of this population to chemotherapy may also prove unfavourable in certain circumstances given the recent identification of a MAIT cell derived-lymphoma (McGregor et al., 2014).

Despite high expression of MDR1, MAIT cells remained susceptible to the anti-proliferative effect of tacrolimus and MPA (Figures 6-6 & 6-7), while retaining their ability to express IFNγ in response to *E.coli*-pulsed THP1s. This suggests that while MAIT cells were unable to efflux immunosuppressants to a degree able to confer resistance, they were protected from any inhibitory effect on their activation. This is particularly surprising in regards to tacrolimus, which inhibits TCR signal transduction through calcineurin (Taylor et al., 2005) yet did not inhibit MR1-presented ligand from signalling through the Vα7.2 MAIT cell TCR. However, the effect on cytokine production in response to TCR stimulation in conventional T cells was not determined in this assay, which specifically

activates MAIT cells (Ussher et al., 2014), and therefore whether MAIT cells remain functional preferentially over other T cells cannot be determined. The immunosuppressive effect of prednisolone on MAIT and other T cells was also not detected in these assays, however MAIT cells did remain functional after culture with this corticosteroid (Figure 6-8).

Together, this would suggest that MAIT cells remain functional in patients receiving tacrolimus and/or MPA and/or prednisolone, in immunosuppressive regimens post-transplantation, and could, therefore, represent potential mediators of rejection. What the source of the ligand in these cases would be is not known, although complete asepsis during surgery is impossible (Fox, 1997) and may introduce sources of bacterial ligand. The existence of further MAIT cell ligands in addition to derivatives of the riboflavin pathway (Corbett et al., 2014; Kjer-Nielsen et al., 2012), including self molecules, is also a distinct possibility. Cross-reactivity of MAIT cells to MR1 from different species (Huang et al., 2009; Le Bourhis et al., 2010) suggests that inter-individual reactivity may be possible, as well as indicating further impediments to successful xenotransplantation. In the absence of specific ligand, MAIT cells can also be activated by a combination of IL-12 and IL-18 produced in response to TLR activation of APCs (Ussher et al., 2014), which presents another pathway by which MAIT cells may be activated, while also opening up the possibility that MAIT cells may respond (indirectly) to the danger signals induced by tissue injury and reperfusion during transplantation (Matzinger, 1994; Wood and Goto, 2012). It would be interesting, therefore, to examine the effect of immunosuppression on the ability of MAIT cells to respond to cytokine stimulation. Furthermore, tissue rejection by T cells is predominantly mediated through cytotoxic attack of the transplanted organ (Wood and Goto, 2012). MAIT cells have recently been identified as cytotoxic, inducing lysis of both infected APCs (Kurioka et al., 2014) and epithelial cells (Le Bourhis et al., 2013). Therefore the cytotoxicity of MAIT cells following exposure to immunosuppressants should also be assessed, to determine their potential for inducing rejection of transplanted tissues by this mechanism. Immunosuppression regimens frequently utilise combinations of drugs, and therefore determining whether MAIT cells maintain responsive after exposure to multiple drugs would also be of interest. A preliminary experiment (in three donors only) suggests that after exposure to a combination of tacrolimus (10ng/ml), MPA (4mg/ml) and prednisolone (50ng/ml) MAIT cell

function is not significantly affected, although an average of 34% reduction in the percentage of MAIT cells responding was observed (Appendix VI.ii).

Perhaps the most informative data, however, would be that of MAIT cell number and function in transplant patients undergoing immunosuppressive therapy. The *in vitro* data presented here suggests that MAIT cell numbers would decrease in peripheral blood during immunosuppression, reflective of the inhibition of proliferation. However, a decrease may also reflect specific redistribution, with MAIT cells being a naturally tissue-homing population (Dusseaux et al., 2011; Treiner et al., 2003). Therefore, detection of MAIT cells within transplanted tissues, for example by immunohistochemistry, would be further indicative of a role for these cells in the immune response to transplantation, and potentially rejection. Indeed, MAIT cell recruitment to tissues has previously been implicated in the pathogenesis of GVHD, with decreased levels of circulating CD161++CD8+ T cells correlated with the development of chronic GVHD (van der Waart et al., 2012). Again, this was related to their expression of MDR1 and consequent ability to resist immunosuppression, with CD161++CD8+ T cells in this case demonstrating enhanced ability to proliferate in the presence of CsA compared to conventional CD8+ T cells.

While MAIT cells may be implicated in the deleterious side effects of transplantation (such as rejection or GVHD), escape of inhibition may also enable MAIT cells to provide protection against opportunistic bacterial infections during the non-specific immunosuppression resultant from any drug regimen. The role of these cells in such settings, therefore, warrants further investigation and could be influential in informing drug regimen choice.

6.6 Summary

- Both CD161++ and CD161+ CD8+ T cells expressed elevated levels of MDR1 and greater Rh123 efflux capacity than CD161−CD8+ T cells, with the CD161++ population displaying the highest of both
- CD161+CD8+ T cells did not show preferential protection against daunorubicin cytotoxicity, and there was no significant difference in the expression of MDR1 on CD161+ vs CD161− CMV-specific CD8+ T cells
- MAIT cells were susceptible to the immunosuppressive activity of tacrolimus and MPA, but retained functional activity in response to *E.coli* after exposure to both these drugs and exposure to prednisolone

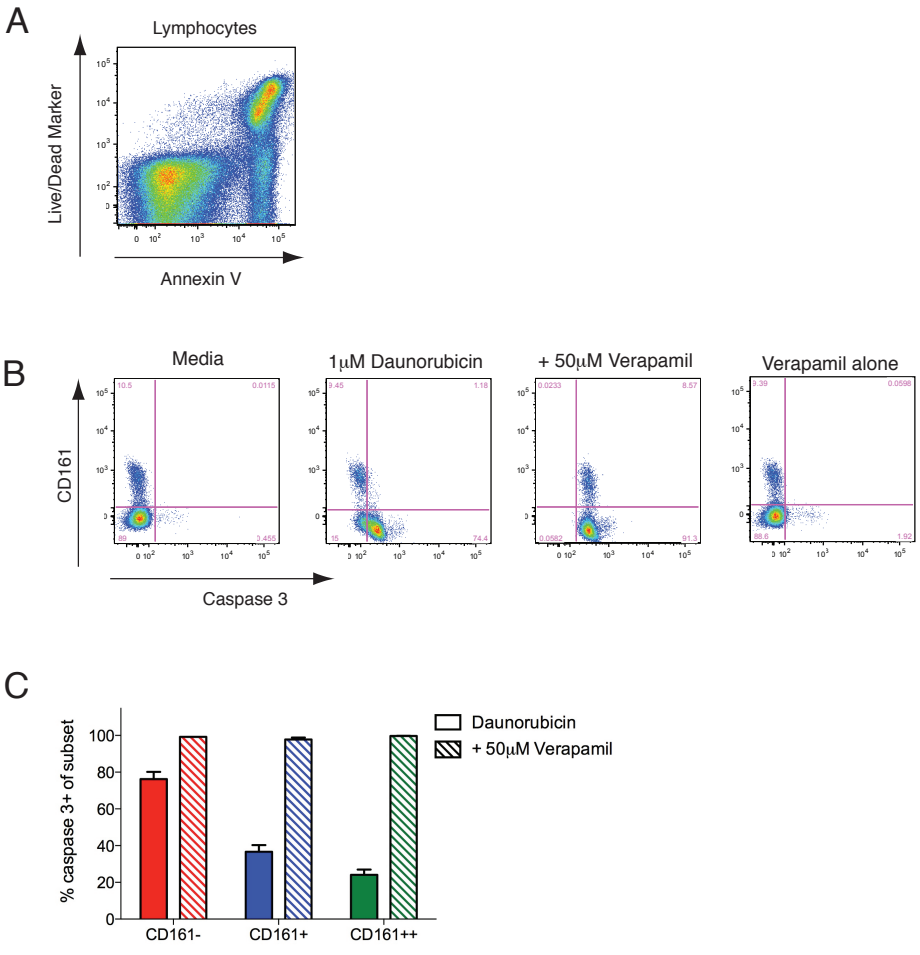

Appendix VI.i: MAIT cells survive daunorubicin cytotoxicity through MDR1. **A**) Representative flow cytometry plot of lymphocytes cultured with daunorubicin and stained with Annexin V and an amine-reactive Live/Dead marker. **B**) Representative flow cytometry plots of caspase 3 expression by CD8+CD3+ lymphocytes after culture with media, 1μM Daunorubicin with or without the MDR1 inhbitor verapamil (50μM) for 48hrs. Cells cultured with verapamil alone are also shown. **C**) Cumulative data for percentage of each subset, excluding CCR7+CD45RA+ naive cells, expressing caspase 3 after culture with daunorubicin alone (block colour) or with verapamil (hatched bars) (n=5).

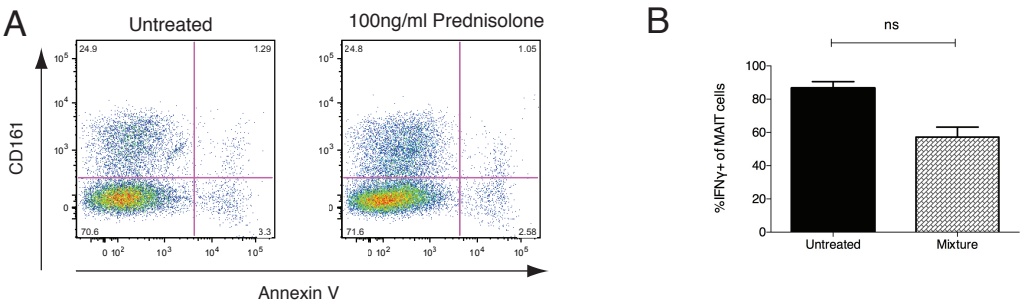

Appendix VI.ii: Culture of PBMCs with immunosuppressants. **A**) Representative flow cytometry plots of Annexin V staining of CD8+CD3+ lymphocytes cultured in medium alone (untreated) or 100ng/ml prednisolone for 4 days. **B**) After culture with a mixture of 10ng/ml tacrolimus, 4mg/ml MPA and 50ng/ml Prednisolone for 4 days, cells were removed and incubated for 5hr with THP1s preincubated with *E.coli* as per Chapter 2 - Materials & Methods. The histogram shows cumulative data for the precentage of MAIT cells expressing IFNγ in response (n=3). ns = not-significant by paired t-test.

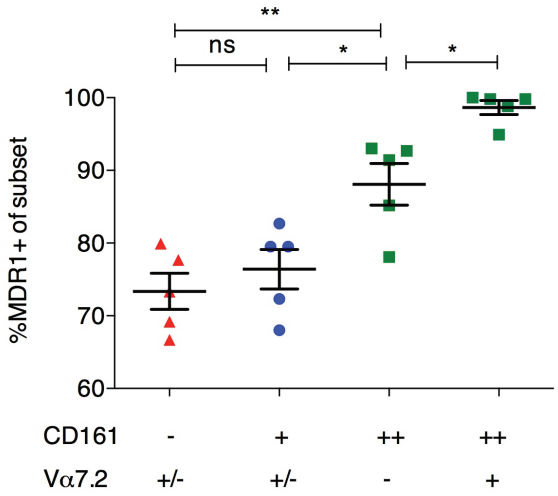

Appendix VI.iii: MDR1 expression by Va7.2- CD161++ CD8+ T cells. Cumulative data for percentage of each subset, divided based upon expression of CD161 and Va7.2, expressing MDR1 as determined by flow cytometry, (n=5). **p<0.01, *p<0.05, ns = not significant by one-way ANOVA with Tukey's multiple comparisons test.

7. Discussion

T cell expression of CD161 was identified two decades ago, on both CD4+ and CD8+ (Lanier et al., 1994), and later on TCRγδ+, T cells (Battistini et al., 1997). Indeed, a quarter of both TCRαβ+ T cells (Lanier et al., 1994) and TCRγδ+ T cells (Battistini et al., 1997) express this C-type lectin. While one population of CD161 positive CD4+ T cells was described (Takahashi et al., 2006), comprising Th17 cells (Cosmi et al., 2008) and a population of pro-inflammatory Treg cells (Pesenacker et al., 2013), two populations expressing either intermediate or high levels are evident amongst CD8+ T cells (Takahashi et al., 2006). The latter was subsequently identified to predominantly express the invariant TCR α chain characteristic of MAIT cells (Martin et al., 2009), namely Vα7.2-Jα33 . Amongst CD161 expressing T lymphocytes most is known regarding CD161++ MAIT cells (which are predominantly CD8+ (Walker et al., 2012)) and CD161+CD4+ Th17 cells, both of which share a type 17 phenotype (Billerbeck et al., 2010; Cosmi et al., 2008; Dusseaux et al., 2011) (see Figure 1-2). In this thesis, other T cell subsets expressing CD161 were investigated, together with and in comparison to the better known CD161++ CD8+ MAIT and CD161+CD4+ T cell populations. In particular the phenotype and function of CD8+ T cells expressing intermediate levels of CD161, the CD161+CD8+ T cell population, was examined.

7.1 T lymphocytes expressing CD161 share common features

7.1.1 Utilising multi-dimensional data

The development of technologies that generate multi-dimensional data, such as mRNA microarrays and CyTOF, has both emphasised phenotypic and functional variation within cell subsets, and revealed relationships across them. For example, Newell *et al.* (2012) utilised CyTOF and unsupervised PCA analysis to illustrate phenotypic diversity amongst

CD8+ T cells, while simultaneously highlighting a high degree of interrelatedness between CD8+ T cell subsets. Chapter 3 represents one of the first phenotypic descriptions of MAIT cells by CyTOF. Despite inclusion of only 'conventional' T cell markers within the 23-parameter panel, rather than the unique markers characteristic of MAIT cells, PCA emphasised the distinctiveness of this population, which segregated within a discrete niche in the spectrum of CD8+ T cell phenotypes.

Whole transcriptome analysis by microarray has further revealed that memory T and B cells display a transcriptional signature that is shared with hematopoietic stem cells (Luckey et al., 2006), and transcripts that distinguish T and B cells are also expressed amongst other lymphocyte cell types (Painter et al., 2011). This indicates that expression patterns and their consequent phenotypes may be shared across previously defined divisions. In a similar way, mRNA microarray data for CD161 positive T cells, including TCRγδ+, CD4+ and both populations of CD8+ T cells, was compared in Chapter 3. Although this was performed in a limited number of donors in each case, and on multiple microarray platforms, stringent normalisation and criteria for significance enabled a CD161++/MAIT cell transcriptional signature to be identified that is enriched in all T cells expressing CD161.

7.1.2 Response to IL-12 and IL-18 is an innate-like characteristic of all CD161 expressing T cells

One of the significantly upregulated genes conserved across CD161 positive T cells of all lineages was IL18Rα. Expression of this receptor was related to the ability of these cells to respond to IL-18 in combination with IL-12, inducing an innate TCR-independent response. Although this has previously been described for CD161++ CD8+ T cells, including MAIT cells (Ussher et al., 2014) and confirmed here for Vα7.2–CD161++, this is the first time this has been described for other T cell subsets – establishing CD161 as a marker of cells with an enhanced 'innate' ability to respond to this stimulus. Furthermore, this identified a previously unappreciated CD161++ subset amongst CD4+ and TCRγδ+ T cells.

7.1.3 Focus on upregulated, rather than downregulated, genes

While this study has focused on upregulated genes, the majority of genes shared between CD161 expressing T cell subsets were downregulated. It would be of interest to further investigate the effect of these downregulated transcripts on cell phenotype. Previously, Turtle et al. (2011) found that multiple proteins that positively regulate TCR signalling were expressed at lower levels in CD161^{hi}, compared with CD161^{lo}, CD8+ T cells, including *ITK* and *MAL*. Interestingly, these genes were also contained within the set of core downregulated genes identified here, being shared between all CD161 positive T cells (Table 3-2). Turtle and colleagues subsequently identified an important role for specific innate cytokines, including IL-12, in inducing proliferation and enabling effector function in these cells. Futhermore, Wencker et al. (2014) recently described murine innate-like TCR$\gamma\delta$+ T cells to be TCR hypo-responsive in the periphery yet to require TCR signalling for development within the thymus. They suggest that innate-like T cells require developmental activation of the TCR which then alters TCR responsiveness, consequently freeing the cells to respond to innate signals, potentially by the induction of high expression of cytokine receptors. Using this new criterion for identification of innate-like lymphocytes they were able to identify an additional innate-like murine TCR$\gamma\delta$+ T cell subset that also responded selectively to IL-12 and IL-18.

7.1.4 CD161 as a co-stimulatory receptor; overcoming the TCR hyporesponsiveness of innate-like lymphocytes

MAIT cells are a member of the innate-like lymphocyte family (Gapin, 2009; Margulies, 2014), and the TCR hypo-responsiveness of this population can be overcome by cytokine-mediated activation or co-stimulation through CD28 (Turtle et al., 2011). CD161 itself has been described to function as a costimulatory receptor, increasing the response of iNKT and MAIT cells to stimulation through the TCR (Exley et al., 1998; Fergusson et al., 2014). Wencker *et al.* (2014) suggest that an enhanced responsiveness to innate cytokine signals is a feature of all innate-like T cells, and is coupled to hypo-responsiveness of the

TCR. CD161 marks T cells with the enhanced ability to respond to innate cytokine signals. The TCR responsiveness of these populations has not been assayed, but could be determined by measuring cytosolic calcium concentrations upon TCR cross-linking, as described (Wencker et al., 2014). If, as suggested, these cells also display TCR hypo-responsiveness, then expression of CD161 may help to overcome the reduced reactivity of the TCR in these innate-like T cells.

7.1.5 TCR signalling and selection of innate-like lymphocytes

This new definition of innate-like lymphocytes, proposed by Wencker *et al.* (2014), identifies the main role of the TCR to be during development, where strong activation via the TCR induces both hypo-responsiveness and the ability to respond to innate cytokine signals. Interestingly, the innate-like TCRγδ+ T cell subset identified by this group to respond selectively to IL-12 plus IL-18 did so without elevated expression of IL18R, with cells responding only poorly to this stimulation in fact expressing higher levels of the receptor. Therefore, response of these T cells to cytokines likely results from both expression of specific cytokine receptors and a pre-programmed effector programme. The transcription factor PLZF is required (Kovalovsky et al., 2008; Savage et al., 2008) and sufficient (Savage et al., 2011) for the innate-like characteristics of iNKT cells. In the absence of PLZF, iNKT cells remained naïve, were unable to secrete IL-4 together with IFNγ, and failed to home to peripheral tissues (Kovalovsky et al., 2008; Savage et al., 2008). Similarly, PLZF expression was required for the innate-like phenotype of a subset of murine TCRγδ+ T cells (Kreslavsky et al., 2009). Interestingly, TCR cross-linking of immature TCRγδ+ thymocytes induced expression of PLZF (Kreslavsky et al., 2009), suggesting that agonist selection may be required for PLZF induction. Recent studies of DN intraepithelial lymphocytes (Mayans et al., 2014; McDonald et al., 2014) suggest a similar role for high levels of TCR signalling during development in programming these cells to home to the intestinal epithelium. Together, this suggests a model analogous to that of natural (n)Treg cells, where a threshold level of self-reactivity may be required for selection of innate-like lymphocytes within the thymus and induction of their innate-like characteristics (Figure 7-1).

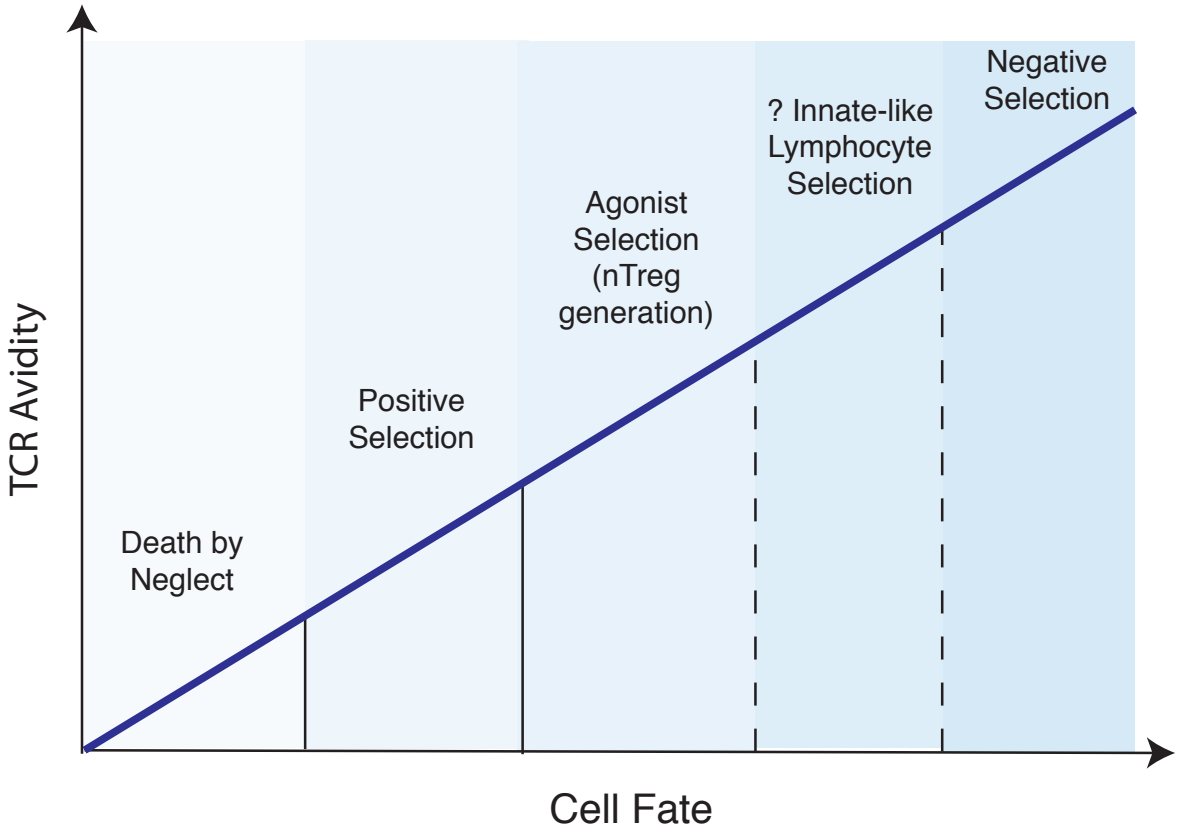

Figure 7-1: Model of agonist selection of innate-like lymphocytes.
The avidity of the TCR (y axis) determines the fate of developing thymocytes (x axis) within the thymus. Various studies suggest that innate-like lymphocytes require strong TCR signals for selection and induction of innate-like characteristics. Adapted from Kurd *et al.* (2014).

7.1.6 Transcriptional control of the CD161 phenotype

While the selection of innate-like lymphocytes and the transcription factors that control their innate-like phenotype are being investigated, what induces the expression of CD161 and its associated phenotype has not yet been determined. A model for the selection of CD161 expressing thymocytes is represented in Figure 7-2. The identification, here, of a transcriptional signature enriched in all T lymphocytes expressing CD161 is strongly indicative of a master transcription factor. Both RORγt (*RORC*) and PLZF (*ZBTB16*) appear likely candidates, both being contained within the core transcription signature of upregulated genes identified in Chapter 3. As described above, PLZF is associated with the innate-like phenotype of iNKT cells (Kovalovsky et al., 2008; Savage et al., 2008), and also that of MAIT cells (Savage et al., 2008; Walker et al., 2012). In particular, PLZF appears to be important in the constitutive memory phenotype of these cells, with PLZF deficient iNKT cells displaying a naïve phenotype (Kovalovsky et al., 2008; Savage et al., 2008), as do transgenic murine MAIT cells which lack PLZF (Martin et al., 2009). CD161 expression is also associated with memory phenotype in all T cell lineages (Maggi et al., 2010; Takahashi et al., 2006). However, the role of PLZF in inducing this memory phenotype may in fact be indirect (Weinreich et al., 2010). Nonetheless CD161 expression is reduced in iNKT, TCRγδ+ and CD8+ T cells in a PLZF deficient patient (Eidson et al., 2011), suggesting a role for this transcription factor in expression of this marker. CD161 expression is also related to production of IL-17 across all T cell subtypes, associated with their expression of RORγt (Maggi et al., 2010), even amongst Treg cells (Pesenacker et al., 2013). Signalling via CD161 may also function to induce a type 17 phenotype (Bai et al., 2014). Furthermore, transduction of CD161−CD4+ T cells with RORγt induced expression of CD161 (Maggi et al., 2010). However, not all CD161 positive cells express significant levels of RORγt or IL-17, with expression restricted to CD161++, and not displayed by CD161+, cells amongst CD8+ T cells (Billerbeck et al., 2010). It also remains to be seen whether Vα7.2− CD161++CD8+ T cells share the ability to secrete IL-17 displayed by MAIT cells (Dusseaux et al., 2011).

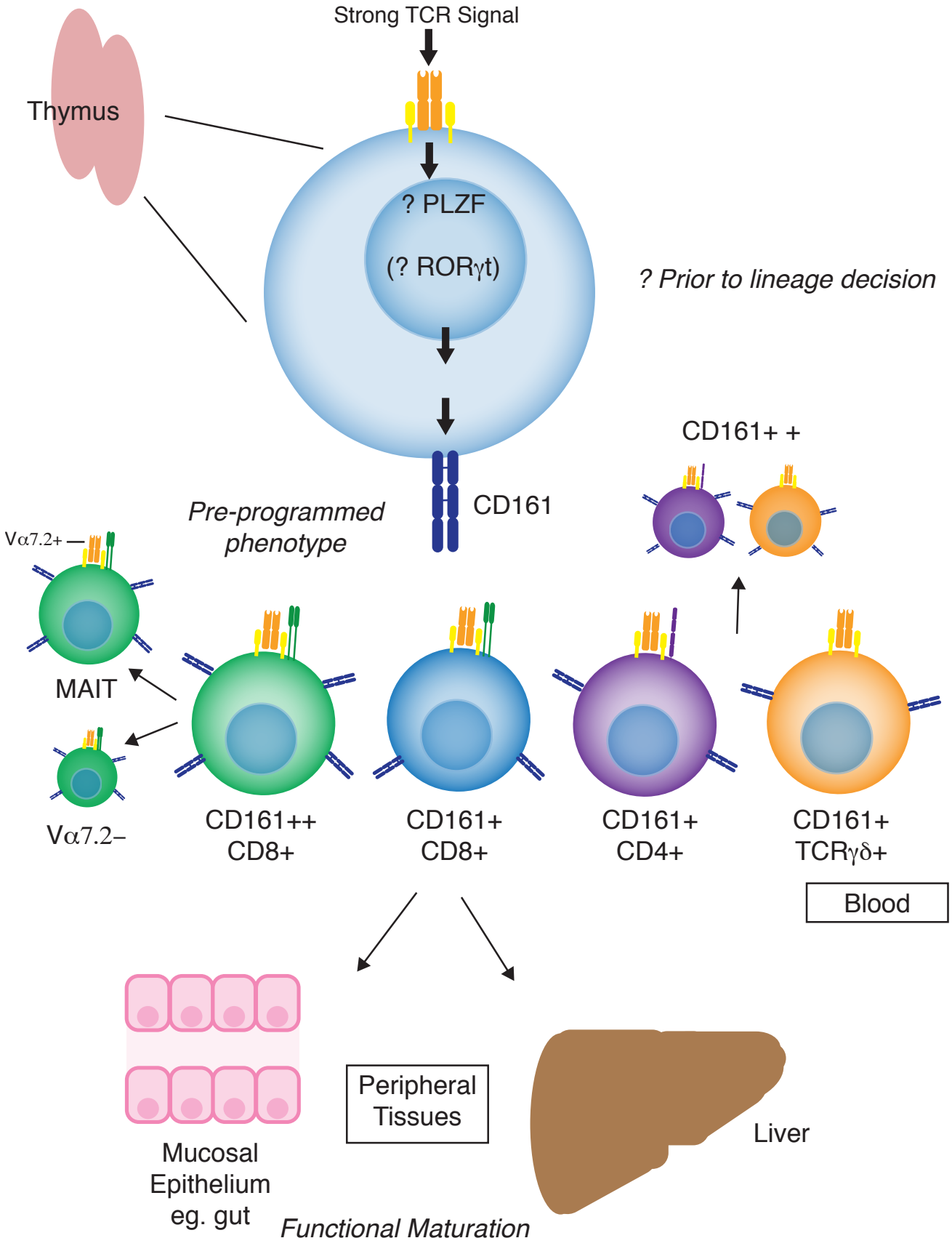
Strong TCR Signal
Thymus
? PLZF
(? RORγt)
? Prior to lineage decision
CD161+ +
CD161
Pre-programmed
phenotype
Vα7.2+
MAIT
Vα7.2–
CD161++
CD8+
CD161+
CD8+
CD161+
CD4+
CD161+
TCRγδ+
Blood
Peripheral
Tissues
Liver
Mucosal
Epithelium
eg. gut
Functional Maturation

Figure 7-2: Model of CD161 expressing lymphocyte selection. The quality of the TCR signal during thymic development induces CD161 expression in certain developing thymocytes, potentially through expression of specific transcription factors. This TCR signal may be conferred by differing antigen presenting cells and molecules, for example Vα7.2+ MAIT cells are thought to be selected by MR1-expressing double positive thymocytes. Expression of CD161 also indicates the programming of these cells with the associated phenotype, including an ability to respond to IL-12 + IL-18. Programming to a "CD161 phenotype"" may even occur prior to CD4/CD8 lineage decisions. Once mature, these lymphocytes enter the bloodstream where, after birth, Vα7.2+ MAIT cells expand from the CD161++CD8+ T cell pool and these populations home to peripheral tissues such as the gut and liver.

IL18Rα, a gene shown here to be highly related to CD161 and the innate-like ability of CD161 positive T cells to respond to cytokines, does not contain binding sites for either of these transcription factors within its promoter[2]. It is possible, therefore, that these transcription factors act indirectly on expression of IL18Rα. However, as demonstrated by Wencker *et al.* (2014) elevated expression of the IL18R is not directly associated with the ability to respond to cytokine stimulation. Further, IL18R expression is acquired during peripheral maturation of MAIT cells within mucosal tissue and the liver, while MAIT cells are already CD161++ in human foetal thymi (Leeansyah et al., 2014), suggesting that expression of these two markers is indeed regulated differently. Although the role for PLZF and RORγt, or other transcription factors, in controlling the CD161 phenotype is difficult to determine within the human system (and the current lack of a direct murine homologue to CD161 rendering it impossible to study within the mouse), techniques such as Chromatin Immunoprecipitation Sequencing (ChIP-Seq) may provide important clues.

[2] http://www.sabiosciences.com/chipqpcrsearch.php?gene=IL18R1&factor=Over+200+TF&species_id=0&ninfo=n&ngene=n&nfactor=y visited: 27.08.14

7.2 CD161+CD8+ T cells

7.2.1 CD161+CD8+ T cells display features of innate-like T lymphocytes

High levels of CD161 have already been described to mark CD8+ T cells with the ability to respond to innate stimulation by IL-12 plus IL-18, whether Vα7.2+ or Vα7.2– (Ussher et al., 2014). This was extended here to include CD8+ T cells expressing lower levels of CD161: the CD161+CD8+ T cell population. Although CD161+CD8+ T cells were polyclonal in terms of their TCR repertoire, and were classically MHC class I-restricted, this population displayed certain other features of innate-like T cells (see Table 1-1). Presence of this population was detected in both the healthy liver and gut in Chapter 4, suggestive of an ability to home to peripheral tissues, and potentially associated with their elevated expression of CXCR6. CD161+CD8+ T cells also expressed higher transcript, and to as lesser extent protein, levels of the transcription factor PLZF than CD8+ T cells lacking CD161; a transcription factor highly connected to innate-like lymphocytes and associated with their memory phenotype (Constantinides et al., 2014; Kovalovsky et al., 2008; Kreslavsky et al., 2009; Prince et al., 2014), as discussed above. Likewise, CD161+CD8+ T cells displayed a memory phenotype in the majority in the adult circulation, although CD161 is not simply an activation or memory marker; memory CD161– CD8+ T cells were also apparent and naïve CD161– CD8+ T cells remained CD161– upon activation, as described in Chapter 5. Furthermore, naïve CD161+CD8+ T cells were present within UCB and appeared pre-programmed to their adult phenotype, already expressing elevated levels of IL18Rα, MDR1 and PLZF.

7.2.2 CD161+CD8+ T cells reflect features of MAIT cells

Naïve CD161++CD8+ T cells are also present within UCB, representing the pre-programmed progenitors of MAIT cells (Walker et al., 2012). Indeed, many of the features pre-programmed within CD161+CD8+ T cells are similarly pre-programmed in this CD161++CD8+ T cell population, including expression of PLZF and IL18Rα. This shared

phenotype was apparent within the adult circulation also, with both mRNA microarray (Chapter 3) and flow cytometric protein analysis (Chapter 4) demonstrating shared expression of many markers by both CD161+ and CD161++/MAIT CD8+ T cells, with expression levels correlating with that of CD161 i.e. CD161++ CD8+ T cells express the highest levels of all markers. Furthermore, Chapter 6 described both populations to express elevated levels of the multidrug efflux pump MDR1 and to efflux the fluorescent substrate Rh123. Thus, CD161+CD8+ T cells reflect many features of MAIT cells (Figure 7-3). However, MAIT cells express low levels of the cytotoxicity effectors perforin and granzyme B in the resting state (Kurioka et al., 2014), while the CD161+CD8+ T cell population was highly enriched for these molecules. Upon activation, MAIT cells upregulate both granzyme B and perforin and display potent cytotoxicity against antigen-presenting target cells (Kurioka et al., 2014). While CD161+CD8+ T cells were shown here to be equipped for killing, their ability to induce apoptosis of target cells has not yet been assayed.

The majority of work presented here was performed on cells isolated from the circulation. However, both CD161++/MAIT cells and CD161+CD8+ T cells were found within the healthy human liver and gut, indicating a shared propensity to home to peripheral tissues. Analysis of these populations within tissues may reveal differing phenotypes from those described here for circulating cells. MAIT cells were originally described as enriched within the gut (Treiner et al., 2003), and were consequently named as 'mucosally-associated'. However, MAIT cells are more prominently enriched within the human liver, as shown here and elsewhere (Billerbeck et al., 2010; Dusseaux et al., 2011). In contrast, while CD161+CD8+ T cells were a minor population of T cells within the liver, they were the major CD161 expressing CD8+ subset within the gut.

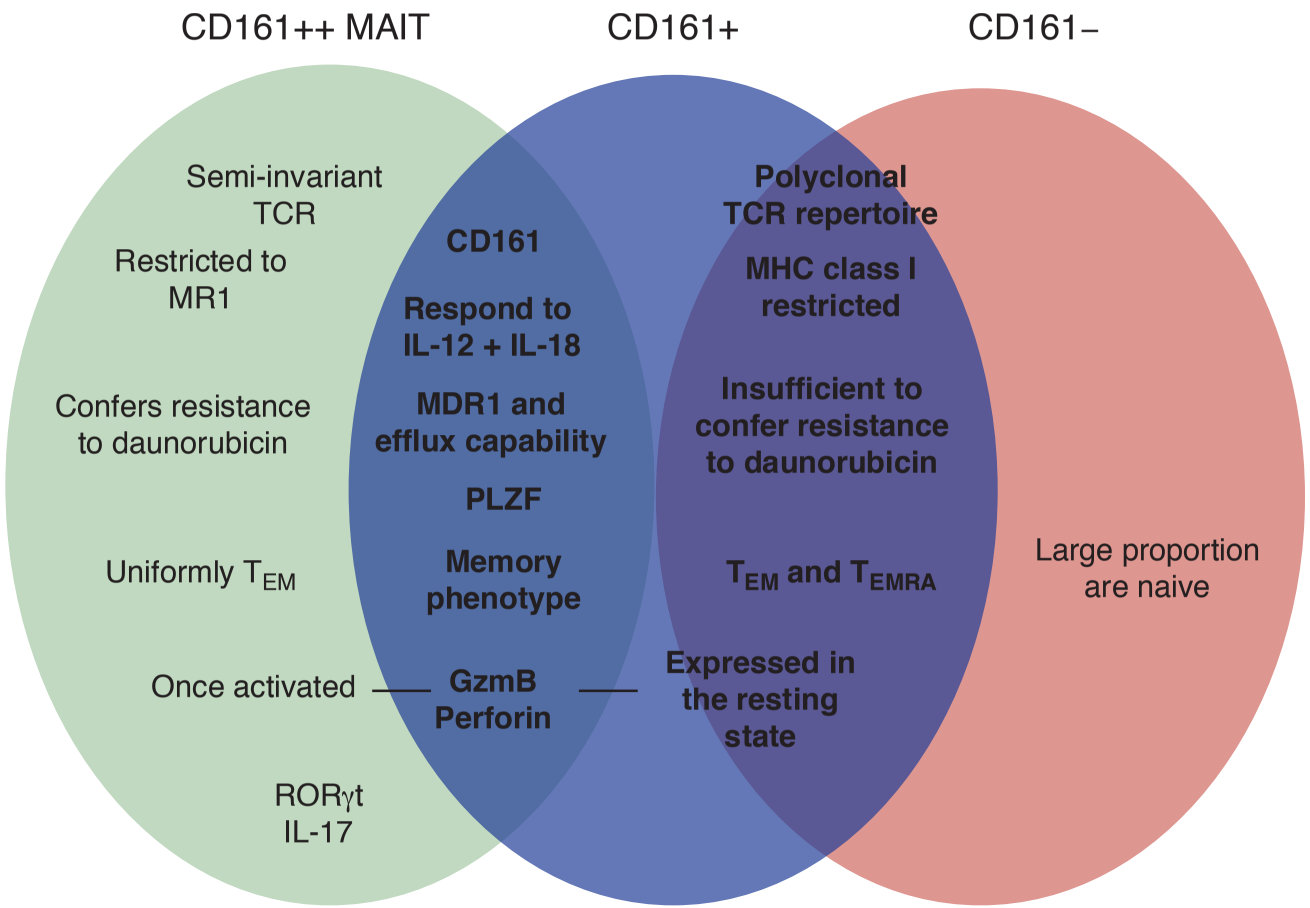

Figure 7-3: CD161+CD8+ T cells lie between CD161++ MAIT and CD161− CD8+ T cells. CD161+CD8+ T cells reflect many of the phenotypic characteristics of MAIT cells, but display a polyclonal TCR repertoire that is highly correlated with that of CD161−CD8+ T cells, suggestive of a developmental relationship. The figure summarises some of the features which are shared between CD161+CD8+ T cells and the other CD8+ T cell subsets.

7.3 CD161 and Disease

7.3.1 CD161+CD8+ T cells and tissue-specific diseases

The presence of CD161+CD8+ T cells within the healthy gut suggests a role for these cells in immune homeostasis within this tissue, which comes into contact with a large number of foreign and commensal antigens daily. Indeed, inflammation of the bowel is concomitant with an influx of CD161−CD8+ T cells, such as seen in IBD (shown in Chapter 4), and hence a dilution of CD161+CD8+ T cells. This is in contrast to CD161+CD4+ T cells, which also represent both a circulating and gut-resident population, but are the predominant subset of infiltrating CD4+ T cells in CD (Kleinschek et al., 2009). MAIT cells are also enriched in inflamed, compared to healthy, tissue in CD, with a specific reduction in CD8+ MAIT cells from the peripheral blood (Serriari et al., 2014). This implicates CD161++ MAIT and CD161+CD4+ T cells, and likely their production of IL-17 which is increased in each case (Kleinschek et al., 2009; Serriari et al., 2014), in the pathogenesis of inflammation of the bowel, while CD161+CD8+ T cells are more associated with a healthy, balanced intestinal environment.

CD161+CD8+ T cells were only a minor population within the liver, yet a role for this population in hepatotropic infections is implied by their enrichment in HCV and HBV-targeting CTL populations (Northfield et al., 2008). The significance of this enrichment was investigated here by examining the phenotype of this population both in health and in chronic HCV infection. In health, a higher proportion of the CD161+CD8+ population expressed cytotoxic effectors perforin and granzyme B than CD161−. While expression of both these markers was significantly reduced within the CD161− population in the peripheral blood of HCV patients, the CD161+CD8+ population maintained expression of both. This may prove important in the cytotoxic killing of HCV-infected cells, which contributes both to control of viral replication and to liver damage (Klenerman and Thimme, 2012). However, CD8+ T cells may also control replication by non-cytolytic mechanisms, especially by the secretion of IFNγ (Klenerman and Thimme, 2012). In healthy blood, the CD161+CD8+ population was polyfunctional in regards to cytokine production – particularly in terms of IFNγ and IL-2 dual secretion. In chronic HCV

infection, the proportion of dual-secreting CD161+CD8+ T cells was significantly reduced, which may be associated with T cell exhaustion (Klenerman and Thimme, 2012), although the expression of exhaustion markers, such as programmed death 1 (PD1) (Wherry et al., 2007), was not examined here. If proven to be important in controlling viral replication, then inducing enrichment of CD161+ anti-viral cells with these functional attributes by vaccination strategies would be a logical objective. In strategies utilising viral vectors already under investigation, CD161+ anti-HCV cells were induced that expressed higher levels of granzyme B, but not of perforin, compared to viral-specific CD161– CD8+ T cells.

Importantly, whether CD161+CD8+ T cells are in fact recruited to the liver upon HCV infection was not determined in this study. Interestingly, the majority of CD8+ T cells in the infected liver are not HCV-specific (Klenerman and Thimme, 2012). MAIT cells are markedly enriched within the liver during chronic hepatitis (Billerbeck et al., 2010), and while they are not anti-viral, a role in viral infections such as these is enabled due to their ability to make TCR-independent responses to IL-12 and IL-18 (Ussher et al., 2014).

7.3.2 A common pathway of activation: protective or pathogenic?

As demonstrated in Chapter 3, all CD161 positive T cells possess the ability to respond to stimulation by IL-12 plus IL-18. This enables these cell subsets to respond (by production of IFNγ) in any pathological setting where IL-12 and IL-18 is produced by activated APCs (eg. Rintahaka et al. 2008). In the infectious setting, IFNγ production induced by IL-12 and IL-18 was of major importance in control of dengue virus infection (Fagundes et al., 2011). Further, the control of *Mycobacterium bovis* BCG growth by MAIT cells was dependent on IFNγ, and IL-12 secretion by infected macrophages, while recognition of MR1 played only a minor role (Chua et al., 2012). This pathway may also be active in certain autoimmune diseases. For example, macrophages from the synovium of rheumatoid arthritis (RA) patients produced IL-18 which synergistically enhanced IL-12-induced IFNγ production by T cells (Yamamura et al., 2001). In this case, activation of this pathway appears pathogenic rather than protective. This pathway, therefore, may provide an appealing therapeutic opportunity in which multiple cellular mediators can be

targeted simultaneously, but with more specificity than broadly immunosuppressive drugs such as leflunomide used in the treatment of RA (Lorenz, 2003).

7.3.3 Challenges to therapy posed by expression of MDR1

The success of such treatments, and indeed that of other immunosuppressive drugs, is hampered by the resistance conferred through expression of MDR1, capable of effluxing a variety of drugs from the cellular cytoplasm to the extracellular space (Gottesman et al., 2002). In Chapter 6, both CD161++ and CD161+ CD8+ T cells were shown to express functional MDR1, with expression sufficient to render CD161++ MAIT cells resistant to daunorubicin and other immunosuppressive drugs *in vitro*. Whether these results accurately reflect the case *in vivo* remains to be determined. MDR1 (*ABCB1*) was also contained within the core upregulated genes enriched in all CD161 expressing T cells, although whether CD161+ CD4+ and TCRγδ+ T cells express functional MDR1 capable of protecting these cells from various drugs was not investigated. However, it was recently shown that a subset of Th17 cells expressed MDR1 and that these cells were resistant to steroids, a 'first-line' therapy in the treatment of many autoimmune diseases (Ramesh et al., 2014). Furthermore, not only were these drugs ineffectual against these T cells, but they specifically selected for this population within mixed T cell cultures, with the proportion of MDR1+ CD4+ T cells increasing in steroid-treated cultures (Ramesh et al., 2014). If, as suggested (Annibali et al., 2011; Kleinschek et al., 2009; Poggi et al., 1999b), CD161 positive T cells are pathogenic in autoimmune disease, then MDR1-conferred resistance to the steroids customarily used in their treatment would not only account for the frequent occurrence of steroid-resistant disease, but further result in an enrichment in the pathology-causing cell population. Thus, determining the MDR1 activity, and further the function of CD161 expressing T cells, in both health and disease becomes vitally important.

7.4 Concluding Remarks

Characterisation of lymphocytes traditionally relies on the identification of unique markers, differentially expressed by cells with correspondingly disparate functions. In contrast to this, the marker CD161 is expressed by subsets of cells across these previously defined divisions. Although the function of CD161 itself has remained controversial, it has been extensively used as a marker of a type 17 phenotype, expressed by IL-17 producing CD161++ MAIT, CD161+ Th17, CD161+ TCRγδ+, and even CD161+ Treg cells. This, together with the expression of CD161 by pre-committed precursors in UCB and thymocytes, suggested that CD161 may be a marker of a distinct transcriptional, phenotypic, and potentially also functional, programme. In agreement with this, this thesis describes CD161 to mark cells enriched for a transcriptional signature across CD4+, CD8+ and TCRγδ+ T cells, which included expression of genes such as *CXCR6*, *IL18Rα* and *ABCB1* (MDR1). However, the transcriptional regulator(s) which control the expression of this phenotype, of which CD161 is a marker, remains to be defined. While CD161 has previously been described to mark cells with potential to secrete IL-17 (Maggi et al., 2010), it has been shown here to also mark cells with the innate ability to respond to cytokine stimulation, being induced to produce IFNγ by a combination of IL-12 plus IL-18. The potential of IL-12 and IL-18 to specifically induce additional effector functions requires further investigation. The CD161+CD4+ population includes Th17 cells (Cosmi et al., 2008) and Treg cells (Pesenacker et al., 2013) both of which display IL-17 secretion, but which have not been distinguished from the bulk population here. Therefore it is not known whether these subsets display an equal ability to respond to specific stimulation by IL-12 plus IL-18. However, the CD161+CD8+ T cell population, which lacks IL-17 production (Billerbeck et al., 2010), did respond to cytokine stimulation. The phenotype and function of this population had not previously been described, but is explored in depth within, to reveal a memory population with potent effector functions that reflect characteristics of CD161++ MAIT cells. Furthermore, this phenotype was pre-programmed and present in naïve precursors within UCB. The exact pathway of development of this population has not been fully elucidated, although it was clear that CD161 expression is not easily induced amongst the CD161−CD8+ population. The

significance of MDR1 expression by this population has also been explored, but not fully determined. However, shared, albeit higher, expression of MDR1 by MAIT cells rendered them functionally resistant to immunosuppressive drugs. This opens the possibility that these cells, both MAIT and CD161+CD8+, remain pathological in disease settings where treatment is rendered ineffective due to expression of MDR1. Having determined many of the features of the CD161+CD8+ T cell population, their role in various disease settings remains to be determined. Their ability to respond in an antigen-independent manner, as indeed is shared by other CD161 expressing lymphocytes, renders their potential impact to be both wide and significant.

References

Ahmed, R., Bevan, M.J., Reiner, S.L., Fearon, D.T., 2009. The precursors of memory: models and controversies. Nat. Rev. Immunol. 9, 662–8.

Aita, T., Yamamura, M., Kawashima, M., Okamoto, A., 2004. Expression of Interleukin 12 Receptor (IL-12R) and IL-18R on CD4+ T Cells from Patients with Rheumatoid Arthritis. J. Rheumatol. 31, 448–456.

Aldemir, H., Prod'homme, V., Dumaurier, M.-J., Retiere, C., Poupon, G., Cazareth, J., Bihl, F., Braud, V.M., 2005. Cutting Edge: Lectin-Like Transcript 1 Is a Ligand for the CD161 Receptor. J. Immunol. 175, 7791–7795.

Alves, N.L., Hooibrink, B., Arosa, F.A., Lier, A.W. Van, 2003. IL-15 induces antigen-independent expansion and differentiation of human naive CD8+ T cells in vitro. Blood 102, 2541–2546.

Annibali, V., Ristori, G., Angelini, D.F., Serafini, B., Mechelli, R., Cannoni, S., Romano, S., Paolillo, A., Abderrahim, H., Diamantini, A., Borsellino, G., Aloisi, F., Battistini, L., Salvetti, M., 2011. CD161(high)CD8+T cells bear pathogenetic potential in multiple sclerosis. Brain 134, 542–54.

Annunziato, F., Cosmi, L., Santarlasci, V., Maggi, L., Liotta, F., Mazzinghi, B., Parente, E., Filì, L., Ferri, S., Frosali, F., Giudici, F., Romagnani, P., Parronchi, P., Tonelli, F., Maggi, E., Romagnani, S., 2007. Phenotypic and functional features of human Th17 cells. J. Exp. Med. 204, 1849–1861.

Appay, V., van Lier, R. a W., Sallusto, F., Roederer, M., 2008. Phenotype and function of human T lymphocyte subsets: consensus and issues. Cytometry. A 73, 975–83.

Arase, H., Arase, N., Ogasawara, K., 1992. An NK1.1+ CD4+CD8- single-positive thymocyte subpopulation that expresses a highly skewed T-cell antigen receptor Vbeta family. Proc. Natl. Acad. Sci. 89, 6506–6510.

Ariotti, S., Hogenbirk, M.A., Dijkgraaf, F.E., Visser, L.L., Hoekstra, M.E., Song, J.-Y., Jacobs, H., Haanen, J.B., Schumacher, T.N., 2014. Skin-resident memory CD8+ T cells trigger a state of tissue-wide pathogen alert. Science (80-.). DOI: 10.1126/science.1254803.

Ashida, K., Terada, T., Kitamura, Y., Kaibara, N., 1998. Expression of E-cadherin, alpha-catenin, beta-catenin, and CD44 (standard and variant isoforms) in human cholangiocarcinoma: an immunohistochemical study. Hepatology 27, 974–82.

Aust, J.G., Gays, F., Mickiewicz, K.M., Buchanan, E., Brooks, C.G., 2009. The expression and function of the NKRP1 receptor family in C57BL/6 mice. J. Immunol. 183, 106–16.

Azzoni, L., Zatsepina, O., Abebe, B., Bennett, I.M., Kanakaraj, P., Perussia, B., 1998. Differential transcriptional regulation of CD161 and a novel gene, 197/15a, by IL-2, IL-15, and IL-12 in NK and T cells. J. Immunol. 161, 3493–500.

Bachmann, M., Horn, K., Poleganov, M.A., Paulukat, J., Nold, M., Pfeilschifter, J., Mühl, H., 2006. Interleukin-18 secretion and Th1-like cytokine responses in human peripheral blood mononuclear cells under the influence of the toll-like receptor-5 ligand flagellin. Cell. Microbiol. 8, 289–300.

Bai, A., Moss, A., Kokkotou, E., Usheva, A., Sun, X., Cheifetz, A., Zheng, Y., Longhi, M.S., Gao, W., Wu, Y., Robson, S.C., 2014. CD39 and CD161 Modulate Th17 Responses in Crohn's Disease. J. Immunol. 193, doi:10.4049/jimmunol.1400346.

Barnes, E., Folgori, A., Capone, S., Swadling, L., Aston, S., Kurioka, A., Meyer, J., Huddart, R., Smith, K., Townsend, R., Brown, A., Antrobus, R., Ammendola, V., Naddeo, M., O'Hara, G., Willberg, C., Harrison, A., Grazioli, F., Esposito, M.L., Siani, L., Traboni, C., Oo, Y.Y., Adams, D., Hill, A., Colloca, S., Nicosia, A., Cortese, R., Klenerman, P., 2012. Novel adenovirus-based vaccines induce broad and sustained T cell responses to HCV in man. Sci. Transl. Med. 4, 1–11.

Battistini, L., Borsellino, G., Sawicki, G., Poccia, F., Salvetti, M., Ristori, G., Brosnan, C.F., 1997. Phenotypic and cytokine analysis of human peripheral blood gamma delta T cells expressing NK cell receptors. J. Immunol. 159, 3723–30.

Beckman, E.M., Melin, A., Behar, S.M., Sieling, P.A., Chatterjee, D., Furlong, S.T., Matsumoto, R., Rosat, J.P., Modlin, R., Porcelli, S.A., 1996. CD1c Restricts Responses of Mycobacteria-Specific T Cells. J. Immunol. 157, 2795–2803.

Bendelac, A., Lantz, O., Quimby, M.E., Yewdell, J.W., Bennink, J.R., Brutkiewicz, R.R., 1995. CD1 recognition by mouse NK1+ T lymphocytes. Science 268, 863–5.

Bendelac, A., Savage, P.B., Teyton, L., 2007. The biology of NKT cells. Annu. Rev. Immunol. 25, 297–336.

Betts, M.R., Nason, M.C., West, S.M., De Rosa, S.C., Migueles, S. a, Abraham, J., Lederman, M.M., Benito, J.M., Goepfert, P. a, Connors, M., Roederer, M., Koup, R. a, 2006. HIV nonprogressors preferentially maintain highly functional HIV-specific CD8+ T cells. Blood 107, 4781–9.

Billerbeck, E., Kang, Y.-H., Walker, L., Lockstone, H., Grafmueller, S., Fleming, V., Flint, J., Willberg, C.B., Bengsch, B., Seigel, B., Ramamurthy, N., Zitzmann, N., Barnes, E.J., Thevanayagam, J., Bhagwanani, A., Leslie, A., Oo, Y.H., Kollnberger, S., Bowness, P., Drognitz, O., Adams, D.H., Blum, H.E., Thimme, R., Klenerman, P., 2010. Analysis of CD161 expression on human CD8+ T cells defines a distinct functional subset with tissue-homing properties. Proc. Natl. Acad. Sci. U. S. A. 107, 3006–11.

Boles, K.S., Barten, R., Kumaresan, P.R., Trowsdale, J., Mathew, P.A., 1999. Cloning of a new lectin-like receptor expressed on human NK cells. Immunogenetics 50, 1–7.

Bonneville, M., O'Brien, R.L., Born, W.K., 2010. Gammadelta T cell effector functions: a blend of innate programming and acquired plasticity. Nat. Rev. Immunol. 10, 467–478.

Borst, P., Schinkel, A.H., Smit, J.J.M., Wagenaar, E., Deemter, L.V.A.N., Smith, A.J., Eijdems, E.W.H.M., 1994. Classical and novel forms of multidrug resistance and the physiological functions of P-glycoprotein in mammals. Pharmac. Ther. 60, 289–299.

Bouneaud, C., Garcia, Z., Kourilsky, P., Pannetier, C., 2005. Lineage relationships, homeostasis, and recall capacities of central- and effector-memory CD8 T cells in vivo. J. Exp. Med. 201, 579–90.

Bryceson, Y.T., March, M.E., Ljunggren, H.-G., Long, E.O., 2006. Activation, coactivation, and costimulation of resting human natural killer cells 214, 73–91.

Butcher, S., Arney, K.L., Cook, G.P., 1998. MAFA-L, an ITIM-containing receptor encoded by the human NK cell gene complex and expressed by basophils and NK cells. Eur. J. Immunol. 28, 3755–62.

Caligiuri, M.A., 2008. Human natural killer cells. Blood 112, 461–9.

Carlyle, J.R., Jamieson, A.M., Gasser, S., Clingan, C.S., Arase, H., Raulet, D.H., 2004. Missing self-recognition of Ocil/Clr-b by inhibitory NKR-P1 natural killer cell receptors. Proc. Natl. Acad. Sci. U. S. A. 101, 3527–3532.

Casorati, G., De Libero, G., Lanzavecchia, A., Migonet, N., 1989. Molecular Analysis of Human gamma/delta+ Clones from Thymus and Peripheral Blood. J. Exp. Med. 170, 1521–1535.

Cepek, K.L., Shaw, S.K., Parker, C.M., Russell, G.J., Morrow, J.S., Rimm, D.L., Brenner, M.B., 1994. Adhesion between epithelial cells and T lymphocytes mediated by E-cadherin and the alphaEbeta7 integrin. Nature 372, 190–193.

Chaix, J., Tessmer, M.S., Hoebe, K., Fuseri, N., Ryffel, B., Dalod, M., Alexopoulou, L., Beutler, B., Brossay, L., Vivier, E., Walzer, T., 2008. Cutting Edge: Priming of NK Cells by IL-18. J. Immunol. 181, 1627–1631.

Chaudhary, P.M., Roninson, I.B., 1991. Expression and activity of P-glycoprotein, a multidrug efflux pump, in human hematopoietic stem cells. Cell 66, 85–94.

Chowers, Y., Holtmeier, W., Harwood, J., Morzycka-wroblewska, E., Kagnoff, M.F., 1994. The Vdelta1 T Cell Receptor Repertoire in Human Small Intestine and Colon. J. Exp. Med. 180, 183–190.

Chua, W.-J., Truscott, S.M., Eickhoff, C.S., Blazevic, A., Hoft, D.F., Hansen, T.H., 2012. Polyclonal mucosa-associated invariant T cells have unique innate functions in bacterial infection. Infect. Immun. 80, 3256–67.

Constantinides, M.G., McDonald, B.D., Verhoef, P.A., Bendelac, A., 2014. A committed precursor to innate lymphoid cells. Nature 508, 397–401.

Corbett, A.J., Eckle, S.B.G., Birkinshaw, R.W., Liu, L., Patel, O., Mahony, J., Chen, Z., Reantragoon, R., Meehan, B., Cao, H., Williamson, N.A., Strugnell, R.A., Van Sinderen, D., Mak, J.Y.W., Fairlie, D.P., Kjer-Nielsen, L., Rossjohn, J., McCluskey, J., 2014. T-cell activation by transitory neo-antigens derived from distinct microbial pathways. Nature 509, 361–5.

Cosgrove, C., Ussher, J.E., Rauch, A., Gärtner, K., Kurioka, A., Hühn, M.H., Adelmann, K., Kang, Y.-H., Fergusson, J.R., Simmonds, P., Goulder, P., Hansen, T.H., Fox, J., Günthard, H.F., Khanna, N., Powrie, F., Steel, A., Gazzard, B., Phillips, R.E., Frater, J., Uhlig, H., Klenerman, P., 2013. Early and nonreversible decrease of CD161++ /MAIT cells in HIV infection. Blood 121, 951–61.

Cosmi, L., De Palma, R., Santarlasci, V., Maggi, L., Capone, M., Frosali, F., Rodolico, G., Querci, V., Abbate, G., Angeli, R., Berrino, L., Fambrini, M., Caproni, M., Tonelli, F., Lazzeri, E., Parronchi, P., Liotta, F., Maggi, E., Romagnani, S., Annunziato, F., 2008. Human interleukin 17–producing cells originate from a CD161+CD4+ T cell precursor. J. Exp. Med. 205, 1903–1916.

Croxford, J.L., Miyake, S., Huang, Y.-Y., Shimamura, M., Yamamura, T., 2006. Invariant V(alpha)19i T cells regulate autoimmune inflammation. Nat. Immunol. 7, 987–94.

Davey, M.S., Morgan, M.P., Liuzzi, A.R., Tyler, C.J., Khan, M.W.A., Szakmany, T., Hall, J.E., Moser, B., Eberl, M., 2014. Microbe-Specific Unconventional T Cells Induce Human Neutrophil Differentiation into Antigen Cross-Presenting Cells. J. Immunol. 193.

De Jong, A., Cheng, T.-Y., Huang, S., Gras, S., Birkinshaw, R.W., Kasmar, A.G., Van Rhijn, I., Peña-Cruz, V., Ruan, D.T., Altman, J.D., Rossjohn, J., Moody, D.B., 2014. CD1a-autoreactive T cells recognize natural skin oils that function as headless antigens. Nat. Immunol. 15, 177–85.

De Santo, C., Arscott, R., Booth, S., Karydis, I., Jones, M., Asher, R., Salio, M., Middleton, M., Cerundolo, V., 2010. Invariant NKT cells modulate the suppressive activity of IL-10-secreting neutrophils differentiated with serum amyloid A. Nat. Immunol. 11, 1039–46.

Dieli, F., Troye-Blomberg, M., Ivanyi, J., Fournié, J.J., Krensky, a M., Bonneville, M., Peyrat, M. a, Caccamo, N., Sireci, G., Salerno, a, 2001. Granulysin-dependent killing of intracellular and extracellular Mycobacterium tuberculosis by Vgamma9/Vdelta2 T lymphocytes. J. Infect. Dis. 184, 1082–5.

Dusseaux, M., Martin, E., Serriari, N., Péguillet, I., Premel, V., Louis, D., Milder, M., Le Bourhis, L., Soudais, C., Treiner, E., Lantz, O., 2011. Human MAIT cells are xenobiotic-resistant, tissue-targeted, CD161hi IL-17-secreting T cells. Blood 117, 1250–9.

Eberl, M., Hintz, M., Reichenberg, A., Kollas, A.-K., Wiesner, J., Jomaa, H., 2003. Microbial isoprenoid biosynthesis and human γδ T cell activation. FEBS Lett. 544, 4–10.

Eidson, M., Wahlstrom, J., Beaulieu, A.M., Zaidi, B., Carsons, S.E., Crow, P.K., Yuan, J., Wolchok, J.D., Horsthemke, B., Wieczorek, D., Sant'Angelo, D.B., 2011. Altered development of NKT cells, γδ T cells, CD8 T cells and NK cells in a PLZF deficient patient. PLoS One 6, e24441.

Exley, M., Garcia, J., Balk, S.P., Porcelli, S., 1997. Requirements for CD1d Recognition by Human Invariant Valpha24+ CD4-CD8- T Cells. J. Exp. Med. 186, 109–120.

Exley, M., Porcelli, S., Furman, M., Garcia, J., Balk, S., 1998. CD161 (NKR-P1A) Costimulation of CD1d-dependent Activation of Human T Cells Expressing Invariant Valpha24JalphaQ T cell Receptor alpha Chains. J. Exp. Med. 188, 867–876.

Fagundes, C.T., Costa, V. V, Cisalpino, D., Amaral, F.A., Souza, P.R.S., Souza, R.S., Ryffel, B., Vieira, L.Q., Silva, T. a, Atrasheuskaya, A., Ignatyev, G., Sousa, L.P., Souza, D.G., Teixeira, M.M., 2011. IFN-γ production depends on IL-12 and IL-18

combined action and mediates host resistance to dengue virus infection in a nitric oxide-dependent manner. PLoS Negl. Trop. Dis. 5, e1449.

Fearon, D.T., Manders, P., Wagner, S.D., 2001. Arrested differentiation, the self-renewing memory lymphocyte, and vaccination. Science 293, 248–50.

Fergusson, J.R., Smith, K.E., Fleming, V.M., Rajoriya, N., Newell, E.W., Simmons, R., Marchi, E., Björkander, S., Kang, Y.-H., Swadling, L., Kurioka, A., Sahgal, N., Lockstone, H., Baban, D., Freeman, G.J., Sverremark-Ekström, E., Davis, M.M., Davenport, M.P., Venturi, V., Ussher, J.E., Willberg, C.B., Klenerman, P., 2014. CD161 Defines a Transcriptional and Functional Phenotype across Distinct Human T Cell Lineages. Cell Rep. 9, 1–14.

Folgori, A., Spada, E., Pezzanera, M., Ruggeri, L., Mele, A., Garbuglia, A.R., Perrone, M.P., Del Porto, P., Piccolella, E., Cortese, R., Nicosia, A., Vitelli, A., 2006. Early impairment of hepatitis C virus specific T cell proliferation during acute infection leads to failure of viral clearance. Gut 55, 1012–9.

Fox, N.J., 1997. Space, sterility and surgery: circuits of hygiene in the operating theatre. Soc. Sci. Med. 45, 649–57.

Fromm, M.F., 2002. The influence of MDR1 polymorphisms on P-glycoprotein expression and function in humans. Adv. Drug Deliv. Rev. 54, 1295–310.

Gadola, S.D., Dulphy, N., Salio, M., Cerundolo, V., 2002. Valpha24-JalphaQ-Independent, CD1d-Restricted Recognition of alpha-Galactosylceramid by Human CD4+ and CD8alphabeta+ T Lymphocytes. J. Immunol. 168, 5516–5520.

Gamadia, L.E., M., van L.E.M., Remmerswaal, E.B.M., Yong, S., Surachno, S., Wertheim-van Dillen, P.M.E., ten Berge, I.J.M., van Lier, R.A.W., 2014. The Size and Phenotype of Virus-Specific T Cell Populations Is Determined by Repetitive Antigenic Stimulation and Environmental Cytokines. J. Immunol. 172, 6107–6114.

Gapin, L., 2009. Where do MAIT cells fit in the family of unconventional T cells? PLoS Biol. 7, e1000070.

Gattinoni, L., Lugli, E., Ji, Y., Pos, Z., Paulos, C.M., Quigley, M.F., Almeida, J.R., Gostick, E., Yu, Z., Carpenito, C., Wang, E., Douek, D.C., Price, D. a, June, C.H., Marincola, F.M., Roederer, M., Restifo, N.P., 2011. A human memory T cell subset with stem cell-like properties. Nat. Med. 17, 1290–7.

Georgel, P., Radosavljevic, M., Macquin, C., Bahram, S., 2011. The non-conventional MHC class I MR1 molecule controls infection by Klebsiella pneumoniae in mice. Mol. Immunol. 48, 769–75.

Giraud, C., Manceau, S., Treluyer, J.-M., 2010. ABC transporters in human lymphocytes: expression, activity and role, modulating factors and consequences for antiretroviral therapies. Expert Opin. Drug Metab. Toxicol. 6, 571–89.

Glimcher, L., Shen, F.W., Cantor, H., 1977. Identification of a Cell-Surface Antigen Selectively Expressed on the Natural Killer Cell. J. Exp. Med. 145, 1–9.

Godfrey, D.I., MacDonald, H.R., Kronenberg, M., Smyth, M.J., Van Kaer, L., 2004. NKT cells: what's in a name? Nat. Rev. Immunol. 4, 231–7.

Gold, M.C., Cerri, S., Smyk-Pearson, S., Cansler, M.E., Vogt, T.M., Delepine, J., Winata, E., Swarbrick, G.M., Chua, W.J., Yu, Y.Y., Lantz, O., Cook, M.S., Null, M.D., Jacoby, D.B., Harriff, M.J., Lewinsohn, D.A., Hansen, T.H., Lewinsohn, D.M., 2010. Human mucosal associated invariant T cells detect bacterially infected cells. Plos Biol. 8, e1000407.

Gold, M.C., Eid, T., Smyk-Pearson, S., Eberling, Y., Swarbrick, G.M., Langley, S.M., Streeter, P.R., Lewinsohn, D.A., Lewinsohn, D.M., 2013. Human thymic MR1-restricted MAIT cells are innate pathogen-reactive effectors that adapt following thymic egress. Mucosal Immunol. 6, 35–44.

Gottesman, M.M., Fojo, T., Bates, S.E., 2002. Multidrug resistance in cancer: role of ATP-dependent transporters. Nat. Rev. Cancer 2, 48–58.

Gould, J., Getz, G., Monti, S., Reich, M., Mesirov, J.P., 2006. Comparative gene marker selection suite. Bioinformatics 22, 1924–5.

Goverman, J., 2009. Autoimmune T cell responses in the central nervous system. Nat. Rev. Immunol. 9, 393–407.

Greathead, L., Metcalf, R., Gazzard, B., Gotch, F., Steel, A., Kelleher, P., 2014. CD8+/CD161++ mucosal-associated invariant T-cell levels in the colon are restored on long-term antiretroviral therapy and correlate with CD8+ T-cell immune activation. AIDS 28, 1690–1692.

Hamann, D., Baars, P.A., Rep, M.H.G., Hooibrink, B., Kerkhof-garde, S.R., Klein, M.R., Lier, R.A.W. Van, 1997. Phenotypic and Functional Separation of Memory and Effector Human CD8+ T Cells. J. Exp. Med. 186, 1407–1418.

Hansmann, L., Groeger, S., von Wulffen, W., Bein, G., Hackstein, H., 2008. Human monocytes represent a competitive source of interferon-alpha in peripheral blood. Clin. Immunol. 127, 252–64.

Harari, A., Dutoit, V., Cellerai, C., Bart, P.-A., Du Pasquier, R. a, Pantaleo, G., 2006. Functional signatures of protective antiviral T-cell immunity in human virus infections. Immunol. Rev. 211, 236–54.

Hayday, A., 2000. [Gamma][Delta] Cells: a Right Time and a Right Place for a Conserved Third Way of Protection. Annu. Rev. Immunol. 18, 975–1026.

Hintz, M., Reichenberg, A., Altincicek, B., Bahr, U., Gschwind, R.M., Kollas, A., Beck, E., Wiesner, J., Eberl, M., Jomaa, H., 2001. Identification of (E)-4-hydroxy-3-methyl-but-2-enyl pyrophosphate as a major activator for human gammadelta T cells in Escherichia coli. FEBS Lett. 509, 317–322.

Holtmeier, W., Pfänder, M., Hennemann, a, Zollner, T.M., Kaufmann, R., Caspary, W.F., 2001. The TCR-delta repertoire in normal human skin is restricted and distinct from the TCR-delta repertoire in the peripheral blood. J. Invest. Dermatol. 116, 275–80.

Huang, S., Martin, E., Kim, S., Yu, L., Soudais, C., Fremont, D.H., Lantz, O., Hansen, T.H., 2009. MR1 antigen presentation to mucosal-associated invariant T cells was highly conserved in evolution. Proc. Natl. Acad. Sci. U. S. A. 106, 8290–5.

Huber, W., von Heydebreck, A., Sultmann, H., Poustka, A., Vingron, M., 2002. Variance stabilization applied to microarray data calibration and to the quantification of differential expression. Bioinforma. suppl. 1, S96–S104.

Iizuka, K., Naidenko, O. V, Plougastel, B.F.M., Fremont, D.H., Yokoyama, W.M., 2003. Genetically linked C-type lectin-related ligands for the NKRP1 family of natural killer cell receptors. Nat. Immunol. 4, 801–7.

Illes, Z., Shimamura, M., Newcombe, J., Oka, N., Yamamura, T., 2004. Accumulation of V 7.2-J 33 invariant T cells in human autoimmune inflammatory lesions in the nervous system. Int. Immunol. 16, 223–230.

Ishihara, S., Nieda, M., Kitayama, J., Osada, T., Yabe, T., Ishikawa, Y., Nagawa, H., Muto, T., Juji, T., 1999. CD8+NKR-P1A+ T cells preferentially accumulate in human liver. Eur. J. Immunol. 29, 2406–2413.

Ivanov, I.I., McKenzie, B.S., Zhou, L., Tadokoro, C.E., Lepelley, A., Lafaille, J.J., Cua, D.J., Littman, D.R., 2006. The Orphan Nuclear Receptor RORγt Directs the Differentiation Program of Proinflammatory IL-17+ T Helper Cells. Cell 126, 1121–1133.

Jiang, X., Clark, R.A., Liu, L., Wagers, A.J., Fuhlbrigge, R.C., Kupper, T.S., 2012. Skin infection generates non-migratory memory CD8+ T(RM) cells providing global skin immunity. Nature 483, 227–31.

Kaech, S.M., Hemby, S., Kersh, E., Ahmed, R., 2002. Molecular and functional profiling of memory CD8 T cell differentiation. Cell 111, 837–51.

Kaech, S.M., Tan, J.T., Wherry, E.J., Konieczny, B.T., Surh, C.D., Ahmed, R., 2003. Selective expression of the interleukin 7 receptor identifies effector CD8 T cells that give rise to long-lived memory cells. Nat. Immunol. 4, 1191–8.

Kaech, S.M., Wherry, E.J., 2007. Heterogeneity and cell-fate decisions in effector and memory CD8+ T cell differentiation during viral infection. Immunity 27, 393–405.

Kalia, V., Sarkar, S., Subramaniam, S., Haining, W.N., Smith, K.A., Ahmed, R., 2010. Prolonged interleukin-2Ralpha expression on virus-specific CD8+ T cells favors terminal-effector differentiation in vivo. Immunity 32, 91–103.

Kang, Y.-H., Seigel, B., Bengsch, B., Fleming, V.M., Billerbeck, E., Simmons, R., Walker, L., Willberg, C.B., Barnes, E.J., Bhagwanani, A., Oo, Y.H., Blum, H.E., Adams, D.H., Thimme, R., Klenerman, P., 2012. CD161(+)CD4(+) T cells are enriched in the liver during chronic hepatitis and associated with co-secretion of IL-22 and IFN-γ. Front. Immunol. 3, 346.

Kedzierska, K., Venturi, V., Field, K., Davenport, M.P., Turner, S.J., Doherty, P.C., 2006. Early establishment of diverse T cell receptor profiles for influenza-specific CD8(+)CD62L(hi) memory T cells. Proc. Natl. Acad. Sci. U. S. A. 103, 9184–9.

Kjer-Nielsen, L., Patel, O., Corbett, A.J., Le Nours, J., Meehan, B., Liu, L., Bhati, M., Chen, Z., Kostenko, L., Reantragoon, R., Williamson, N.A., Purcell, A.W., Dudek, N.L., McConville, M.J., O'Hair, R.A.J., Khairallah, G.N., Godfrey, D.I., Fairlie, D.P., Rossjohn, J., McCluskey, J., 2012. MR1 presents microbial vitamin B metabolites to MAIT cells. Nature 491, 717–23.

Kleinschek, M.A., Boniface, K., Sadekova, S., Grein, J., Murphy, E.E., Turner, S.P., Raskin, L., Desai, B., Faubion, W.A., de Waal Malefyt, R., Pierce, R.H., McClanahan, T., Kastelein, R.A., 2009. Circulating and gut-resident human Th17 cells express CD161 and promote intestinal inflammation. J. Exp. Med. 206, 525–34.

Klenerman, P., Thimme, R., 2012. T cell responses in hepatitis C: the good, the bad and the unconventional. Gut 61, 1226–34.

Koo, G.C., Peppard, J.R., 1984. Establishment of monoclonal anti-Nk-1.1 antibody. Hybridoma 3, 301–3.

Kovalovsky, D., Uche, O.U., Eladad, S., Hobbs, R.M., Yi, W., Alonzo, E., Chua, K., Eidson, M., Kim, H.-J., Im, J.S., Pandolfi, P.P., Sant'Angelo, D.B., 2008. The BTB-zinc finger transcriptional regulator PLZF controls the development of invariant natural killer T cell effector functions. Nat. Immunol. 9, 1055–64.

Kreslavsky, T., Savage, A.K., Hobbs, R., Gounari, F., Bronson, R., Pereira, P., Pandolfi, P.P., Bendelac, A., von Boehmer, H., 2009. TCR-inducible PLZF transcription factor required for innate phenotype of a subset of gammadelta T cells with restricted TCR diversity. Proc. Natl. Acad. Sci. U. S. A. 106, 12453–8.

Kronenberg, M., 2005. Toward an understanding of NKT cell biology: progress and paradoxes. Annu. Rev. Immunol. 23, 877–900.

Kurioka, A., Ussher, J.E., Cosgrove, C., Clough, C., Fergusson, J., Smith, K., Kang, Y.-H., Walker, L., Hansen, T., Willberg, C.B., Klenerman, P., 2014. MAIT cells are licensed through granzyme exchange to kill bacterially sensitized targets. Mucosal Immunol. In Press.

Kuttruff, S., Koch, S., Kelp, A., Pawelec, G., Rammensee, H., Steinle, A., 2009. NKp80 defines and stimulates a reactive subset of CD8 T cells. Blood 113, 358–369.

Lanier, L.L., Chang, C., Phillips, J.H., 1994. Human NKRP1A. A disulfide-linked homodimer of the C-type lectin superfamily expressed by a subset of NK and T lymphocytes. J. Immunol. 153, 2417–2428.

Lau, L.L., Jamieson, B.D., Somasundaram, T., Ahmed, R., 1994. Cytotoxic T-cell memory without antigen. Nature 369, 648–652.

Lauer, G.M., Barnes, E., Lucas, M., Timm, J., Ouchi, K., Kim, A.Y., Day, C.L., Robbins, G.K., Casson, D.R., Reiser, M., Dusheiko, G., Allen, T.M., Chung, R.T., Walker, B.D., Klenerman, P., 2004. High resolution analysis of cellular immune responses in resolved and persistent hepatitis C virus infection. Gastroenterology 127, 924–936.

Lauwerys, B.R., Renauld, J.C., Houssiau, F.A., 1999. Synergistic proliferation and activation of natural killer cells by interleukin 12 and interleukin 18. Cytokine 11, 822–30.

Le Bourhis, L., Dusseaux, M., Bohineust, A., Bessoles, S., Martin, E., Premel, V., Coré, M., Sleurs, D., Serriari, N.-E., Treiner, E., Hivroz, C., Sansonetti, P., Gougeon, M.-L., Soudais, C., Lantz, O., 2013. MAIT cells detect and efficiently lyse bacterially-infected epithelial cells. PLoS Pathog. 9, e1003681.

Le Bourhis, L., Martin, E., Péguillet, I., Guihot, A., Froux, N., Coré, M., Lévy, E., Dusseaux, M., Meyssonnier, V., Premel, V., Ngo, C., Riteau, B., Duban, L., Robert, D., Huang, S., Rottman, M., Soudais, C., Lantz, O., 2010. Antimicrobial activity of mucosal-associated invariant T cells. Nat. Immunol. 11, 701–8.

Leeansyah, E., Ganesh, A., Quigley, M.F., Sönnerborg, A., Andersson, J., Hunt, P.W., Somsouk, M., Deeks, S.G., Martin, J.N., Moll, M., Shacklett, B.L., Sandberg, J.K., 2013. Activation, exhaustion, and persistent decline of the antimicrobial MR1-restricted MAIT-cell population in chronic HIV-1 infection. Blood 121, 1124–35.

Leeansyah, E., Loh, L., Nixon, D.F., Sandberg, J.K., 2014. Acquisition of innate-like microbial reactivity in mucosal tissues during human fetal MAIT-cell development. Nat. Commun. 5, 3143.

Lehmann, J., Huehn, J., de la Rosa, M., Maszyna, F., Kretschmer, U., Krenn, V., Brunner, M., Scheffold, A., Hamann, A., 2002. Expression of the integrin alpha E beta 7 identifies unique subsets of CD25+ as well as CD25- regulatory T cells. Proc. Natl. Acad. Sci. U. S. A. 99, 13031–6.

Livak, K.J., Schmittgen, T.D., 2001. Analysis of relative gene expression data using real-time quantitative PCR and the 2(-Delta Delta C(T)) Method. Methods 25, 402–8.

Loh, L., Ivarsson, M.A., Michaëlsson, J., Sandberg, J.K., Nixon, D.F., 2014. Invariant natural killer T cells developing in the human fetus accumulate and mature in the small intestine. Mucosal Immunol. 1–11.

Lorenz, H.-M., 2003. T-cell-activation inhibitors in rheumatoid arthritis. BioDrugs 17, 263–70.

Lucas, M., Vargas-Cuero, A.L., Lauer, G.M., Barnes, E., Willberg, C.B., Semmo, N., Walker, B.D., Phillips, R., Klenerman, P., 2004. Pervasive Influence of Hepatitis C Virus on the Phenotype of Antiviral CD8+ T Cells. J. Immunol. 172, 1744–1753.

Luckey, C.J., Bhattacharya, D., Goldrath, A.W., Weissman, I.L., Benoist, C., Mathis, D., 2006. Memory T and memory B cells share a transcriptional program of self-renewal with long-term hematopoietic stem cells. Proc. Natl. Acad. Sci. U. S. A. 103, 3304–9.

Lyons, A.B., Parish, C.R., 1994. Determination of lymphocyte division by flow cytometry. J. Immunol. Methods 171, 131–7.

Macdonald, H.R., 1995. NK1.1+ T Cell Receptor-alpha/beta+ Cells: New Clues to Their Origin, Specificity, and Function. J. Exp. Med. 182, 633–638.

Mackay, B.Y.C.R., Marston, W.L., Dudler, L., 1990. Naive and memory T cell show distinct pathways of lymphocyte recirculation. J. Exp. Med. 171, 801–817.

Mackay, L.K., Rahimpour, A., Ma, J.Z., Collins, N., Stock, A.T., Hafon, M.-L., Vega-Ramos, J., Lauzurica, P., Mueller, S.N., Stefanovic, T., Tscharke, D.C., Heath, W.R., Inouye, M., Carbone, F.R., Gebhardt, T., 2013. The developmental pathway for CD103(+)CD8+ tissue-resident memory T cells of skin. Nat. Immunol. 14, 1294–301.

Maggi, L., Santarlasci, V., Capone, M., Peired, A., Frosali, F., Crome, S.Q., Querci, V., Fambrini, M., Liotta, F., Levings, M.K., Maggi, E., Cosmi, L., Romagnani, S.,

Annunziato, F., 2010. CD161 is a marker of all human IL-17-producing T-cell subsets and is induced by RORC. Eur. J. Immunol. 40, 2174–81.

Margulies, D., 2014. The in-betweeners: MAIT cells join the innate-like lymphocytes gang. J. Exp. Med. 211, 1501–1502.

Martin, E., Treiner, E., Duban, L., Guerri, L., Laude, H., Toly, C., Premel, V., Devys, A., Moura, I.C., Tilloy, F., Cherif, S., Vera, G., Latour, S., Soudais, C., Lantz, O., 2009. Stepwise development of MAIT cells in mouse and human. Plos Biol. 7, e54.

Masopust, D., Vezys, V., Marzo, A.L., Lefrançois, L., 2001. Preferential localization of effector memory cells in nonlymphoid tissue. Science 291, 2413–7.

Masopust, D., Vezys, V., Wherry, E.J., Barber, D.L., Ahmed, R., 2006a. Cutting Edge: Gut Microenvironment Promotes Differentiation of a Unique Memory CD8 T Cell Population. J. Immunol. 176, 2079–2083.

Masopust, D., Vezys, V., Wherry, E.J., Barber, D.L., Ahmed, R., 2006b. Cutting Edge: Gut Microenvironment Promotes Differentiation of a Unique Memory CD8 T Cell Population. J. Immunol. 176, 2079–2083.

Mathew, P.A., Chuang, S.S., Vaidya, S. V, Kumaresan, P.R., Boles, K.S., Pham, H.-T.K., 2004. The LLT1 receptor induces IFN-gamma production by human natural killer cells. Mol. Immunol. 40, 1157–63.

Matzinger, P., 1994. Tolerance, Danger, and the Extended Family. Annu Rev Immunol 12, 991–1045.

Mayans, S., Stepniak, D., Palida, S.F., Larange, A., Dreux, J., Arlian, B.M., Shinnakasu, R., Kronenberg, M., Cheroutre, H., Lambolez, F., 2014. αβT Cell Receptors Expressed by CD4−CD8αβ− Intraepithelial T Cells Drive Their Fate into a Unique Lineage with Unusual MHC Reactivities. Immunity http://dx.doi.org/10.1016/j.immuni.2014.07.010.

McDonald, B.D., Bunker, J.J., Ishizuka, I.E., Jabri, B., Bendelac, A., 2014. Elevated T Cell Receptor Signaling Identifies a Thymic Precursor to the TCRαβ+CD4−CD8β− Intraepithelial Lymphocyte Lineage. Immunity 41, 219–29.

McGregor, S., Shah, A., Raca, G., Mirza, M.K., Smith, S.M., Anastasi, J., Vardiman, J.W., Hyjek, E., Gurbuxani, S., 2014. PLZF staining identifies peripheral T-cell lymphomas derived from innate-like T cells with TRAV1-2-TRAJ33 TCR-alpha rearrangement. Blood 123, 2742–2743.

Meierovics, A., Yankelevich, W.-J.C., Cowley, S.C., 2013. MAIT cells are critical for optimal mucosal immune responses during in vivo pulmonary bacterial infection. Proc. Natl. Acad. Sci. U. S. A. 110, E3119–28.

Melenhorst, J.J., Lay, M.D.H., Price, D.A., Adams, S.D., Zeilah, J., Sosa, E., Hensel, N.F., Follmann, D., Douek, D.C., Davenport, M.P., Barrett, A.J., 2008. Contribution of TCRbeta Locus and HLA to the Shape of the Mature Human Vbeta Repertoire. J. Immunol. 180, 6484–6489.

Michie, C., McLean, A., Alcock, C., Beverley, P.C.L., 1992. Lifespan of human lymphocyte subsets defined by CD45 isoforms. Nature 360, 264–265.

Migueles, S.A., Laborico, A.C., Shupert, W.L., Sabbaghian, M.S., Rabin, R., Hallahan, C.W., Van Baarle, D., Kostense, S., Miedema, F., McLaughlin, M., Ehler, L., Metcalf, J., Liu, S., Connors, M., 2002. HIV-specific CD8+ T cell proliferation is coupled to perforin expression and is maintained in nonprogressors. Nat. Immunol. 3, 1061–8.

Miyazaki, Y., Miyake, S., Chiba, A., Lantz, O., Yamamura, T., 2011. Mucosal-associated invariant T cells regulate Th1 response in multiple sclerosis. Int. Immunol. 23, 529–35.

Morita, C.T., Verma, S., Aparicio, P., Martinez-A., C., Hergen, S., Brenner, M.B., 1991. Functionally distinct subsets of human gamma delta T cells. Eur. J. Immunol. 21, 2999–3007.

Murali-Krishna, K., Lau, L.L., Sambhara, S., Lemonnier, F., Altman, J., Ahmed, R., 1999. Persistence of Memory CD8 T Cells in MHC Class I-Deficient Mice. Science (80-.). 286, 1377–1381.

Neuenhahn, M., Busch, D.H., 2009. The quest for CD8+ memory stem cells. Immunity 31, 702–4.

Newell, E.W., Sigal, N., Bendall, S.C., Nolan, G.P., Davis, M.M., 2012. Cytometry by time-of-flight shows combinatorial cytokine expression and virus-specific cell niches within a continuum of CD8+ T cell phenotypes. Immunity 36, 142–52.

Neyfakh, A.A., Serpinskaya, A.S., Chervonsky, A. V, Apasov, S.G., Kazarov, A.R., 1989. Multidrug-resistance phenotype of a subpopulation of T-lymphocytes without drug selection. Exp. Cell Res. 185, 496–505.

Nishitsuji, H., Funami, K., Shimizu, Y., Ujino, S., Sugiyama, K., Seya, T., Takaku, H., Shimotohno, K., 2013. Hepatitis C virus infection induces inflammatory cytokines and chemokines mediated by the cross talk between hepatocytes and stellate cells. J. Virol. 87, 8169–78.

Nistala, K., Adams, S., Cambrook, H., Ursu, S., Olivito, B., de Jager, W., Evans, J.G., Cimaz, R., Bajaj-Elliott, M., Wedderburn, L.R., 2010. Th17 plasticity in human autoimmune arthritis is driven by the inflammatory environment. Proc. Natl. Acad. Sci. U. S. A. 107, 14751–6.

Northfield, J.W., Kasprowicz, V., Lucas, M., Kersting, N., Bengsch, B., Kim, A., Phillips, R.E., Walker, B.D., Thimme, R., Lauer, G., Klenerman, P., 2008. CD161 expression on hepatitis C virus-specific CD8+ T cells suggests a distinct pathway of T cell differentiation. Hepatology 47, 396–406.

O'Keeffe, J., Doherty, D.G., Kenna, T., Sheahan, K., O'Donoghue, D.P., Hyland, J.M., O'Farrelly, C., 2004. Diverse populations of T cells with NK cell receptors accumulate in the human intestine in health and in colorectal cancer. Eur. J. Immunol. 34, 2110–9.

Painter, M.W., Davis, S., Hardy, R.R., Mathis, D., Benoist, C., 2011. Transcriptomes of the B and T lineages compared by multiplatform microarray profiling. J. Immunol. 186, 3047–57.

Paliard, X., de Waal Malefijt, R., Yssel, H., Blanchard, D., Chrétien, I., Abrams, J., de Vries, J., Spits, H., 1988. Simultaneous production of IL-2, IL-4, and IFN-gamma by activated human CD4+ and CD8+ T cell clones. J. Immunol. 141, 849–55.

Papagno, L., Spina, C. a, Marchant, A., Salio, M., Rufer, N., Little, S., Dong, T., Chesney, G., Waters, A., Easterbrook, P., Dunbar, P.R., Shepherd, D., Cerundolo, V., Emery, V., Griffiths, P., Conlon, C., McMichael, A.J., Richman, D.D., Rowland-Jones, S.L., Appay, V., 2004. Immune activation and CD8+ T-cell differentiation towards senescence in HIV-1 infection. PLoS Biol. 2, 0173–0185.

Park, S.H., Benlagha, K., Lee, D., Balish, E., Bendelac, A., 2000. Unaltered phenotype, tissue distribution and function of Valpha14(+) NKT cells in germ-free mice. Eur. J. Immunol. 30, 620–5.

Parker, C.M., Groh, V., Band, H., Porcelli, S. a, Morita, C., Fabbi, M., Glass, D., Strominger, J.L., Brenner, M.B., 1990. Evidence for extrathymic changes in the T cell receptor gamma/delta repertoire. J. Exp. Med. 171, 1597–612.

Pesenacker, A.M., Bending, D., Ursu, S., Wu, Q., Nistala, K., Wedderburn, L.R., 2013. CD161 defines the subset of FoxP3+ T cells capable of producing proinflammatory cytokines. Blood 121, 2647–2658.

Peterfalvi, A., Gomori, E., Magyarlaki, T., Pal, J., Banati, M., Javorhazy, A., Szekeres-Bartho, J., Szereday, L., Illes, Z., 2008. Invariant Valpha7.2-Jalpha33 TCR is expressed in human kidney and brain tumors indicating infiltration by mucosal-associated invariant T (MAIT) cells. Int. Immunol. 20, 1517–25.

Platanias, L.C., 2005. Mechanisms of type-I- and type-II-interferon-mediated signalling. Nat. Rev. Immunol. 5, 375–86.

Plougastel, B., Dubbelde, C., Yokoyama, W.M., 2001a. Cloning of Clr, a new family of lectin-like genes localized between mouse Nkrp1a and Cd69. Immunogenetics 53, 209–14.

Plougastel, B., Matsumoto, K., Dubbelde, C., Yokoyama, W.M., 2001b. Analysis of a 1-Mb BAC contig overlapping the mouse Nkrp1 cluster of genes: cloning of three new Nkrp1 members, Nkrp1d, Nkrp1e, and Nkrp1f. Immunogenetics 53, 592–8.

Poggi, A., Costa, P., Tomasello, E., Moretta, L., 1998. IL-12-induced up-regulation of NKRP1A expression in human NK cells and consequent NKRP1A-mediated down-regulation of NK cell activation. Eur. J. Immunol. 28, 1611–1616.

Poggi, A., Costa, P., Zocchi, M.R., Moretta, L., 1997. Phenotypic and functional analysis of CD4+ NKRP1A+ human T lymphocytes. Direct evidence that the NKRP1A molecule is involved in transendothelial migration. Eur. J. Immunol. 27, 2345–50.

Poggi, A., Zocchi, M.R., Costa, P., Ferrero, E., Borsellino, G., Placido, R., Galgani, S., Salvetti, M., Gasperini, C., Ristori, G., Brosnan, C.F., Battistini, L., 1999a. IL-12-mediated NKRP1A up-regulation and consequent enhancement of endothelial transmigration of V delta 2+ TCR gamma delta+ T lymphocytes from healthy donors and multiple sclerosis patients. J. Immunol. 162, 4349–4354.

Poggi, A., Zocchi, M.R., Costa, P., Ferrero, E., Borsellino, G., Placido, R., Galgani, S., Salvetti, M., Gasperini, C., Ristori, G., Brosnan, C.F., Battistini, L., 1999b. IL-12-

Mediate NKRP1A Up-Regulation and Consequent Enhancement of Endothelial Transmigration of Vdelta2+ TCRgammadelta+ T Lymphocytes from Healthy Donors and Multiple Sclerosis Patients. J. Immunol. 162, 4349–4354.

Porcelli, S., Yockey, C.E., Brenner, M.B., Balk, S.P., 1993. Analysis of T cell antigen receptor (TCR) expression by human peripheral blood CD4-8- alpha/beta T cells demonstrates preferential use of several V beta genes and an invariant TCR alpha chain. J. Exp. Med. 178, 1–16.

Pozo, D., Vales-Gomez, M., Mavaddat, N., Williamson, S.C., Chisholm, S.E., Reyburn, H., 2006. CD161 (Human NKR-P1A) Signaling in NK Cells Involves the Activation of Acid Sphingomyelinase. J. Immunol. 176, 2397–2406.

Prince, A.L., Watkin, L.B., Yin, C.C., Selin, L.K., Kang, J., Schwartzberg, P.L., Berg, L.J., 2014. Innate PLZF+CD4+ αβ T Cells Develop and Expand in the Absence of Itk. J. Immunol. 193, 673–87.

Qin, G., Mao, H., Zheng, J., Sia, S.F., Liu, Y., Chan, P.-L., Lam, K.-T., Peiris, J.S.M., Lau, Y.-L., Tu, W., 2009. Phosphoantigen-expanded human gammadelta T cells display potent cytotoxicity against monocyte-derived macrophages infected with human and avian influenza viruses. J. Infect. Dis. 200, 858–65.

Rajoriya, N., Fergusson, J.R., Leithead, J., Klenerman, P., 2014. Gamma delta T-lymphocytes in hepatitis C and chronic liver disease Gamma delta T-lymphocytes in hepatitis C and chronic liver disease. Front. Immunol. 5, doi: 10.3389/fimmu.2014.00400.

Ramesh, R., Kozhaya, L., McKevitt, K., Djuretic, I.M., Carlson, T.J., Quintero, M.A., McCauley, J.L., Abreu, M.T., Unutmaz, D., Sundrud, M.S., 2014. Pro-inflammatory human Th17 cells selectively express P-glycoprotein and are refractory to glucocorticoids. J. Exp. Med. 211, 89–104.

Reantragoon, R., Corbett, A.J., Sakala, I.G., Gherardin, N.A., Furness, J.B., Chen, Z., Eckle, S.B.G., Uldrich, A.P., Birkinshaw, R.W., Patel, O., Kostenko, L., Meehan, B., Kedzierska, K., Liu, L., Fairlie, D.P., Hansen, T.H., Godfrey, D.I., Rossjohn, J., McCluskey, J., Kjer-Nielsen, L., 2013. Antigen-loaded MR1 tetramers define T cell receptor heterogeneity in mucosal-associated invariant T cells. J. Exp. Med. 210, 2305–20.

Riegert, P., Wanner, V., Bahram, S., 1998. Genomics, Isoforms, Expression, and Phylogeny of the MHC Class I-Related MR1 Gene. J. Immunol. 161, 4066–4077.

Ringnér, M., 2008. What is principal component analysis ? Nat. Biotechnol. 26, 303–304.

Rintahaka, J., Wiik, D., Kovanen, P.E., Alenius, H., Matikainen, S., 2008. Cytosolic Antiviral RNA Recognition Pathway Activates Caspases 1 and 3. J. Immunol. 180, 1749–1757.

Rosen, D.B., Bettadapura, J., Alsharifi, M., Mathew, P.A., Warren, H.S., Lanier, L.L., 2005. Cutting Edge: Lectin-Like Transcript-1 Is a Ligand for the Inhibitory Human NKR-P1A Receptor. J. Immunol. 175, 7796–7799.

Rosen, D.B., Cao, W., Avery, D.T., Tangye, S.G., Liu, Y.-J., Houchins, J.P., Lanier, L.L., 2008. Functional Consequences of Interactions between Human NKR-P1A and Its

Ligand LLT1 Expressed on Activated Dendritic Cells and B Cells. J. Immunol. 180, 6508–6517.

Saghafian-Hedengren, S., Sverremark-Ekström, E., Linde, A., Lilja, G., Nilsson, C., 2010. Early-life EBV infection protects against persistent IgE sensitization. J. Allergy Clin. Immunol. 125, 433–8.

Saito, H., Kranz, D.M., Takagaki, Y., Hayday, A.C., Eisen, H.N., Tonegawa, S., 1984. Complete primary structure of heterodimeric T-cell receptor deduced from cDNA sequences. Nature 309, 757–762.

Sallusto, F., Lenig, D., Forster, R., Lipp, M., Lanzavecchia, A., 1999. Two subsets of memory T lymphocytes with distinct homing potentials. Nature 401, 708–712.

Sarkar, S., Kalia, V., Haining, W.N., Konieczny, B.T., Subramaniam, S., Ahmed, R., 2008. Functional and genomic profiling of effector CD8 T cell subsets with distinct memory fates. J. Exp. Med. 205, 625–40.

Sathaliyawala, T., Kubota, M., Yudanin, N., Turner, D., Camp, P., Thome, J.J.C., Bickham, K.L., Lerner, H., Goldstein, M., Sykes, M., Kato, T., Farber, D.L., 2013. Distribution and Compartmentalization of Human Circulating and Tissue-Resident Memory T Cell Subsets. Immunity 38, 187–197.

Sato, T., Thorlacius, H., Johnston, B., Staton, T.L., Xiang, W., Littman, D.R., Butcher, E.C., 2005. Role for CXCR6 in recruitment of activated CD8+ lymphocytes to inflamed liver. J. Immunol. 174, 277–283.

Savage, A.K., Constantinides, M.G., Bendelac, A., 2011. Promyelocytic leukemia zinc finger turns on the effector T cell program without requirement for agonist TCR signaling. J. Immunol. 186, 5801–6.

Savage, A.K., Constantinides, M.G., Han, J., Picard, D., Martin, E., Li, B., Lantz, O., Bendelac, A., 2008. The transcription factor PLZF directs the effector program of the NKT cell lineage. Immunity 29, 391–403.

Schenkel, J.M., Fraser, K.A., Beura, L.K., Pauken, K.E., Vezys, V., Masopust, D., 2014. Resident memory CD8 T cells trigger protective innate and adaptive immune responses. Science (80-.). DOI: 10.1126/science.1254536.

Seach, N., Guerri, L., Le Bourhis, L., Mburu, Y., Cui, Y., Bessoles, S., Soudais, C., Lantz, O., 2013. Double-positive thymocytes select mucosal-associated invariant T cells. J. Immunol. 191, 6002–9.

Serriari, N.-E., Eoche, M., Lamotte, L., Lion, J., Fumery, M., Marcelo, P., Chatelain, D., Barre, a, Nguyen-Khac, E., Lantz, O., Dupas, J.-L., Treiner, E., 2014. Innate mucosal-associated invariant T (MAIT) cells are activated in inflammatory bowel diseases. Clin. Exp. Immunol. 176, 266–74.

Shimizu, Y., Minemura, M., Murata, H., Hirano, K., Nakayama, Y., Higuchi, K., Watanabe, A., Yasuyama, T., Tsukada, K., 2003. Preferential accumulation of CD103+ T cells in human livers; its association with extrathymic T cells. J. Hepatol. 39, 918–924.

Shin, H., Iwasaki, A., 2013. Tissue-resident memory T cells. Immunol. Rev. 255, 165–181.

Spada, E., Mele, A., Berton, A., Ruggeri, L., Ferrigno, L., Garbuglia, A.R., Perrone, M.P., Girelli, G., Del Porto, P., Piccolella, E., Mondelli, M.U., Amoroso, P., Cortese, R., Nicosia, A., Vitelli, A., Folgori, A., 2004. Multispecific T cell response and negative HCV RNA tests during acute HCV infection are early prognostic factors of spontaneous clearance. Gut 53, 1673–81.

Spada, F.M., Grant, E.P., Peters, P.J., Sugita, M., Melián, A., Leslie, D.S., Lee, H.K., Donselaar, E. Van, Hanson, D.A., Krensky, A.M., Majdic, O., Porcelli, S.A., Morita, C.T., Brenner, M.B., 2000. Self-recognition of CD1 by gamma/delta T cells: implications for innate immunity. J. Exp. Med. 191, 937–48.

Spanakis, N.E., Garinis, G.A., Alexopoulos, E.C., Patrinos, G.P., Menounos, P.G., Sklavounou, A., Manolis, E.N., Gorgoulis, V.G., Valis, D., 2002. Cytokine Serum Levels in Patients With Chronic HCV Infection. J. Clin. Lab. Anal. 46, 40–46.

Subramanian, A., Tamayo, P., Mootha, V.K., Mukherjee, S., Ebert, B.L., Gillette, M.A., Paulovich, A., Pomeroy, S.L., Golub, T.R., Lander, E.S., Mesirov, J.P., 2005. Gene set enrichment analysis : A knowledge-based approach for interpreting genome-wide. Proc. Natl. Acad. Sci. 102, 15545–50.

Swain, S.L., 1999. Class II-Independent Generation of CD4 Memory T Cells from Effectors. Science (80-.). 286, 1381–1383.

Takahashi, T., Dejbakhsh-Jones, S., Strober, S., 2006. Expression of CD161 (NKR-P1A) Defines Subsets of Human CD4 and CD8 T Cells with Different Functional Activities. J. Immunol. 176, 211–216.

Tanaka, Y., Morita, C.T., Tanaka, Y., Nieves, E., Brenner, M.B., Bloom, B.R., 1995. Natural and synthetic non-peptide antigens recognised by human gamma delta T cells. Nature 375, 155–158.

Taylor, A.L., Watson, C.J.E., Bradley, J.A., 2005. Immunosuppressive agents in solid organ transplantation: Mechanisms of action and therapeutic efficacy. Crit. Rev. Oncol. Hematol. 56, 23–46.

The International Multiple Sclerosis Genetics Consortium, 2007. Risk Alleles for Multiple Sclerosis Identified by a Genomewide Study. N. Engl. J. Med. 357, 851–862.

Tilloy, F., Treiner, E., Park, S., Garcia, C., Lemonnier, F., de la Salle, H., Bendelac, A., Bonneville, M., Lantz, O., 1999. An Invariant T Cell Receptor alpha Chain Defines a Novel TAP-independent Major Histocompatibility Complex Class Ib-restricted alpha/beta T cell Subpopulation in Mammals. J. Exp. Med. 189, 1907–1921.

Treiner, E., Duban, L., Bahram, S., Radosavljevic, M., Wanner, V., Tilloy, F., Affaticati, P., Gilfillan, S., Lantz, O., 2003. Selection of evolutionarily conserved mucosal-associated invariant T cells by MR1. Nature 422, 164–9.

Triebel, F., Hercend, T., 1989. Subpopulations of human peripheral T gamma delta lymphocytes. Immunol. Today 10, 186–8.

Turner, D.L., Bickham, K.L., Thome, J.J., Kim, C.Y., D'Ovidio, F., Wherry, E.J., Farber, D.L., 2014. Lung niches for the generation and maintenance of tissue-resident memory T cells. Mucosal Immunol. 7, 501–10.

Turtle, C.J., Delrow, J., Joslyn, R.C., Swanson, H.M., Basom, R., Tabellini, L., Delaney, C., Heimfeld, S., Hansen, J.A., Riddell, S.R., 2011. Innate signals overcome acquired TCR signaling pathway regulation and govern the fate of human CD161hi CD8alpha+ semi-invariant T cells. Blood 118, 2752–2762.

Turtle, C.J., Swanson, H.M., Fujii, N., Estey, E.H., Riddell, S.R., 2009. A distinct subset of self-renewing human memory CD8+ T cells survives cytotoxic chemotherapy. Immunity 31, 834–44.

Uss, E., Rowshani, A.T., Hooibrink, B., Lardy, N.M., van Lier, R.A.W., ten Berge, I.J.M., 2006. CD103 is a marker for alloantigen-induced regulatory CD8+ T cells. J. Immunol. 177, 2775–2783.

Ussher, J.E., Bilton, M., Attwod, E., Shadwell, J., Richardson, R., de Lara, C., Mettke, E., Kurioka, A., Hansen, T.H., Klenerman, P., Willberg, C.B., 2014. CD161++CD8+ T cells, including the MAIT cell subset, are specifically activated by IL-12+IL-18 in a TCR-independent manner. Eur. J. Immunol. 44, 195–203.

Van der Waart, A.B., van der Velden, W.J.F.M., van Halteren, A.G.S., Leenders, M.J.L.G., Feuth, T., Blijlevens, N.M.A., van der Voort, R., Dolstra, H., 2012. Decreased Levels of Circulating IL17-Producing CD161+CCR6+ T Cells Are Associated with Graft-versus-Host Disease after Allogeneic Stem Cell Transplantation. PLoS One 7, e50896.

Van Rhijn, I., Kasmar, A., de Jong, A., Gras, S., Bhati, M., Doorenspleet, M.E., de Vries, N., Godfrey, D.I., Altman, J.D., de Jager, W., Rossjohn, J., Moody, D.B., 2013. A conserved human T cell population targets mycobacterial antigens presented by CD1b. Nat. Immunol. 14, 706–13.

Vavassori, S., Kumar, A., Wan, G.S., Ramanjaneyulu, G.S., Cavallari, M., El Daker, S., Beddoe, T., Theodossis, A., Williams, N.K., Gostick, E., Price, D.A., Soudamini, D.U., Voon, K.K., Olivo, M., Rossjohn, J., Mori, L., De Libero, G., 2013. Butyrophilin 3A1 binds phosphorylated antigens and stimulates human γδ T cells. Nat. Immunol. 14, 908–16.

Veiga-Fernandes, H., Walter, U., Bourgeois, C., McLean, a, Rocha, B., 2000. Response of naïve and memory CD8+ T cells to antigen stimulation in vivo. Nat. Immunol. 1, 47–53.

Venturi, V., Kedzierska, K., Tanaka, M.M., Turner, S.J., Doherty, P.C., Davenport, M.P., 2008. Method for assessing the similarity between subsets of the T cell receptor repertoire. J. Immunol. Methods 329, 67–80.

Vitale, M., Bottino, C., Sivori, S., Sanseverino, L., Castriconi, R., Marcenaro, E., Augugliaro, R., Moretta, L., Moretta, A., 1998. NKp44, a novel triggering surface molecule specifically expressed by activated natural killer cells, is involved in non-major histocompatibility complex-restricted tumor cell lysis. J. Exp. Med. 187, 2065–2072.

Vitale, M., Falco, M., Castriconi, R., Parolini, S., Zambello, R., Semenzato, G., Biassoni, R., Bottino, C., Moretta, L., Moretta, a, 2001. Identification of NKp80, a novel triggering molecule expressed by human NK cells. Eur. J. Immunol. 31, 233–42.

Voehringer, D., Koschella, M., Pircher, H., 2002. Lack of proliferative capacity of human effector and memory T cells expressing killer cell lectin-like receptor G1 (KLRG1). Blood 100, 3698–3702.

Wakim, L.M., Waithman, J., van Rooijen, N., Heath, W.R., Carbone, F.R., 2008. Dendritic cell-induced memory T cell activation in nonlymphoid tissues. Science 319, 198–202.

Wakim, L.M., Woodward-Davis, A., Liu, R., Hu, Y., Villadangos, J., Smyth, G., Bevan, M.J., 2012. The molecular signature of tissue resident memory CD8 T cells isolated from the brain. J. Immunol. 189, 3462–71.

Walker, L.J., Kang, Y.H., Smith, M.O., Tharmalingham, H., Ramamurthy, N., Fleming, V.M., Sahgal, N., Leslie, A., Oo, Y., Geremia, A., Scriba, T.J., Hanekom, W. a., Lauer, G.M., Lantz, O., Adams, D.H., Powrie, F., Barnes, E., Klenerman, P., 2012. Human MAIT and CD8 alpha alpha cells develop from a pool of type-17 precommitted CD8+ T cells. Blood 119, 422–433.

Wang, G.C., Dash, P., McCullers, J.A., Doherty, P.C., Thomas, P.G., 2012. T cell receptor αβ diversity inversely correlates with pathogen-specific antibody levels in human cytomegalovirus infection. Sci. Transl. Med. 4, 128ra42.

Weinreich, M.A., Odumade, O. a, Jameson, S.C., Hogquist, K.A., 2010. T cells expressing the transcription factor PLZF regulate the development of memory-like CD8+ T cells. Nat. Immunol. 11, 709–16.

Welte, S., Kuttruff, S., Waldhauer, I., Steinle, A., 2006. Mutual activation of natural killer cells and monocytes mediated by NKp80-AICL interaction. Nat. Immunol. 7, 1334–42.

Wencker, M., Turchinovich, G., Di Marco Barros, R., Deban, L., Jandke, A., Cope, A., Hayday, A.C., 2014. Innate-like T cells straddle innate and adaptive immunity by altering antigen-receptor responsiveness. Nat. Immunol. 15, 80–7.

Wherry, E.J., Ha, S.-J., Kaech, S.M., Haining, W.N., Sarkar, S., Kalia, V., Subramaniam, S., Blattman, J.N., Barber, D.L., Ahmed, R., 2007. Molecular signature of CD8+ T cell exhaustion during chronic viral infection. Immunity 27, 670–84.

Wong, E.B., Akilimali, N.A., Govender, P., Sullivan, Z.A., Cosgrove, C., Pillay, M., Lewinsohn, D.M., Bishai, W.R., Walker, B.D., Ndung'U, T., Klenerman, P., Kasprowicz, V.O., 2013. Low levels of peripheral CD161++CD8+ mucosal associated invariant T (MAIT) cells are found in HIV and HIV/TB co-infection. PLoS One 8, e83474.

Wood, K.J., Goto, R., 2012. Mechanisms of rejection: current perspectives. Transplantation 93, 1–10.

Xu, B., Pizarro, J.C., Holmes, M.A., McBeth, C., Groh, V., Spies, T., Strong, R.K., 2011. Crystal structure of a gammadelta T-cell receptor specific for the human MHC class I homolog MICA. Proc. Natl. Acad. Sci. U. S. A. 108, 2414–9.

Yamamura, M., Kawashima, M., Taniai, M., Yamauchi, H., Tanimoto, T., Kurimoto, M., Morita, Y., Ohmoto, Y., Makino, H., 2001. Interferon-gamma-inducing activity of interleukin-18 in the joint with rheumatoid arthritis. Arthritis Rheum. 44, 275–85.

Yokoyama, W.M., Seaman, W.E., 1993. The Ly-49 and NKR-P1 gene families encoding lectin-like receptors on natural killer cells: the NK gene complex. Annu. Rev. Immunol. 11, 613–35.

Yoshimoto, T., Paul, W.E., 1994. CD41pos, NKI.lpos T Cells Promptly Produce Interleukin 4 in Response to In Vivo Challenge with Anti-CD3. J. Exp. Med. 179, 1285–1295.

Zimmerli, S.C., Harari, A., Cellerai, C., Vallelian, F., Bart, P., Pantaleo, G., 2005. HIV-specific IFN-gamma/IL-2-secreting CD8 T cells support CD4-independent proliferation of HIV-1-specific CD8 T cells. Proc. Natl. Acad. Sci. 102, 7239–7244.

Zimmermann, C., Brduscha-Riem, K., Blaser, C., Zinkernagel, R.M., Pircher, H., 1996. Visualization, Characterization, and Turnover of CD8+ Memory T Cells in Virus-infected Hosts. J. Exp. Med. 183, 1367–1375.

APPENDIX

List of Publications

J.R. Fergusson, K.E Smith, V.M. Fleming, N. Rajoriya, E.W. Newell, R. Simmons, E. Marchi, S. Björkander, Y-H. Kang, L. Swadling, A. Kurioka, N. Sahgal, H. Lockstone, D. Baban, G.J. Freeman, E. Sverremark-Ekström, M.M. Davis, M.P. Davenport, V. Venturi, J.E. Ussher, C.B. Willberg, P. Klenerman (2014) CD161 defines a transcriptional and functional phenotype shared across distinct human T cell lineages *Cell Reports* 9, 1-14

L. Xue, J.R. Fergusson, M. Salimi, I. Panse, J.E. Ussher, N. Sahgal, A. Barrow, S.L. Vinall, D. Jackson, M.G. Hunter, R. Pettipher, G. Ogg, P. Klenerman (2014) Prostaglandin D2 and leukotriene E4 synergise to stimulate diverse Th2 functions and Th2 cell/neutrophil crosstalk *J. Allergy Clin. Immunol.* doi: 10. 1016/j.jaci/2014/09/006

A. Kurioka, J.E. Ussher, C. Cosgrove, J.R. Fergusson, K. Smith, C. Clough, Y-H. Kang, L.J. Walker, T.H. Hansen, C.B. Willberg, P. Klenerman (2014) MAIT cells are licensed through granzyme exchange to kill bacterially sensitized targets *Mucosal Immunology* doi: 10. 1038/mi.2014.81

L. Swadling, S. Capone, R.D. Antrobus, A. Brown, R. Richardson, E.W. Newell, J. Halliday, C. Kelly, D. Bowen, J.R. Fergusson, A. Kurioka, V. Ammendola, M. Del Sorbo, F. Grazioli, M.L. Esposito, L. Siani, C. Traboni, A. Hill, S. Colloca, M.M. Davis, A. Nicosia, R. Cortese, A. Folgori, P. Klenerman, E. Barnes (2014) A human vaccine strategy based on chimpanzee adenoviral and MVA vectors that primes, boosts and sustains functional HCV-specific T-cell memory *Sci. Trans. Med.* 6(261):261ra153

N. Rajoriya, J.R. Fergusson, J.A. Leithead, P. Klenerman (2014) Gamma delta T-lymphocytes in hepatitis C and chronic liver disease *Frontiers in Immunology* doi: 10.3389/fimmu.2014.00400

L.J. Walker, E. Marrinan, M. Muenchhoff, J.R. Fergusson, H. Kloverpris, H. Cheroutre, E. Barnes. P. Goulder, P. Klenerman (2013) CD8 alpha alpha expression marks terminally differentiated human CD8+ T cells expanded in chronic viral infection Frontiers in Immunology doi: 10.3389/fimmu.2013.00223

C. Cosgrove, J.E. Ussher, A. Rauch, K. Gärtner, A. Kurioka, M. H. Hühn, K. Adelmann, Y-H. Kang, J.R. Fergusson, P. Simmonds, P. Goulder, T.H. Hansen, J. Fox, H.F. Günthard, N. Khanna, F. Powrie, A. Steel, B. Gazzard, R.E. Phillips, J. Frater, H. Uhlig, P. Klenerman (2013) Early and nonreversible decrease of CD161++/MAIT cells in HIV infection *Blood* 121(6):951-61

J.R. Fergusson, V.M. Fleming, P. Klenerman (2011) CD161-expressing human T cells *Frontiers in Immunology* doi: 10.3389/fimmu.2011.00036

Article

Cell Reports

CD161 Defines a Transcriptional and Functional Phenotype across Distinct Human T Cell Lineages

Graphical Abstract

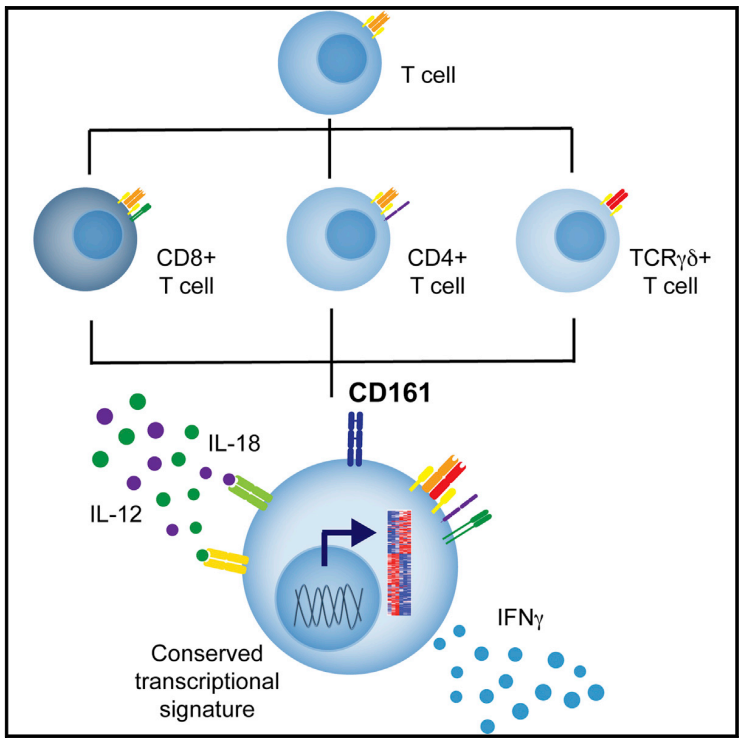

Authors

Joannah R. Fergusson, Kira E. Smith, ..., Christian B. Willberg, Paul Klenerman

Correspondence

paul.klenerman@ndm.ox.ac.uk

In Brief

T lymphocytes are conventionally divided into subsets based on expression of coreceptors, cytokines, and surface molecules. Using CyTOF and mRNA microarray analysis, Fergusson et al. identify T lymphocytes that express the C-type lectin CD161 to share a transcriptional profile and innate function across these previously defined subsets.

Highlights

CD161 expression defines specific T cell subsets, including CD8+, CD4+, and TCRγδ+

CD161-expressing lymphocytes possess a conserved transcriptional signature

CD161-expressing lymphocytes display a shared innate response to IL-12+18

CD161 can act as a costimulatory receptor

Accession Numbers

GSE62099

Fergusson et al., 2014, Cell Reports 9, 1075–1088
November 6, 2014 ©2014 The Authors
http://dx.doi.org/10.1016/j.celrep.2014.09.045

Cell Reports
Article

OPEN ACCESS
CellPress

CD161 Defines a Transcriptional and Functional Phenotype across Distinct Human T Cell Lineages

Joannah R. Fergusson,[1] Kira E. Smith,[1] Vicki M. Fleming,[1,2] Neil Rajoriya,[1] Evan W. Newell,[3,4] Ruth Simmons,[1] Emanuele Marchi,[1] Sophia Björkander,[5] Yu-Hoi Kang,[1] Leo Swadling,[1] Ayako Kurioka,[1] Natasha Sahgal,[6] Helen Lockstone,[6] Dilair Baban,[6] Gordon J. Freeman,[7] Eva Sverremark-Ekström,[5] Mark M. Davis,[3] Miles P. Davenport,[8] Vanessa Venturi,[8] James E. Ussher,[1,9] Christian B. Willberg,[1] and Paul Klenerman[1,10,*]

[1]Peter Medawar Building for Pathogen Research, University of Oxford, Oxford OX1 3SY, UK
[2]Department of Microbiology and Infectious Disease, Oxford University Hospitals NHS Trust, Oxford OX3 9DU, UK
[3]Department of Microbiology and Immunology, Stanford University, Stanford, CA 94305, USA
[4]Agency for Science, Technology and Research (A*STAR), Singapore Immunology Network (SIgN), Singapore 138632, Singapore
[5]Department of Molecular Biosciences, The Wenner-Gren Institute, Stockholm University, 106 91 Stockholm, Sweden
[6]Bioinformatics and Statistical Genetics Core, Wellcome Trust Centre for Human Genetics, University of Oxford, Oxford OX3 7BN, UK
[7]Dana Farber Cancer Institute, Harvard Medical School, Boston, MA 02215, USA
[8]Department of Haematology, Prince of Wales Hospital, Kensington, NSW NS2 2052, Australia
[9]Department of Microbiology and Immunology, University of Otago, Dunedin 9054, New Zealand
[10]NIHR Oxford Biomedical Research Centre, John Radcliffe Hospital, Oxford OX3 9TU, UK
*Correspondence: paul.klenerman@ndm.ox.ac.uk
http://dx.doi.org/10.1016/j.celrep.2014.09.045
This is an open access article under the CC BY license (http://creativecommons.org/licenses/by/3.0/).

SUMMARY

The C-type lectin CD161 is expressed by a large proportion of human T lymphocytes of all lineages, including a population known as mucosal-associated invariant T (MAIT) cells. To understand whether different T cell subsets expressing CD161 have similar properties, we examined these populations in parallel using mass cytometry and mRNA microarray approaches. The analysis identified a conserved CD161++/MAIT cell transcriptional signature enriched in CD161+CD8+ T cells, which can be extended to CD161+ CD4+ and CD161+TCRγδ+ T cells. Furthermore, this led to the identification of a shared innate-like, TCR-independent response to interleukin (IL)-12 plus IL-18 by different CD161-expressing T cell populations. This response was independent of regulation by CD161, which acted as a costimulatory molecule in the context of T cell receptor stimulation. Expression of CD161 hence identifies a transcriptional and functional phenotype, shared across human T lymphocytes and independent of both T cell receptor (TCR) expression and cell lineage.

INTRODUCTION

T lymphocytes form a major arm of the adaptive response, with somatic recombination of the T cell receptor (TCR) enabling recognition of a wide variety of antigens, coupled with the ability to form immunological memory. Although developing from a common thymic precursor, T lymphocytes may develop to express a TCR composed of either γδ chains or, more conventionally in humans, of αβ. TCRαβ+ T cells subsequently develop to be either CD8+ or CD4+, displaying distinct functions and restricted by major histocompatibility complex (MHC) class I or II molecules, respectively. These subsets display further subdivisions, with differentiation of CD4+ T cells into defined helper cell subsets characterized by unique cytokine production, transcription factor expression, and surface phenotype. For example, the more recently defined Th17 subset is characterized by secretion of interleukin (IL)-17, the master transcription factor RORγt (Annunziato et al., 2007), and expression of the C-type lectin CD161 (Cosmi et al., 2008).

Expression of CD161 is not restricted to CD4+ Th17 cells, however. Originally a marker of natural killer (NK) cells (Lanier et al., 1994; Yokoyama and Seaman, 1993), T cell expression of CD161 was identified two decades ago on both CD4+ and CD8+ (Lanier et al., 1994), and later on TCRγδ+ (Battistini et al., 1997), T cells. Indeed, a quarter of both TCRαβ+ T cells (Lanier et al., 1994) and TCRγδ+ T cells (Battistini et al., 1997) express this C-type lectin, and thus CD161 is expressed by a large proportion of human T cells. Within CD8+ T cells, two populations are evident, expressing either intermediate or high levels of CD161 (CD161+ or CD161++; Takahashi et al., 2006), with the latter shown to consist mainly of mucosal-associated invariant T (MAIT) cells (Martin et al., 2009; Ussher et al., 2014).

MAIT cells are a family of innate-like human T cells that display a somatically recombined yet semi-invariant TCR, composed of the TCR α chain Vα7.2-Jα33/12/20 (Reantragoon et al., 2013; Tilloy et al., 1999) paired with a biased Vβ repertoire (Reantragoon et al., 2013; Walker et al., 2012). Expression of this TCR restricts MAIT cells to the MHC class Ib antigen-presenting molecule MR1, which presents riboflavin precursors (Corbett et al., 2014; Kjer-Nielsen et al., 2012) produced by a variety of bacteria to

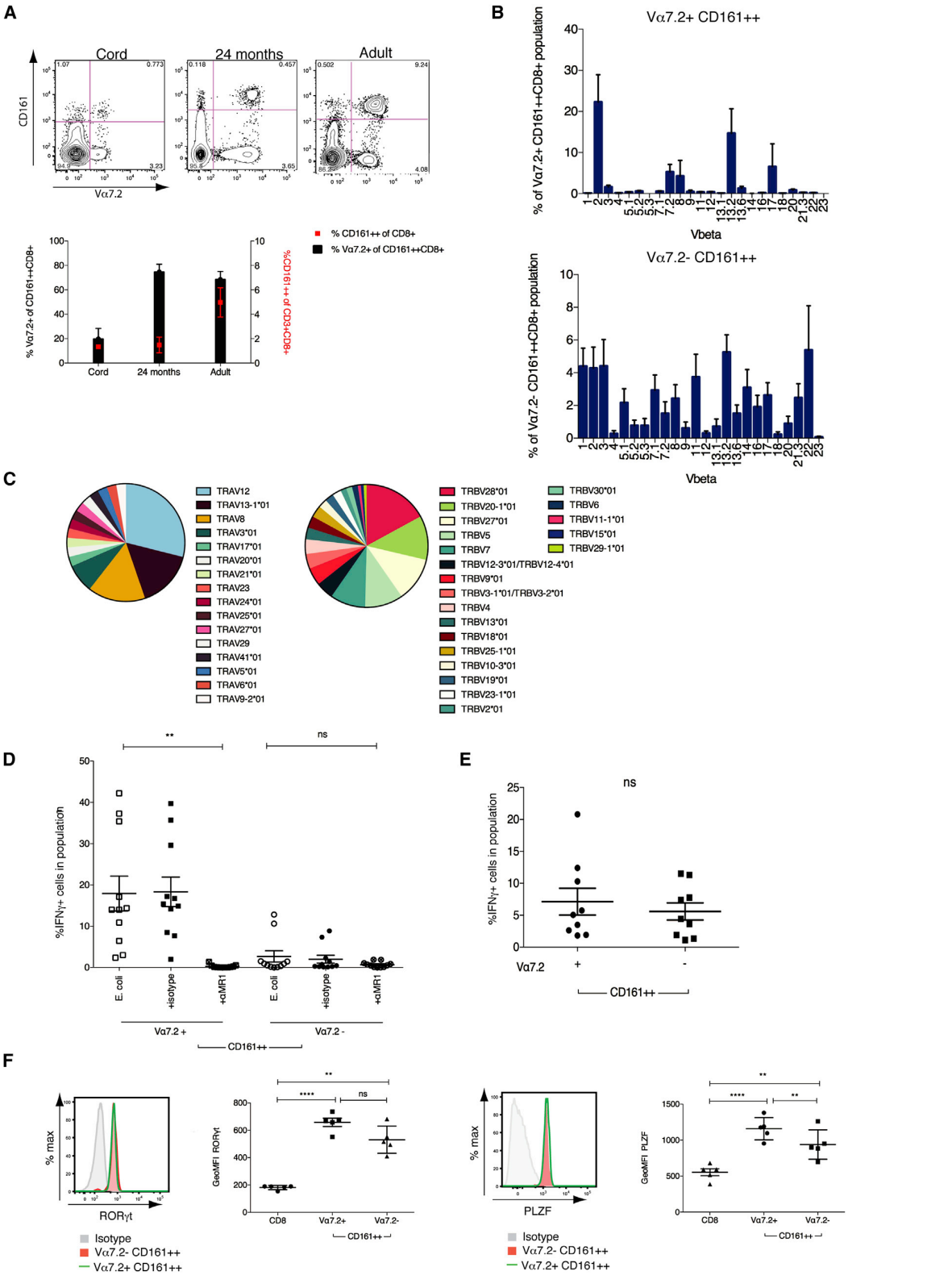

(legend on next page)

OPEN ACCESS CellPress

activate MAIT cells. Whereas originally identified within the double-negative T cell fraction (Porcelli et al., 1993), approximately 90% of MAIT cells in humans are CD8+ (either CD8αα or αβ; Walker et al., 2012), although a minor fraction of CD4+ MAIT cells also exists (Reantragoon et al., 2013). Yet, independently of coreceptor expression, all MAIT cells are identified by high expression of CD161 (Dusseaux et al., 2011; Martin et al., 2009).

CD161 is a homodimeric C-type lectin, which represents the single human ortholog of the family of *NKRP1* genes in rodents (Lanier et al., 1994), and thus study of MAIT and CD161-expressing T cells is currently restricted to the human system. Murine NKRP1 receptors recognize non-MHC ligands of the C-type lectin-related (Clr) family, encoded by genes interspersed within the *NKRP1* genes themselves (Iizuka et al., 2003; Plougastel et al., 2001). Similarly, CD161 binds the human ortholog of Clr-b, known as lectin-like transcript 1 (LLT1) (Aldemir et al., 2005; Rosen et al., 2005). Whereas the outcome of CD161 ligation on NK cells is generally accepted to be inhibitory (Aldemir et al., 2005; Lanier et al., 1994; Rosen et al., 2005), the effect on T cells is less clear, with reports of both costimulatory (Aldemir et al., 2005; Exley et al., 1998) and inhibitory (Le Bourhis et al., 2013; Rosen et al., 2008) effects.

Both CD161++ MAIT cells and CD161+CD4+ T cells display a type 17 phenotype (Billerbeck et al., 2010; Cosmi et al., 2008; Dusseaux et al., 2011). This phenotype appears preprogrammed, with precursors of both MAIT and Th17 cells identified within umbilical cord blood by expression of CD161 (Cosmi et al., 2008; Walker et al., 2012). Indeed, a highly significant correlation in gene expression in CD161++CD8+ T cells between cord blood and adults was demonstrated, despite only a minor proportion of CD161++CD8+ T cells expressing the MAIT cell TCR at birth (Walker et al., 2012). Furthermore, CD161 has previously been shown to identify T cells with the potential to produce IL-17 (Maggi et al., 2010). Therefore, we asked whether expression of CD161 marked cells with a shared phenotypic or transcriptional profile, both within and across previously defined T cell subsets, and further whether this corresponded to a specific shared function between these otherwise disparate cell types.

RESULTS

CD161++ CD8+ T Cells, Including Both Vα7.2+ MAIT and Vα7.2− Populations, Share a Common Phenotype

MAIT cells express an invariant TCR α chain (Vα7.2) together with high levels of CD161 (Dusseaux et al., 2011) and predominantly express the CD8 coreceptor (>90%; Walker et al., 2012). Whereas Vα7.2+ MAIT cells represent the vast majority of the CD161++ CD8+ T cell population (<95%) in adult blood, a population of CD161++CD8+ T cells that are Vα7.2− is also evident (Figure 1A), comprising an average of 11.41% (±6.99%) of CD161++CD8+ T cells in healthy adults. We first investigated the identity of this additional CD161++CD8+ T cell population in relation to MAIT cells. In cord blood, where CD161++CD8+ T cells are already preprogrammed to a MAIT-like, type-17 phenotype (Walker et al., 2012), this Vα7.2− population comprised the major proportion of CD161++CD8+ T cells (84.69% ± 8.44%). After birth, Vα7.2+ MAIT cell expansion drives the MAIT cell domination of the CD161++ population (Gold et al., 2013; Leeansyah et al., 2014), and a corresponding reduction in the proportion of Vα7.2− cells was seen. This was evident as early as 24 months, where the MAIT cell population represented nearly 75% of the CD161++CD8+ T cell population (Figure 1A).

In addition to invariant expression of Vα7.2, MAIT cells display semi-invariant TCR β usage (Figure 1B) with predominant use of Vβ2 and Vβ13.2, as previously described (Reantragoon et al., 2013; Walker et al., 2012). In contrast, a panel of Vβ antibodies revealed nondiscriminate Vβ usage by Vα7.2− CD161++CD8+ T cells. We further investigated the TCR repertoire of this population by TCR sequencing, performed on single cells, as described (Wang et al., 2012). This confirmed Vβ usage by Vα7.2− CD161++CD8+ T cells to be polyclonal. Furthermore, polyclonality within α chain usage was also evident, with expression of a variety of α chains both within and between donors (Figure 1C).

The semi-invariant MAIT cell TCR recognizes bacterially derived riboflavin precursors presented by the antigen-presenting molecule MR1 (Corbett et al., 2014; Kjer-Nielsen et al., 2012). MHC-tetramer-positive populations against various viral epitopes are rarely CD161++ (J.R.F., unpublished data). Therefore, to establish the MR1 reactivity of Vα7.2− CD161++CD8+ T cells, we used a 5 hr coculture assay in which we have previously described MAIT cells to be activated via the TCR to produce interferon γ (IFNγ) (Ussher et al., 2014). Here, THP1s were incubated with fixed *Escherichia coli* (*E. coli*) overnight and then cultured with sort-purified Vα7.2+ or Vα7.2− CD161++CD8+ T cells. As expected, CD161++Vα7.2+ MAIT cells produced IFNγ in response to THP1s + *E. coli*, and these responses were blocked by addition of anti-MR1 (Figure 1D). Whereas in two donors, a limited MR1-mediated response by Vα7.2− CD161++CD8+ T cells to *E.coli* was apparent, the majority of

Figure 1. Polyclonal Vα7.2−CD161++ CD8+ T Cells Are Not Activated in an MR1-Dependent Manner but, like MAIT Cells, Respond to Stimulation by IL-12+IL-18

(A) Percentage Vα7.2+ of CD161++CD8+ T cells (histogram) and percentage CD161++ of CD8+ T cells (red point) in cord (n = 3), 24 month (n = 8), and adult blood (n = 8). Representative flow cytometry plots shown above.

(B) Comparison of TCR Vβ usage by Vα7.2+ and Vα7.2− CD161++ CD8+ T cells using a TCR Vβ antibody panel.

(C) Proportional Vα (38 sequences) and Vβ (129 sequences) usage by Vα7.2− CD161++CD8+ T cells as determined by single-cell TCR sequencing (n = 3).

(D) Percentage of IFNγ expression by Vα7.2+ or Vα7.2− CD161++ CD8+ T cell subsets cocultured with THP1 cells exposed to *E. coli* in the presence or absence of anti-MR1 (10 μg/ml) or corresponding isotype control (n = 11). **p < 0.01; one-way ANOVA with Dunnett's multiple comparisons test compared to *E. coli* alone.

(E) Percentage of IFNγ expression by sorted Vα7.2+ or Vα7.2− CD161++CD8+ T cells incubated overnight with IL-12 + IL-18 at 50 ng/ml (n = 9). ns, not significant by paired t test.

(F) Transcription factor expression as determined by flow cytometry. Graphs show GeoMFI of RORγt (left) and PLZF (right) by conventional CD8+ T cells (CD3+CD8+ cells excluding CD161++) and Vα7.2+ or Vα7.2− CD161++ CD8+ T cells (n = 5). ****p < 0.0001; **p < 0.01; one-way ANOVA with Tukey's multiple comparison test. Representative histograms show isotype (gray), Vα7.2+ (green line), and Vα7.2− (red) for each transcription factor.

All data are represented as mean ± SEM. See also Figure S1.

OPEN ACCESS
CellPress

donors did not respond to bacteria. No response was observed in sorted conventional (MHC-restricted) CD161+CD8+ T cells (data not shown). This was reflected in 24-month-old donors where no response was observed from Vα7.2− CD161++CD8+ T cells when peripheral blood mononuclear cells (PBMCs) were incubated for 5 hr with *E. coli*-loaded THP1s (Figure S1).

In addition to MR1-mediated stimulation through the TCR, MAIT cells are also activated by a combination of IL-12+IL-18 in a TCR-independent, innate manner, a characteristic that was shared by other CD161++CD8+ T cells (Ussher et al., 2014). Gating of both CD161++CD8+ T cell populations in adult, 24-month-old, and cord blood donors again showed that both Vα7.2+ and Vα7.2− portions were capable of IFNγ production (Figure S1). We confirmed this in sorted adult populations, where both Vα7.2+ and Vα7.2− CD161++CD8+ T cells produced IFNγ in response to cytokine stimulation (Figure 1E), indicating this as a feature of CD161++CD8+ T cells as a whole.

We next asked whether Vα7.2− CD161++CD8+ T cells shared the characteristic transcription factor expression of MAIT cells, namely expression of RORγt, associated with the type-17 profile of MAIT cells (Billerbeck et al., 2010; Dusseaux et al., 2011) and promyelocytic leukemia zinc finger (PLZF), related to the innate-like effector differentiation of MAIT and NK T (NKT) cells (Savage et al., 2008). Expression of these transcription factors by Vα7.2− CD161++CD8+ was significantly ($p < 0.01$) higher than in conventional CD8+ T cells but expressed on average at slightly lower levels than MAIT cells (Figure 1F). Vα7.2− CD161++CD8+ T cells also principally displayed an effector memory (CD62L− CD45RA−) phenotype, as seen in Vα7.2+ MAIT cells (Figure S1).

Together, these results illustrate that, despite different TCR expression and restriction, both Vα7.2+ MAIT and Vα7.2− CD161++CD8+ T cells share a preprogrammed phenotype and an innate ability to respond to cytokine stimulation and can therefore be viewed as a common population related through high expression of CD161.

Analysis of CD161-Expressing CD8+ T Cells by CyTOF

Next, we wanted to investigate whether expression of CD161, and specifically different levels of expression, defined distinct CD8+ T cell phenotypes (Figure 2A). To do this, we assayed expression of 23 markers (see the Supplemental Experimental Procedures) simultaneously across phorbol 12-myristate 13-acetate (PMA) + ionomycin-stimulated CD8+ T cells by mass cytometry (CyTOF), using principal-component analysis (PCA) to integrate the patterns of expression into a smaller number of summary values (Newell et al., 2012). PCA looks for directions, or components, that cumulatively account for the variation contained within the data set, with the first four components here accounting for >60% of the total variation (Figure 2B). This analysis allowed the patterns of expression of all 23 markers to be summarized for each cell, which can then be viewed on a 2D or 3D plot, thereby allowing the different CD8+ T cell populations to be viewed in relation to one another.

When stimulated CD8+ T cells were plotted upon the first three components, CD161++ cells occupied a distinct niche compared to the other CD8+ T cell subsets (Figure 2C; Movie S1). Similarly, when plotted in 2D on component 1, which accounts for the most variation, and component 4, to which CD161 contributed the most to the variation described (component loading; Figure 2B), CD161++ cells again occupied a distinct niche among the spectrum of CD8+ T cell phenotypes (Figure 2D).

The progression in phenotypes of CD8+ T cells that expressed differing levels in CD161, and the niches they occupied, could be most clearly seen when components 1,2, and 4 were viewed together (Movie S2). In addition to CD8+ T cells that express high levels of CD161, a population of CD8+ T cells that express low, or intermediate, levels of CD161 is also apparent in the circulation (CD161+; Figure 2A). These cells displayed an overlap with the phenotypic niche of CD161++ cells (Movie S1; Figure 2D).

The Phenotypic and Transcriptional Profile of CD161+CD8+ T Cells Overlaps with CD161++CD8+ T Cells

To explore in more depth the phenotypic overlap of CD161+ and CD161++/MAIT CD8+ T cells, we probed genome-wide RNA expression of these CD8+ T cell populations by microarray. Previously, we identified a set of genes differentially expressed by CD161++CD8+ T cells compared to CD161− CD8+ T cells (Figure 3A; Billerbeck et al., 2010). This included the upregulated expression of RORγt, CXCR6, and IL18 receptor (IL18R). Given the dominance of MAIT cells within the CD161++CD8+ T cell population, these markers are consequently thought to be descriptive of the MAIT cell subset as well. Similarly, we performed microarray analysis on CD161+CD8+ T cells in comparison to CD161−CD8+ T cells in the same donors (Figure 3B) and identified 544 differentially expressed genes. When compared with the CD161++/MAIT cell transcriptional signature, 79% of those genes significantly differentially expressed by CD161+ CD8+ T cells were shared by CD161++CD8+ T cells (Figure 3C; Tables S1 and S2). Although the majority of shared genes were downregulated, among the 107 shared upregulated genes were those characteristic of MAIT cells, including *CCR6*, *CXCR6*, *ABCB1* (encoding MDR1), and *IL18R* (Billerbeck et al., 2010; Dusseaux et al., 2011).

Next, we analyzed the gene expression data as a whole using gene set enrichment analysis (GSEA) (Subramanian et al., 2005), rather than limiting analysis to significant genes, which may miss relevant biological differences or pathway effects. GSEA orders the genes into a ranked list according to their differential expression between CD161+ and CD161− CD8+ T cells. The locations of the CD161++CD8+ T-cell-associated genes, divided into upregulated (those upregulated within CD161++CD8+ T cells) or downregulated (upregulated within CD161−CD8+ T cells; Figure 3A) genes, within this ranked list were then identified. We found significant enrichment of genes upregulated in CD161++ CD8+ T cells in CD161+CD8+ T cells (normalized enrichment score [NES] = 3.79; $p < 0.001$) and corresponding enrichment of downregulated genes with those genes more associated with a CD161− phenotype (NES = −3.12; $p < 0.001$; Figure 3D).

The correlation of CD161 expression with a number of "MAIT cell markers" identified among these shared upregulated genes was then investigated at the protein level using flow cytometric analysis. To prevent skewing by the differing proportions of each subset, defined as CD161++, CD161+, and

OPEN ACCESS
CellPress

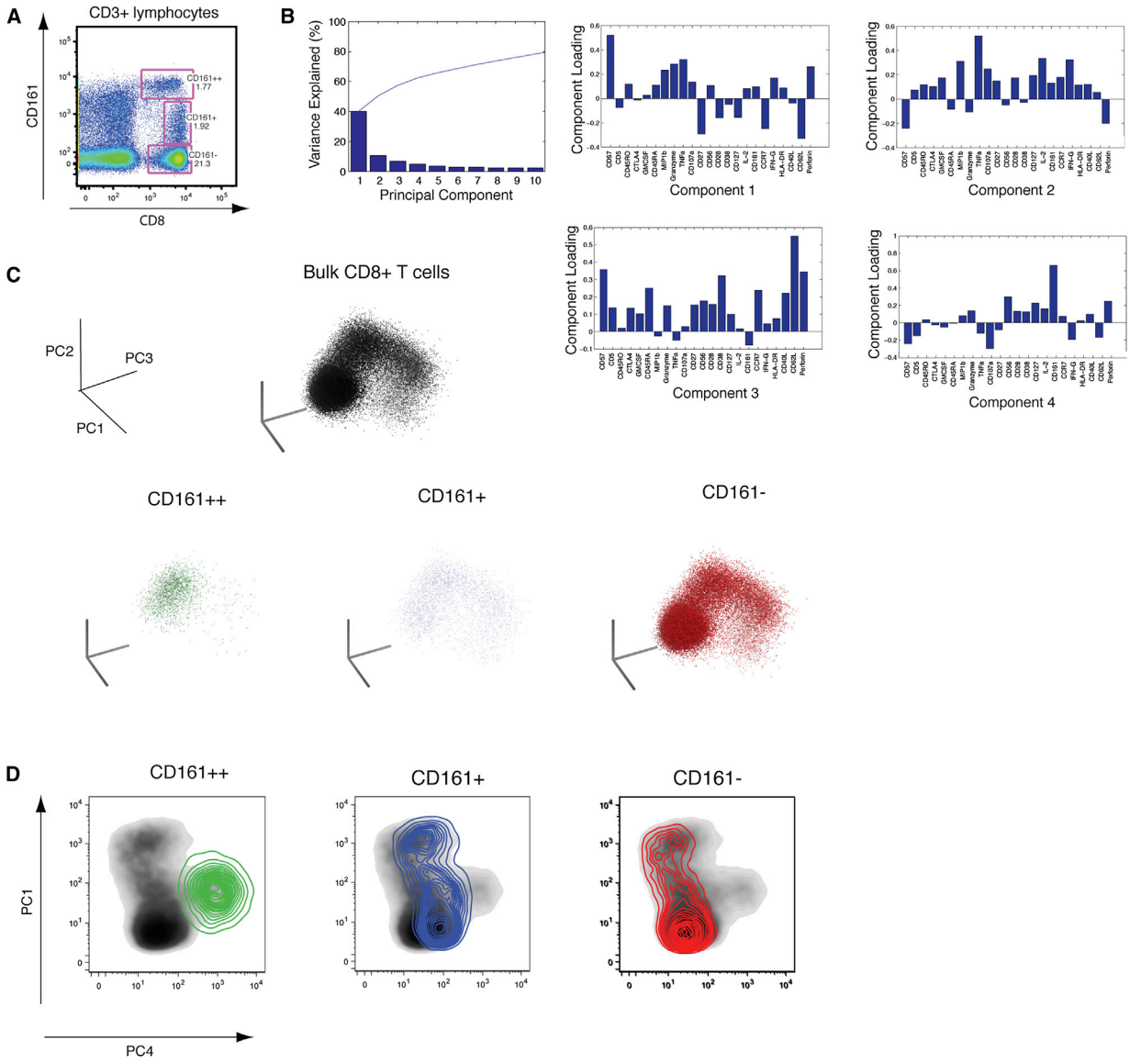

Figure 2. CyTOF and Principal-Component Analysis Reveals CD161++ Cells to Be Unique among CD8+ T Cells

(A) Representative flow cytometry plot of the division of CD8+ T cells into three subsets based upon expression of CD161.

(B) Data generated for PMA + ionomycin-stimulated CD8+ T cells were analyzed by principal-component analysis (PCA). The percent variation explained is plotted for each component (bars) and cumulatively (line), and the PCA parameter loadings (weighting coefficients) for the first four components are shown.

(C) Stimulated CD8+ T cells from one representative donor are plotted on the first three components as a bulk population (black) and for the three subsets: CD161++ (green); CD161+ (blue); and CD161− (red).

(D) Density plots of bulk-stimulated CD8+ T cells are plotted on component 1 and component 4 and are overlaid with contour density of plots of CD161++ (green), CD161+ (blue), and CD161− (red) cells.

CD161− (Figure 2A), we gated on each individual subset and plotted the expression levels of each marker, taken as geometric mean fluorescence intensity (GeoMFI), in relation to that of CD161 expression (Figure 3E). This revealed a highly significant correlation ($p < 0.0001$) between the levels of CD161 expressed and the expression of the CCR6 ($r^2 = 0.9143$), CXCR6 ($r^2 = 0.9258$), MDR1 ($r^2 = 0.9322$), and IL18Rα ($r^2 = 0.9554$). Therefore, expression of CD161 by CD8+ T cells correlates with a phenotypic signature that includes a distinct set of chemokine and cytokine receptors.

Conserved Transcriptional Changes in CD161-Expressing CD4+ and TCRγδ+ T Cells

A population of CD4+ T cells expressing CD161 is also apparent in the adult circulation and cord blood (Figure 4A). Both

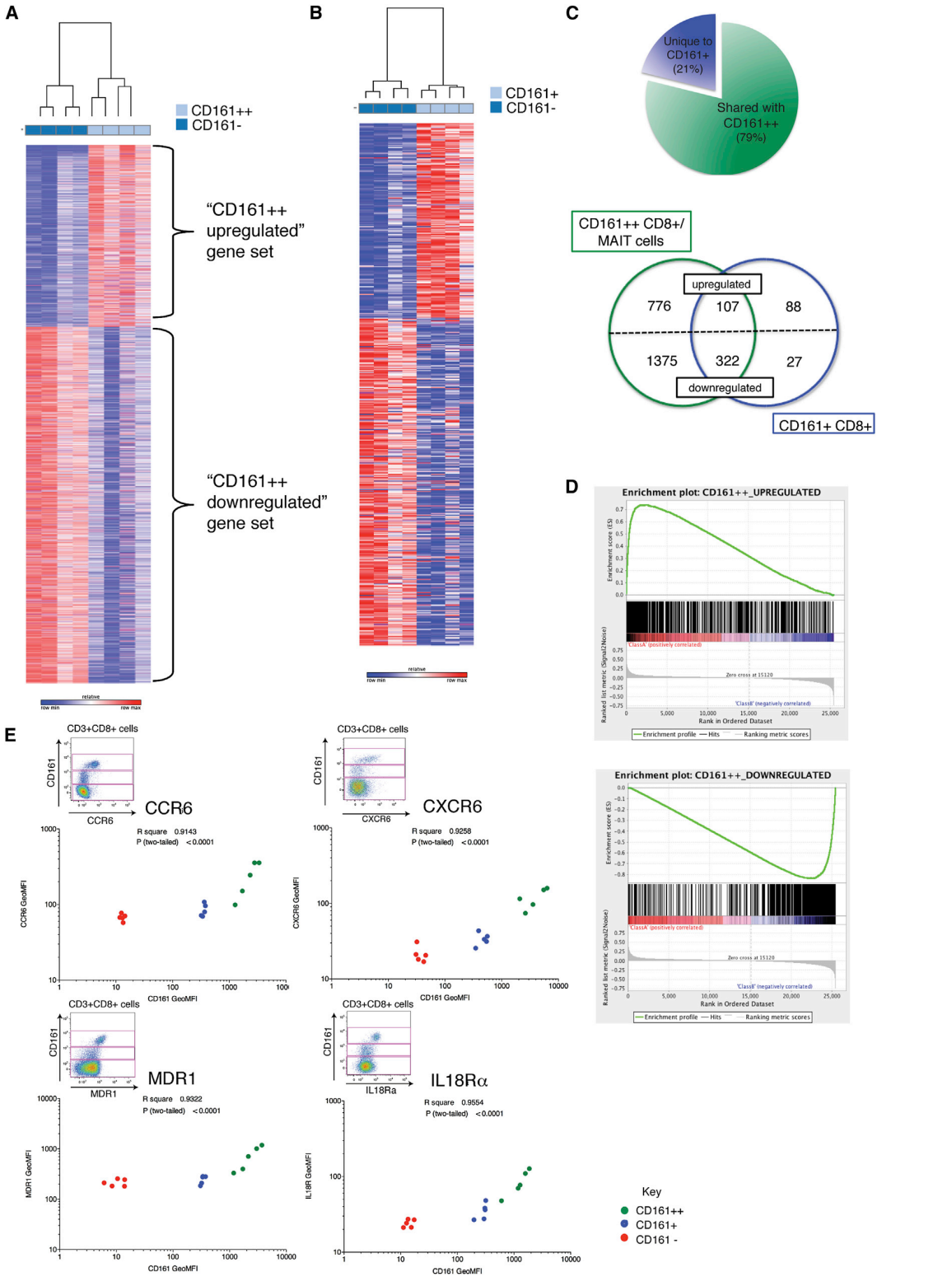

(legend on next page)

OPEN ACCESS CellPress

CD161+CD4+ T cells (Cosmi et al., 2008; Maggi et al., 2010) and CD161++ CD8+/MAIT cells (Billerbeck et al., 2010; Dusseaux et al., 2011) have been associated with a type-17 phenotype. Therefore, we investigated phenotypic overlap on a global scale by performing gene-expression profiling of CD161+CD4+ T cells by microarray. Genes significantly differentially expressed compared to CD161−CD4+ T cells were identified and compared to the CD161++CD8+ gene data set. CD161+CD4+ T cells shared a third of distinguishing genes with CD161++CD8+ T cells, including *IL18RAP* (Figure 4B; Tables S3 and S4). Again, GSEA demonstrated significant enrichment ($p < 0.001$) of those genes upregulated in CD161++CD8+ T cells in the CD161+CD4+ transcriptional profile (NES = 2.45) and downregulated genes with the CD161−CD4+ phenotype (NES = −3.04; Figure 4C), demonstrating concordance of transcriptional profiles, independently of coreceptor expression among TCRαβ+ T cells expressing CD161.

To investigate whether the CD161++/MAIT phenotype was also enriched in T cells expressing a different TCR, we extended our analysis to TCRγδ+ T cells. Again, both CD161+ and CD161− TCRγδ+ T cells are evident within the adult circulation and cord blood (Figure 4D). Gene-expression analysis was performed on sorted CD161+ and CD161− TCRγδ+ T cells and those genes significantly differentially expressed identified (Figure 4E). Approximately a fifth of these were again shared with the CD161++ CD8+ gene data set, including *IL18R1* and *ABCB1*, which encodes MDR1 (Tables S5 and S6). As seen for CD8+ and CD4+ T cells, GSEA revealed the CD161++CD8+ gene set to be significantly enriched ($p < 0.001$) in CD161+TCRγδ+ T cells, corresponding to both upregulated (NES = 2.78) and downregulated (NES = −2.62) genes (Figure 4F), despite a reduced number of genes being shared.

Overall, CD161 expression can distinguish distinct populations of T cells within each T cell lineage, whether CD8+, CD4+, or TCRγδ+, with a defined CD161++/MAIT-cell-associated transcriptional signature enriched within this CD161-positive subset. Moreover, comparison of the leading edge gene set (the core set of genes that account for this enrichment) from each T cell population distinguished a core of 124 upregulated (Table 1) and 199 downregulated (Table S7) genes commonly enriched in all CD161-expressing T cells and which therefore defines the CD161-associated transcriptional signature. This included upregulated expression of *ABCB1* (MDR1), *RORC* (RORγ), *ZBTB16* (PLZF), *IL12RB2*, and *IL18R1*.

A Common Functional Correlate of CD161 Expression in All T Cell Subsets

IL18R was one of the defining components of the leading edge gene set associated with CD161 expression. The receptor is composed of two subunits: IL18Rα and IL18RAP. *IL18R1* (IL18Rα) was significantly upregulated in CD161+TCRγδ+ ($p < 0.01$) and both CD161-positive populations of CD8+ ($p < 0.0001$) T cells and *IL18RAP* significantly upregulated in all CD161-expressing T cell subsets ($p < 0.0001$; Figure 5A). Expression was confirmed at the protein level by flow cytometry, which also revealed a previously unappreciated CD161++ IL18Rα++ subset among CD4+ and TCRγδ+ T cells (Figure 5B). Gating of these three subsets (CD161++, CD161+, and CD161−) revealed a significant correlation between CD161 expression and IL18Rα expression (Figure 5C) among CD4+ ($p < 0.0001$) and TCRγδ+ ($p = 0.0001$) T cells, as for CD8+ T cells (Figure 3E).

We recently described that elevated expression of IL18R enables CD161++CD8+/MAIT cells to be activated by IL-12+IL-18 in a TCR-independent manner (Ussher et al., 2014). As genes encoding both subunits of the IL-18R and *IL12RB2* were contained within the core leading edge set of CD161-associated upregulated genes (Table 1), we assayed IFNγ production in response to overnight stimulation with IL-12+IL-18 in CD8+, CD4+, and TCRγδ+ T cells. IFNγ production was apparent by intracellular cytokine staining in all three T cell lineages and particularly apparent within the CD161++ population of each (Figure 5D). Although CD4+ MAIT cells do exist (Reantragoon et al., 2013), IFNγ responses were not restricted to Vα7.2+CD4+ T cells (Figure S2). We correlated this response to IL12+IL18 with the levels of CD161 expressed by gating on the three CD161 populations (CD161++, CD161+, and CD161−) within each T cell lineage, as previously (Figure 5B). As expected, there was a significant correlation between levels of CD161 expressed by each population and the percentage of that population expressing IFNγ in response to IL-12+IL-18 (Figure 5E), with the greatest responses seen by the CD161++ population in each.

Together, these results demonstrate CD161-positive T lymphocytes to be related both in terms of gene expression and function, including elevated expression of IL18R in the resting state. This is linked to their shared ability to make an innate response to cytokine stimulation by IL-12+IL-18, which is independent of the TCR yet correlated to expression of CD161.

Regulation by CD161

Expression of CD161 by NK cells is generally accepted to negatively regulate NK cell functions (Aldemir et al., 2005; Lanier et al., 1994; Rosen et al., 2005), whereas the effect of CD161 ligation on T cell function is less clear (Aldemir et al., 2005; Exley et al., 1998; Le Bourhis et al., 2013; Rosen et al., 2008). To investigate the role of CD161 in the response to IL12+IL18, we ligated CD161 by adding biotin beads coated with anti-CD161 into the culture.

Figure 3. CD161+CD8+ T Cells Share a CD161++ Transcriptional Signature and Phenotypic Profile

(A) Heatmap showing 3,025 significantly ($p < 0.05$) differentially expressed transcripts between CD161++ and CD161− CD8+ T cells in four donors. Subsets clustered by one minus Pearson correlation.

(B) Heatmap showing 544 significantly differentially expressed genes between CD161+ and CD161− CD8+ T cells in the same four donors. Subsets clustered by one minus Pearson correlation.

(C) Pie chart shows proportion of genes differentially expressed by CD161+ that are shared with CD161++ (79%) when compared to CD161− CD8+ T cells. Venn diagram shows breakdown of upregulated and downregulated genes unique to or shared by each subset.

(D) Gene set enrichment summary plots for vsn-normalized CD161+ versus CD161− CD8+ T cell ranked genes and CD161++ upregulated (top) and downregulated (bottom) gene sets. Normalized enrichment score (NES) = 3.79, $p < 0.001$ upregulated genes; NES = −3.12, $p < 0.001$ downregulated genes.

(E) GeoMFI of CD161 for CD161++ (green), CD161+ (blue), and CD161− (red) CD8+ T cell subsets correlated with GeoMFI of CCR6 ($r^2 = 0.9143$; $p < 0.0001$), CXCR6 ($r^2 = 0.9258$; $p < 0.0001$), MDR1 ($r^2 = 0.9322$; $p < 0.0001$), and IL18Rα ($r^2 = 0.9554$; $p < 0.0001$); n = 5. Representative flow cytometry plots shown for each.

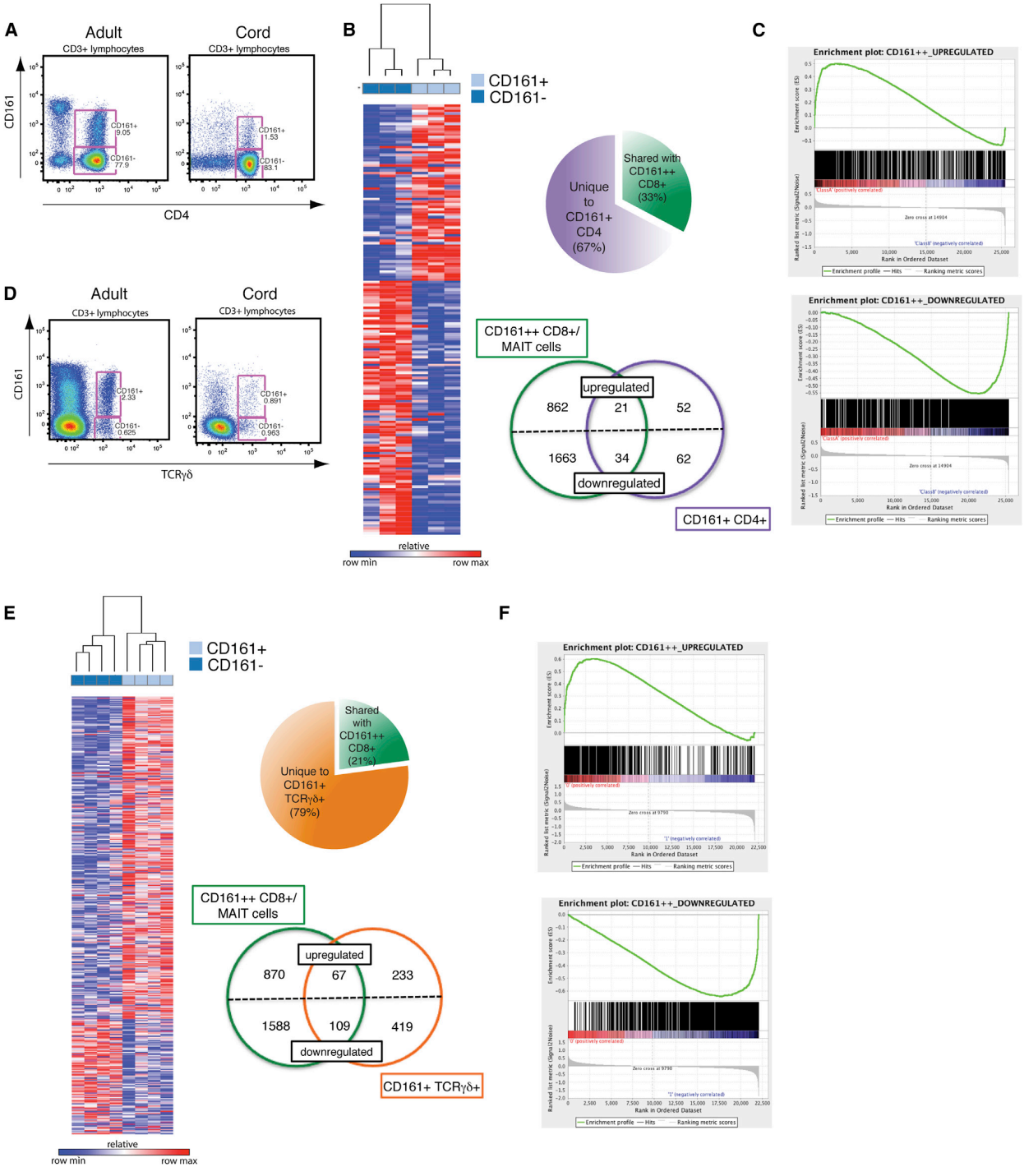

Figure 4. CD161+CD4+ and CD161+TCRγδ+ T Cells Are Enriched for the CD161++CD8+/MAIT Transcriptional Signature

(A) Representative flow cytometry plot showing CD161+CD4+ T cells within adult and cord blood.

(B) Heatmap showing 169 significantly differentially expressed genes between CD161+ and CD161− CD4+ T cells in three donors. Subsets clustered by one minus Pearson correlation. Pie chart shows proportion of genes differentially expressed by CD161+CD4+ that are shared with CD161++CD8+ (33%), when compared to their CD161− counterparts. Venn diagram shows breakdown of upregulated and downregulated genes unique to or shared by each subset.

(legend continued on next page)

OPEN ACCESS
CellPress

Table 1. Core Transcriptional Signature of CD161-Associated Upregulated Genes

ABCA2	*CTNNA1*	*IGFBP4*	*MYO1F*	*SESN1*
ABCB1	*CTSH*	*IL12RB2*	*NADK*	*SIPA1L2*
ACTN4	*CXCR6*	*IL15*	*NBEAL2*	*SLAMF1*
ADCY9	*CXXC5*	*IL18R1*	*NETO2*	*SLC1A5*
ADRB2	*CYB561*	*IL18RAP*	*NPC1*	*SLC2A8*
AGPAT4	*CYFIP1*	*IL23R*	*PBX4*	*SLC7A5*
ALCAM	*DENND3*	*IRAK2*	*PERP*	*SLCO3A1*
ARNTL	*DUSP5*	*JSRP1*	*PHACTR2*	*SMAD3*
AUTS2	*EIF2C4*	*KIAA1539*	*PHLDA1*	*SMAD7*
B4GALT1	*ELOVL4*	*KIF5C*	*PIK3AP1*	*SNAI3*
CACNA2D2	*ELOVL6*	*KLRB1*	*PLCB1*	*SYNE2*
CACNA2D4	*ERN1*	*KLRG1*	*PLEKHG3*	*SYTL2*
CAMTA1	*FAM43A*	*LAG3*	*PLXNC1*	*THBS1*
CAPN12	*FAS*	*LATS2*	*PODXL*	*TLE1*
CCR2	*FOSL2*	*LONRF3*	*PRDM1*	*TNF*
CD58	*GALM*	*LTB4R*	*PRDM8*	*TNFRSF18*
CD72	*GBP5*	*LTK*	*PRF1*	*TNFSF14*
CERK	*GFPT2*	*MAFF*	*PTGDS*	*TPM2*
CFH	*GPR65*	*MAP3K5*	*PTPRM*	*VCL*
CLCF1	*GPR68*	*MAP3K8*	*RAB11FIP1*	*VLDLR*
CLIC5	*GTF3C1*	*MATK*	*RASD1*	*WNT1*
COL5A1	*GZMA*	*ME1*	*RHBDF2*	*YPEL1*
COL5A3	*GZMK*	*METRNL*	*RORA*	*ZBTB16*
COLQ	*IFI44*	*MICALCL*	*RORC*	*ZDHHC14*
CREB3L2	*IFNGR1*	*MYO1D*	*RPPH1*	

Leading-edge analysis was performed on the enriched CD161++CD8+ T cell upregulated gene set in all T cell subsets. The leading-edge gene set was compared from each T cell population and a core set of 124 genes identified and listed in alphabetical order. Those referred to in the text are underlined.

Ligation of CD161, either by its ligand LLT1 or anti-CD161, induces transient downregulation in CD161 expression (Figure S3). Therefore, this analysis could only be reliably performed on MAIT cells, which can be tracked independently through expression of Vα7.2. Ligation of CD161 had no effect on MAIT cell expression of IL18R (Figure 6A) or IFNγ production in response to IL-12+IL-18 (Figure 6B). Previously, CD161 has been shown to regulate responses only in the context of TCR stimulation (Aldemir et al., 2005; Exley et al., 1998); therefore, we examined the effect of CD161 ligation in addition to stimulation through the TCR. Ligation of CD161 induced a significant increase in IFNγ ($p < 0.01$) and tumor necrosis factor alpha (TNF-α) ($p < 0.05$) production when MAIT cells were stimulated with anti-CD3 and anti-CD28 compared to cells stimulated with anti-CD3 and anti-CD28 alone (Figures 6C and 6D). This suggests, along with published data (Aldemir et al., 2005; Exley et al., 1998) and other data using soluble anti-CD161 (data not shown), that CD161 can act as a costimulatory receptor to increase the response to TCR stimulation.

DISCUSSION

Conventionally, T lymphocyte subsets have been identified and divided based upon the expression of sets of proteins, including cell surface markers, cytokines, and nuclear transcription factors. The C-type lectin CD161 is expressed by a large proportion of cells within each of these previously defined subsets, including MAIT, CD4+ and CD8+, and both TCRαβ+ and TCRγδ+ T cells. Despite the diverse phenotypes and functions of these individual T cell subsets, associated with their recognition of distinct antigens on specific antigen-presenting molecules, we have demonstrated these cell lineages to be related by a shared transcriptional signature and innate-like function and marked by expression of CD161.

Among those T cells expressing the highest levels of CD161 is the population of innate-like, unconventional T cells known as MAIT cells. This population is distinct in terms of TCR expression (Tilloy et al., 1999), antibacterial function (Le Bourhis et al., 2010), and type-17-related transcriptional and phenotypic profile (Billerbeck et al., 2010). This study represents a phenotypic description of CD161++CD8+ MAIT cells by multiparametric mass cytometry (CyTOF). Despite inclusion of only "conventional" T cell markers within the 23-parameter panel, rather than the unique markers characteristic of MAIT cells, PCA emphasized the distinctiveness of this population, which segregates within a discrete niche in the spectrum of CD8+ T cell phenotypes. It would be of interest to identify the location of the Vα7.2− CD161++CD8+ T cell population in relation to Vα7.2+ MAIT cells within the spectrum of CD8+ T cell phenotypes, which was precluded here by the absence of an isotope-tagged Vα7.2 antibody.

Although the Vα7.2− CD161++CD8+ T cell population is highly heterogeneous in terms of both TCR α and β chain expression, both Vα7.2+ and Vα7.2− CD161++ subsets expressed a memory phenotype and elevated levels of the polarizing transcription factors RORγt and PLZF. The central role of PLZF in directing the innate-like functions of NKT and MAIT cells (Savage et al., 2008) and other innate lymphocytes (Constantinides et al., 2014) has recently been revealed. The shared expression by Vα7.2− CD161++CD8+ T cells, early in development (Walker et al., 2012), suggests that these cells may also display innate characteristics. We investigated whether diverse Vα7.2− cells represented a population analogous to type II NKT cells (Godfrey

(C) Gene set enrichment summary plots for vsn-normalized CD161+ versus CD161− CD4+-T-cell-ranked genes and CD161++CD8+ upregulated (left) and downregulated (right) genes. NES = 2.45, $p < 0.001$ upregulated genes; NES = −3.04, $p < 0.001$ downregulated genes.
(D) Representative flow cytometry plot showing CD161+TCRγδ+ T cells within adult and cord blood.
(E) Heatmap showing 828 significantly differentially expressed genes between CD161+ and CD161− TCRγδ+ T cells in four donors. Subsets clustered by one minus Pearson correlation. Pie chart shows proportion of genes differentially expressed by CD161+TCRγδ+ that are shared with CD161++CD8+ (21%), when compared to their CD161− counterparts. Venn diagram shows breakdown of upregulated and downregulated genes unique to or shared by each subset.
(F) Gene set enrichment summary plots for vsn-normalized CD161+ versus CD161− TCRγδ+-T-cell-ranked genes and CD161++CD8+ upregulated (left) and downregulated (right) genes. NES = 2.78, $p < 0.001$ upregulated genes; NES = −2.62, $p < 0.001$ downregulated genes.

OPEN ACCESS
CellPress

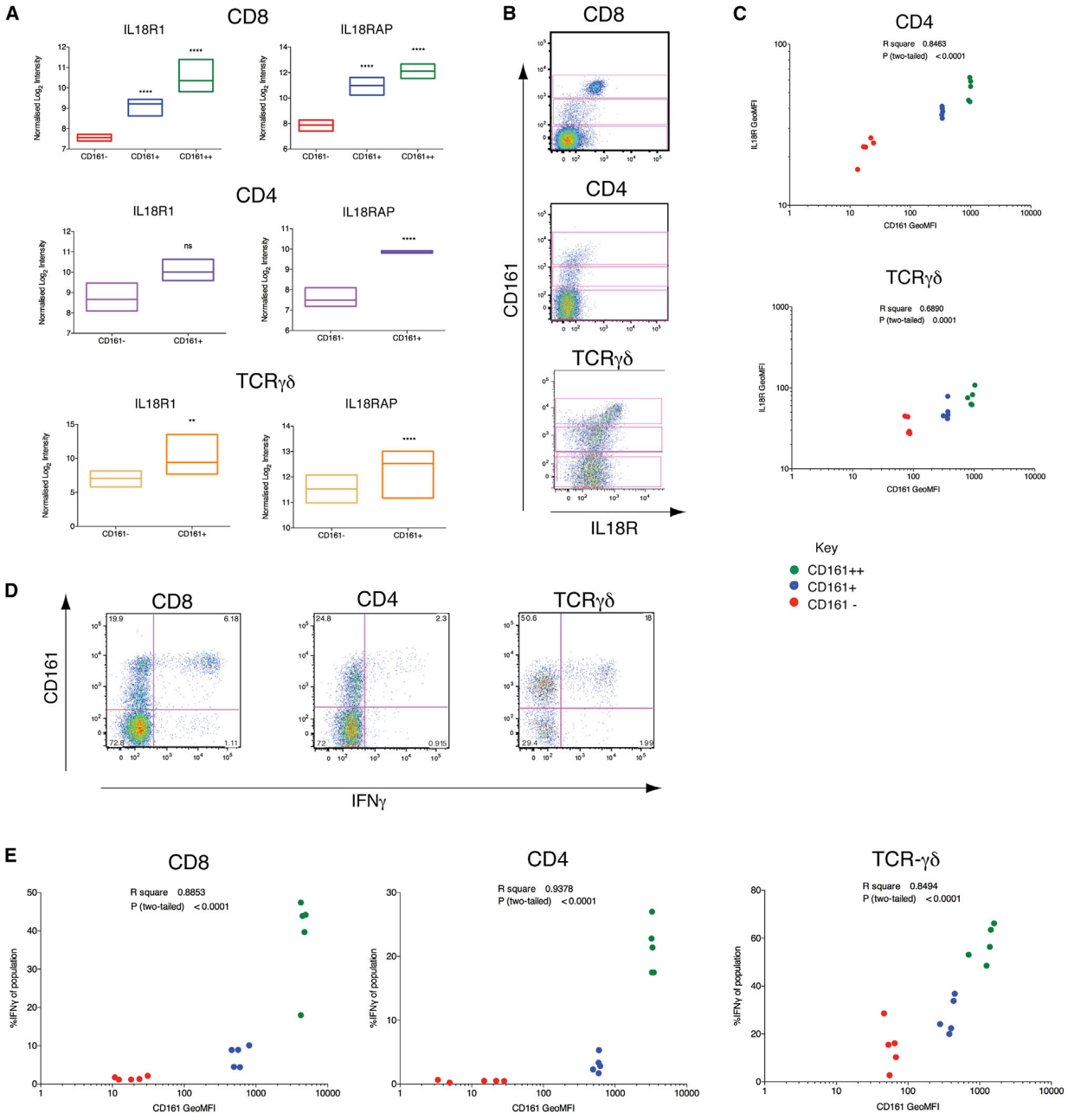

Figure 5. CD161-Positive T Cell Subsets Express Elevated Levels of IL18Rα and Respond to Stimulation by IL-12+IL-18

(A) Relative expression levels of IL18R subunits by CD161-positive and CD161-negative sorted T cells and statistical significance from mRNA expression analyses after normalization and correction for multiple testing. **p < 0.01; ****p < 0.0001. Floating bars show minimum and maximum values, with a line at the mean.

(B) Representative flow cytometry plots for IL18Rα expression in each T cell lineage, revealing CD161++, CD161+, and CD161− subsets in each (gated).

(C) GeoMFI of CD161 for CD161++ (green), CD161+ (blue), and CD161− (red) subsets in CD4+ and TCRγδ+ T cells correlated with GeoMFI of IL18Rα. CD4 r^2 = 0.8463, p < 0.0001; TCRγδ r^2 = 0.6890, p < 0.0001 (n = 5).

(D) PBMCs were stimulated overnight with 50 ng/ml IL-12+IL-18. Representative flow cytometry plots for IFNγ expression by gated CD8+, CD4+, and TCRγδ+ CD3+ live lymphocytes.

(E) GeoMFI of CD161 for CD161++ (green), CD161+ (blue), and CD161− (red) subsets in CD8+, CD4+, and TCRγδ+ T cells correlated with percentage of each subset expressing IFNγ in response to overnight stimulation with IL-12+IL-18. CD8 r^2 = 0.8853, p < 0.0001; CD4 r^2 = 0.9378, p < 0.0001; TCRγδ r^2 = 0.8494, p < 0.0001 (n = 5).

See also Figure S2.

OPEN ACCESS
CellPress

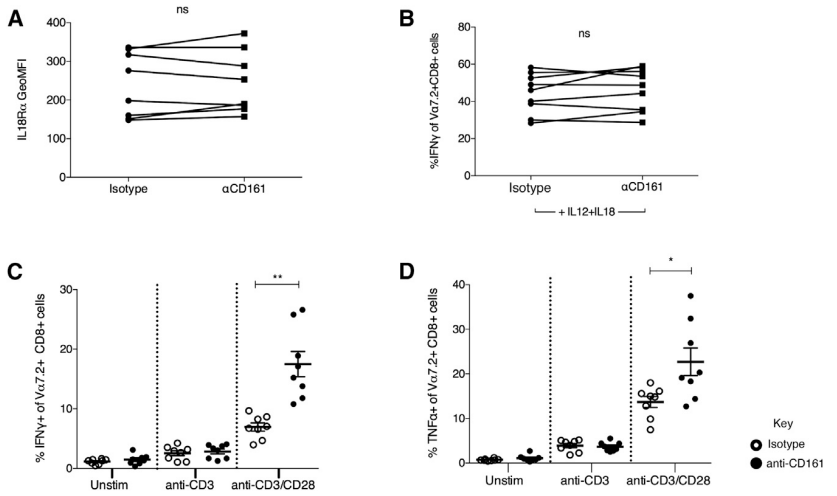

Figure 6. CD161 Regulates TCR-Dependent, but Not TCR-Independent, Responses

(A) GeoMFI of IL18Rα on Vα7.2+CD8+CD3+ cells incubated for 18 hr with biotin beads coated with either IgG2a isotype or anti-CD161. ns, not significant by paired t test (n = 9).

(B) Percentage of Vα7.2+CD8+CD3+ cells expressing IFNγ when cultured with 50 ng/ml IL-12+IL-18 for 18 hr in the presence of biotin beads coated with either IgG2a isotype or anti-CD161. ns, not significant by paired t test (n = 9).

(C and D) Percentage of Vα7.2+CD8+CD3+ cells expressing IFNγ (C) or TNF-α (D) when cultured overnight with TCR-stimulating biotin beads, coated either with anti-CD3 or anti-CD3 + anti-CD28, in combination with IgG2a isotype (open circles) or anti-CD161 (filled circles). *$p < 0.05$ and **$p < 0.01$ by repeated-measures one-way ANOVA (n = 8).

Data are represented as mean ± SEM. See also Figure S3.

et al., 2004), which recognize identical ligands to invariant NKT cells, an additional innate-like lymphocyte subset, despite diverse TCR expression (Gadola et al., 2002). It appears that Vα7.2− CD161++CD8+ T cells are not MR1 responsive in the majority of donors; however, this does not rule out the possibility that this population may be reactive to other nonclassical ligands and warrants further investigation. Nonetheless, like Vα7.2+ MAIT cells, Vα7.2− CD161++CD8+ T cells are specifically activated by stimulation by IL-12+IL18, as shown here and elsewhere (Ussher et al., 2014), representing a shared innate-like feature of both populations of CD161++CD8+ T cells.

As MAIT cells displayed a phenotypic and functional relationship to Vα7.2− CD161++CD8+ T cells, we utilized mRNA microarray analysis to examine the relationship of MAIT cells to other CD161-expressing T cell subsets. Previously, whole transcriptome analysis by microarray has revealed that memory T and B cells display a transcriptional signature that is shared with hematopoietic stem cells (Luckey et al., 2006), and transcripts that distinguish T and B cells are also expressed among other lymphocyte cell types (Painter et al., 2011). This indicates that expression patterns and their consequent phenotypes may be shared across previously defined divisions and may further be suggestive of shared functional characteristics. In a similar way, analysis of mRNA microarray data for CD161-positive T cells, including TCRγδ+, CD4+, and both populations of CD8+ T cells, revealed a CD161-associated transcriptional signature enriched in all T lymphocytes expressing CD161 and led to the identification of a shared functional attribute.

The core transcriptional profile of CD161-expressing T cells included genes for subunits of both the IL-12 and IL-18 receptors, with high IL18Rα expression conserved across CD161-positive T cells of all lineages. Expression of this receptor was related to the ability of these cells to respond to IL-18 in combination with IL-12, inducing the innate TCR-independent production of IFNγ. Although this has previously been described for CD161++ CD8+ T cells, including MAIT cells (Ussher et al., 2014) and confirmed here for Vα7.2−CD161++, this has not been described for other T cell subsets, with CD161++ subsets in all lineages, identified among CD4+ and TCRγδ+ T cells, displaying the highest response levels. This establishes CD161 as a marker of cells with an enhanced "innate" ability to respond to this stimulus. Furthermore, this TCR-independent pathway suggests a means by which these populations may be activated in the inflammatory conditions in which they have been implicated (Annibali et al., 2011; Billerbeck et al., 2010; Kang et al., 2012; Kleinschek et al., 2009; Poggi et al., 1999).

The significance of CD161 expression by T cells has not yet been fully determined. However, CD161 has previously been applied as a marker of IL-17-expressing T cells (Maggi et al., 2010), particularly Th17 cells (Cosmi et al., 2008), and may be involved in the induction of this phenotype (Bai et al., 2014). Whereas CD161 was shown here to mark cells with an innate-like ability to respond to cytokine stimulation, ligation of CD161 had no effect on this response. Instead, CD161 was demonstrated to function as a costimulatory receptor in the context of TCR stimulation. This effect may differ from those shown by others (Le Bourhis et al., 2013; Rosen et al., 2008) due to differences in the presentation of anti-CD161 or in the clones used (see Figure S3D).

MAIT cells have previously been described to be hyporesponsive to stimulation through the TCR (Turtle et al., 2011), a feature recently suggested to characterize all innate-like lymphocytes (Wencker et al., 2014). This was related to low expression levels of genes for multiple proteins that positively regulate TCR signaling, including the genes *ITK* and *MAL* (Turtle et al., 2011). Interestingly, these genes were also contained within the set of core downregulated genes we identified here, being shared between all CD161-expressing T cells (Table S7). If similarly TCR hyporesponsive, then by acting as a costimulatory receptor, CD161 may help to overcome the reduced reactivity of the TCR in these innate-like T cells (Wencker et al., 2014). Induction of TCR hyporesponsiveness during development of innate-like T cells has also been associated with the ability to respond to cytokine stimulation and interestingly enabled identification by Wencker et al. (2014) of an innate-like murine TCRγδ+ T cell subset that also responded selectively to IL-12 and IL-18.

OPEN ACCESS
CellPress

In contrast to the current paradigms of T cell subdivision, this study identifies a phenotype and function that is shared across T cell lineages and marked by expression of CD161. Here, we describe CD161 to identify cells with a shared transcriptional profile, including high expression of IL18R, and capable of making innate-type responses to cytokine stimulation. Therefore, expression of CD161 marks human T cells with a distinct phenotype that is independent of lineage and identifies a family of related lymphocytes with innate characteristics that includes MAIT cells.

EXPERIMENTAL PROCEDURES

Cells

PBMCs were obtained from adults (whole blood leukocyte cones; NHS Blood and Transplant), 24 month olds (prospective birth cohort; Saghafian-Hedengren et al., 2010), and umbilical cord blood samples (Stem Cell Services, NHS Blood and Transplant) after appropriate ethical review. These were rested overnight or stored in liquid nitrogen until required.

THP-1 cells (ECACC) were incubated with paraformaldehyde-fixed *E. coli* (DH5α; Invitrogen) at 25 bacteria per cell overnight. PMBCs (24-month donors) or sort-purified CD8+ T cells (adults; sorted on a MoFlo; Beckman Coulter Genomics) were then added for a 5 hr coculture. Anti-MR1 (clone 26.5, kindly provided by T.H. Hansen) or IgG2a isotype control (BD Biosciences) was added at 10 μg/ml. For IL-12 + IL-18 stimulations, IL-12 (Miltenyi Biotec) and IL-18 (R&D Systems) were added at 50 ng/ml overnight. In all cases, brefeldin A (eBioscience) was added for the final 4 hr of incubation.

TCR Sequencing

T cell receptor sequencing of single cells was performed as previously described (Wang et al., 2012). In brief, Vα7.2+ and Vα7.2− CD161++CD8+ T cells were sorted (MoFlo; Beckman Coulter) as single cells into wells of a 96-well plate containing 2.5 μl of iScript cDNA Synthesis reaction mixture (Bio-Rad) with 0.1% Triton X-100. TCR transcripts for each cell were amplified by multiplex nested PCR using one unit of Platinum Taq DNA polymerase High Fidelity, 10× PCR buffer, 2 mM magnesium sulfate and 0.2 mM deoxynucleotide triphosphate (Invitrogen), 2.5 pmol of each external TRAV and TRBV primer and 10 pmol of each external TRAC and TRBC in the first round, or the same concentration of either internal TRAV and TRAC or internal TRBV and TRBC primers in the second round (primers as detailed in Wang et al., 2012). The PCR conditions were 95°C for 2 min, followed by 35 cycles of 95°C for 20 s, 52°C for 20 s, 72°C for 45 s, followed by one cycle of 72°C for 7 min. PCR products were purified and sequenced with the corresponding TRAC or TRBC primer.

Microarrays

Cell sorting, RNA extraction, and microarray analysis of CD161 subsets within CD8+ T cells was performed as previously described (Billerbeck et al., 2010).

CD4+ T cells were isolated from three donors by magnetic bead enrichment (EasySep; STEMCELL Technologies) and CD161 subsets selected by staining anti-CD161-phycoerythrin (PE); Beckman Coulter) followed by purification with anti-PE MicroBeads (Miltenyi Biotec). Purity, as determined by flow cytometry, was >95% for all samples. Total RNA was extracted using an RNeasy Mini Kit (QIAGEN) and quality measured using the ND 1000 Spectrophotometer (Saveen Werner). cRNA was amplified and purified using Illumina TotalPrep RNA amplification kit (Ambion) and hybridized to the Illumina HumanWG-6 v3.0 Expression BeadChip (Illumina).

For gene-expression profiling of TCRγδ+ T cell subsets, T cells were enriched from PBMCs from four donors as per the manufacturer's instructions (EasySep T cell enrichment kit; STEMCELL Technologies). CD3+TCRγδ+ CD161+ or CD161− were sorted using a FACSAria (BD Biosciences). Cell pellets were snap frozen and sent to Miltenyi Biotec Genomic Services (Bergisch Gladbach) for RNA extraction and hybridization to Agilent Whole Human Genome Oligo Microarray.

Microarray features were normalized using variance-stabilizing normalization (vsn) (Huber et al., 2002) using R (http://cran.r-project.org/) and Bioconductor (http://bioconductor.org) packages. Gene lists of interest were generated from those genes >2-fold up/downregulated and with a $p < 0.05$ for comparison using the Venn diagram module of GenePattern (Gould et al., 2006). Heatmaps were generated using GENE-E (http://www.broadinstitute.org/cancer/software/GENE-E/index.html). Gene set enrichment analysis was performed using GSEA version 2.0.14 (Subramanian et al., 2005).

CyTOF

PBMCs were stimulated for 3 hr with 150 ng/ml PMA + 1 μM ionomycin in RPMI plus brefeldin A and monensin (eBioscience), 2.5 μg/ml anti-CD107α, 1.25 μg/ml anti-CD107b (BD Bioscience), and 10 μM TAPI-2 (VWR International). Following stimulation, cells were resuspended in cytometry buffer (PBS + 0.05% sodium azide + 2 mM EDTA + 2% fetal calf serum) and stained with isotope-tagged antibodies before being acquired on the CyTOF. For the detailed protocol, see Newell et al. (2012) and the Supplemental Experimental Procedures.

Statistical Analysis

Statistical analysis was performed using Prism version 6 software (GraphPad). Data are represented as mean ± SEM. ****$p < 0.0001$; ***$p < 0.001$; **$p < 0.01$; *$p < 0.05$; and ns, not significant, as stated in figure legends.

ACCESSION NUMBERS

The NCBI Gene Expression Omnibus accession number for the microarray data reported in this paper is GSE62099.

SUPPLEMENTAL INFORMATION

Supplemental Information includes Supplemental Experimental Procedures, three figures, seven tables, and two movies and can be found with this article online at http://dx.doi.org/10.1016/j.celrep.2014.09.045.

AUTHOR CONTRIBUTIONS

J.R.F. designed, performed, and analyzed experiments and wrote the manuscript. K.E.S. designed, performed, and analyzed the CD161 ligation experiments. V.M.F., N.R., and Y.-H.K. performed the microarrays. All remaining authors contributed to specific experiments. P.K. designed experiments and provided overall guidance.

ACKNOWLEDGMENTS

The authors would like to thank T. Hansen for the kind provision of the MR1-blocking antibody, N. Rust for sorting expertise, C. Marchant for technical support, and all members of the laboratory for helpful discussion and support. J.R.F is supported by the Wellcome Trust IITM Programme (092871/Z/10/Z). This work was also supported by the Wellcome Trust (WT091663MA), the Medical Research Council, the NIHR Biomedical Research Centre (Oxford), the Nuffield Department of Clinical Medicine (Oxford), the James Martin School for the 21st Century (Oxford), the NIH (NIAD U19AI 082630), and the Oxford Dominions Trust.

Received: June 16, 2014
Revised: August 28, 2014
Accepted: September 24, 2014
Published: October 23, 2014

REFERENCES

Aldemir, H., Prod'homme, V., Dumaurier, M.-J., Retiere, C., Poupon, G., Cazareth, J., Bihl, F., and Braud, V.M. (2005). Cutting edge: lectin-like transcript 1 is a ligand for the CD161 receptor. J. Immunol. *175*, 7791–7795.

Annibali, V., Ristori, G., Angelini, D.F., Serafini, B., Mechelli, R., Cannoni, S., Romano, S., Paolillo, A., Abderrahim, H., Diamantini, A., et al. (2011).

OPEN ACCESS
CellPress

CD161(high)CD8+T cells bear pathogenetic potential in multiple sclerosis. Brain *134*, 542–554.

Annunziato, F., Cosmi, L., Santarlasci, V., Maggi, L., Liotta, F., Mazzinghi, B., Parente, E., Filì, L., Ferri, S., Frosali, F., et al. (2007). Phenotypic and functional features of human Th17 cells. J. Exp. Med. *204*, 1849–1861.

Bai, A., Moss, A., Kokkotou, E., Usheva, A., Sun, X., Cheifetz, A., Zheng, Y., Longhi, M.S., Gao, W., Wu, Y., and Robson, S.C. (2014). CD39 and CD161 Modulate Th17 Responses in Crohn's Disease. J. Immunol. *193*, 3366–3377.

Battistini, L., Borsellino, G., Sawicki, G., Poccia, F., Salvetti, M., Ristori, G., and Brosnan, C.F. (1997). Phenotypic and cytokine analysis of human peripheral blood gamma delta T cells expressing NK cell receptors. J. Immunol. *159*, 3723–3730.

Billerbeck, E., Kang, Y.-H., Walker, L., Lockstone, H., Grafmueller, S., Fleming, V., Flint, J., Willberg, C.B., Bengsch, B., Seigel, B., et al. (2010). Analysis of CD161 expression on human CD8+ T cells defines a distinct functional subset with tissue-homing properties. Proc. Natl. Acad. Sci. USA *107*, 3006–3011.

Constantinides, M.G., McDonald, B.D., Verhoef, P.A., and Bendelac, A. (2014). A committed precursor to innate lymphoid cells. Nature *508*, 397–401.

Corbett, A.J., Eckle, S.B.G., Birkinshaw, R.W., Liu, L., Patel, O., Mahony, J., Chen, Z., Reantragoon, R., Meehan, B., Cao, H., et al. (2014). T-cell activation by transitory neo-antigens derived from distinct microbial pathways. Nature *509*, 361–365.

Cosmi, L., De Palma, R., Santarlasci, V., Maggi, L., Capone, M., Frosali, F., Rodolico, G., Querci, V., Abbate, G., Angeli, R., et al. (2008). Human interleukin 17-producing cells originate from a CD161+CD4+ T cell precursor. J. Exp. Med. *205*, 1903–1916.

Dusseaux, M., Martin, E., Serriari, N., Péguillet, I., Premel, V., Louis, D., Milder, M., Le Bourhis, L., Soudais, C., Treiner, E., and Lantz, O. (2011). Human MAIT cells are xenobiotic-resistant, tissue-targeted, CD161hi IL-17-secreting T cells. Blood *117*, 1250–1259.

Exley, M., Porcelli, S., Furman, M., Garcia, J., and Balk, S. (1998). CD161 (NKR-P1A) costimulation of CD1d-dependent activation of human T cells expressing invariant V α 24 J α Q T cell receptor α chains. J. Exp. Med. *188*, 867–876.

Gadola, S.D., Dulphy, N., Salio, M., and Cerundolo, V. (2002). Valpha24-JalphaQ-independent, CD1d-restricted recognition of alpha-galactosylceramide by human CD4(+) and CD8alphabeta(+) T lymphocytes. J. Immunol. *168*, 5514–5520.

Godfrey, D.I., MacDonald, H.R., Kronenberg, M., Smyth, M.J., and Van Kaer, L. (2004). NKT cells: what's in a name? Nat. Rev. Immunol. *4*, 231–237.

Gold, M.C., Eid, T., Smyk-Pearson, S., Eberling, Y., Swarbrick, G.M., Langley, S.M., Streeter, P.R., Lewinsohn, D.A., and Lewinsohn, D.M. (2013). Human thymic MR1-restricted MAIT cells are innate pathogen-reactive effectors that adapt following thymic egress. Mucosal Immunol. *6*, 35–44.

Gould, J., Getz, G., Monti, S., Reich, M., and Mesirov, J.P. (2006). Comparative gene marker selection suite. Bioinformatics *22*, 1924–1925.

Huber, W., von Heydebreck, A., Sültmann, H., Poustka, A., and Vingron, M. (2002). Variance stabilization applied to microarray data calibration and to the quantification of differential expression. Bioinformatics *18* (*Suppl 1*), S96–S104.

Iizuka, K., Naidenko, O.V., Plougastel, B.F.M., Fremont, D.H., and Yokoyama, W.M. (2003). Genetically linked C-type lectin-related ligands for the NKRP1 family of natural killer cell receptors. Nat. Immunol. *4*, 801–807.

Kang, Y.-H., Seigel, B., Bengsch, B., Fleming, V.M., Billerbeck, E., Simmons, R., Walker, L., Willberg, C.B., Barnes, E.J., Bhagwanani, A., et al. (2012). CD161(+)CD4(+) T cells are enriched in the liver during chronic hepatitis and associated with co-secretion of IL-22 and IFN-γ. Front Immunol *3*, 346.

Kjer-Nielsen, L., Patel, O., Corbett, A.J., Le Nours, J., Meehan, B., Liu, L., Bhati, M., Chen, Z., Kostenko, L., Reantragoon, R., et al. (2012). MR1 presents microbial vitamin B metabolites to MAIT cells. Nature *491*, 717–723.

Kleinschek, M.A., Boniface, K., Sadekova, S., Grein, J., Murphy, E.E., Turner, S.P., Raskin, L., Desai, B., Faubion, W.A., de Waal Malefyt, R., et al. (2009). Circulating and gut-resident human Th17 cells express CD161 and promote intestinal inflammation. J. Exp. Med. *206*, 525–534.

Lanier, L.L., Chang, C., and Phillips, J.H. (1994). Human NKR-P1A. A disulfide-linked homodimer of the C-type lectin superfamily expressed by a subset of NK and T lymphocytes. J. Immunol. *153*, 2417–2428.

Le Bourhis, L., Martin, E., Péguillet, I., Guihot, A., Froux, N., Coré, M., Lévy, E., Dusseaux, M., Meyssonnier, V., Premel, V., et al. (2010). Antimicrobial activity of mucosal-associated invariant T cells. Nat. Immunol. *11*, 701–708.

Le Bourhis, L., Dusseaux, M., Bohineust, A., Bessoles, S., Martin, E., Premel, V., Coré, M., Sleurs, D., Serriari, N.-E., Treiner, E., et al. (2013). MAIT cells detect and efficiently lyse bacterially-infected epithelial cells. PLoS Pathog. *9*, e1003681.

Leeansyah, E., Loh, L., Nixon, D.F., and Sandberg, J.K. (2014). Acquisition of innate-like microbial reactivity in mucosal tissues during human fetal MAIT-cell development. Nat Commun *5*, 3143.

Luckey, C.J., Bhattacharya, D., Goldrath, A.W., Weissman, I.L., Benoist, C., and Mathis, D. (2006). Memory T and memory B cells share a transcriptional program of self-renewal with long-term hematopoietic stem cells. Proc. Natl. Acad. Sci. USA *103*, 3304–3309.

Maggi, L., Santarlasci, V., Capone, M., Peired, A., Frosali, F., Crome, S.Q., Querci, V., Fambrini, M., Liotta, F., Levings, M.K., et al. (2010). CD161 is a marker of all human IL-17-producing T-cell subsets and is induced by RORC. Eur. J. Immunol. *40*, 2174–2181.

Martin, E., Treiner, E., Duban, L., Guerri, L., Laude, H., Toly, C., Premel, V., Devys, A., Moura, I.C., Tilloy, F., et al. (2009). Stepwise development of MAIT cells in mouse and human. PLoS Biol. *7*, e54.

Newell, E.W., Sigal, N., Bendall, S.C., Nolan, G.P., and Davis, M.M. (2012). Cytometry by time-of-flight shows combinatorial cytokine expression and virus-specific cell niches within a continuum of CD8+ T cell phenotypes. Immunity *36*, 142–152.

Painter, M.W., Davis, S., Hardy, R.R., Mathis, D., and Benoist, C.; Immunological Genome Project Consortium (2011). Transcriptomes of the B and T lineages compared by multiplatform microarray profiling. J. Immunol. *186*, 3047–3057.

Plougastel, B., Dubbelde, C., and Yokoyama, W.M. (2001). Cloning of Clr, a new family of lectin-like genes localized between mouse Nkrp1a and Cd69. Immunogenetics *53*, 209–214.

Poggi, A., Zocchi, M.R., Costa, P., Ferrero, E., Borsellino, G., Placido, R., Galgani, S., Salvetti, M., Gasperini, C., Ristori, G., et al. (1999). IL-12-mediated NKRP1A up-regulation and consequent enhancement of endothelial transmigration of V delta 2+ TCR gamma delta+ T lymphocytes from healthy donors and multiple sclerosis patients. J. Immunol. *162*, 4349–4354.

Porcelli, S., Yockey, C.E., Brenner, M.B., and Balk, S.P. (1993). Analysis of T cell antigen receptor (TCR) expression by human peripheral blood CD4-8- alpha/beta T cells demonstrates preferential use of several V beta genes and an invariant TCR alpha chain. J. Exp. Med. *178*, 1–16.

Reantragoon, R., Corbett, A.J., Sakala, I.G., Gherardin, N.A., Furness, J.B., Chen, Z., Eckle, S.B.G., Uldrich, A.P., Birkinshaw, R.W., Patel, O., et al. (2013). Antigen-loaded MR1 tetramers define T cell receptor heterogeneity in mucosal-associated invariant T cells. J. Exp. Med. *210*, 2305–2320.

Rosen, D.B., Bettadapura, J., Alsharifi, M., Mathew, P.A., Warren, H.S., and Lanier, L.L. (2005). Cutting edge: lectin-like transcript-1 is a ligand for the inhibitory human NKR-P1A receptor. J. Immunol. *175*, 7796–7799.

Rosen, D.B., Cao, W., Avery, D.T., Tangye, S.G., Liu, Y.-J., Houchins, J.P., and Lanier, L.L. (2008). Functional consequences of interactions between human NKR-P1A and its ligand LLT1 expressed on activated dendritic cells and B cells. J. Immunol. *180*, 6508–6517.

Saghafian-Hedengren, S., Sverremark-Ekström, E., Linde, A., Lilja, G., and Nilsson, C. (2010). Early-life EBV infection protects against persistent IgE sensitization. J. Allergy Clin. Immunol. *125*, 433–438.

Savage, A.K., Constantinides, M.G., Han, J., Picard, D., Martin, E., Li, B., Lantz, O., and Bendelac, A. (2008). The transcription factor PLZF directs the effector program of the NKT cell lineage. Immunity *29*, 391–403.

Subramanian, A., Tamayo, P., Mootha, V.K., Mukherjee, S., Ebert, B.L., Gillette, M.A., Paulovich, A., Pomeroy, S.L., Golub, T.R., Lander, E.S., and Mesirov, J.P. (2005). Gene set enrichment analysis: a knowledge-based approach for interpreting genome-wide expression profiles. Proc. Natl. Acad. Sci. USA *102*, 15545–15550.

Takahashi, T., Dejbakhsh-Jones, S., and Strober, S. (2006). Expression of CD161 (NKR-P1A) defines subsets of human CD4 and CD8 T cells with different functional activities. J. Immunol. *176*, 211–216.

Tilloy, F., Treiner, E., Park, S.H., Garcia, C., Lemonnier, F., de la Salle, H., Bendelac, A., Bonneville, M., and Lantz, O. (1999). An invariant T cell receptor alpha chain defines a novel TAP-independent major histocompatibility complex class Ib-restricted alpha/beta T cell subpopulation in mammals. J. Exp. Med. *189*, 1907–1921.

Turtle, C.J., Delrow, J., Joslyn, R.C., Swanson, H.M., Basom, R., Tabellini, L., Delaney, C., Heimfeld, S., Hansen, J.A., and Riddell, S.R. (2011). Innate signals overcome acquired TCR signaling pathway regulation and govern the fate of human CD161(hi) CD8α^+ semi-invariant T cells. Blood *118*, 2752–2762.

Ussher, J.E., Bilton, M., Attwod, E., Shadwell, J., Richardson, R., de Lara, C., Mettke, E., Kurioka, A., Hansen, T.H., Klenerman, P., and Willberg, C.B. (2014). CD161++ CD8+ T cells, including the MAIT cell subset, are specifically activated by IL-12+IL-18 in a TCR-independent manner. Eur. J. Immunol. *44*, 195–203.

Walker, L.J., Kang, Y.H., Smith, M.O., Tharmalingham, H., Ramamurthy, N., Fleming, V.M., Sahgal, N., Leslie, A., Oo, Y., Geremia, A., et al. (2012). Human MAIT and CD8$\alpha\alpha$ cells develop from a pool of type-17 precommitted CD8+ T cells. Blood *119*, 422–433.

Wang, G.C., Dash, P., McCullers, J.A., Doherty, P.C., and Thomas, P.G. (2012). T cell receptor $\alpha\beta$ diversity inversely correlates with pathogen-specific antibody levels in human cytomegalovirus infection. Sci. Transl. Med. *4*, 28ra42.

Wencker, M., Turchinovich, G., Di Marco Barros, R., Deban, L., Jandke, A., Cope, A., and Hayday, A.C. (2014). Innate-like T cells straddle innate and adaptive immunity by altering antigen-receptor responsiveness. Nat. Immunol. *15*, 80–87.

Yokoyama, W.M., and Seaman, W.E. (1993). The Ly-49 and NKR-P1 gene families encoding lectin-like receptors on natural killer cells: the NK gene complex. Annu. Rev. Immunol. *11*, 613–635.

frontiers in IMMUNOLOGY

MINI REVIEW ARTICLE
published: 30 August 2011
doi: 10.3389/fimmu.2011.00036

CD161-expressing human T cells

Joannah R. Fergusson[1]*, Vicki M. Fleming[2] and Paul Klenerman[2,3]

[1] *Sir William Dunn School of Pathology, University of Oxford, Oxford, UK*
[2] *Peter Medawar Building for Pathogen Research, University of Oxford, Oxford, UK*
[3] *Biomedical Research Centre, John Radcliffe Hospital, Oxford, UK*

Edited by:
Liisa Kaarina Selin, University of Massachusetts Medical School, USA

Reviewed by:
Joshua J. Obar, Montana State University, USA
Kristin Hogquist, University of Minnesota, USA

****Correspondence:***
Joannah R. Fergusson, Sir William Dunn School of Pathology, South Parks Road, Oxford OX1 3RE, UK.
e-mail: joannah.fergusson@path.ox.ac.uk

Expression of the Natural Killer cell receptor CD161 has recently been identified on a subset of T cells, including both CD4+ T helper and CD8+ T cells. Expression of this molecule within the adult circulation is restricted to those T cells with a memory phenotype. However, the distinct properties of these T cell populations is yet to be fully determined, although expression of CD161 has been related to the secretion of interleukin-17, and therefore to a type 17 phenotype. Recent studies have aimed to determine both the origin of these cells and the significance of CD161 expression as either a marker of specific cell types or as an effector and regulator of lymphocyte function, and hence to characterize the role of these CD161+ cells within a variety of human diseases in which they have been implicated.

Keywords: CD161, interleukin-17, T cells, T helper 17 cells, NK cells, NK-T cells, NKRP1

INTRODUCTION

The study of immunology is largely based on the division of leukocytes into families, lineages, and subsets; from division between innate and adaptive immunity, to categorization based on surface molecule expression and cytokine secretion. Many of those surface molecules involved in identification of subtype also reflect effector function. However, as further cells are identified these divisions become less distinct, with some cells demonstrating features from one or more of the previously defined subsets. As these molecules are often involved in effector function, common expression of molecules between lineages may suggest overlapping functions.

One set of divisions which are becoming increasingly "blurred" are those between T lymphocytes, Natural Killer (NK) cells, and NK-T cells. These subsets share common expression of specific molecules, including the C-type lectin CD161. This surface molecule was originally identified as the human homolog of the NKRP1 glycoproteins expressed on rodent NK cells, demonstrating 46–47% homology with its rodent counterparts. Human NKRP1A, or CD161, is composed of a disulfide-linked homodimer of ~40 kDa subunits. It is expressed by the majority of NK cells and approximately 24% of peripheral T cells (Lanier et al., 1994), including both γδ and αβ TCR-expressing subsets (Maggi et al., 2010) and NK-T cells. As NK-T cells compose less than 1% of human peripheral blood T cells (Gumperz et al., 2002), the remaining CD161+ T cells must represent a distinct lineage of T lymphocytes (Takahashi et al., 2006).

However, the implication of CD161 expression by these T cells remains to be fully determined – is CD161 simply a phenotypic marker; identifying T cells of a common activation state and/or lineage? Or does this C-type lectin perform some significant effector function itself? This review aims to explore recent advances in the characterization of CD161-expressing T cells, concentrating particularly on human αβ-TCR T cells, and through this to evaluate the importance of expression to immune function and hence to human disease.

CD161 AS A PHENOTYPIC MARKER OF T CELLS

CD161 expression is not unique to any predefined T cell subset. Lanier et al. (1994) originally identified expression on both CD4+ and CD8+ T cells, with a higher surface density on the latter. More recently, CD161 expression has also been demonstrated on CD4−CD8− double negative (DN) TCRαβ+ and TCRγδ+ T cells (Maggi et al., 2010). Further analysis has identified two CD161+CD8+ populations (Takahashi et al., 2006; Billerbeck et al., 2010), with intermediate or high CD161 expression levels, and one CD161+CD4+ T cell population expressing intermediate levels of CD161 only (Takahashi et al., 2006; Kang et al., unpublished observation), as shown in **Figure 1**. The functional relationship between the two populations of CD161 positive CD8+ T cells, and the significance of a $CD161^{high}$ population within CD8+ T cells which is largely absent from the CD4+ population, is yet to be fully defined.

CD161 AS A MARKER IL-17 PRODUCING CELLS

The identity of these CD161-expressing T subsets remained elusive until CD161 was identified as being significantly upregulated in T helper (Th) 17 clones compared to those of Th1 and Th2 (Cosmi et al., 2008). These CD4+ Th17 cells represent a novel helper cell subset, which secrete both IL-17A and IL-17F and express the master transcription factor retinoic acid-related orphan receptor (ROR)γt (Ivanov et al., 2006). In peripheral blood, IL-17 secreting CD4+ cells are contained within the CD161+ fraction and these cells express RORγt. Hence, CD161 is considered a hallmark of Th17 cells.

As a result of the correlation between IL-17 secretion and CD161 amongst Th17 cells, Maggi et al. (2010) investigated CD161 expression in other T cells capable of producing IL-17. In addition to Th17 cells, IL-17 secreting CD8+ T cells have also been isolated from the circulation of healthy individuals (Kondo et al., 2009). Interestingly, in all T cell subsets, including these CD8+ T cells, the ability to secrete IL-17 was virtually restricted

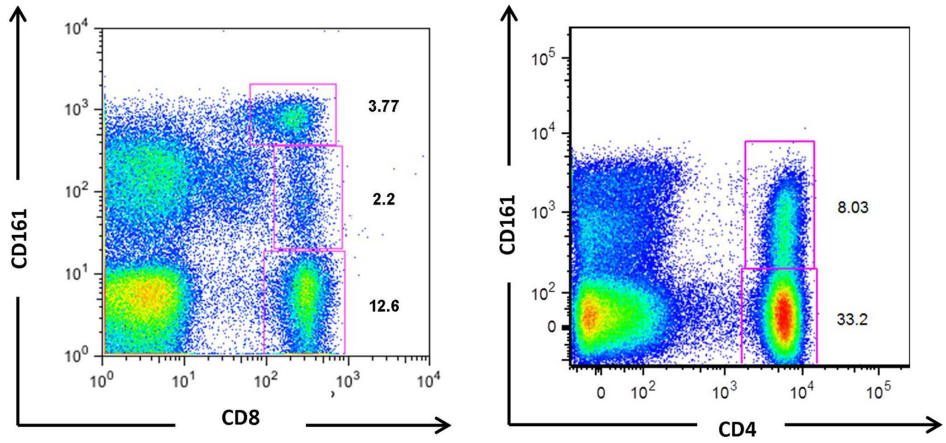

FIGURE 1 | CD161-expressing populations in CD8+ and CD4+ T cells. Flow cytometric analyses of T cells from healthy individuals demonstrate the existence of three populations of CD8+ T cells; CD161^{-}, CD161^{int}, and CD161^{high}, and two CD4+ T cell populations; CD161^{-} and CD161^{int}. Some donors may display a CD161^{high} CD4+ population, but in the majority CD161 positive CD4+ T cells comprise a single population with intermediate expression levels.

to those cells expressing CD161. These CD161+ cells express the Th17 transcription factor RORγt. Furthermore, Maggi et al. (2010) demonstrated that naïve CD161−CD4+ T cells transduced with RORγt produced IL-17 and upregulated CD161 expression, while inhibition of RORγt downregulated both IL-17 and CD161 expression in Th17 clones. Similarly, RORγt transduction in differentiating CD8+ T cells induced high levels of IL-17 production when these cells were cultured in the presence of Th17-polarizing cytokines (Huber et al., 2009). Thus, the observed correlation between IL-17 production and CD161 expression may result from dual control of gene expression by the transcription factor RORγt, which may be activated or upregulated under type 17-polarizing conditions.

CD8+ T cells capable of secreting IL-17 have been further characterized by Billerbeck et al. (2010). This study demonstrated IL-17 secretion amongst CD8+ T cells was restricted to those expressing high levels of CD161. CD161^{high}CD8+ cells display a phenotype similar to Th17 cells, such as the upregulated expression of RORγt, CCR6, and IL-18R, and as such have been described as Tc17 cells. Although these cells express the CD8 co-receptor, Tc17 cells display reduced cytotoxic potential compared to conventional CD8+ effector T cells associated with a low expression of granzyme B and perforin, and reduced cytotoxic degranulation as measured by CD107a upregulation. Tc17 populations independently described in mice also displayed limited cytolytic capability, with only a very small fraction positive for granzyme B (Hamada et al., 2009; Huber et al., 2009).

AREAS OF CONTROVERSY

However, several opposing theories have recently emerged regarding the identity of CD8+ T cells expressing high levels of CD161, summarized in **Table 1**. CD161, when co-expressed with IL-18Rα, has also been suggested as a marker of a prototypical CD8+ population known as memory stem cells (Turtle et al., 2009), which survive cytotoxic chemotherapy through the rapid efflux of cytotoxic drugs. Like those cells described by Billerbeck et al. (2010), these memory cells expressed low levels of granzyme B and perforin, demonstrated reduced proliferation, and were CD28+ and CD27+. However, Dusseaux et al. (2011) suggest that in healthy adults CD161^{high}CD8+ T cells largely represent mucosal associated invariant T (MAIT) cells; an innate-like T cell subset which express the invariant TCRα chain Vα7.2 – Jα33 and are restricted by MHC-related molecule 1 (MR1; Martin et al., 2009). Approximately 10% of MAIT cells were found to express IL-17 in response to PMA and ionomycin and these cells expressed RORγt. MAIT cells have therefore also been suggested to represent Tc17 cells. However, while Tc17 cells can react to viral peptides (Billerbeck et al., 2010), MAIT cells were unable to react to virus-infected APCs (Le Bourhis et al., 2010). Further studies are consequently required to clarify the degree of overlap between these putative cell types. Current analysis of Tc17 cells indicates that although the majority, like MAIT cells, are Vα7.2+, these cells do not completely encompass the CD161^{high} population (Walker et al., 2010).

CD161 AND MEMORY PHENOTYPE

Despite this disagreement regarding TCR usage, in all studies CD161 expression is consistently associated with a memory phenotype within the adult circulation, being described in CD4+ (Takahashi et al., 2006; Annunziato et al., 2007; Cosmi et al., 2008; Kleinschek et al., 2009), CD8+ (Takahashi et al., 2006; Maggi et al., 2010), DN TCRαβ+, and TCRγδ+ T cells (Maggi et al., 2010). Whereas approximately half of CD161^{int}CD4+ T cells display a central memory phenotype, being CD62L+ CCR7+, less than 1% of CD161^{high}CD8+CD45RO+ cells expressed this phenotype, and are therefore classed as being effector memory cells (Takahashi et al., 2006). This may suggest that CD161 expression is acquired as a result of immune stimulation, and may itself be a memory marker. However, CD161 negative cells do not alter in CD161 expression with anti-CD2, -CD3 and -CD28 stimulation, and influenza-specific cells did not express CD161 after re-stimulation, even in the presence of cytokines (Northfield et al., 2008), implying that CD161 is not simply a marker of activation.

Table 1 | Three parallel characterizations of CD161^{high}CD8+ T cells.

	MAIT cells (Martin et al., 2009; Gold et al., 2010; Dusseaux et al., 2011)	Tc17 cells (Northfield et al., 2008; Billerbeck et al., 2010)	CD8 memory stem cells (Turtle et al., 2009)
Surface phenotype	Vα7.2+ CD161^{high} IL-18Rα+	CD161^{high} IL-18R+	CD161^{high} IL-18Rα+Rh123-effluxing
Frequency	∼1 in 10 mature CD8 or DN T cells	1 in 6 circulating CD8+ T cells	Low
Cord blood	Present: CD45RA+CD161^{high} IL-18Rα+	Present: CD45RA+ CD161^{high} CCR6+	Absent
IL-17 production	Yes	Yes	Unknown
RORγt	Expressed	Expressed	Unknown
Tissue trophism	High numbers in liver and intestine	Enriched in liver during inflammation, enriched in healthy tonsillar, and epithelial kidney tissue	None
Specificity	Respond to bacterially infected APCs	Some specificity for HCV demonstrated, but not for other viruses, e.g., HIV, CMV, and influenza	Respond to APCs pulsed with viral peptides

This table illustrates both the similarities and differences between the main observations concerning the phenotype of CD161^{high}CD8+ T cells. Billerbeck et al. (2010) characterize these cells as Tc17 cells, reflecting their similarity to Th17 cells, while Turtle et al. (2009) identified high expression of CD161 as a marker of CD8+ memory stem cells. A recent study by Dusseaux et al. (2011), however, suggests that both these cell types represent the previously characterized MAIT cell population.

Furthermore, CD161 is expressed both by a subset of T cells in the fetal liver and on a minor population of CD3+ thymocytes (Lanier et al., 1994; Martin et al., 2009). This indicates, therefore, that expression is induced early in ontogeny. CD161^{int}CD4+ (Cosmi et al., 2008) and CD161^{high}CD8+ (Martin et al., 2009; Billerbeck et al., 2010) T cells have also been isolated from umbilical cord blood (UCB), where they display a naïve phenotype. When cultured in the presence of Th17-polarizing cytokines, development of IL-17 production is restricted to the CD161+CD4+CD45RA+ fraction (Cosmi et al., 2008), implying that Th17 cells originate from a CD161+CD4+ T cell progenitor. This suggests that those CD161+ cells identified in cord blood represent the precursors of memory CD161+ T cells found in adults. What induces the maturation of these cells to display a memory phenotype after birth is yet to be defined.

CD161 AS AN EFFECTOR MOLECULE

It is clear that determining the function of CD161 would greatly aid the functional phenotyping of those cells expressing this C-type lectin. Crosslinking of CD161 by anti-CD161 antibodies has previously had variable effects on both human NK and T cells. Aldemir et al. (2005), observed that ligation of CD161 was not sufficient to trigger IFN-γ production by T cells, yet did enhance secretion with the simultaneous engagement of CD3. Conversely, Rosen et al. (2005, 2008) found that crosslinking of CD161 did not affect cytokine production in CD4+ T cells, but reduced TNFα production by CD8+ T cells in a proportion of donors tested.

CD161 LIGANDS

As the only human ortholog of the rodent NK receptor family known as NKRP1, a central aim in determining the function of CD161 is the identification of this receptor's ligand(s). Seven murine NKRP1 genes have thus far been identified, termed *Nkrp1a-g* (with *Nkrp1e* thought to be a pseudogene; Plougastel et al., 2001a), heterogeneously expressed by NK cells (Aust et al., 2009). In C57BL/6 mice NKR-P1C carries the NK cell antigenic marker NK1.1 (Glimcher et al., 1977; Koo and Peppard, 1984) and also marks murine NK-T cells (MacDonald, 1995). This NKRP1 receptor may also be expressed during activation of CD8+ T cells (Aust et al., 2009). Unlike classical NK cell receptors, NKRP1 receptors recognize non-MHC ligands of the C-type lectin related (Clr) family, encoded by genes interspersed within the *Nkrp1* genes themselves (Plougastel et al., 2001b; Iizuka et al., 2003). Yet, like other NK cell receptors, *Nkrp1* gene products can be classified as either activating or inhibitory. NKRP1A, C and F contain charged residues within their transmembrane domains, and are therefore considered to be activating receptors, inducing NK cytolytic activity, while NKRP1B and NKRP1D lack charged transmembrane residues and deliver inhibitory signals when crosslinked (Aust et al., 2009). NKRP1B and D appear to be closely related inhibitory molecules, expressed in BALB/c and C57BL/6 mice, respectively, with the *Nkrp1d* gene of C57BL/6 mice suggested to represent a divergent allele of the *Nkrp1b* gene of other strains (Carlyle et al., 2006). Both NKRP1B and D bind the Clr-b protein osteoclast inhibitory lectin (Ocil; Carlyle et al., 2004). The human ortholog of this ligand, also known as lectin-like transcript 1 (LLT1), was simultaneously identified by two groups as a ligand for CD161 in humans (Aldemir et al., 2005; Rosen et al., 2005). This interaction, conserved between mouse and man, may suggest that NKRP1B and D represent the closest relations to human CD161. The suggested ligands for murine NKRP1 receptors and human CD161 are shown in **Figure 2**.

In humans, LLT1 is thought to be expressed by both activated APCs (Aldemir et al., 2005; Rosen et al., 2008) and lymphocytes (Aldemir et al., 2005). Despite transcripts and proteins of CD161 being identical between NK and T cells, ligation by LLT1 appears to induce opposing effects in these subsets, inhibiting or enhancing IFNγ production, respectively. A subsequent CD161 ligand, related to LLT1, has also been recently identified, termed proliferation-induced lymphocyte-associated receptor (PILAR; Huarte et al., 2008). As its name implies, PILAR is expressed on lymphocytes and expression is upregulated in T cells upon TCR stimulation. In the absence of CD28 costimulation, PILAR increases the proliferation of naïve T cells, suggesting that CD161 acts as a costimulatory receptor, enhancing proliferation through interaction with PILAR. Lately, however, the interaction between PILAR and CD161 has

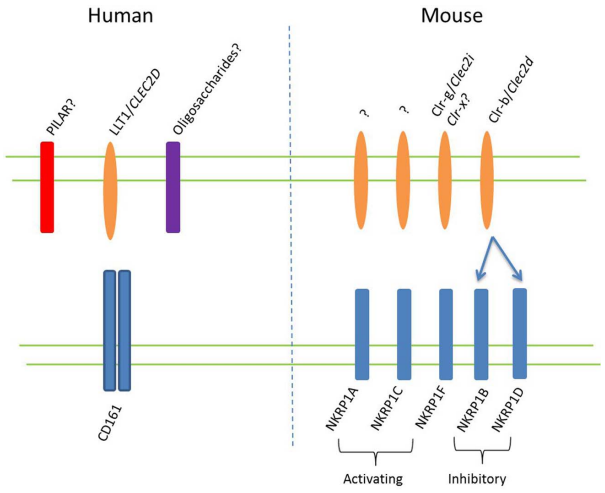

FIGURE 2 | NKRP1 ligands in mouse and man. Putative ligands for CD161, expressed on human T lymphocytes, are shown on the left side of the figure. The CD161 ortholog in mice exists as a family of genes, known as NKRP1 receptors, which are thought to consist of at least three activating and two inhibitory receptors, as shown on the right. The ligands for these receptors are Clr proteins, with the two known ligands depicted. A recent study suggested that NKRP1F may also recognize Clr-x (Aust et al., 2009).

been disputed, and it has been suggested that the PILAR gene encodes a ligand (termed keratinocyte-associated C-type lectin, KACL) which interacts with a distinct receptor, a further C-type lectin named NKp65 (Spreu et al., 2010).

CD161 AND TISSUE HOMING

CD161 has also been proposed to play a role in transendothelial migration. CD161+ cells migrated across endothelial cell monolayers to a greater extent than CD161−CD4+ lymphocytes (Poggi et al., 1997), and this was reduced by incubation with anti-CD161 monoclonal antibody. This may occur through binding of CD161 to acidic oligosaccharides on the endothelial cell surface, as has been shown in NK cells (Bezouska et al., 1994). Interestingly, migration occurred without chemotactic stimuli, which may be indicative of a preference of these cells to home to specific tissues. Indeed, both CD4+ and CD8+ CD161+ T cells make up more than half of T cells in the healthy human intestine (O'Keeffe et al., 2004) and CD161-expressing CD8+ T cells appear to home to the liver (Ishihara et al., 1999).

CD161 EXPRESSION AND DISEASE

CD161+ T CELLS AND INFECTION

These cells are also selectively recruited during inflammation, with CD4+ (Kang et al., unpublished observation) and CD8+ CD161+ T cells enriched in the liver in response to both hepatic infection and non-alcoholic steatohepatitis (Billerbeck et al., 2010). CD8+ T cells specific for HCV and hepatitis B (HBV), but not HIV, cytomegalovirus (CMV), or influenza, express significant levels of CD161 (Northfield et al., 2008) and these T cells display responses against HCV-derived peptides (Billerbeck et al., 2010). $CD161^{int}$CD4+ T cells are also markedly enriched in the liver of patients with HCV (Kang et al., unpublished observation) and HCV-specific Th17 cells have been described (Rowan et al., 2008). Expression of CD161, particularly on CD8+ T cells, may therefore differentiate responses within specific organs such as the liver. Yet the role of these cells in either disease control or immune-mediated damage is largely unknown. Recently, Wang et al., correlated levels of IL-17 with degree of fibrosis in HBV infection, with intrahepatic IL-17 localized to fibrotic regions (Wang et al., 2011). Conversely, secretion of IL-22 by these cells may in fact be hepatoprotective (Zenewicz et al., 2007; Kang et al., unpublished observation).

However, these cells are not limited to liver-specific responses. Tc17 populations within mice protect against lethal influenza infection (Hamada et al., 2009), an effect shown to be due, at least partially, to their secretion of IL-17. CD161+ MAIT cells, on the other hand, respond to bacterially infected cells, including both APCs (Le Bourhis et al., 2010) and *Mycobacterium tuberculosis*-infected lung epithelial cells (Gold et al., 2010), suggesting a role in detection and control of bacterial infections. MAIT cells are thought to be unresponsive to virus-induced or virus-derived ligands (Le Bourhis et al., 2010). Resolution of CD161-expressing CD8+ T cell specificity, in addition to aiding classification, would also assist the identification of their role within human disease.

CD161+ T CELLS IN AUTOIMMUNE DISEASE

In contrast to the situation with host defense, much research has concentrated on the role of $CD161^{int}$CD4+ T cells in autoimmune disease, which was previously considered to be Th1-driven (Cua et al., 2003). IL-17 knockout mice exhibit delayed onset, reduced severity, and early recovery of experimental autoimmune encephalomyelitis (EAE), the murine model of multiple sclerosis (MS). In humans, IL-17 levels are increased in patients with MS (Lock et al., 2002) and IL-17+ T cells have been identified within MS brain lesions (Tzartos et al., 2008). Patients with MS also display a significantly higher percentage of peripheral blood $CD161^{high}$CD8+ T cells than healthy individuals (Annibali et al., 2011). More specifically, polymorphisms in CD161 have recently been implicated in MS, suggesting a role for CD161 itself in autoimmune pathogenesis (Hafler et al., 2007).

CD161-expressing T cells have also been implicated in other autoimmune diseases. High proportions of $CD161^{int}$CD4+ T cells were found in inflammatory infiltrates of patients with psoriasis (Cosmi et al., 2008) and Crohn's disease (CD; Kleinschek et al., 2009). Indeed, $CD161^{int}$CD4+ T cells demonstrated a 20-fold increase in gut samples from patients with CD compared to healthy controls and those isolated from the blood produced significantly more IL-17 on stimulation with PMA and ionomycin. Tc17 cells are also significantly enriched in inflammatory infiltrates from donors with psoriatic and rheumatoid arthritis (RA; Billerbeck et al., 2010). However, the significance of CD161 expression by both Th17 and Tc17 within the disease process has yet to be determined.

CONCLUSION AND FUTURE WORK

CD161 expression is evident within all T cell subsets, and is associated with cells expressing a memory phenotype in the adult circulation. However, CD161 does not simply represent a marker

of activation, memory, or exhaustion. Neither stimulation nor re-stimulation induced expression in CD161− cells, and CD161+ cells express only low levels of the exhaustion marker PD-1 (Northfield et al., 2008; Billerbeck et al., 2010). Furthermore, CD161 expression has been identified in naïve cells within UCB (Cosmi et al., 2008; Billerbeck et al., 2010), with CD45RA+CD161+CD4+ T cells expressing high levels of mRNA for RORγt, IL-23R, and CCR6. CCR6 is also expressed on CD161^{high}CD8+ T cells isolated from cord blood (Billerbeck et al., 2010). This suggests that these CD161 positive cells, while apparently naïve, represent a population precommitted to a distinct pathway of differentiation.

During ontogeny T cells develop within the thymus, where lineage commitments such as CD4 vs. CD8 co-receptor expression are made. These fate decisions influence the phenotype of these cells upon their release into the periphery. Interestingly, single positive thymocytes from the post-natal thymus which express CD161 have also been identified (Lanier et al., 1994; Cosmi et al., 2008; Martin et al., 2009). This, together with early expression of RORγt and characteristic cytokine receptors in UCB CD161+ lymphocytes, suggests that expression of CD161 may indicate an early lineage commitment made by cells during development. Indeed, this decision may even be made prior to division into CD4 or CD8 subtype, with the possible pathways by which CD161+ cells develop illustrated in **Figure 3**. It appears that these CD161+ thymocytes represent the precursors of those memory Th17 and Tc17 cells identified within the adult circulation. Expression of CD161 early in ontogeny could also explain the identification by Turtle et al. (2009) of CD161^{high}CD8+ T cells with stem cell-like properties. Expression of CD161 during development suggests that these cells may become precommitted to display characteristics of a "CD161 positive" phenotype, possessing shared characteristics independent of helper/cytotoxic lineage, such as IL-17 secretion. As such, this phenotypic commitment may be decided prior to further lineage development, as suggested in **Figure 3A**. Programmed chemokine receptor expression in CD161+ naïve cells, such as CCR6, may also indicate the ability of these cells to preferentially home to specific tissues, where they are found in elevated numbers (Huarte et al., 2008; Spreu et al., 2010). Evidently the development of CD161-expressing cells is still largely unexplored. However, clarification of the significance of CD161 expression during ontogeny may provide clues regarding the function of this unique cell type.

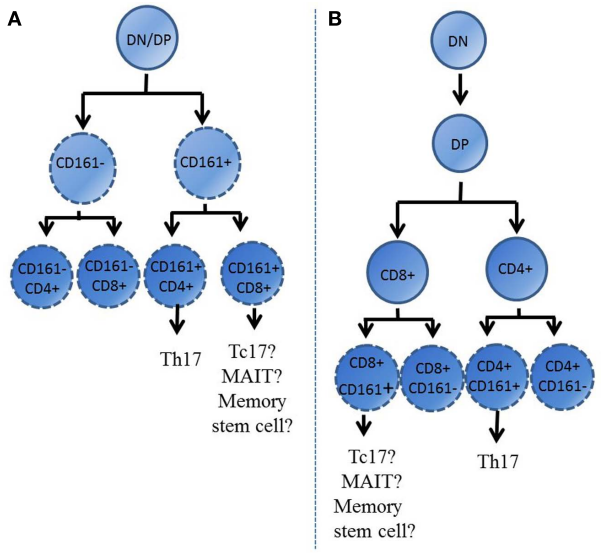

FIGURE 3 | Expression of CD161 early during the development of T cells within the thymus. This figure illustrates two possible pathways by which CD161 expression may be determined during development; either before co-receptor expression is decided **(A)** or at the single positive stage, when T cells are either CD4+ or CD8+ **(B)**. Th17 cells only develop from CD161+ CD4+ cells, however these cells can also develop into Th1 or Th2 cells. DN, double negative; DP, double positive.

As CD161 marks T cells with the ability to secrete IL-17 (Maggi et al., 2010), expression of CD161 during development would appear to commit cells to a type 17 pathway of differentiation. However, CD161 expression was also identified on IFNγ+ and IFN-γ/IL-17 co-secreting CD8+ (Billerbeck et al., 2010) and CD4+ T cells (Cosmi et al., 2008). CD4+IL-17+IFNγ+ cells have been termed Th17-1 (Jadidi-Niaragh and Mirshafiey, 2011) and express the chemokine receptors CCR6 and CXCR3, distinguishing them from Th17 cells which express CCR6 and CCR4 (Acosta-Rodriguez et al., 2007). However, whether these cells represent a stable subset or a transitional phenotype (El-behi et al., 2010) is yet to be resolved, with the latter case suggesting plasticity within the Th17 phenotype. Indeed, human Th17 clones have been shown to demonstrate a degree of plasticity when stimulated in the presence of IL-12, downregulating RORγt while upregulating the Th1 transcription factor T-bet, with these cells subsequently producing IFN-γ in addition to IL-17 (Annunziato et al., 2007). Therefore, while CD161 is agreed to mark Th17 cells, and descriptions of these cells are extensive, the dual functionality demonstrated by some also reveals the difficulty in exclusively categorizing T cells into distinct subsets.

It is clear that much is left to be determined regarding the significance of CD161 expression, and further of different levels of expression, by this subset of human T cells. Studies to identify this receptor's ligands, and more importantly the effect of ligand binding on T cell function, will provide clues regarding the purpose of CD161 expression. In addition, characterization of both the phenotype and function of these subsets is fundamental to enabling their role within human diseases to be determined. The suggestion that CD161 supports activation-induced expansion of T cells (Huarte et al., 2008), and the implication of CD161 polymorphisms within MS (Hafler et al., 2007) could identify CD161, or indeed other receptors on CD161+ T cells, as potential therapeutic targets in the treatment of a wide range of diseases.

ACKNOWLEDGMENTS

We are grateful to Lucy Walker, Yu-Hoi Kang, Chris B. Willberg, and Kira Smith for work referred to in this article. Joannah R. Fergusson is funded by the Wellcome Trust, Vicki M. Fleming, and Paul Klenerman by Wellcome Trust (WT091663MA), MRC, NIHR Biomedical Research Centre, Oxford, the James Martin School for twenty first Century, Oxford, and the NIH NIAID 1U19AI082630-01.

REFERENCES

Acosta-Rodriguez, E. V., Rivino, L., Geginat, J., Jarrossay, D., Gattorno, M., Lanzavecchia, A., Sallusto, F., and Napolitani, G. (2007). Surface phenotype and antigenic specificity of human interleukin 17-producing T helper memory cells. *Nat. Immunol.* 8, 639–646.

Aldemir, H., Pro'homme, V., Dumaurier, M., Retiere, C., Poupon, G., Cazareth, J., Bihl, F., and Braud, V. M. (2005). Cutting edge: lectin-like transcript 1 is a ligand for the CD161 receptor. *J. Immunol.* 175, 7791–7795.

Annibali, V., Ristori, G., Angelini, D. F., Serafini, B., Mechelli, R., Cannoni, S., Romano, S., Paolillo, A., Abderrahim, H., Diamantini, A., Borsellino, G., Aloisi, F., Battistini, L., and Salvetti, M. (2011). CD161highCD8+T cells bear pathogenetic potential in multiple sclerosis. *Brain* 134, 542–554.

Annunziato, F., Cosmi, L., Santarlasci, V., Maggi, L., Liotta, F., Mazzinghi, B., Parente, E., Filí, L., Ferri, S., Frosali, F., Giudici, F., Romagnani, P., Parronchi, P., Tonelli, F., Maggi, E., and Romagnani, R. (2007). Phenotypic and functional features of human Th17 cells. *J. Exp. Med.* 204, 1849–1861.

Aust, J. G., Gays, F., Mickiewicz, K. M., Buchanan, E., and Brooks, C. G. (2009). The expression and function of the NKRP1 receptor family in C57BL/6 mice. *J. Immunol.* 183, 106–111.

Bezouska, K., Yuen, C. T., O'Brien, J., Childs, R. A., Chai, W., Lawson, A. M., Drbal, K., Fiserová, A., Pospísil, M., and Feizi, T. (1994). Oligosaccharide ligands for NKR-P1 protein activate NK cells and cytotoxicity. *Nature* 372, 150–157.

Billerbeck, E., Kang, Y., Walker, L., Lockstone, H., Grafmueller, S., Fleming, V., Flint, J., Willberg, C. B., Bengsch, B., Seigel, B., Ramamurthy, N., Zitzmann, N., Barnes, E. J., Thevanayagam, J., Bhagwanani, A., Leslie, A., Oo, Y. H., Kollnberger, S., Bowness, P., Drognitz, O., Adams, D. H., Blum, H. E., Thimme, R., and Klenerman, P. (2010). Analysis of CD161 expression on human CD8+ T cells defines a distinct functional subset with tissue-homing properties. *Proc. Natl. Acad. Sci. U.S.A.* 107, 3006–3011.

Carlyle, J. R., Jamieson, A. M., Gasser, S., Clingan, C. S., Arase, H., and Raulet, D. H. (2004). Missing self-recognition of Ocil/Clr-b by inhibitory NKR-P1 natural killer cell receptors. *Proc. Natl. Acad. Sci. U.S.A.* 101, 3527–3532.

Carlyle, J. R., Mesci, A., Ljutic, B., Belanger, S., Tai, L. H., Rousselle, E., Troke, A. D., Proteau, M. F., and Makrigiannis, A. P. (2006). Molecular and genetic basis for strain-dependent NK1.1 alloreactivity of mouse NK cells. *J. Immunol.* 176, 7511–7524.

Cosmi, L., De Palma, R., Santarlasci, V., Maggi, L., Capone, M., Frosali, F., Rodolico, G., Querci, V., Abbate, G., Angeli, R., Berrino, L., Fambrini, M., Caproni, M., Tonelli, F., Lazzeri, E., Parronchi, P., Liotta, F., Maggi, E., Romagnani, S., and Annunziato, F. (2008). Human interleukin 17–producing cells originate from a CD161+CD4+ T cell precursor. *J. Exp. Med.* 205, 1903–1916.

Cua, D. J., Sherlock, J., Chen, Y., Murphy, C. A., Joyce, B., Seymour, B., Lucian, L., To, W., Kwan, S., Churakova, T., Zurawski, S., Wiekowski, M., Lira, S. A., Gorman, D., Kastelein, R. A., and Sedgwick, J. D. (2003). Interleukin-23 rather than interleukin-12 is the critical cytokine for autoimmune inflammation of the brain. *Nature* 421, 744–748.

Dusseaux, M., Martin, E., Serriari, N., Peguillet, I., Premel, V., Louis, D., Milder, M., Le Bourhis, L., Soudais, C., Treiner, E., and Lantz, O. (2011). Human MAIT cells are xenobiotic resistant, tissue-targeted, CD161hi IL-17 secreting T cells. *Blood* 117, 1250–1259.

El-behi, M., Rostami, A., and Ciric, B. (2010). Current views on the roles of Th1 and Th17 cells in experimental autoimmune encephalomyelitis. *J. Neuroimmune Pharmacol.* 5, 189–197.

Glimcher, L., Shen, F. W., Cantor, H. (1977). Identification of a cell-surface antigen selectively expressed on the natural killer cell. *J. Exp. Med.* 145, 1–9.

Gold, M. C., Cerri, S., Smyk-Pearson, S., Cansler, M. E., Vogt, T. M., Delepine, J., Winata, E., Swarbrick, G. M., Chua, W. J., Yu, Y. Y. L., Lantz, O., Cook, M. S., Null, M. D., Jacoby, D. B., Harriff, M. J., Lewinsohn, D. A., Hansen, T. H., and Lewinsohn, D. M. (2010). Human mucosal associated invariant T cells detect bacterially infected cells. *PLoS Biol.* 8, e1000407. doi: 10.1371/journal.pbio.1000407

Gumperz, J. E., Miyake, S., Yamamura, T., and Brenner, M. B. (2002). Functionally distinct subsets of CD1d-restricted natural killer T cells revealed by CD1d tetramer staining. *J. Exp. Med.* 195, 625–636.

Hafler, D. A., Compston, A., Sawcer, S., Lander, E. S., Daly, M. J., De Jager, P. L., de Bakker, P. I., Gabriel, S. B., Mirel, D. B., Ivinson, A. J., Pericak-Vance, M. A., Gregory, S. G., Rioux, J. D., McCauley, J. L., Haines, J. L., Barcellos, L. F., Cree, B., Oksenberg, J. R., and Hauser, S. L. (2007). Risk alleles for multiple sclerosis identified by a genomewide study. *N. Engl. J. Med.* 357, 851–862.

Hamada, H., Garcia-Hernandez, M. D. L. L., Reome, J. B., Misra, S. K., Strutt, T. M., McKinstry, K. K., Cooper, A. M., Swain, S. L., and Dutton, R. W. (2009). Tc17, a unique subset of CD8 T cells that can protect against lethal influenza challenge. *J. Immunol.* 182, 3469–3481.

Huarte, E., Cubillos-Ruiz, J. R., Nesbeth, Y. C., Scarlett, U. K., Martinez, D. G., Engle, X. A., Rigby, W. F., Pioli, P. A., Guyre, P. M., and Conejo-Garcia, J. R. (2008). PILAR is a novel modulator of human T-cell expansion. *Blood* 112, 1259–1268.

Huber, M., Heink, S., Grothe, H., Guralnik, A., Reinhard, K., Elflein, K., Hünig, T., Mittrücker, H. W., Brüstle, A., Kamradt, T., and Lohoff, M. (2009). Th17-like developmental process leads to CD8+ Tc17 cells with reduced cytotoxic activity. *Eur. J. Immunol.* 39, 1716–1725.

Iizuka, K., Naidenko, O. V., Plougastel, B. F., Fremont, D. H., and Yokoyama, W. M. (2003). Genetically linked C-type lectin-related ligands for the NKRP1 family of natural killer cell receptors. *Nat. Immunol.* 4, 801–807.

Ishihara, S., Nieda, M., Kitayama, J., Osada, T., Yabe, T., Ishikawa, Y., Nagawa, H., Muto, T., and Juji, T. (1999). CD8+NKR-P1A+ T cells preferentially accumulate in human liver. *Eur. J. Immunol.* 29, 2406–2413.

Ivanov, I. I., McKenzie, B. S., Zhou, L., Tadokoro, C. E., Lepelley, A., Lafaille, J. J., and Cua, D. J., and Littman, D. R. (2006). The orphan nuclear receptor RORγt directs the differentiation program of proinflammatory IL-17+ T helper cells. *Cell* 126, 1121–1133.

Jadidi-Niaragh, F., and Mirshafiey, A. (2011). Th17 cell, the new player of neuroinflammatory process in multiple sclerosis. *Scand. J. Immunol.* 74, 1–13.

Kleinschek, M. A., Boniface, K., Sadekova, S., Grein, J., Murphy, E. E., Turner, S. P., Raskin, L., Desai, B., Faubion, W. A., de Waal Malefyt, R., Pierce, R. H., McClanahan, T., and Kastelein, R. A. (2009). Circulating and gut-resident human Th17 cells express CD161 and promote intestinal inflammation. *J. Exp. Med.* 206, 525–534.

Kondo, T., Takata, H., Matsuki, F., and Takiguchi, M. (2009). Cutting edge: Phenotypic characterization and differentiation of human CD8+ T cells producing IL-17. *J. Immunol.* 182, 1794–1798.

Koo, G. C., and Peppard, J. R. (1984). Establishment of monoclonal anti-Nk-1.1 antibody. *Hybridoma* 3, 301–303.

Lanier, L., Chang, C., and Phillips, J. (1994). Human NKR-P1A. A disulfide-linked homodimer of the C-type lectin superfamily expressed by a subset of NK and T lymphocytes. *J. Immunol.* 153, 2417–2428.

Le Bourhis, L., Martin, E., Péguillet, I., Guihot, A., Froux, N., Coré, M., Lévy, E., Dusseaux, M., Meyssonnier, V., Premel, V., Ngo, C., Riteau, B., Duban, L., Robert, D., Rottman, M., Soudais, C., and Lantz, O. (2010). Antimicrobial activity of mucosal-associated invariant T cells. *Nat. Immunol.* 11, 701–708.

Lock, C., Hermans, G., Pedotti, R., Brendolan, A., Schadt, E., Garren, H., Langer-Gould, A., Strober, S., Cannella, B., Allard, J., Klonowski, P., Austin, A., Lad, N., Kaminski, N., Galli, S. J., Oksenberg, J. R., Raine, C. S., Heller, R., and Steinman, L. (2002). Gene-microarray analysis of multiple sclerosis lesions yields new targets validated in autoimmune encephalomyelitis. *Nat. Med.* 8, 500–508.

MacDonald, H. R. (1995). NK1.1+ T cell receptor-alpha/beta+ cells: new clues to their origin, specificity, and function. *J. Exp. Med.* 182, 633–638.

Maggi, L., Santarlasci, V., Capone1, M., Peired, A., Frosali, F., Crome, S., Querci, V., Fambrini, M., Liotta, F., Levings, M., Maggi, E., Cosmi, L., Romagnani, S., and Annunziato, F. (2010). CD161 is a marker of all human IL-17-producing T-cell subsets and is induced by RORC. *Eur. J. Immunol.* 40, 2174–2181.

Martin, E., Treiner, E., Duban, L., Guerri, L., Laude, H., Toly, C., Premel, V., Devys, A., Moura, I. C., Tilloy, F., Cherif, S., Vera, G., Latour, S., Soudais, C., and Lantz, O. (2009). Stepwise development of MAIT cells in mouse and human. *PLoS Biol.* 7, e54. doi: 10.1371/journal.pbio.1000054

Northfield, J. W., Kasprowicz, V., Lucas, M., Kersting, N., Bengsch, B., Kim, A., Phillips, R. E., Walker, B. D., Thimme, R., Lauer, G., and Klenerman, P. (2008). CD161 expression on hepatitis C virus-specific CD8+ T cells suggests a distinct pathway of T cell differentiation. *Hepatology* 47, 396–406.

O'Keeffe, J., Doherty, D., Kenna, T., Sheahan, K., O'Donoghue, D., Hyland, J., and O'Farrelly, C. (2004). Diverse populations of T cells with NK cell receptors accumulate in the human intestine in health and in colorectal cancer. *Eur. J. Immunol.* 34, 2110–2119.

Plougastel, B., Matsumoto, K., Dubbelde, C., and Yokoyama, W. M. (2001a). Analysis of a 1-Mb BAC contig overlapping the mouse Nkrp1 cluster of genes: cloning of three new Nkrp1 members, Nkrp1d, Nkrp1e, and Nkrp1f. *Immunogenetics* 53, 592–598.

Plougastel, B. F., Dubbelde, C., and Yokoyama, W. M. (2001b). Cloning of Clr, a new family of lectin-like genes localized between mouse Nkrp1a and Cd69. *Immunogenetics* 53, 209–214.

Poggi, A., Costa, P., Zocchi, M. R., and Moretta, L. (1997). NKRP1A molecule is involved in transendothelial migration of CD4+ human T lymphocytes. *Immunol. Lett.* 57, 121–123.

Rosen, D. B., Bettadapura, J., Alsharifi, M., Mathew, P. A., Warren, H. S., and Lanier, L. L. (2005). Cutting edge: lectin-like transcript-1 is a ligand for the inhibitory human NKR-P1A receptor. *J. Immunol.* 175, 7796–7799.

Rosen, D. B., Cao, W., Avery, D. T., Tangye, S. G., Liu, Y., Houchins, J. P., and Lanier, L. L. (2008). Functional consequences of interactions between human NKR-P1A and its ligand LLT1 expressed on activated dendritic cells and B cells. *J. Immunol.* 180, 6508–6517.

Rowan, A. G., Fletcher, J. M., Ryan, E. J., Moran, B., Hegarty, J. E., O'Farrelly, C., and Mills, K. H. (2008). Hepatitis C virus-specific Th17 cells are suppressed by virus-induced TGF-β. *J. Immunol.* 181, 4485–4494.

Spreu, J., Kuttruff, S., Stejfova, V., Dennehy, K. M., Schittek, B., and Steinle, A. (2010). Interaction of C-type lectin-like receptors NKp65 and KACL facilitates dedicated immune recognition of human keratinocytes. *Proc. Natl. Acad. Sci. U.S.A.* 107, 5100–5105.

Takahashi, T., Dejbakhsh-Jones, S., and Strober, S. (2006). Expression of CD161 (NKR-P1A) defines subsets of human CD4 and CD8 T cells with different functional activities. *J. Immunol.* 176, 211–216.

Turtle, C. J., Swanson, H. M., Fujii, N., Estey, E. H., and Riddell, S. R. (2009). A distinct subset of self-renewing human memory CD8+ T cells survives cytotoxic chemotherapy. *Immunity* 31, 834–844.

Tzartos, J. S., Friese, M. A., Craner, M. J., Palace, J., Newcombe, J., Esiri, M. M., and Fugger, L. (2008). Interleukin-17 production in central nervous system-infiltrating T cells and glial cells is associated with active disease in multiple sclerosis. *Am. J. Pathol.* 172, 146–155.

Walker, L., Kang, Y., Smith, M., Oo, Y., Barnes, E., Lauer, G., Adams, D. H., and Klenerman, P. (2010). P74 CD161 expressing CD8+ T-cells; elusive players in viral hepatitis. *Gut* 59(Suppl. 2), A100.

Wang, L., Chen, S., Xu, K. (2011). IL-17 expression is correlated with hepatitis B-related liver diseases and fibrosis. *Int. J. Mol. Med.* 27, 385–392.

Zenewicz, L. A., Yancopoulos, G. D., Valenzuela, D. M., Murphy, A. J., Karow, M., and Flavell, R. A. (2007). Interleukin-22 but not interleukin-17 provides protection to hepatocytes during acute liver inflammation. *Immunity* 27, 647–659.

Conflict of Interest Statement: The authors declare that the research was conducted in the absence of any commercial or financial relationships that could be construed as a potential conflict of interest.

Received: 07 May 2011; accepted: 11 August 2011; published online: 30 August 2011.

Citation: Fergusson JR, Fleming VM and Klenerman P (2011) CD161-expressing human T cells. Front. Immun. ***2****:36. doi: 10.3389/fimmu.2011.00036*

This article was submitted to Frontiers in Immunological Memory, a specialty of Frontiers in Immunology.

Copyright © 2011 Fergusson, Fleming and Klenerman. This is an open-access article subject to a non-exclusive license between the authors and Frontiers Media SA, which permits use, distribution and reproduction in other forums, provided the original authors and source are credited and other Frontiers conditions are complied with.

Posters presented at International Meetings

Presented at the 7th International symposium on CD1 and NKT cells (2013)





UNIVERSITY OF OXFORD

MAIT cells and their relations

Analysis by CyTOF and Microarray reveals MAIT cells to be unique yet related

J. Fergusson[1], E.W. Newell[2,3], L. Swadling[1], A. Kurioka[1], N. Rajoriya[1], M. M. Davis[3], J.E. Ussher[1], P. Klenerman[1,4]

[1]Peter Medawar Building for Pathogen Research, Nuffield Department of Medicine, University of Oxford, UK; [2]Department of Microbiology and Immunology, Stanford University, Stanford, CA; [3] Agency for Science, Technology and Research, Singapore [4]National Institute for Health Research Biomedical Research Centre, John Radcliffe Hospital, Oxford, UK

BACKGROUND

- Mucosal Associated Invariant T (MAIT) cells are characterised by high expression of the C-type lectin CD161 (CD161^{++}).
- CD161 was originally identified as a marker of NK cells, and is also expressed by CD4$^+$, CD8$^+$ and γδ T cells.
- Does expression of CD161 across subsets indicate related phenotype and function?

METHODS

CD161-expressing lymphocytes from healthy donors were analysed by CyTOF and microarray. Gene expression profiling was performed on either the Agilent or Illumina platform, and normalised signal intensities used to calculate differential gene expression. Expression of 23 markers by PMA + ionomycin stimulated cells was assessed by CyTOF and analysed by principal component analysis (PCA).

RESULTS

1. CD161^{++} MAIT cells occupy a distinct niche amongst CD8$^+$ T cells

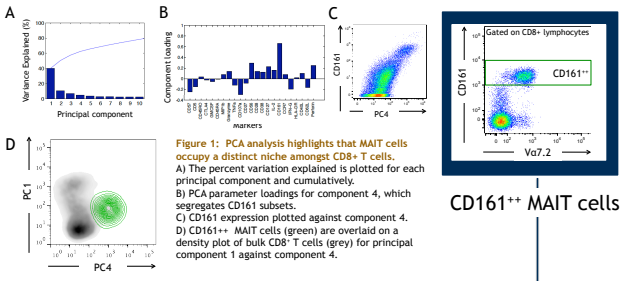

Figure 1: PCA analysis highlights that MAIT cells occupy a distinct niche amongst CD8+ T cells.
A) The percent variation explained is plotted for each principal component and cumulatively.
B) PCA parameter loadings for component 4, which segregates CD161 subsets.
C) CD161 expression plotted against component 4.
D) CD161++ MAIT cells (green) are overlaid on a density plot of bulk CD8$^+$ T cells (grey) for principal component 1 against component 4.

CD161^{++} MAIT cells

Expression of 23 markers by stimulated CD8$^+$ T cells was measured by CyTOF and analysed by principal component analysis (PCA). This unsupervised analysis derives summary 'principal components' which best explain the variation in the entire dataset, with the first four principal components accounting for ~60% of variation within CD8$^+$ T cells (Figure 1A). The majority of the variation, summarised by component 1, tracks with variation due to naïve/memory phenotype. However, variation summarised by component 4 (Figure 1B) appears to correlate with CD161 expression (Figure 1 C). Consequently, when these components are visualised on a 2D plot (Figure 1D), MAIT cells can be distinguished by component 4, and are seen to occupy a distinct niche amongst CD8$^+$ T cells.

CD161$^+$ CD8$^+$ T cells | CD161$^+$ NK cells | CD161$^+$ γδ cells

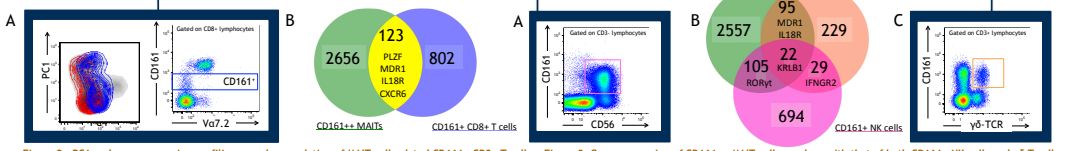

Figure 2: PCA and gene expression profiling reveal a population of MAIT cell-related CD161+ CD8+ T cells.
A) Gating of CD161+ CD8+ T cells (blue) by FACS and overlay of this population on component 1 vs component 4 of bulk CD8+ T cells (grey) and CD161- CD8+ T cells (red) by CyTOF and PCA.
B) Venn diagram displaying overlap (yellow) in genes differentially expressed by CD161++ MAITs (green) and CD161+ CD8+ T cells (blue) compared to their CD161- counterparts.

Figure 3: Gene expression of CD161++ MAIT cells overlaps with that of both CD161+ NK cells and γδ T cells.
A) FACS plot showing the presence of both CD161+ and CD161- NK (CD56+) cells
B) Venn diagram displaying overlap in genes differentially expressed by CD161++ MAITs (green), CD161+ NK cells (pink) and CD161+ γδ T cells (orange).
C) FACS plot showing the presence of both CD161+ and CD161- γδ T cells

2. CD161$^+$ CD8$^+$ T cells are MAIT-cell related NKT cells

Component 4 also reveals a population of CD161$^+$ CD8$^+$ T cells (blue) which is distinct from bulk CD161$^-$ CD8$^+$ T cells (red), but is intermediate to MAIT cells. This population is also apparent by flow cytometry (Figure 2A). CD161$^+$ CD8$^+$ T cells overlap MAIT cells in terms of gene expression, sharing 123 differentially expressed genes (Figure 2B), including shared expression of the NKT cell transcription factor PLZF, but not of the IL-17 associated transcription factor RORγt characteristic of MAIT cells.

3. CD161 marks a family of inter-related lymphocytes which includes MAIT cells

CD161 is also expressed by a subset of NK cells (Figure 3A) and γδ T cells (Figure 3C). Gene expression of these CD161+ cells versus their CD161- counterparts was analysed and compared to that of MAIT cells. Interestingly, MAIT cells share more genes with CD161$^+$ NK cells than CD161$^+$ γδ T cells. CD161$^+$ NK cells share 127 differentially expressed genes with MAIT cells, including RORγt, and 117 genes with CD161$^+$ γδ T cells, including IL18R and MDR1.

Conclusion: While MAIT cells are unique, expression of CD161 incorporates them into a family of lymphocytes related by phenotype and function, including shared expression of master transcription factors, eg. PLZF and RORγt, and potential to respond to cytokine stimulation, eg. IL18R expression*.

Email: joannah.fergusson@path.ox.ac.uk

* see Ussher *et al.* in press, and poster "CD161^{++}CD8$^+$ T cells, including the MAIT cell subset, are specifically activated by IL-12+IL-18 in a TCR-independent manner"

Photo credit: Greg Smolonski

wellcome trust

PRINTED BY: www.SCIENCEPOSTERS.co.uk

Presented at the European Congress in Immunology (2012)

A Novel Subset of Anti-Viral T Cells: the CD161^{dim} CD8^{+} population

J.R. Fergusson[1], J.E. Ussher[1], E.W. Newell[2] and P. Klenerman[1,3]

[1]Peter Medawar Building for Pathogen Research, Nuffield Department of Medicine, University of Oxford, United Kingdom; [2]Department of Microbiology and Immunology, Stanford University, Stanford, CA; [3]National Institute for Health Research Biomedical Research Centre, John Radcliffe Hospital, Oxford, United Kingdom

wellcome trust

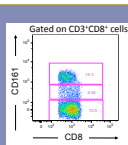

Figure 1: CD161 expression divides CD8^{+} T cells into distinct subsets. CD161^{bright} CD8^{+} T cells include MAIT cells, while CD161^{dim} CD8^{+} T cells are yet to be characterised.

Background:

CD8^{+} T cells are important in the control of viral infections and can be divided into subsets based upon expression of the C-type lectin CD161 (**Figure 1**). Although the function of CD161 is not yet known, expression of high levels (CD161^{bright}) identifies a recently described subset of anti-bacterial T cells known as mucosal associated invariant T (MAIT) cells. These cells express a semi-invariant T cell receptor and are restricted by the non-polymorphic MHC class I related molecule MR1. However, a further subset of CD8^{+} T cells which express lower levels of CD161, the CD161^{dim} CD8^{+} population, is also apparent within both cord blood and the adult circulation, where they can comprise up to 60% of the CD8^{+} T cell pool. However, their phenotype and function have yet to be described. This population includes viral-specific cells, as shown in **Figure 2**, and therefore constitute a potentially important population in the context of viral infections, including hepatitis C in which they have been shown to be enriched (Northfield et.al., 2008).

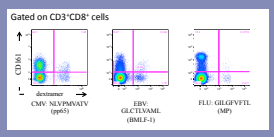

Figure 2: Viral-specific cells are found in both CD161^{dim} and CD161^{neg} CD8^{+} T cell populations. Dextramers were used to identify CD8^{+} T cells specific for epitopes from CMV, EBV and influenza.

1. CD161^{dim} CD8^{+} cells are a unique T cell population

Method: Gene expression profiling of CD161^{dim} CD8^{+} vs CD161^{neg} CD8^{+} T cells was performed using Agilent 60K Whole Genome Oligo Microarray (Agilent Technologies). Normalized signal intensities were used to calculate a list of genes detected in >3 samples, with a fold change >2 and a p-value <0.01. This data was used to produce a heatmap of relative gene expression and to perform hierarchical clustering (GENE-E).

Results: The heatmap in **Figure 3** shows relative gene expression of genes significantly differentially expressed in CD161^{dim} vs CD161^{neg} CD8^{+} T cells. Hierarchical clustering segregates the samples based upon CD161 subtype and therefore demonstrates that CD161^{dim} CD8^{+} T cells have a gene expression profile which is unique from CD161^{neg} CD8^{+} T cells. Among the significantly upregulated genes within the CD161^{dim} population are those shared with CD161^{bright} MAIT cells including IL18R, CXCR6, the transcription factor ZBTB16 and the the multi drug transporter MDR1.

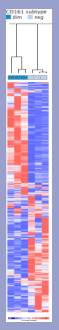

Figure 3 (Right): Heatmap and hierarchical clustering demonstrate the unique gene expression profile of CD161^{dim} CD8^{+} T cells compared to memory CD161^{neg} CD8^{+} T cells.

2. CD161^{dim} CD8^{+} T cells express a functional multi drug transporter, MDR1

Method: In the efflux assay, PBMCs were loaded with efflux buffer containing RPMI 1640 + 1% BSA + 10μg/ml Rho123 for 1hr on ice. Cells were then washed and cultured for 30min at 37°C (efflux) or on ice (loading control), in the absence or presence of 50μM verapamil hydrochloride.

Results: Significantly more CD161^{dim} CD8^{+} T cells express MDR1 than CD161^{neg}, but not to the same extent as in the CD161^{bright} population (**Figure 4A**). MDR1 in the CD161^{dim} population is functional with the ability to efflux its fluorescent substrate Rho123 to a greater degree than in CD161^{neg} cells. Efflux is inhibited by the MDR1 inhibitor verapamil hydrochloride (**Figure 4B-C**).

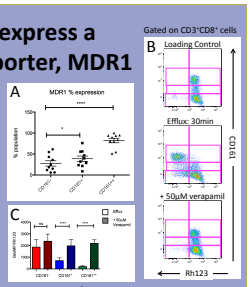

Figure 4: CD161^{dim} CD8^{+} T cells express functional MDR1 and display increased ability to efflux drugs compared to CD161^{neg} CD8^{+} T cells. A) CD161^{dim} CD8^{+} T cells express significantly more surface MDR1 than CD161^{neg}. **B)** A representative example of a Rh123 efflux assay. **C)** CD161^{dim} CD8^{+} T cells show increased efflux of Rho123, which is inhibited by verapamil hydrochloride.

2. Analysis of CD161^{dim} CD8^{+} T cells by Cytometry by Time-of-Flight (CyTOF)

Surface:	Atomic Mass:
CD3	Cd Qdot
CD57	115
CD3	141
CD5	143
CD45RO	144
CTLA4	145
CD8	146
CD45RA	148
CD4	149
CD27	154
CD13	156
CD33	156
CD19	157
CD16	158
CD56	159
CD28	160
CD38	161
GammaDelta-FITC	162
CD127	165
CD161-APC	167
CCR7	168
HLA-DR	171
PD-1-PE	173
Intracellular:	**Atomic Mass**
CD69	142
CTLA4	145
GMCSF	147
MIP1b	150
Granzyme B	151
TNFa	152
CD107a+b	153
IL17	164
IL-2	166
IFNg	170
CD45	172
Other:	**Atomic Mass**
CMV-tetramer	163, 169
FLU-tetramers	169, 175
HCV-tetramers	155, 163
DNA	191, 193
Live/Dead	103, 115
"cell length"	N/A

Figure 5: CyTOF Panel

Method: Cells were stimulated for 3 hours with PMA + Ionomycin before being stained with a panel of heavy metal isotope labelled antibodies against both phenotypic and functional markers (**Figure 5**), in addition to iridium-conjugated DNA interchelators, tagged live/dead chelators and peptide-MHC tetramers for cytomegalovirus (CMV), influenza and hepatitis C virus (HCV). Cells were then analysed by single-cell mass cytometry (cytometry by time-of-flight or CyTOF), which vaporizes the sample and quantifies the relative abundance of heavy metal isotopes. DNA content and cell length were used to identify single cells and live cells identified as live/dead chelator negative. Cells were then gated upon surface marker expression, as shown in **Figure 6**.

Advantages:

- Single-cell analysis of **>45 simultaneous parameters**
- No interference from spectral overlap = **no compensation**
- Limited/**no background** as isotopes are nonbiological
- Similarity in **sensitivity** across all probes
- **Highly accurate** quantitation

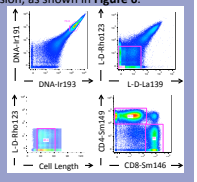

Figure 6: Gating strategy used with CyTOF

Results: CD161^{dim} CD8^{+} T cells demonstrated a striking enrichment in expression of a variety of cytotoxic markers. CD16, the FcγRIII associated with antibody-dependent cellular cytotoxicity (ADCC) in NK cells, was confined to the CD161^{dim} population when analysed by CyTOF (**Figure 7A**). This enrichment was confirmed by flow cytometry (**Figure 7B**), which showed more variability in expression between subsets. CD56, a further NK cell marker, also appeared enriched in CD161^{dim} cells, in addition to granzyme B and perforin. Furthermore, CD161^{dim} CD8^{+} T cells displayed a greater degree of combinatorial staining with these cytotoxic markers (**Figure 7C**). Therefore, the CD161^{dim} CD8^{+} T cell population is enriched in cytotoxic markers, with a potential role in control of viral infection by ADCC.

Figure 7: Analysis by CyTOF reveals enrichment of cytotoxicity markers within the CD161^{dim} CD8^{+} T cell population. A) Staining of CD8^{+} CD161 subsets for NK cell markers CD16 and CD56, and cytotoxic granule components granzyme B and perforin. **B)** Flow cytometry confirms enrichment of CD16 expression within the CD161^{dim} CD8^{+} T cell population. **C)** Pie charts indicate the proportion of each population expressing a combination of cytotoxicity markers.

Conclusions:

- **CD161^{dim} CD8^{+} T cells are a unique population of T cells which have the potential to efflux cytotoxic drugs and show a significant enrichment in cytotoxic markers compared to other CD8^{+} T cell subsets.**